CTGF and lymphangiogenesis in renal and peritoneal fibrosis

Hiroshi Kinashi

Cover: Bonsai, a popular product in Kinashi town, Kagawa, Japan. Green color is derived from dextran labeled with fluorescein isothiocyanate.

Printed by: Gildeprint - The Netherlands
ISBN: 978-94-6233-556-1

Financial support for the publication of this thesis was gratefully provided by the Dutch Kidney Foundation and the department of Pathology (UMC Utrecht)

CTGF and lymphangiogenesis in renal and peritoneal fibrosis

腎臓と腹膜の線維化における CTGF とリンパ管新生
（日本語の要約付き）

CTGF en lymfangiogenese in nier- en peritoneaalfibrose
(met een samenvatting in het Nederlands)

Proefschrift

ter verkrijging van de graad van doctor aan de Universiteit Utrecht op gezag van de rector magnificus, prof.dr. G.J. van der Zwaan, ingevolge het besluit van het college voor promoties in het openbaar te verdedigen op dinsdag 14 maart 2017 des ochtends te 10.30 uur

door

Hiroshi Kinashi

geboren op 11 februari 1978 te Ube, Japan

Promotoren: Prof.dr. R. Goldschmeding
Prof.dr. Y. Ito

Copromotor: Dr. T.Q. Nguyen

CONTENTS

1

General introduction

Pathophysiological considerations regarding CTGF involvement and lymphangiogenesis in renal and peritoneal fibrosis

Peritoneal fibrosis

Long-term peritoneal dialysis (PD) treatment induces morphological change of peritoneum and loss of ultrafiltration accompanied with high peritoneal solute transport. Several factors such as uremia, exposure to dialysate, and peritonitis episodes contribute to peritoneal injury. We describe the PD-related pathophysiology of peritoneal fibrosis, angiogenesis, and lymphangiogenesis.

Mesothelial cells

A monolayer of mesothelial cells cover the surface of peritoneum in healthy subjects. Mesothelial cells provide the local defense and predominantly regulate peritoneal homeostasis including synthesis of cytokines, growth factors, and matrix proteins.[1,2]

Prolonged PD procedure induces mesothelial cell activation, cell hypertrophy, and some degree of mesothelial denudation.[3] Glucose as an osmotic agent of dialysate inhibits mesothelial cell proliferation,[4] and induces mitochondrial DNA damage and apoptosis of mesothelial cells.[5,6] Glucose degradation products (GDPs) are also toxic for cells in the peritoneum.[7] Glucose and GDPs increase production of inflammatory cytokines and growth factors in mesothelial cells, such as monocyte chemoattractant protein-1 (MCP-1),[8,9,10] transforming growth factor-β (TGF-β),[10,11] and vascular endothelial growth factor (VEGF)-A.[12]

High osmolarity also contributes to the bioincompatibility of PD solutions. Shrinkage and apoptosis of mesothelial cells can be induced by exposure to hyperosmolar solutions.[13,14] Both the polyol pathway and osmolarity contribute to the induction of TGF-β and MCP-1 in mesothelial cells.[10] Osmotic stress increases transcriptional activity of nuclear factor-κB (NF-κB) and nuclear factor of activated T cells 5 (NFAT5). NFAT5 not only plays a key role in the protection of cells against hyperosmotic stresses but also induces inflammatory mediators and growth factors.[15,16] In addition, NF-κB and NFAT5 mediate the induction of MCP-1 in mesothelial cells.[17,18]

Furthermore, PD treatment induces loss of epithelial differentiation and acquisition of more mesenchymal characteristics of mesothelial cells (epithelial-to-mesenchymal transdifferentiation, or EMT), which is initiated by profibrotic and inflammatory cytokines including TGF-β1 and interleukin (IL)-1β.[19]

Submesothelial fibrosis

Also uremia itself affects peritoneal membrane. Peritoneal thickness is increased in uremic patients who have not received dialysis treatment (120-140 μm) compared to healthy subjects (50-60 μm).[3,20] Several proteoglycan components are increased in peritoneum of uremic patients.[21] Uremic patients show a variety of peritoneal solute transport rate at the beginning of PD, which is correlated with peritoneal macrophage infiltration.[22] In a rat

uremic model with subtotal nephrectomy it was demonstrated that uremia increased nitric oxide synthase (NOS), VEGF-A, and fibroblast growth factor (FGF) expression in association with higher peritoneal permeability, vascular proliferation, and fibrosis.[23] Increased expression of advanced glycation end products (AGE) and of the cell surface receptor for AGE (RAGE) were induced by carbonyl stress in uremia. Inhibition of AGE-RAGE signaling improved peritoneal function and fibrosis in uremic rats.[24,25]

Myofibroblasts that play an important role in peritoneal fibrosis can be derived from different origins such as resident fibroblasts, endothelial cells, and bone marrow derived cells.[26] Mesothelial cells can also directly contribute to fibrosis by undergoing EMT followed by migration into the submesothelium and production of extracellular matrix.[19] Glucose in the dialysis solution stimulates fibroblast proliferation with increased secretion of extracellular matrix proteins, leading to peritoneal fibrosis.[27,28,29]

Peritonitis is an important cause of peritoneal membrane injury, which leads to peritoneal fibrosis, neoangiogenesis, and peritoneal dysfunction.[3] Peritonitis causes exfoliation of mesothelial cells, loss of underlying basement membrane, and loss of microvilli and cell-cell contact in remaining mesothelial cells.[30] Severe peritonitis induces exudation of fibrin on the surface of peritoneum accompanied with inflammatory cell infiltration.[31] Bacterial peritonitis rapidly increases the total number of cells in the peritoneum, including neutrophils and macrophages, which can last for several weeks after clinical remission of peritonitis. Similarly, proinflammatory cytokines and fibrogenic growth factors, such as IL-1β, IL-6, TGF-β, and FGF were increased through at least 6 weeks despite clinical resolution of peritonitis.[32]

Among various molecular mechanisms, the TGF-β plays a central role in peritoneal fibrosis. PD patients with peritoneal fibrosis showed high level of TGF-β/Smad signaling which activates the transcription of target genes and induces EMT.[33,34] Blocking of TGF-β signaling reduced fibrosis, neoangiogenesis, and EMT, and improved peritoneal function in a rodent model.[26]

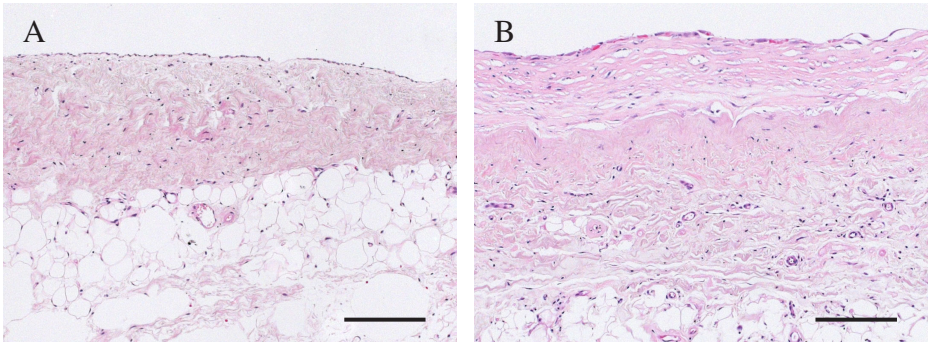

Histological change of human parietal peritoneum (hematoxylin and eosin stain, scale bars: 200 μm)

A: Uremia itself induced peritoneal membrane thickening before the initiation of PD treatment.
B: Mesothelial cell detachment and submesothelial extracellular matrix accumulation progressed after 10 years of PD treatment.

Angiogenesis

Peritoneal capillaries are embedded in a loose adipose layer under the submesothelium.[35] Peritoneal neoangiogenesis and high vascular permeability cause an increase of small solute transport accompanied with rapid reduction of glucose-driven osmotic pressure, which contribute to a loss of ultrafiltration. High blood vessel density and vascular subendothelial hyalinization were observed in the peritoneum of patients with membrane failure.[3] Exposure to glucose-based dialysate results in the deposition of AGE in peritoneal interstitium and microvascular walls of PD patients. AGE accumulation was correlated with interstitial fibrosis, vascular sclerosis, and impaired ultrafiltration.[36] In addition, peritoneal neoangiogenesis and fibrosis develop in parallel. Overexpression of TGF-β1 induced rat peritoneal fibrosis accompanied with neoangiogenesis through induction of VEGF-A production in mesothelial cells.[37]

VEGF-A is a central regulator of angiogenesis and vascular permeability.[38] VEGF-A expression in human PD effluents was correlated with peritoneal permeability for small solutes and loss of ultrafiltration.[39] GDPs induce VEGF-A production in mesothelial cells and endothelial cells.[12] AGE induces angiogenesis through the induction of autocrine signaling VEGF-A in microvascular endothelial cells.[40] Mesothelial cells that have undergone EMT produced higher amounts of VEGF-A than ‘‘normal’’ epithelial-differentiated mesothelial cells.[41]

The angiopoietin (Ang)/Tie-2 pathway plays a major role in the triggering of neoangiogenesis.[42] Ang-1 and Ang-2 act as ligands for the endothelium-specific tyrosine kinase receptor, Tie-2. Ang-1 constantly activates Tie-2 phosphorylation to maintain vascular integrity and homeostasis in healthy adult vasculature, while, Ang-2 blocks Ang-1/Tie-2 activation as an antagonist of Ang-1, which initiates angiogenic sprouting.[42] Increased levels of VEGF-A and Ang-2 in rat peritoneum of a uremic PD model positively correlated with blood vessel density which was accompanied with high peritoneal transport and decreased ultrafiltration.[43] Treatment with a soluble Tie-2 fusion protein reduced Ang-2 expression and suppressed peritoneal angiogenesis in PD-treated uremic rats.[44]

Peritonitis episodes strongly induce peritoneal inflammation. Proinflammatory cytokines, IL-1β and tumor necrosis factor (TNF)-α are mainly produced by macrophages in the early response to peritonitis.[45] Overexpression of IL-1β or TNF-α in rat peritoneum induced angiogenesis, high peritoneal permeability, and loss of ultrafiltration accompanied with increased expression of VEGF-A, TGF-β1, and extracellular matrix. Changes in peritoneal structure and function by TNF-α were transient, while IL-1β led to sustained vascularization and fibrosis.[46] IL-6 also promotes angiogenesis by stimulating proliferation, migration, and matrigel tube formation of circulating blood endothelial progenitor cells.[47]

Plasma and dialysate IL-6 and VEGF-A levels in PD patients were increased in association with high peritoneal solute transport. A positive correlation was observed between dialysate IL-6 and dialysate VEGF-A.[48]

Mast cells contribute to peritoneal angiogenesis by producing angiogenic factors.[49] Chronic exposure to peritoneal dialysate dramatically increased omental mast cells.[50] Specific reduction of mast cells by using mast cell-deficient rats or treatment of mast cell stabilizer reduced peritoneal leukocyte recruitment, omental fibrosis, and angiogenesis in a rat PD model.[51]

Lymphangiogenesis

Lymphatic vessels drain extravasated tissue fluid and return it to the blood circulation, which maintains interstitial homeostasis.[52] Peritoneal lymphatic vessels continuously absorb dialysate during PD treatment, which reduces effective ultrafiltration.[53] Over 10 years ago, several clinical studies showed that increased lymphatic absorption was related to long-term PD procedures and ultrafiltration failure (UFF).[54,55] However, since then the accuracy of estimated lymphatic absorption based on the disappearance rate of intraperitoneally administered macromolecules, such as radioactive iodinated serum albumin or dextran, generated considerable debate.[56,57] After that, lymphatics of PD has been less studied. On the other hand, the recent discovery of several useful lymphatic markers has contributed importantly to the clarification of the regulation and role of lymphangiogenesis in a variety of diseases.[58,59,60,61] VEGF-C/D and VEGF receptor (VEGFR)-3 have been recognized as the central signaling molecules driving lymphangiogenesis.[62,63]

We demonstrated that lymphangiogenesis is associated with PD-induced peritoneal fibrosis.[64] The VEGF-C protein level in human PD effluents was increased in association with high peritoneal solute transport and was correlated with the TGF-β1 concentration in PD effluents.[64,65] VEGF-C mRNA expression and lymphatic markers was increased in peritoneal biopsies of UFF patients and was correlated with peritoneal thickness.[64] VEGF-C expression was mainly upregulated in mesothelial cells and macrophages in human peritoneal biopsies with bacterial peritonitis. In addition, VEGF-C expression in cultured mesothelial cells and macrophages was increased by TGF-β1 treatment.[64,66] In the rat peritoneal fibrosis model induced by chlorhexidine gluconate (CG) the expression of lymphatic vessels and VEGF-C was increased and accompanied with peritoneal inflammation and fibrosis.[64] The diaphragm contains a specialized lymphatic absorption system that includes lymphatic lacunae and mesothelial stomata.[67] We observed dramatic induction of dilated giant lymphatic vessels in the diaphragm in association with CG-induced peritoneal fibrosis. Increased expression of lymphatic vessels and VEGF-C was reduced by treatment with TGF-β type I receptor inhibitor.[64] Thus, TGF-β promotes VEGF-C production in peritoneal cells, which leads to lymphangiogenesis during peritoneal fibrosis. Treatment with a cyclooxygenase-2 (COX-2) inhibitor also reduced peritoneal lymphangiogenesis in the experimental PD model,[64,68] which might be mediated by

reduction of VEGF-C production in macrophages.[69] Interestingly, in the rat remnant kidney model it was demonstrated that chronic kidney disease itself induced peritoneal fibrosis, lymphangiogenesis, and high lymphatic absorption rate, independent of exposure of PD solution.[70]

Icodextrin, a glucose polymer derived from starch is one of the alternatives to glucose as an osmotic agent in peritoneal dialysate. Icodextrin is only slowly absorbed from the peritoneal cavity, and mainly by lymphatic vessels, because its molecular weight is too large for transport into blood capillaries.[71] Therefore, icodextrin solutions can provide stable ultrafiltration for long dwells particularly in patients with high peritoneal solute transport and UFF. We investigated the role of lymphangiogenesis in ultrafiltration of both a conventional glucose-based solution and an icodextrin solution.[72] For this, we treated mice with soluble VEGFR-3, a decoy receptor to trap VEGF-C/D, specifically suppressing VEGF-D-dependent lymphangiogenesis without changes of inflammation, fibrosis, and angiogenesis in the diaphragm of mice subjected to a peritoneal fibrosis model induced by methylglyoxal, which is a toxic GDP.[72] Inhibition of lymphangiogenesis by soluble VEGFR-3 treatment improved impaired ultrafiltration of icodextrin solution. Peritoneal equilibration tests revealed that, when using the glucose-based solution, treatment with soluble VEGFR-3 did not change peritoneal solute transport (glucose, creatinine) and tended to increase impaired ultrafiltration volume.[72] Icodextrin solution has been widely used because it reduces metabolic effects of peritoneal glucose exposure and acts as a stable osmotic gradient for long dwells.[71] However, it has been reported that the icodextrin solution did not improve ultrafiltration in some patients with UFF, which might be caused by increased lymphatic absorption with lymphangiogenesis.[73] The popularization of new peritoneal dialysates like icodextrin solution might lead to further focus on the function of lymphatic vessels in association with PD treatment.

Lymphangiogenesis and fibrosis in the kidney

Lymphangiogenesis has also been reported in kidney diseases. Aminopeptidase p and podoplanin are discriminatory markers for vascular and lymphatic endothelial cells in rat remnant kidneys, and proliferation of lymphatic vessels was observed in tubulointerstitial fibrotic area accompanied with rarefaction of blood vessels.[74] In human kidney transplant rejection, prominent lymphangiogenesis was observed within nodular mononuclear infiltrates, and it is speculated that lymphatic vessels not only drainage inflammatory infiltrate but also maintain the immune response by producing lymphatic chemokine which attracts inflammatory cells.[75] Donor-derived macrophages might differentiate into lymphatic endothelial cells, which contribute lymphangiogenesis in human renal transplants.[76] In our previous study with a total of 124 human kidney biopsies undergoing diagnostic evaluation, lymphangiogenesis was observed in a variety of kidney diseases, which was significantly correlated with the degree of renal interstitial fibrosis.[77] During obstructive nephropathy, TGF-β increases VEGF-C expression in renal tubular cells and macrophages, which leads to lymphangiogenesis.[66,78]

Unlike the clear contribution of lymphatic absorption in the physiology of PD, it might be difficult to show the general therapeutic strategy with regulation of lymphangiogenesis in kidney diseases. For instance, the mammalian target of rapamycin (mTOR) inhibitors is known to impede lymphatic endothelial cells growth through impairing the VEGF-C downstream signaling.[79] In renal transplantation model, one of the mTOR inhibitors, sirolimus inhibited lymphangiogenesis in association with attenuated development of chronic kidney allograft injury.[80] In contrast, VEGF-C treatment attenuated lung allograft rejection by inducing lymphangiogenesis, which improved clearance of detrimental hyaluronan from the lung allografts.[61] However, during aspiration pneumonia increased lymphangiogenesis is observed, and treatment with VEGFR inhibitor or VEGFR-3 specific inhibitor improved inflammation and oxygen saturation.[81] In addition, specific blocking of lymphangiogenesis by anti-VEGFR-3 antibody did not prevent inflammation, interstitial fibrosis, and proteinuria in a rat model of proteinuric nephropathy.[82] Thus, the requirement for lymphangiogenesis and efficacy of therapeutic intervention varies depending on organ and etiology of disease, and further studies are needed to understand the role of renal lymphangiogenesis in a variety of kidney diseases.

CTGF as an angiogenic and pro-fibrotic factor

Connective tissue growth factor (CTGF, CCN-2) is a member of the CCN (CTGF/Cyr61/Nov) family of matricellular proteins. Although CCN-specific receptor has not been found yet, CCNs bind and modulate multi-ligands and receptors for other matricellular molecules.[83] CCNs play important roles in development, inflammation, cancer progression, tissue repair, and fibrosis.[83] CTGF is known as an important determinant of fibrotic tissue remodeling.[84] CTGF is highly expressed in many fibrotic disorders and plays a key role in extracellular matrix production and profibrotic activities mediated by other growth factors.[85,86] CTGF is also known as a regulator of angiogenesis. CTGF can promote angiogenesis in part by mediating TGF-β downstream and adhesive signalings such as integrins and heparin sulfate proteoglycan.[87] On the other hand, CTGF binds to VEGF-A, and inhibits VEGF-A-induced angiogenesis.[87-89] The role of CTGF in angiogenesis may depend on tissue specificity and etiology of diseases.

CTGF strongly contributes to the development and progression of chronic kidney disease (CKD).[90] CTGF is overexpressed in various kidney diseases, such as diabetic nephropathy,[91] hypertensive nephrosclerosis,[92] crescentic glumerulonephritis,[93] and renal allograft fibrosis.[94] CTGF expression correlates with the severity of renal fibrosis.[91,95] TGF-β induces CTGF expression in multiple cell types including mesangial cells and renal tubular epithelial cells.[96,97] On the other hand, CTGF modulates TGF-β signaling by direct physical interaction.[85]

Reduction of CTGF has been reported as an effective antifibrotic strategy in experimental kidney diseases. Several reports showed that an approximate 50% reduction of CTGF is capable of reducing fibrotic development in moderate models of obstructive,[98] diabetic,[99] and allograft nephropathy,[100] and the remnant kidney model.[101] Interestingly, we have

shown that 50% reduction of CTGF is not sufficient to attenuate fibrotic development in severe models of kidney diseases.[102] We estimate that further CTGF reduction might prevent fibrosis in severe kidney disease models because 50% reduction of CTGF level is still higher than baseline CTGF level. FG-3019, a human monoclonal antibody against CTGF, was studied in a small phase-I clinical trial on patients with diabetic nephropathy and found to significantly reduce albuminuria.[103]

CTGF levels in plasma and urine were increased in type I diabetic patients with nephropathy.[104,105] Urinary CTGF correlated with urinary albumin excretion and glomerular filtration rate in patients with diabetic nephropathy.[105] Urinary CTGF also correlated with progression of microalbuminuria which is an early finding of diabetic nephropathy.[106] In renal transplantation recipients, urinary CTGF levels were associated with the degree of interstitial fibrosis, and urinary CTGF expression at 3 months was associated with the progression of renal allograft fibrosis two years after transplantation.[94]

CTGF is also involved in PD-associated peritoneal fibrosis. CTGF expression is increased in human PD effluents and human peritoneal biopsy samples in association with high peritoneal solute transport rate and UFF.[107] Peritonitis episodes markedly increase the CTGF level in human PD effluents.[108] CTGF is mainly enhanced in mesothelial cells and fibroblast-like cells in human fibrotic peritoneum with UFF.[107] CTGF production by human peritoneal mesothelial cells is regulated by GDP, AGE, and TGF-β.[107-109] Thus, CTGF plays an important role in both renal and peritoneal fibrosis.

Aims and Outline of this Thesis

Lymphangiogenesis is associated with renal and peritoneal fibrosis. Peritoneal lymphangiogenesis might play an important role in the mechanism of UFF. Lymphangiogenesis has also been associated with fibrosis of the kidney. The mechanism underlying fibrosis-associated lymphangiogenesis are only poorly understood. Although CTGF is an important fibrosis mediator, and has been implicated in blood vessel formation, nothing is known about its possible involvement in fibrosis-associated lymphangiogenesis. In this thesis I present my investigations into the role of CTGF and lymphangiogenesis in renal and peritoneal fibrosis.

Chapter 2 summarizes and discusses representative animal models of PD-associated peritonitis, including our newly generated scraping and zymosan models that mimic peritoneal injury associated with fibrosis and neoangiogenesis caused by bacterial or fungal peritonitis. **Chapter 3** is the first study showing lymphangiogenesis during peritoneal fibrosis. We analyzed expression of VEGF-C and lymphatic vessels in human samples in association with peritoneal fibrosis and UFF. Induction of VEGF-C by TGF-β was evaluated in in vitro. In addition, peritoneal lymphangiogenesis was also evaluated in a rat peritoneal fibrosis model. In **Chapter 4**, we investigated the role of VEGF-C/D-VEGFR-3 signaling in lymphangiogenesis in peritoneal injury and function in a mouse peritoneal fibrosis model by the treatment with adenoviral transfection of soluble VEGFR-3. In **Chapter 5**, we studied the relationship between CTGF and lymphangiogenesis in human peritoneal samples, cultured mesothelial cells, and a rat peritoneal fibrosis model.

Lymphatic vessels develop also during renal interstitial fibrosis. In **Chapter 6** we identify a possible mechanism of lymphangiogenesis in a rat model of obstructive nephropathy. **Chapter 7** focuses on CTGF involvement in renal lymphangiogenesis. We explored the effect of reducing CTGF expression on fibrosis and lymphangiogenesis in a mouse model of obstructive nephropathy. In addition, we also analyzed the interaction between CTGF and VEGF-C in vitro. Age is associated with progression of CKD, which is at least in part attributed to accumulation of fibrosis. However it is known whether also the rate of progression of fibrosis is increasing with age. In **Chapter 8**, we investigated the effect of age on the development of renal tissue damage and fibrosis in a mouse model of obstructive nephropathy using young and old mice, and identified a role of CTGF in age-associated differences in tissue response to injury. CTGF has also been identified as an important mediator of renal allograft fibrosis. In **Chapter 9**, we therefore evaluated whether early tubulointerstitial CTGF expression predicts progression of interstitial fibrosis and tubular atrophy as well as functional deterioration in human transplanted kidney biopsies.

References

1. Yung S, Chan TM. Intrinsic cells: mesothelial cells -- central players in regulating inflammation and resolution. Perit Dial Int. 2009;29 (Suppl 2):S21-7.
2. Yung S, Chan TM. Pathophysiological changes to the peritoneal membrane during PD-related peritonitis: the role of mesothelial cells. Mediators Inflamm. 2012;2012:484167.
3. Williams JD, Craig KJ, Topley N, et al. Morphologic changes in the peritoneal membrane of patients with renal disease. J Am Soc Nephrol. 2002;13:470-9.
4. Ciszewicz M, Wu G, Tam P, Polubinska A, et al. Changes in peritoneal mesothelial cells phenotype after chronic exposure to glucose or N-acetylglucosamine. Transl Res. 2007;150:337-42.
5. Ishibashi Y, Sugimoto T, Ichikawa Y, et al. Glucose dialysate induces mitochondrial DNA damage in peritoneal mesothelial cells. Perit Dial Int. 2002;22:11-21.
6. Boulanger E, Wautier MP, Gane P, et al. The triggering of human peritoneal mesothelial cell apoptosis and oncosis by glucose and glycoxydation products. Nephrol Dial Transplant. 2004;19:2208-16.
7. Witowski J, Jörres A. Glucose degradation products: relationship with cell damage. Perit Dial Int. 2000;20(Suppl 2):S31-6.
8. Haslinger B, Mandl-Weber S, Sellmayer A, et al. Effect of high glucose concentration on the synthesis of monocyte chemoattractant protein-1 in human peritoneal mesothelial cells: involvement of protein kinase C. Nephron. 2001;87:346-51.
9. Lee SK, Kim BS, Yang WS, et al. High glucose induces MCP-1 expression partly via tyrosine kinase-AP-1 pathway in peritoneal mesothelial cells. Kidney Int. 2001;60:55-64.
10. Wong TY, Phillips AO, Witowski J, et al. Glucose-mediated induction of TGF-beta 1 and MCP-1 in mesothelial cells in vitro is osmolality and polyol pathway dependent. Kidney Int. 2003;63:1404-16.
11. Kang DH, Hong YS, Lim HJ, et al. High glucose solution and spent dialysate stimulate the synthesis of transforming growth factor-beta1 of human peritoneal mesothelial cells: effect of cytokine costimulation. Perit Dial Int. 1999;19:221-30.
12. Inagi R, Miyata T, Yamamoto T, et al. Glucose degradation product methylglyoxal enhances the production of vascular endothelial growth factor in peritoneal cells: role in the functional and morphological alterations of peritoneal membranes in peritoneal dialysis. FEBS Lett. 1999;463:260-4.
13. Breborowicz A, Polubinska A, Oreopoulos DG. Changes in volume of peritoneal mesothelial cells exposed to osmotic stress. Perit Dial Int. 1999;19:119-23.
14. Alscher DM, Biegger D, Mettang T, et al. Apoptosis of mesothelial cells caused by unphysiological characteristics of peritoneal dialysis fluids. Artif Organs. 2003;27:1035-40.
15. Burg MB, Ferraris JD, Dmitrieva NI. Cellular response to hyperosmotic stresses. Physiol Rev. 2007;87:1441-74.

16. Neuhofer W. Role of NFAT5 in inflammatory disorders associated with osmotic stress. Curr Genomics. 2010;11:584-90.
17. Matsuo H, Tamura M, Kabashima N, et al. Prednisolone inhibits hyperosmolarity-induced expression of MCP-1 via NF-kappaB in peritoneal mesothelial cells. Kidney Int. 2006;69:736-46.
18. Küper C, Beck FX, Neuhofer W. NFAT5 contributes to osmolality-induced MCP-1 expression in mesothelial cells. Mediators Inflamm. 2012;2012:513015.
19. Yáñez-Mó M, Lara-Pezzi E, Selgas R, et al. N Engl J Med. 2003 Jan 30;348(5):403-13. N Engl J Med. 2003;348:403-13.
20. Honda K, Hamada C, Nakayama M, et al. Impact of uremia, diabetes, and peritoneal dialysis itself on the pathogenesis of peritoneal sclerosis: a quantitative study of peritoneal membrane morphology. Clin J Am Soc Nephrol. 2008;3:720-8.
21. Osada S, Hamada C, Shimaoka T, et al. Alterations in proteoglycan components and histopathology of the peritoneum in uraemic and peritoneal dialysis (PD) patients. Nephrol Dial Transplant. 2009;24:3504-12.
22. Sawai A, Ito Y, Mizuno M, et al. Peritoneal macrophage infiltration is correlated with baseline peritoneal solute transport rate in peritoneal dialysis patients. Nephrol Dial Transplant. 2011;26:2322-32.
23. Combet S, Ferrier ML, Van Landschoot M, et al. Chronic uremia induces permeability changes, increased nitric oxide synthase expression, and structural modifications in the peritoneum. J Am Soc Nephrol. 2001;12:2146-57.
24. Kakuta T, Tanaka R, Satoh Y, et al. Pyridoxamine improves functional, structural, and biochemical alterations of peritoneal membranes in uremic peritoneal dialysis rats. Kidney Int. 2005;68:1326-36.
25. De Vriese AS, Tilton RG, Mortier S, et al. Myofibroblast transdifferentiation of mesothelial cells is mediated by RAGE and contributes to peritoneal fibrosis in uraemia. Nephrol Dial Transplant. 2006;21:2549-55.
26. Loureiro J, Aguilera A, Selgas R, et al. Blocking TGF-β1 protects the peritoneal membrane from dialysate-induced damage. J Am Soc Nephrol. 2011;22:1682-95.
27. Higuchi C, Sanaka T, Sato T, et al. The effect of glucose on the proliferation of peritoneal fibroblasts. Adv Perit Dial. 1997;13:253-6.
28. Higuchi C, Nihei H. The role of protein kinase C activity in the proliferation of peritoneal fibroblasts. Perit Dial Int. 1999;19(Suppl 2):S353-7.
29. Breborowicz A, Wisniewska J, Polubinska A, et al. Role of peritoneal mesothelial cells and fibroblasts in the synthesis of hyaluronan during peritoneal dialysis. Perit Dial Int. 1998;18:382-6.
30. Verger C, Luger A, Moore HL, et al. Acute changes in peritoneal morphology and transport properties with infectious peritonitis and mechanical injury. Kidney Int. 1983;23:823-31.

31. Tawada M, Ito Y, Hamada C, et al. Vascular Endothelial Cell Injury Is an Important Factor in the Development of Encapsulating Peritoneal Sclerosis in Long-Term Peritoneal Dialysis Patients. PLoS One. 2016;11:e0154644.
32. Lai KN, Lai KB, Lam CW, et al. Changes of cytokine profiles during peritonitis in patients on continuous ambulatory peritoneal dialysis. Am J Kidney Dis. 2000;35:644-52.
33. Duan WJ, Yu X, Huang XR, et al. Opposing roles for Smad2 and Smad3 in peritoneal fibrosis in vivo and in vitro. Am J Pathol. 2014;184:2275-84.
34. Zhou Q, Bajo MA, Del Peso G, et al. Preventing peritoneal membrane fibrosis in peritoneal dialysis patients. Kidney Int. 2016;90:515-24.
35. Nessim SJ, Perl J, Bargman JM. The renin-angiotensin-aldosterone system in peritoneal dialysis: is what is good for the kidney also good for the peritoneum? Kidney Int. 2010;78:23-8.
36. Honda K, Nitta K, Horita S, et al. Accumulation of advanced glycation end products in the peritoneal vasculature of continuous ambulatory peritoneal dialysis patients with low ultra-filtration. Nephrol Dial Transplant. 1999;14:1541-9.
37. Margetts PJ, Kolb M, Galt T, et al. Gene transfer of transforming growth factor-beta1 to the rat peritoneum: effects on membrane function. J Am Soc Nephrol. 2001;12:2029-39.
38. Shibuya M. Vascular endothelial growth factor and its receptor system: physiological functions in angiogenesis and pathological roles in various diseases. J Biochem. 2013;153:13-9.
39. Zweers MM, de Waart DR, Smit W, et al. Growth factors VEGF and TGF-beta1 in peritoneal dialysis. J Lab Clin Med. 1999;134:124-32.
40. Yamagishi Si, Yonekura H, Yamamoto Y, et al. Advanced glycation end products-driven angiogenesis in vitro. Induction of the growth and tube formation of human microvascular endothelial cells through autocrine vascular endothelial growth factor. J Biol Chem. 1997;272:8723-30.
41. Aroeira LS, Aguilera A, Selgas R, et al. Mesenchymal conversion of mesothelial cells as a mechanism responsible for high solute transport rate in peritoneal dialysis: role of vascular endothelial growth factor. Am J Kidney Dis. 2005;46:938-48.
42. Scholz A, Plate KH, Reiss Y. Angiopoietin-2: a multifaceted cytokine that functions in both angiogenesis and inflammation. Ann N Y Acad Sci. 2015;1347:45-51.
43. Yuan J, Fang W, Ni Z, et al. Peritoneal morphologic changes in a peritoneal dialysis rat model correlate with angiopoietin/Tie-2. Pediatr Nephrol. 2009;24:163-70.
44. Xiao J, Guo J, Liu XX, et al. Soluble Tie2 fusion protein decreases peritoneal angiogenesis in uremic rats. Mol Med Rep. 2013;8:267-71.
45. Visser CE, Brouwer-Steenbergen JJ, Struijk G, et al. Production of IL-1 beta and TNF-alpha by peritoneal macrophages depends on the bacterial species and the inoculum. Adv Perit Dial. 1997;13:201-4.

46. Margetts PJ, Kolb M, Yu L, et al. Inflammatory cytokines, angiogenesis, and fibrosis in the rat peritoneum. Am J Pathol. 2002;160:2285-94.
47. Fan Y, Ye J, Shen F, et al. Interleukin-6 stimulates circulating blood-derived endothelial progenitor cell angiogenesis in vitro. J Cereb Blood Flow Metab. 2008;28:90-8.
48. Pecoits-Filho R, Araújo MR, Lindholm B, et al. Plasma and dialysate IL-6 and VEGF concentrations are associated with high peritoneal solute transport rate. Nephrol Dial Transplant. 2002;17:1480-6.
49. Nienartowicz A, Sobaniec-Łotowska ME, Jarocka-Cyrta E, et al. Mast cells in neoangiogenesis. Med Sci Monit. 2006;12:RA53-6.
50. Zareie M, Hekking LH, Driesprong BA, et al. Accumulation of omental mast cells during peritoneal dialysis. Perit Dial Int. 2001;21(Suppl 3):S373-6.
51. Zareie M, Fabbrini P, Hekking LH, et al. Novel role for mast cells in omental tissue remodeling and cell recruitment in experimental peritoneal dialysis. J Am Soc Nephrol. 2006;17:3447-57.
52. Norrmén C, Tammela T, Petrova TV, et al. Biological basis of therapeutic lymphangiogenesis. Circulation. 2011;123:1335-51.
53. Mactier RA, Khanna R, Twardowski Z, et al. Contribution of lymphatic absorption to loss of ultrafiltration and solute clearances in continuous ambulatory peritoneal dialysis. J Clin Invest. 1987;80:1311-6.
54. Fusshöller A, zur Nieden S, Grabensee B, et al. Peritoneal fluid and solute transport: influence of treatment time, peritoneal dialysis modality, and peritonitis incidence. J Am Soc Nephrol. 2002;13:1055-60.
55. Smit W, Schouten N, van den Berg N, et al. Analysis of the prevalence and causes of ultrafiltration failure during long-term peritoneal dialysis: a cross-sectional study. Perit Dial Int. 2004;24:562-70.
56. Krediet RT. The effective lymphatic absorption rate is an accurate and useful concept in the physiology of peritoneal dialysis. Perit Dial Int. 2004;24:309-13.
57. Flessner M. Effective lymphatic absorption rate is not a useful or accurate term to use in the physiology of peritoneal dialysis. Perit Dial Int. 2004;24:313-6.
58. Alitalo A, Detmar M. Interaction of tumor cells and lymphatic vessels in cancer progression. Oncogene. 2012;31:4499-508.
59. Kim H, Kataru RP, Koh GY. Inflammation-associated lymphangiogenesis: a double-edged sword? J Clin Invest. 2014;124:936-42.
60. Dashkevich A, Hagl C, Beyersdorf F, et al. VEGF Pathways in the Lymphatics of Healthy and Diseased Heart. Microcirculation. 2016;23:5-14.
61. Cui Y, Liu K, Monzon-Medina ME, et al. Therapeutic lymphangiogenesis ameliorates established acute lung allograft rejection. J Clin Invest. 2015;125:4255-68.
62. Zheng W, Aspelund A, Alitalo K. Lymphangiogenic factors, mechanisms, and applications. J Clin Invest. 2014;124:878-87.

63. Coso S, Bovay E, Petrova TV. Pressing the right buttons: signaling in lymphangiogenesis. Blood. 2014;123:2614-24.
64. Kinashi H, Ito Y, Mizuno M, et al. TGF-β1 promotes lymphangiogenesis during peritoneal fibrosis. J Am Soc Nephrol. 2013;24:1627-42.
65. Yang WS, Tsai TJ, Shih CL, et al. Intraperitoneal vascular endothelial growth factor C level is related to peritoneal dialysis ultrafiltration. Blood Purif. 2009;28:69-74.
66. Suzuki Y, Ito Y, Mizuno M, et al. Transforming growth factor-β induces vascular endothelial growth factor-C expression leading to lymphangiogenesis in rat unilateral ureteral obstruction. Kidney Int. 2012;81:865-79.
67. Abu-Hijleh MF, Habbal OA, Moqattash ST. The role of the diaphragm in lymphatic absorption from the peritoneal cavity. J Anat. 1995;186:453-67.
68. Fabbrini P, Schilte MN, Zareie M, et al. Celecoxib treatment reduces peritoneal fibrosis and angiogenesis and prevents ultrafiltration failure in experimental peritoneal dialysis. Nephrol Dial Transplant. 2009;24:3669-76.
69. Iwata C, Kano MR, Komuro A, et al. Inhibition of cyclooxygenase-2 suppresses lymph node metastasis via reduction of lymphangiogenesis. Cancer Res. 2007;67:10181-9.
70. Vlahu CA, de Graaff M, Aten J, et al. Lymphangiogenesis and Lymphatic Absorption Are Related and Increased in Chronic Kidney Failure, Independent of Exposure to Dialysis Solutions. Adv Perit Dial. 2015;31:21-5.
71. García-López E, Lindholm B, Davies S. An update on peritoneal dialysis solutions. Nat Rev Nephrol. 2012;8:224-33.
72. Terabayashi T, Ito Y, Mizuno M, et al. Vascular endothelial growth factor receptor-3 is a novel target to improve net ultrafiltration in methylglyoxal-induced peritoneal injury. Lab Invest. 2015;95:1029-43.
73. Thodis E, Passadakis P, Panagoutsos S, et al. Failure of icodextrin to provide adequate ultrafiltration in continuous ambulatory peritoneal dialysis patients. Adv Perit Dial. 1999;15:171-4.
74. Matsui K, Nagy-Bojarsky K, Laakkonen P, et al. Lymphatic microvessels in the rat remnant kidney model of renal fibrosis: aminopeptidase p and podoplanin are discriminatory markers for endothelial cells of blood and lymphatic vessels. J Am Soc Nephrol. 2003;14:1981-9.
75. Kerjaschki D, Regele HM, Moosberger I, et al. Lymphatic neoangiogenesis in human kidney transplants is associated with immunologically active lymphocytic infiltrates. J Am Soc Nephrol. 2004;15:603-12.
76. Kerjaschki D, Huttary N, Raab I, et al. Lymphatic endothelial progenitor cells c ontribute to de novo lymphangiogenesis in human renal transplants. Nat Med. 2006;12:230-4.
77. Sakamoto I, Ito Y, Mizuno M, et al. Lymphatic vessels develop during tubulointerstitial fibrosis. Kidney Int. 2009;75:828-38.

78. Lee AS, Lee JE, Jung YJ, et al. Vascular endothelial growth factor-C and -D are involved in lymphangiogenesis in mouse unilateral ureteral obstruction. Kidney Int. 2013;83:50-62.
79. Huber S, Bruns CJ, Schmid G, et al. Inhibition of the mammalian target of rapamycin impedes lymphangiogenesis. Kidney Int. 2007;71:771-7.
80. Palin NK, Savikko J, Koskinen PK. Sirolimus inhibits lymphangiogenesis in rat renal allografts, a novel mechanism to prevent chronic kidney allograft injury. Transpl Int. 2013;26:195-205.
81. Nihei M, Okazaki T, Ebihara S, et al. Chronic inflammation, lymphangiogenesis, and effect of an anti-VEGFR therapy in a mouse model and in human patients with aspiration pneumonia. J Pathol. 2015;235:632-45.
82. Yazdani S, Hijmans RS, Poosti F, et al. Targeting tubulointerstitial remodeling in proteinuric nephropathy in rats. Dis Model Mech. 2015;8:919-30.
83. Lau LF. Cell surface receptors for CCN proteins. J Cell Commun Signal. 2016;10:121-7.
84. Perbal B. CCN proteins: multifunctional signalling regulators. Lancet. 2004;363:62-4.
85. Abreu JG, Ketpura NI, Reversade B, et al. Connective-tissue growth factor (CTGF) modulates cell signalling by BMP and TGF-beta. Nat Cell Biol. 2002;4:599-604.
86. Xu H, Li P, Liu M, et al. CCN2 and CCN5 exerts opposing effect on fibroblast proliferation and transdifferentiation induced by TGF-β. Clin Exp Pharmacol Physiol. 2015;42:1207-19.
87. Pi L, Shenoy AK, Liu J, et al. CCN2/CTGF regulates neovessel formation via targeting structurally conserved cystine knot motifs in multiple angiogenic regulators. FASEB J. 2012;26:3365-79.
88. Inoki I, Shiomi T, Hashimoto G, et al. Connective tissue growth factor binds vascular endothelial growth factor (VEGF) andinhibits VEGF-induced angiogenesis. FASEB J. 2002;16:219-21.
89. Hashimoto G, Inoki I, Fujii Y, et al. Matrix metalloproteinases cleave connective tissue growth factor and reactivateangiogenic activity of vascular endothelial growth factor 165. J Biol Chem. 2002;277:36288-95.
90. Falke LL, Goldschmeding R, Nguyen TQ. A perspective on anti-CCN2 therapy f or chronic kidney disease. Nephrol Dial Transplant. 2014;29(Suppl 1):i30-i37.
91. Ito Y, Aten J, Bende RJ, et al. Expression of connective tissue growth factor in human renal fibrosis. Kidney Int. 1998;53:853-61.
92. Ito Y, Aten J, Nguyen TQ, et al. Involvement of connective tissue growth factor in human and experimental hypertensive nephrosclerosis. Nephron Exp Nephrol. 2011;117:e9-20.
93. Kanemoto K, Usui J, Nitta K, et al. In situ expression of connective tissue growth factor in human crescentic glomerulonephritis. Virchows Arch. 2004;444:257-63.

94. Metalidis C, van Vuuren SH, Broekhuizen R, et al. Urinary connective tissue growth factor is associated with human renal allograft fibrogenesis. Transplantation. 2013;96:494-500.
95. Yokoi H, Sugawara A, Mukoyama M, et al. Role of connective tissue growth factor in profibrotic action of transforming growth factor-beta: a potential target for preventing renal fibrosis. Am J Kidney Dis. 2001;38(4 Suppl 1):S134-8.
96. Castro NE, Kato M, Park JT, et al. Transforming growth factor β1 (TGF-β1) enhances expression of profibrotic genes through a novel signaling cascade and microRNAs in renal mesangial cells. J Biol Chem. 2014;289:29001-13.
97. Luo DD, Phillips A, Fraser D. Bone morphogenetic protein-7 inhibits proximal tubular epithelial cell Smad3 signaling via increased SnoN expression. Am J Pathol. 2010;176:1139-47.
98. Yokoi H, Mukoyama M, Nagae T, et al. Reduction in connective tissue growth factor by antisense treatment ameliorates renal tubulointerstitial fibrosis. J Am Soc Nephrol. 2004;15:1430-40.
99. Guha M, Xu ZG, Tung D, et al. Specific down-regulation of connective tissue growth factor attenuates progression of nephropathy in mouse models of type 1 and type 2 diabetes. FASEB J. 2007;21:3355-68.
100. Luo GH, Lu YP, Song J, et al. Inhibition of connective tissue growth factor by small interfering RNA prevents renal fibrosis in rats undergoing chronic allograft nephropathy. Transplant Proc. 2008;40:2365-9.
101. Okada H, Kikuta T, Kobayashi T, et al. Connective tissue growth factor expressed in tubular epithelium plays a pivotal role in renal fibrogenesis. J Am Soc Nephrol. 2005;16:133-43.
102. Falke LL, Dendooven A, Leeuwis JW, et al. Hemizygous deletion of CTGF/CCN2 does not suffice to prevent fibrosis of the severely injured kidney. Matrix Biol. 2012;31:421-31.
103. Adler SG, Schwartz S, Williams ME, et al. Phase 1 study of anti-CTGF monoclonal antibody in patients with diabetes and microalbuminuria. Clin J Am Soc Nephrol. 2010;5:1420-8.
104. Roestenberg P, van Nieuwenhoven FA, Wieten L, et al. Connective tissue growth factor is increased in plasma of type 1 diabetic patients with nephropathy. Diabetes Care. 2004;27(5):1164-70.
105. Nguyen TQ, Tarnow L, Andersen S, et al. Urinary connective tissue growth factor excretion correlates with clinical markers of renal disease in a large population of type 1 diabetic patients with diabetic nephropathy. Diabetes Care. 2006;29:83-8.
106. Tam FW, Riser BL, Meeran K, et al. Urinary monocyte chemoattractant protein-1 (MCP-1) and connective tissue growth factor (CCN2) as prognostic markers for progression of diabetic nephropathy. Cytokine. 2009;47:37-42.

107. Mizutani M, Ito Y, Mizuno M, et al. Connective tissue growth factor (CTGF/CCN2) is increased in peritoneal dialysis patients with high peritoneal solute transport rate. Am J Physiol Renal Physiol. 2010;298:F721-33.
108. Zarrinkalam KH, Stanley JM, Gray J, et al. Connective tissue growth factor and its regulation in the peritoneal cavity of peritoneal dialysis patients. Kidney Int. 2003;64:331-8.
109. Leung JC, Chan LY, Tam KY, et al. Regulation of CCN2/CTGF and related cytokines in cultured peritoneal cells under conditions simulating peritoneal dialysis. Nephrol Dial Transplant. 2009;24:458-69.

2

Review of bacterial and non-bacterial models of inflammation-induced models of peritoneal injury and fibrosis

Submitted

Yasuhiko Ito[1], Hiroshi Kinashi[1,2], Yasuhiro Suzuki[1] and Mizuno Masashi[1]

[1]Department of Nephrology and Renal Replacement Therapy, Nagoya University Graduate School of Medicine, Nagoya, Japan
[2]Department of Pathology, University Medical Center Utrecht, Utrecht, The Netherlands

Abstract
Peritonitis is an important complication of peritoneal dialysis (PD). Several animal peritonitis models have been described, including bacterial and fungal models that are useful for studying inflammation in peritonitis. However, these models have limitations for investigating peritoneal fibrosis induced by acute inflammation, and present difficulties in handling the infected animals. Here, we present an overview of representative animal models of PD-associated bacterial and non-bacterial peritonitis, including our novel animal models (scraping and zymosan models) that mimic peritoneal injury associated with fibrosis and neoangiogenesis caused by bacterial or fungal peritonitis.

Introduction

There are several reasons why peritonitis is important in peritoneal dialysis (PD) treatment. First, peritonitis remains an important cause of death in PD patients. The mortality rate for peritonitis is approximately 3% (1, 2), and peritonitis is a contributing cause of death in more than 10% of PD patients (3). Second, peritonitis remains an important factor in withdrawal from PD. In the PD registry of the Nagoya group from both 2005 to 2007 (4) and 2010 to 2012 (5), the most common reasons for withdrawal from PD have been PD-related peritonitis, followed by dialysis failure/ultrafiltration failure, and social problems such as lack of family support. PD peritonitis is primarily caused by gram-positive organisms that typically result from touch contamination. The mean incidence of peritonitis as reported twice from a study over a 3-year period was 1 episode every 42.8 (4) and 47.3 (5) patient-months, respectively. Third, peritonitis presents a risk for the development of encapsulating peritoneal sclerosis (EPS) (6). The duration of peritonitis is independently associated with EPS (7). In particular, fungal and Pseudomonas infections put patients at a higher risk for the development of EPS (8). Fourth, peritonitis is one of the risks for a decrease in residual renal function. The number of peritonitis episodes has been reported to be an independent predictor of the development of anuria (9). Fifth, peritonitis is an important cause of peritoneal membrane injury, which leads to peritoneal fibrosis, neoangiogenesis and peritoneal dysfunction (10).

The characteristic features of chronic peritoneal damage in PD treatment are the loss of ultrafiltration capacity associated with morphological submesothelial fibrosis with extracellular matrix accumulation, and neoangiogenesis. The pathogenesis of peritoneal fibrosis is attributed to a combination of bioincompatible factors in PD fluid (PDF), and peritonitis, especially repeated episodes of peritonitis (11). We have reported that uremia is associated with inflammation of the peritoneal membrane (12). Histologically, acute peritonitis can cause morphological damage to the peritoneum (10, 13). Detachment and disintegration of mesothelial cells is observed, along with the appearance of fibrin exudation and numerous infiltrating cells, ultimately resulting in internal structures becoming unrecognizable (6). Therefore, peritonitis may play a crucial role in the development of peritoneal damage leading to peritoneal membrane failure.

Animal models of peritonitis are important for establishing new information and therapies to improve peritoneal damage induced by peritonitis.

Peritonitis models induced by bacteria or fungus

There are several reports of animal models of peritonitis induced by bacteria or fungi (Table 1). The pathogenic microorganisms used to induce peritonitis include Staphylococcus aureus (14-18), Staphylococcus epidermidis (19, 20), Pseudomonas aeruginosa (21) and Candida albicans (22). These models of bacterial peritonitis have been mainly used to elucidate the mechanism of inflammation in the membrane and the mechanism of acute peritoneal membrane failure. However, the acute peritonitis model is not typically used to study peritoneal fibrosis.

A catheter-induced model of gram-positive bacterial peritonitis has been developed, which is an acute bacterial peritonitis model with bacteria originating from skin flora due to lack of aseptic precautions (23-25). In subsequent studies, these researchers used a model of lipopolysaccharide (LPS)-induced peritonitis instead of the gram-positive bacteria-induced peritonitis model (26, 27). They investigated the role of nitric oxide (NO) released by endothelial NO synthase (eNOS) in the gram-positive bacterial peritonitis model (23) and the LPS-induced peritonitis model (27), and suggested that the selective inhibition of eNOS might ameliorate the poor peritoneal function caused by acute peritonitis. They reported that mice injected with LPS developed a cloudy dialysate with increased white blood cell counts and NO metabolite levels, and inflammatory cell infiltration in the peritoneum, observations that are similar to the gram-positive peritonitis model.

The mechanisms of inflammation were studied in the bacterial and fungal peritonitis models; however, these models were not used to investigate the long-term complications such as fibrosis and neoangiogenesis.

Non-bacterial peritonitis models

Currently, the number of reports in which investigators use the non-bacterial peritonitis model is increasing. The non-bacterial model is convenient and useful for handling animals and performing experiments. We suggest that a model of peritoneal fibrosis induced in a peritonitis model will help identify new strategies for preventing peritoneal fibrosis. Many studies have used the LPS-induced peritoneal injury model (26-36). LPS derived from Escherichia coli (Sigma, St. Louis, MO) is frequently used (26-30, 33, 35). A method involving a single LPS dose was used to study peritoneal inflammation and dysfunction (26-29). Rat peritoneal inflammation and significant changes in neoangiogenesis were caused by daily administration of PDF over 3 weeks following an initial exposure to LPS (29-35).

Another non-bacterial peritonitis model induced by administration of lyophilized cell-free supernatants from Staphylococcus epidermidis has been used to study the regulation of inflammation and leukocyte trafficking (11, 37). Hurst et al. showed that interleukin-6 (IL-6)/soluble IL-6 receptor trans-signaling, which involves signal transducer and activator of transcription 3 (STAT3) activation, regulates chemokine secretion and polymorphonuclear neutrophil apoptosis in the peritoneal cavity. These mechanisms of inflammation and leukocyte trafficking have been clearly shown in the non-bacterial model.

Here, we introduce a model of peritoneal fibrosis that we generated in rats and mice that is induced by acute inflammation with mechanical scraping, the so-called “scraping model”.

Scraping model

We first reported the scraping model as a non-bacterial, peritonitis-induced peritoneal fibrosis model (38). After opening the rat abdomen under anesthesia, the right parietal peritoneum received hand-driven scratching for 1 min using the edge of a 15-ml centrifuge tube (Figure 1). Rats freely consumed food with or without NaCl loading after surgery (38-

40). Similarly, in mice, the right parietal peritoneum was scraped for 90 s with the cap of an injection needle.

In this model (Figure 2), neutrophil infiltration with fibrin exudation from the scraped peritoneum was demonstrated at 6 to 24 h after surgery. The predominant infiltrating cells switched to a mononuclear population on day 3, and inflammation gradually decreased thereafter. From days 7 to 14, the peritoneum became markedly thickened with the accumulation of alpha-smooth muscle actin (α-SMA)-positive fibroblasts and type III collagen. Mesothelial cells were not detected at 6 to 24 h after scraping, while approximately 30% and 70% of the total peritoneal length was covered with mesothelial cells on days 3 and 14, respectively. Increased CD31-positive blood vessel density was observed, which peaked at day 14. Transforming growth factor-β (TGF-β) and plasminogen activator inhibitor-1 (PAI-1) expression increased rapidly starting on day 3 and peaked at day 14. TGF-β and PAI-1 mRNA expression was upregulated from day 3 and peaked at day 7. In contrast, monocyte chemotactic protein-1 (MCP-1) mRNA rapidly increased and peaked at day 3. The pathology of this model in the early stage is characterized by strong infiltration of neutrophils and macrophages. The latter stage of this model is characterized by fibrosis and neoangiogenesis. In addition, peritoneal membrane permeability increased in rats that underwent bilateral scraping (38). The pathological features and time course of this model are summarized in Figures 2 and 3A.

Using this model, we investigated the effects of mineralocorticoid receptor (MR) blockade with salt loading (38). The local renin-angiotensin-aldosterone system (RAAS) is thought to play a role in peritoneal injury in PD patients (41). Peritoneal mesothelial cells have been observed to express angiotensinogen, angiotensin-converting enzyme (ACE), and angiotensin II type 1 receptors (AT1R) (42, 43). We found that MRs were expressed by rat fibroblasts and scraped peritoneum. Treatment with spironolactone suppressed macrophage infiltration, neoangiogenesis and fibrosis, which is associated with the suppression of TGF-β and PAI-1 expression, thereby resulting in improvement of peritoneal dysfunction, including ultrafiltration, glucose transport, and albumin leakage (38). The effects of spironolactone have also been shown in the LPS-induced peritoneal injury model (36).

In addition, we demonstrated the effects of atrial natriuretic peptide (ANP) in this model (39). ANP has been used as a diuretic and vasodilator in clinical settings. ANP has been shown to play an important function in the inhibition of RAAS (44, 45). ANP and brain natriuretic peptide (BNP) have been reported to prevent cardiac fibrosis (44, 46) and renal fibrosis (47-49), and to reduce infarct size in acute myocardial infarction (50). We demonstrated that AT1-R, ACE, and atrial natriuretic peptide receptor (NPR-A) mRNA expression were increased and peaked at days 14, 7, and 7, respectively. ANP administration resulted in a significant reduction in macrophage infiltration, fibrosis, and neoangiogenesis (39). In this model, the salt loading progression of peritoneal fibrosis is likely to be involved in local RAAS activation. Administration of an MR blocker or ANP with antibiotics may prevent peritoneal membrane dysfunction associated with fibrosis and neoangiogenesis in human bacterial peritonitis. In a small study, 25 mg/day of

spironolactone for 6 months was shown to reduce CD20 and collagen IV levels in the human peritoneal membrane (51). Recently, the scraping model was used to study the effectiveness of cell therapy using the mesothelial cells to prevent peritoneal damage in PD patients (52).

Zymosan-induced fungal peritonitis model

By modifying the scraping model, we established the zymosan-induced fungal peritonitis model. Although fungal peritonitis is not common, yeast infection with the most common Candida species results in a poor outcome with high mortality (53-55). The 2016 International Society for Peritoneal Dialysis guidelines recommends removal of the PD catheter in fungal peritonitis (56). Several clinical observations have suggested that EPS could be induced by a single occurrence of fungal peritonitis (56-60). The cell walls of many types of yeast activate various signaling reactions, including the complement system (61). Complement maintains host homeostasis by eliminating microorganisms and irregular cells and also regulates cellular immunity. The complement system in the peritoneum is continuously active at low levels, and complement regulators (CRegs) regulate complement activation. Irregular activation of complement leads to tissue damage in many diseases (62, 63).

We demonstrated the expression of CRegs, Crry, CD55, and CD59 in rat peritoneum, especially along the mesothelial cell layer (64). In rat peritoneum, combined blockade of Crry and CD59 induced severe focal inflammation with edema (65). We examined the state of complement activation in the aforementioned rat scraping model, and C3 and C3b were transiently present in the inflammatory stage at day 3 (64). Zymosan is abundant in the cell walls of fungi, and activates the complement system through the alternative pathway (66).

We demonstrated that administration of zymosan after scraping promoted severe peritoneal injury that is pathologically similar to human fungal peritonitis. Zymosan (5 mg/rat/day, 2 mg/mouse/day) mixed with PDF was intraperitoneally injected into the rat or mouse abdominal cavity for up to 5 days after scraping the rat or mouse peritoneum (40, 64, 67). Macroscopic findings in the zymosan rats showed the presence of a few white plaques at day 3, and yellow-white plaques at day 5, while no plaques were found in the control scraping model. Plaque fusion resulted in the formation of a yellow-white sheet covering the peritoneum with numerous small vessels running into the plaques, which suggests the occurrence of peritoneal neovascularization in the zymosan model at day 5. Peritoneal thickening associated with severe infiltration of inflammatory cells continued and remained present in the zymosan model at day 36, while the peritoneum was of normal appearance in the control scraping rats.

In recent experiments, we found that disease severity was affected by the lots of the zymosan (Sigma-Aldrich, St. Louis, MO). Expression of CRegs, Crry, CD55, and CD59 transiently decreased in the control scraping model at day 5. In contrast, CRegs expression was further decreased in the zymosan model at day 5, and continued decreasing up to day 18. Complement activation products, C3b and membrane attack complex (MAC), were

clearly found in the zymosan model from day 1 to 5, and small amounts of these products remained at days 18 and 36. The time course of this model is summarized in Figure 3B.

Systemic complement depletion by cobra venom factor or local suppression of complement activation by Crry-immunoglobulin or soluble complement receptor 1 dramatically reduced complement activation, peritoneal thickening and inflammation. These findings clearly indicated that the zymosan model is a complement-dependent model of severe proliferative peritonitis (64). Fungal peritonitis is known to be one of the causes of EPS. Subsequently, we successfully demonstrated that further enhancement of complement activation by inhibiting CRegs and enhancing systemic activation with cobra venom factor in the zymosan model induced fibrin exudation, which is the initial event of EPS (68).

Other models of non-bacterial peritoneal injury associated with inflammation and fibrosis

Administration of PDF into the abdominal cavity of rats and mice by repeated intraperitoneal injection or implanting a catheter is a method used to study the pathophysiological changes of the peritoneum associated with PD (69-83). Daily intraperitoneal injection of 4.25% glucose dialysate into the rat abdominal cavity for 1 week induced an increased peritoneal membrane transport rate and the absence of the peritoneal surface layer, as observed by electron microscopy (69, 70). Daily injection of PDF (100 ml/kg, once or twice daily) was performed for up to 8 or 12 weeks to obtain morphological changes in the rat peritoneum (71-73). Implantation of a silicon catheter into the rat abdomen was reported to amplify peritoneal inflammation from PDF through a foreign body reaction (74). However, the peritoneum of rats that received only a puncture without infusion of any solution showed no functional or pathological changes (73, 75).

A model of renal insufficiency, such as 5/6 nephrectomy, was used in combination with PDF infusion to closely model the clinical situation of peritoneal dialysis patients and to understand the influence of PD on residual renal function (76, 77). Daily intraperitoneal exposure of 1.5-3.0 ml of 4.25% glucose PDF for 4 or 5 weeks, with or without implanting a catheter, produced peritoneal dysfunction and morphological changes, such as fibrosis and neoangiogenesis, in mice (78-83).

Chronic intraperitoneal exposure to chemical irritation (chlorhexidine gluconate; CG) is used as an experimental model of peritoneal fibrosis with inflammation and EPS. Suga et al. developed a CG-induced peritoneal fibrosis model in rats (84). Daily injection of 0.1% CG in 15% ethanol, dissolved in 2-3 ml saline per 200 g body weight, was administered in the rat peritoneal cavity (85-87). At day 7, the peritoneal tissue was partially thickened with edema and showed initial accumulation of connective tissues and modest cell migration. At day 14, significant alterations were found, including peritoneal thickening with edema, cell infiltration, and neoangiogenesis. At day 21 to 28, the peritoneal tissue was markedly thickened and showed remarkable proliferation of collagen fibers. The number of macrophages gradually increased in the thickened areas and reached a maximum at day 21.

At day 28, neoangiogenesis had decreased, whereas collagen fibrils had accumulated. At day 35, fibrillary elements with cell infiltration occupied the submesothelial zone. Peritoneal resting for 3 weeks after 3 weeks of CG exposure ameliorated some functional parameters in the peritoneum; however, elevated peritoneal thickness and fibrosis continued during the resting period (88-91). Placing an infusion pump in the rat abdominal cavity was reported as an alternative administration route for CG (92-94).

A lower dosage of CG is an option for producing mild peritoneal injury (95-96). Mice were given daily intraperitoneal administration of 0.3 ml or 10 ml saline /kg body weight containing 0.1% CG in 15% ethanol (97, 98). Peritoneal fibrosis and increased infiltration of mononuclear cells were observed over time. Peritoneal fibrosis reached the chronic inflammatory stage, and macroscopic evidence of EPS was observed by 8 weeks. Lower doses of CG or shorter time courses produced milder and more infrequent development of peritoneal fibrosis (99, 100). Recent studies showed that a standard peritoneal fibrosis model could be produced in mice following treatment with 0.1% CG every other day or 3 times a week for 1-3 weeks (101-108).

Glucose degradation products contained in PDF contribute to the biocompatibility of conventional PDF and are risk factors for EPS. Methylglyoxal (MGO) is an extremely toxic glucose degradation product, and administration of PDF containing MGO can be used as an animal peritoneal fibrosis model. Rats were given intraperitoneal injections of 100 ml/kg of 2.5% glucose PDF (pH 5.0) containing 20 mM MGO every day for 3 weeks (109-111). Peritoneal function decreased significantly, and peritoneal fibrous thickening with proliferation of mesenchymal-like mesothelial cells and abdominal cocoon were induced. The combination of low doses of MGO and adenine-induced renal failure accelerated the progression of fibrous peritoneal thickening, whereas both MGO and renal failure alone did not (112). Intraperitoneal injection of PDF (100 ml/kg) containing 20 or 40 mM MGO for 5 consecutive days per week for 3 weeks induced peritoneal injury in mice (113,114). We clearly showed the presence of severe lymphangiogenesis in the diaphragm of both the CG and MGO models (96, 114). TGF-β is a central mediator of peritoneal fibrosis. Overexpression of TGF-β1 driven by intraperitoneal adenovirus administration induced peritoneal fibrosis through epithelial mesenchymal transition, neoangiogenesis, and poor peritoneal function in mice (115-118) and rats (119, 120). Other chemical irritants, such as deoxycholate (121), household bleach (122) and acidic solutions (123), were also reported to produce peritoneal inflammation, fibrosis, and abdominal cocoon in rats.

Conclusions

Non-bacterial peritonitis models are convenient and useful for animal handling and performing experiments. The peritoneum in the scraping model showed signs of peritonitis initially and fibrosis at a later stage. These pathological changes, along with alterations in solute transport, mimic those observed in bacterial peritonitis. This model is useful for exploring strategies for the treatment and prevention of peritoneal fibrosis and membrane failure. The zymosan model is useful for studying the mechanisms of fungal peritonitis and

the drugs used to reduce peritoneal damage induced by fungal peritonitis. Anti-complement therapy might be useful as a therapeutic in human fungal peritonitis and related peritoneal damage. Other non-bacterial models, such as CG and MGO models, are also useful for investigating the pathophysiology of fibrosis with inflammation, angiogenesis, and lymphangiogenesis.

Appendices

We presented the main part of this review at the International Society for Peritoneal Dialysis-Asia Pacific Chapter Meeting (ISPD-APCM); September 27-29, 2013; Grand Hotel, Taipei, Taiwan.

Acknowledgement

This work was supported in part by a Grant-in-Aid for Scientific Research from the Ministry of Education, Science and Culture of Japan (YI, # 20590972) and by the 2014 and 2015 research grant from the Aichi Kidney Foundation (YI).

Disclosures

All the authors declared no competing interests.

References

1. Brown MC, Simpson K, Kerssens JJ, Mactier RA, Scottish Renal Registry. Peritoneal dialysis-associated peritonitis rates and outcomes in a national cohort are not improving in the post-millennium (2000-2007). Perit Dial Int 2011; 31:639-50.
2. Davenport A. Peritonitis remains the major clinical complication of peritoneal dialysis: the London, UK, peritonitis audit 2002-2003. Perit Dial Int 2009; 29:297-302.
3. Pajek J, Hutchison AJ, Bhutani S, Brenchley PE, Hurst H, Perme MP1, et al. Outcomes of peritoneal dialysis patients and switching to hemodialysis: a competing risks analysis. Perit Dial Int 2014; 34:289-98.
4. Mizuno M, Ito Y, Tanaka A, Suzuki Y, Hiramatsu H, Watanabe M, et al. Peritonitis is still an important factor for withdrawal from peritoneal dialysis therapy in the Tokai area of Japan. Clin Exp Nephrol 2011; 15:727-37.
5. Mizuno M, Ito Y, Suzuki Y, Sakata F, Saka Y, Hiramatsu T, et al. Recent analysis of status and outcomes of peritoneal dialysis in the Tokai area of Japan: the second report of the Tokai peritoneal dialysis registry. Clin Exp Nephrol 2016; DOI 10.1007/s10157-016-1249-9.
6. Tawada M, Ito Y, Hamada C, Honda K, Mizuno M, Suzuki Y, et al. Vascular Endothelial Cell Injury Is an Important Factor in the Development of Encapsulating Peritoneal Sclerosis in Long-Term Peritoneal Dialysis Patients. PLoS One 2016; 11:e0154644.
7. Nakao M, Yokoyama K, Yamamoto I, Matsuo N, Tanno Y, Ohkido I, et al. Risk factors for encapsulating peritoneal sclerosis in long-term peritoneal dialysis: a retrospective observational study. Ther Apher Dial 2014; 18:68-73.
8. Kawanishi H, Moriishi M. Epidemiology of encapsulating peritoneal sclerosis in Japan. Perit Dial Int 2005; 25(Suppl 4):S14-8.
9. Szeto CC, Kwan BC, Chow KM, Chung S, Yu V, Cheng PM, et al. Predictors of residual renal function decline in patients undergoing continuous ambulatory peritoneal dialysis. Perit Dial Int 2015; 35:180-8.
10. Williams JD, Craig KJ, Topley N, Von Ruhland C, Fallon M, Newman GR, et al. Morphologic changes in the peritoneal membrane of patients with renal disease. J Am Soc Nephrol 2002; 13:470-9.
11. Devuyst O, Margetts PJ, Topley N. The pathophysiology of the peritoneal membrane. J Am Soc Nephrol 2010; 21:1077-85.
12. Sawai A, Ito Y, Mizuno M, Suzuki Y, Toda S, Ito I, et al. Peritoneal macrophage infiltration is correlated with baseline peritoneal solute transport rate in peritoneal dialysis patients. Nephrol Dial Transplant 2011; 26:2322-32.
13. Verger C, Luger A, Moore HL, Nolph KD. Acute changes in peritoneal morphology and transport properties with infectious peritonitis and mechanical injury. Kidney Int 1983; 23:823-31.
14. Catalan MP, Esteban J, Subirá D, Egido J, Ortiz A; Grupo de Estudios Peritoneales de Madrid-FRIAT/IRSIN. Inhibition of caspases improves bacterial clearance in experimental peritonitis. Perit Dial Int 2003; 23:123-6.
15. Calame W, Afram C, Blijleven N, Hendrickx RJ, Namavar F, Beelen RH. Establishing an experimental infection model for peritoneal dialysis: effect of inoculum and volume. Perit Dial Int 1993; 13(Suppl 2):S79-80.
16. Welten AG, Zareie M, van den Born J, ter Wee PM, Schalkwijk CG, Driesprong BA, et al. In vitro and in vivo models for peritonitis demonstrate unchanged neutrophil migration after exposure to dialysis fluids. Nephrol Dial Transplant 2004; 19:831-9.

17. van Westrhenen R, Westra WM, van den Born J, Krediet RT, Keuning ED, Hiralall J, et al. Alpha-2-macroglobulin and albumin are useful serum proteins to detect subclinical peritonitis in the rat. Perit Dial Int 2006; 26:101-7.
18. Akman S, Koyun M, Gelen T, Coskun M. Comparison of intraperitoneal antithrombin III and heparin in experimental peritonitis. Pediatr Nephrol 2008; 23:1327-30.
19. Mactier RA, Moore H, Khanna R, Shah J. Effect of peritonitis on insulin and glucose absorption during peritoneal dialysis in diabetic rats. Nephron 1990; 54:240-4.
20. Gallimore B, Gagnon RF, Richards GK. Response of chronic renal failure mice to peritoneal Staphylococcus epidermidis challenge: impact of repeated peritoneal instillation of dialysis solution. Am J Kidney Dis 1989; 14:184-95.
21. Finelli A, Burrows LL, DiCosmo FA, DiTizio V, Sinnadurai S, Oreopoulos DG, et al. Colonization-resistant antimicrobial-coated peritoneal dialysis catheters: evaluation in a newly developed rat model of persistent Pseudomonas aeruginosa peritonitis. Perit Dial Int 2002; 22:27-31.
22. Kretschmar M, Hube B, Bertsch T, Sanglard D, Merker R, Schröder M, et al. Germ tubes and proteinase activity contribute to virulence of Candida albicans in murine peritonitis. Infect Immun 1999; 67:6637-42.
23. Ni J, Moulin P, Gianello P, Feron O, Balligand JL, Devuyst O. Mice that lack endothelial nitric oxide synthase are protected against functional and structural modifications induced by acute peritonitis. J Am Soc Nephrol 2003; 14:3205-16.
24. Combet S, Van Landschoot M, Moulin P, Piech A, Verbavatz JM, Goffin E, et al. Regulation of aquaporin-1 and nitric oxide synthase isoforms in a rat model of acute peritonitis. J Am Soc Nephrol 1999; 10:2185-96.
25. Ferrier ML, Combet S, van Landschoot M, Stoenoiu MS, Cnops Y, Lameire N, et al. Inhibition of nitric oxide synthase reverses changes in peritoneal permeability in a rat model of acute peritonitis. Kidney Int 2001; 60:2343-50.
26. Ni J, Cnops Y, McLoughlin RM, Topley N, Devuyst O. Inhibition of nitric oxide synthase reverses permeability changes in a mouse model of acute peritonitis. Perit Dial Int 2005; 25(Suppl 3):S11-4.
27. Ni J, McLoughlin RM, Brodovitch A, Moulin P, Brouckaert P, Casadei B, et al. Nitric oxide synthase isoforms play distinct roles during acute peritonitis. Nephrol Dial Transplant 2010; 25:86-96.
28. Breborowicz A, Połubinska A, Wu G, Tam P, Oreopoulos DG. N-acetylglucosamine reduces inflammatory response during acute peritonitis in uremic rats. Blood Purif 2006; 24:274-81.
29. Korybalska K, Wieczorowska-Tobis K, Polubinska A, Wisniewska J, Moberly J, Martis L, et al. L-2-oxothiazolidine-4-carboxylate: an agent that modulates lipopolysaccharide-induced peritonitis in rats. Perit Dial Int 2002 ;22:293-300.
30. Kim YL, Kim SH, Kim JH, Kim SJ, Kim CD, Cho DK, et al. Effects of peritoneal rest on peritoneal transport and peritoneal membrane thickening in continuous ambulatory peritoneal dialysis rats. Perit Dial Int 1999; 19(Suppl 2):S384-7.
31. Margetts PJ, Kolb M, Yu L, Hoff CM, Gauldie J. A chronic inflammatory infusion model of peritoneal dialysis in rats. Perit Dial Int 2001; 21(Suppl 3):S368-72.
32. Margetts PJ, Gyorffy S, Kolb M, Yu L, Hoff CM, Holmes CJ, et al. Antiangiogenic and antifibrotic gene therapy in a chronic infusion model of peritoneal dialysis in rats. J Am Soc Nephrol 2002; 13:721-8.

33. Park SH, Lee EG, Kim IS, Kim YJ, Cho DK, Kim YL. Effect of glucose degradation products on the peritoneal membrane in a chronic inflammatory infusion model of peritoneal dialysis in the rat. Perit Dial Int 2004 ;24:115-22.
34. Nie J, Hao W, Dou X, Wang X, Luo N, Lan HY, et al. Effects of Smad7 overexpression on peritoneal inflammation in a rat peritoneal dialysis model. Perit Dial Int 2007; 27:580-8.
35. Song SH, Kwak IS, Yang BY, Lee DW, Lee SB, Lee MY. Role of rosiglitazone in lipopolysaccharide-induced peritonitis: a rat peritoneal dialysis model. Nephrology (Carlton) 2009; 14:155-63.
36. Zhang L, Hao JB, Ren LS, Ding JL, Hao LR. The aldosterone receptor antagonist spironolactone prevents peritoneal inflammation and fibrosis. Lab Invest 2014; 94:839-50.
37. Hurst SM, Wilkinson TS, McLoughlin RM, Jones S, Horiuchi S, Yamamoto N, et al. Il-6 and its soluble receptor orchestrate a temporal switch in the pattern of leukocyte recruitment seen during acute inflammation. Immunity 2001; 14:705-14.
38. Nishimura H, Ito Y, Mizuno M, Tanaka A, Morita Y, Maruyama S, et al. Mineralocorticoid receptor blockade ameliorates peritoneal fibrosis in new rat peritonitis model. Am J Physiol Renal Physiol 2008; 294:F1084-93.
39. Kato H, Mizuno T, Mizuno M, Sawai A, Suzuki Y, Kinashi H, et al. Atrial natriuretic peptide ameliorates peritoneal fibrosis in rat peritonitis model. Nephrol Dial Transplant 2012; 27:526-36.
40. Mizuno M, Ito Y. Rat Models of Acute and/or Chronic Peritoneal Injuries Including Peritoneal Fibrosis and Peritoneal Dialysis Complications. Methods Mol Biol 2016; 1397:35-43.
41. Nessim SJ, Perl J, Bargman JM. The renin-angiotensin-aldosterone system in peritoneal dialysis: is what is good for the kidney also good for the peritoneum? Kidney Int 2010; 78:23-8.
42. Noh H, Ha H, Yu MR, Kim YO, Kim JH, Lee HB. Angiotensin II mediates high glucose-induced TGF-beta1 and fibronectin upregulation in HPMC through reactive oxygen species. Perit Dial Int 2005; 25:38-47.
43. Kiribayashi K, Masaki T, Naito T, Ogawa T, Ito T, Yorioka N, et al. Angiotensin II induces fibronectin expression in human peritoneal mesothelial cells via ERK1/2 and p38 MAPK. Kidney Int 2005; 67:1126-35.
44. Tsuneyoshi H, Nishina T, Nomoto T, Kanemitsu H, Kawakami R, Unimonh O, et al. Atrial natriuretic peptide helps prevent late remodeling after left ventricular aneurysm repair. Circulation 2004; 110(11 Suppl 1):II174-9.
45. Kasama S, Furuya M, Toyama T, Ichikawa S, Kurabayashi M. Effect of atrial natriuretic peptide on left ventricular remodelling in patients with acute myocardial infarction. Eur Heart J 2008; 29:1485-94.
46. Ito T, Yoshimura M, Nakamura S, Nakayama M, Shimasaki Y, Harada E, et al. Inhibitory effect of natriuretic peptides on aldosterone synthase gene expression in cultured neonatal rat cardiocytes. Circulation 2003; 107:807-10.
47. Kasahara M, Mukoyama M, Sugawara A, Makino H, Suganami T, Ogawa Y, et al. Ameliorated glomerular injury in mice overexpressing brain natriuretic peptide with renal ablation. J Am Soc Nephrol 2000; 11:1691-701.
48. Suganami T, Mukoyama M, Sugawara A, Mori K, Nagae T, Kasahara M, et al. Overexpression of brain natriuretic peptide in mice ameliorates immune-mediated renal injury. J Am Soc Nephrol 2001; 12:2652-63.

49. Makino H, Mukoyama M, Mori K, Suganami T, Kasahara M, Yahata K, et al. Transgenic overexpression of brain natriuretic peptide prevents the progression of diabetic nephropathy in mice. Diabetologia 2006; 49:2514-24.
50. Kitakaze M, Asakura M, Kim J, Shintani Y, Asanuma H, Hamasaki T, et al. Human atrial natriuretic peptide and nicorandil as adjuncts to reperfusion treatment for acute myocardial infarction (J-WIND): two randomised trials. Lancet 2007; 370:1483-93.
51. Vazquez-Rangel A, Soto V, Escalona M, Toledo RG, Castillo EA, Polanco Flores NA, et al. Spironolactone to prevent peritoneal fibrosis in peritoneal dialysis patients: a randomized controlled trial. Am J Kidney Dis 2014; 63:1072-4.
52. Kitamura S, Horimoto N, Tsuji K, Inoue A, Takiue K, Sugiyama H, et al. The selection of peritoneal mesothelial cells is important for cell therapy to prevent peritoneal fibrosis. Tissue Eng Part A 2014; 20:529-39.
53. Nagappan R, Collins JF, Lee WT. Fungal peritonitis in continuous ambulatory peritoneal dialysis--the Auckland experience. Am J Kidney Dis 1992; 20:492-6.
54. Wang AY, Yu AW, Li PK, Lam PK, Leung CB, Lai KN, et al. Factors predicting outcome of fungal peritonitis in peritoneal dialysis: analysis of a 9-year experience of fungal peritonitis in a single center. Am J Kidney Dis 2000; 36:1183-92.
55. Felgueiras J, del Peso G, Bajo A, Hevia C, Romero S, Celadilla O, et al. Risk of technique failure and death in fungal peritonitis is determined mainly by duration on peritoneal dialysis: single-center experience of 24 years. Adv Perit Dial 2006; 22:77-81.
56. Li PK, Szeto CC, Piraino B, de Arteaga J, Fan S, Figueiredo AE, et al. ISPD peritonitis recommendations: 2016 Update on prevention and treatment. Perit Dial Int 2016; pdi.2016.00078.
57. Rigby RJ, Hawley CM. Sclerosing peritonitis: the experience in Australia. Nephrol Dial Transplant 1998; 13:154-9.
58. Lee HY, Kim BS, Choi HY, Park HC, Kang SW, Choi KH, et al. Sclerosing encapsulating peritonitis as a complication of long-term continuous ambulatory peritoneal dialysis in Korea. Nephrology (Carlton) 2003; 8(Suppl 1):S33-9.
59. Gupta S, Woodrow G. Successful treatment of fulminant encapsulating peritoneal sclerosis following fungal peritonitis with tamoxifen. Clin Nephrol 2007; 68:125-9.
60. Trigka K, Dousdampanis P, Chu M, Khan S, Ahmad M, Bargman JM, et al. Encapsulating peritoneal sclerosis: a single-center experience and review of the literature. Int Urol Nephrol 2011; 43:519-26.
61. Sorenson WG, Shahan TA, Simpson J. Cell wall preparations from environmental yeasts: effect on alveolar macrophage function in vitro. Ann Agric Environ Med 1998; 5:65-71.
62. Mizuno M, Morgan BP. The possibilities and pitfalls for anti-complement therapies in inflammatory diseases. Curr Drug Targets Inflamm Allergy 2004; 3:87-96.
63. Mizuno M. A review of current knowledge of the complement system and the therapeutic opportunities in inflammatory arthritis. Curr Med Chem 2006; 13:1707-17.
64. Mizuno M, Ito Y, Hepburn N, Mizuno T, Noda Y, Yuzawa Y, et al. Zymosan, but not lipopolysaccharide, triggers severe and progressive peritoneal injury accompanied by complement activation in a rat peritonitis model. J Immunol 2009; 183:1403-12.
65. Mizuno T, Mizuno M, Morgan BP, Noda Y, Yamada K, Okada N, et al. Specific collaboration between rat membrane complement regulators Crry and CD59 protects peritoneum from damage by autologous complement activation. Nephrol Dial Transplant 2011; 26:1821-30.

66. Rawal N, Pangburn MK. C5 convertase of the alternative pathway of complement. Kinetic analysis of the free and surface-bound forms of the enzyme. J Biol Chem 1998; 273:16828-35.
67. Kim H, Mizuno M, Furuhashi K, Katsuno T, Ozaki T, Yasuda K, et al. Rat adipose tissue-derived stem cells attenuate peritoneal injuries in rat zymosan-induced peritonitis accompanied by complement activation. Cytotherapy 2014; 16:357-68.
68. Mizuno M, Ito Y, Mizuno T, Harris CL, Suzuki Y, Okada N, et al. Membrane complement regulators protect against fibrin exudation increases in a severe peritoneal inflammation model in rats. Am J Physiol Renal Physiol 2012; 302:F1245-51.
69. Guo QY, Peng WX, Cheng HH, Ye RG, Lindholm B, Wang T. Hyaluronan preserves peritoneal membrane transport properties. Perit Dial Int 2001; 21:136-42.
70. Wang T, Cheng HH, Liu SM, Wang Y, Wu JL, Peng WX, et al. Increased peritoneal membrane permeability is associated with abnormal peritoneal surface layer. Perit Dial Int 2001; 21(Suppl 3):S345-8.
71. Chunming J, Miao Z, Cheng S, Nana T, Wei Z, Dongwei C, et al. Tanshinone IIA attenuates peritoneal fibrosis through inhibition of fibrogenic growth factors expression in peritoneum in a peritoneal dialysis rat model. Ren Fail 2011; 33:355-62.
72. Lee EA, Oh JH, Lee HA, Kim SI, Park EW, Park KB, et al. Structural and functional alterations of the peritoneum after prolonged exposure to dialysis solutions: role of aminoguanidine. Perit Dial Int 2001; 21:245-53.
73. Musi B, Braide M, Carlsson O, Wieslander A, Albrektsson A, Ketteler M, et al. Biocompatibility of peritoneal dialysis fluids: long-term exposure of nonuremic rats. Perit Dial Int 2004; 24:37-47.
74. Flessner MF, Credit K, Richardson K, Potter R, Li X, He Z, et al. Peritoneal inflammation after twenty-week exposure to dialysis solution: effect of solution versus catheter-foreign body reaction. Perit Dial Int 2010; 30:284-93.
75. Zeltzer E, Klein O, Rashid G, Katz D, Korzets Z, Bernheim J. Intraperitoneal infusion of glucose-based dialysate in the rat--an animal model for the study of peritoneal advanced glycation end-products formation and effect on peritoneal transport. Perit Dial Int 2000; 20:656-61.
76. Nakao A, Nakao K, Takatori Y, Kojo S, Inoue J, Akagi S, et al. Effects of icodextrin peritoneal dialysis solution on the peritoneal membrane in the STZ-induced diabetic rat model with partial nephrectomy. Nephrol Dial Transplant 2010; 25:1479-88.
77. Kihm LP, Müller-Krebs S, Klein J, Ehrlich G, Mertes L, Gross ML, et al. Benfotiamine protects against peritoneal and kidney damage in peritoneal dialysis. J Am Soc Nephrol 2011; 22:914-26.
78. Wang J, Jiang ZP, Su N, Fan JJ, Ruan YP, Peng WX, et al. The role of peritoneal alternatively activated macrophages in the process of peritoneal fibrosis related to peritoneal dialysis. Int J Mol Sci 2013; 14:10369-82.
79. Duan WJ, Yu X, Huang XR, Yu JW, Lan HY. Opposing roles for Smad2 and Smad3 in peritoneal fibrosis in vivo and in vitro. Am J Pathol 2014; 184:2275-84.
80. Yu JW, Duan WJ, Huang XR, Meng XM, Yu XQ, Lan HY. MicroRNA-29b inhibits peritoneal fibrosis in a mouse model of peritoneal dialysis. Lab Invest 2014; 94:978-90.
81. Aroeira LS, Lara-Pezzi E, Loureiro J, Aguilera A, Ramírez-Huesca M, González-Mateo G, et al. Cyclooxygenase-2 mediates dialysate-induced alterations of the peritoneal membrane. J Am Soc Nephrol 2009; 20:582-92.

82. Loureiro J, Aguilera A, Selgas R, Sandoval P, Albar-Vizcaíno P, Pérez-Lozano ML, et al. Blocking TGF-β1 protects the peritoneal membrane from dialysate-induced damage. J Am Soc Nephrol 2011; 22:1682-95.
83. Loureiro J, Sandoval P, del Peso G, Gónzalez-Mateo G, Fernández-Millara V, Santamaria B, et al. Tamoxifen ameliorates peritoneal membrane damage by blocking mesothelial to mesenchymal transition in peritoneal dialysis. PLoS One 2013; 8:e61165.
84. Suga H, Teraoka S, Ota K, Komemushi S, Furutani S, Yamauchi S, et al. Preventive effect of pirfenidone against experimental sclerosing peritonitis in rats. Exp Toxicol Pathol 1995; 47:287-91.
85. Mishima Y, Miyazaki M, Abe K, Ozono Y, Shioshita K, Xia Z, et al. Enhanced expression of heat shock protein 47 in rat model of peritoneal fibrosis. Perit Dial Int 2003; 23:14-22.
86. Nishino T, Miyazaki M, Abe K, Furusu A, Mishima Y, Harada T, et al. Antisense oligonucleotides against collagen-binding stress protein HSP47 suppress peritoneal fibrosis in rats. Kidney Int 2003; 64:887-96.
87. Io H, Hamada C, Ro Y, Ito Y, Hirahara I, Tomino Y. Morphologic changes of peritoneum and expression of VEGF in encapsulated peritoneal sclerosis rat models. Kidney Int 2004; 65:1927-36.
88. Bozkurt D, Hur E, Ulkuden B, Sezak M, Nar H, Purclutepe O, et al. Can N-acetylcysteine preserve peritoneal function and morphology in encapsulating peritoneal sclerosis? Perit Dial Int 2009; 29(Suppl 2):S202-5.
89. Bozkurt D, Sipahi S, Cetin P, Hur E, Ozdemir O, Ertilav M, et al. Does immunosuppressive treatment ameliorate morphology changes in encapsulating peritoneal sclerosis? Perit Dial Int 2009; 29(Suppl 2):S206-10.
90. Ertilav M, Hur E, Bozkurt D, Sipahi S, Timur O, Sarsik B, et al. Octreotide lessens peritoneal injury in experimental encapsulated peritoneal sclerosis model. Nephrology (Carlton) 2011; 16:552-7.
91. Huddam B, Başaran M, Koçak G, Azak A, Yalçın F, Reyhan NH, et al. The use of mycophenolate mofetil in experimental encapsulating peritoneal sclerosis. Int Urol Nephrol 2015; 47:1423-8.
92. Komatsu H, Uchiyama K, Tsuchida M, Isoyama N, Matsumura M, Hara T, et al. Development of a peritoneal sclerosis rat model using a continuous-infusion pump. Perit Dial Int 2008; 28:641-7.
93. Kanda R, Hamada C, Kaneko K, Nakano T, Wakabayashi K, Hara K, et al. Paracrine effects of transplanted mesothelial cells isolated from temperature-sensitive SV40 large T-antigen gene transgenic rats during peritoneal repair. Nephrol Dial Transplant 2014; 29:289-300.
94. Wakabayashi K, Hamada C, Kanda R, Nakano T, Io H, Horikoshi S, et al. Adipose-derived mesenchymal stem cells transplantation facilitate experimental peritoneal fibrosis repair by suppressing epithelial-mesenchymal transition. J Nephrol 2014; 27:507-14.
95. Saito H, Kitamoto M, Kato K, Liu N, Kitamura H, Uemura K, et al. Tissue factor and factor v involvement in rat peritoneal fibrosis. Perit Dial Int 2009; 29:340-51.
96. Kinashi H, Ito Y, Mizuno M, Suzuki Y, Terabayashi T, Nagura F, et al. TGF-β1 promotes lymphangiogenesis during peritoneal fibrosis. J Am Soc Nephrol 2013; 24:1627-42.
97. Ishii Y, Sawada T, Shimizu A, Tojimbara T, Nakajima I, Fuchinoue S, et al. An experimental sclerosing encapsulating peritonitis model in mice. Nephrol Dial Transplant 2001; 16:1262-6.

98. Sawada T, Ishii Y, Tojimbara T, Nakajima I, Fuchinoue S, Teraoka S. The ACE inhibitor, quinapril, ameliorates peritoneal fibrosis in an encapsulating peritoneal sclerosis model in mice. Pharmacol Res 2002; 46:505-10.
99. Tanabe K, Maeshima Y, Ichinose K, Kitayama H, Takazawa Y, Hirokoshi K, et al. Endostatin peptide, an inhibitor of angiogenesis, prevents the progression of peritoneal sclerosis in a mouse experimental model. Kidney Int 2007; 71:227-38.
100. Fukuoka N, Sugiyama H, Inoue T, Kikumoto Y, Takiue K, Morinaga H, et al. Increased susceptibility to oxidant-mediated tissue injury and peritoneal fibrosis in acatalasemic mice. Am J Nephrol 2008; 28:661-8.
101. Yoshio Y, Miyazaki M, Abe K, Nishino T, Furusu A, Mizuta Y, et al. TNP-470, an angiogenesis inhibitor, suppresses the progression of peritoneal fibrosis in mouse experimental model. Kidney Int 2004; 66:1677-85.
102. Nakav S, Kachko L, Vorobiov M, Rogachev B, Chaimovitz C, Zlotnik M, et al. Blocking adenosine A2A receptor reduces peritoneal fibrosis in two independent experimental models. Nephrol Dial Transplant 2009; 24:2392-9.
103. Kokubo S, Sakai N, Furuichi K, Toyama T, Kitajima S, Okumura T, et al. Activation of p38 mitogen-activated protein kinase promotes peritoneal fibrosis by regulating fibrocytes. Perit Dial Int 2012; 32:10-9.
104. Yokoi H, Kasahara M, Mori K, Ogawa Y, Kuwabara T, Imamaki H, et al. Pleiotrophin triggers inflammation and increased peritoneal permeability leading to peritoneal fibrosis. Kidney Int 2012; 81:160-9.
105. Nishino T, Ashida R, Obata Y, Furusu A, Abe K, Miyazaki M, et al. Involvement of lymphocyte infiltration in the progression of mouse peritoneal fibrosis model. Ren Fail 2012; 34:760-6.
106. Sekiguchi Y, Hamada C, Ro Y, Nakamoto H, Inaba M, Shimaoka T, et al. Differentiation of bone marrow-derived cells into regenerated mesothelial cells in peritoneal remodeling using a peritoneal fibrosis mouse model. J Artif Organs 2012; 15:272-82.
107. Hirose M, Nishino T, Obata Y, Nakazawa M, Nakazawa Y, Furusu A, et al. 22-Oxacalcitriol prevents progression of peritoneal fibrosis in a mouse model. Perit Dial Int 2013; 33:132-42.
108. Yokoi H, Kasahara M, Mori K, Kuwabara T, Toda N, Yamada R, et al. Peritoneal fibrosis and high transport are induced in mildly pre-injured peritoneum by 3,4-dideoxyglucosone-3-ene in mice. Perit Dial Int 2013; 33:143-54.
109. Hirahara I, Kusano E, Yanagiba S, Miyata Y, Ando Y, Muto S, et al. Peritoneal injury by methylglyoxal in peritoneal dialysis. Perit Dial Int 2006; 26:380-92.
110. Hirahara I, Ishibashi Y, Kaname S, Kusano E, Fujita T. Methylglyoxal induces peritoneal thickening by mesenchymal-like mesothelial cells in rats. Nephrol Dial Transplant 2009; 24:437-47.
111. Hirahara I, Sato H, Imai T, Onishi A, Morishita Y, Muto S, et al. Methylglyoxal Induced Basophilic Spindle Cells with Podoplanin at the Surface of Peritoneum in Rat Peritoneal Dialysis Model. Biomed Res Int 2015:289751.
112. Onishi A, Akimoto T, Morishita Y, Hirahara I, Inoue M, Kusano E, et al. Peritoneal fibrosis induced by intraperitoneal methylglyoxal injection: the role of concurrent renal dysfunction. Am J Nephrol 2014; 40:381-90.
113. Kitamura M, Nishino T, Obata Y, Furusu A, Hishikawa Y, Koji T, et al. Epigallocatechin gallate suppresses peritoneal fibrosis in mice. Chem Biol Interact 2012; 195:95-104.

114. Terabayashi T, Ito Y, Mizuno M, Suzuki Y, Kinashi H, Sakata F, et al. Vascular endothelial growth factor receptor-3 is a novel target to improve net ultrafiltration in methylglyoxal-induced peritoneal injury. Lab Invest 2015; 95:1029-43.
115. Liu L, Shi CX, Ghayur A, Zhang C, Su JY, Hoff CM, et al. Prolonged peritoneal gene expression using a helper-dependent adenovirus. Perit Dial Int 2009; 29:508-16.
116. Patel P, Sekiguchi Y, Oh KH, Patterson SE, Kolb MR, Margetts PJ. Smad3-dependent and -independent pathways are involved in peritoneal membrane injury. Kidney Int 2010; 77:319-28.
117. Margetts PJ, Hoff C, Liu L, Korstanje R, Walkin L, Summers A, et al. Transforming growth factor β-induced peritoneal fibrosis is mouse strain dependent. Nephrol Dial Transplant 2013; 28:2015-27.
118. Padwal M, Siddique I, Wu L, Tang K, Boivin F, Liu L, et al. Matrix metalloproteinase 9 is associated with peritoneal membrane solute transport and induces angiogenesis through β-catenin signaling. Nephrol Dial Transplant 2016; doi: 10.1093/ndt/qfw076.
119. Margetts PJ, Kolb M, Galt T, Hoff CM, Shockley TR, Gauldie J. Gene transfer of transforming growth factor-beta1 to the rat peritoneum: effects on membrane function. J Am Soc Nephrol 2001; 12:2029-39.
120. Margetts PJ, Bonniaud P, Liu L, Hoff CM, Holmes CJ, West-Mays JA, et al. Transient overexpression of TGF-β1 induces epithelial mesenchymal transition in the rodent peritoneum. J Am Soc Nephrol 2005; 16:425-36.
121. Gotloib L, Wajsbrot V, Cuperman Y, Shostak A. Acute oxidative stress induces peritoneal hyperpermeability, mesothelial loss, and fibrosis. J Lab Clin Med 2004; 143:31-40.
122. Levine S, Saltzman A. Abdominal cocoon: an animal model for a complication of peritoneal dialysis. Perit Dial Int 1996; 16:613-6.
123. Nakamoto H, Imai H, Ishida Y, Yamanouchi Y, Inoue T, Okada H, et al. New animal models for encapsulating peritoneal sclerosis--role of acidic solution. Perit Dial Int 2001; 21(Suppl 3):S349-53.

Representative animal models		Methods	species	experimental period	peritoneal dysfunction	neoangio-genesis	fibrosis	EPS	References
Peritonitis model	Bacteria	Staphylococcus aureus	mouse	2 days	no report	no report	no report	-	(14)
			rat	2 weeks	no report	no report	±	-	(15-18)
		Staphylococcus epidermidi	mouse	2 weeks	no report	no report	no report	-	(20)
		Pseudomonas aeruginosa	rat	1 week	no report	no report	no report	-	(21)
	Fungus	Candida albicans	mouse	1 day	no report	no report	no report	-	(22)
	Performance without aseptic precautions		mouse	1 week	+	+	no report	-	(23)
			rat	1 week	+	+	no report	-	(23-25)
Non-bacterial model		LPS	mouse	1 day	+	no report	no report	-	(26,27)
			rat	1 day	+	no report	no report	-	(28,29)
		PDF with LPS	rat	3-6 weeks	+	+	+	-	(29-36)
		SES	mouse	2 days	no report	no report	no report	-	(11,37)
		Scraping	rat	2 weeks	+	+	+	-	(38,39)
		Zymosan with scraping	rat	5 weeks	no report	+	+	±	(64,67)
		PDF	mouse	4-5 weeks	+	+	+	-	(78-83)
			rat	1-20 weeks	+	+	+	-	(69-77)
		Chlorhexidine	mouse	1-8 weeks	+	+	+	+	(97-108)
			rat	1-8 weeks	+	+	+	+	(84-96)
		Methylglyoxal	mouse	3-7 weeks	+	+	+	+	(113,114)
			rat	3 weeks	+	+	+	+	(109-112)
		TGF-β1	mouse	1-10 weeks	no report	+	+	+	(115-118)
			rat	1-4 weeks	+	+	+	-	(119,120)

Table 1. Summary of representative rodent models used to study peritoneal dialysis and its associated complications.

LPS = lipopolysaccharide; PDF = peritoneal dialysis fluid; SES = a lyophilized cell-free supernatant; TGF-β1 = transforming growth factor-β1; EPS = encapsulating peritoneal sclerosis.

Figures

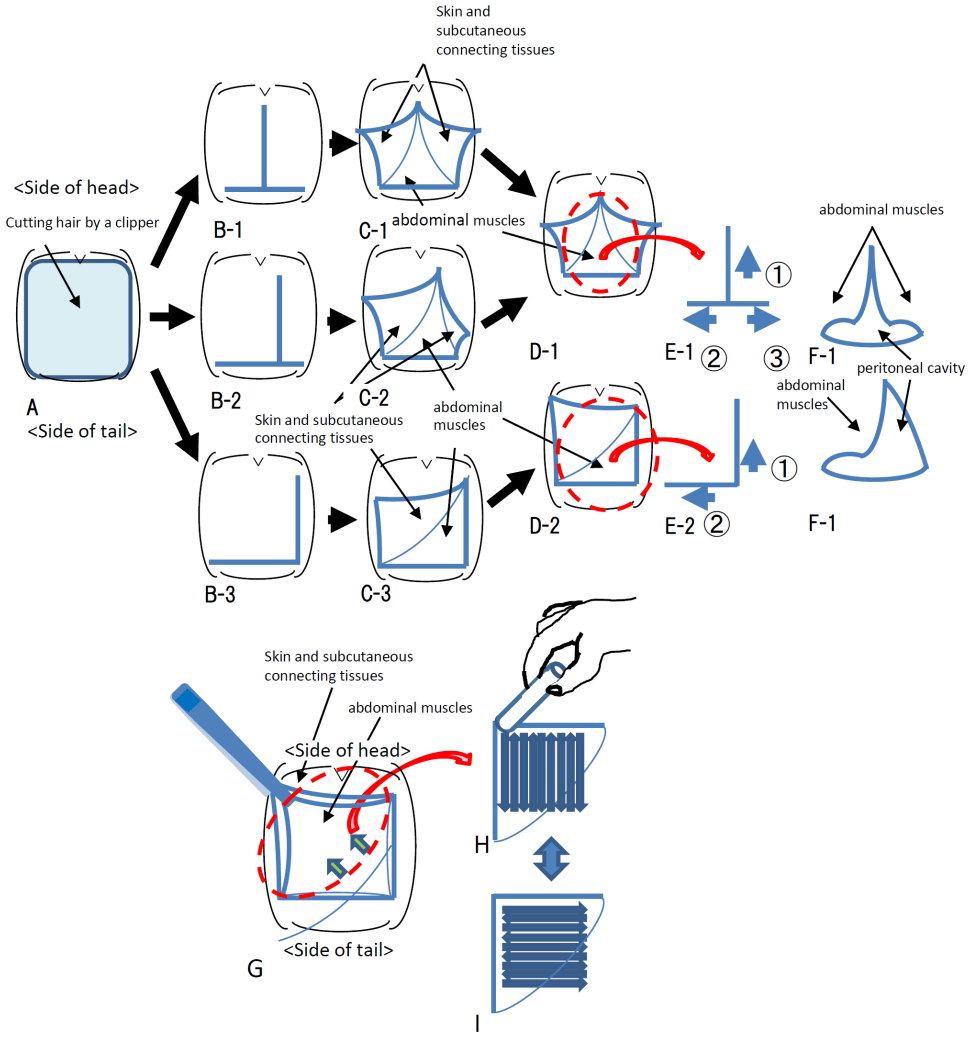

Figure 1. Procedures to generate scraping model. Used by permission from Methods Mol Biol [Ref. 40].

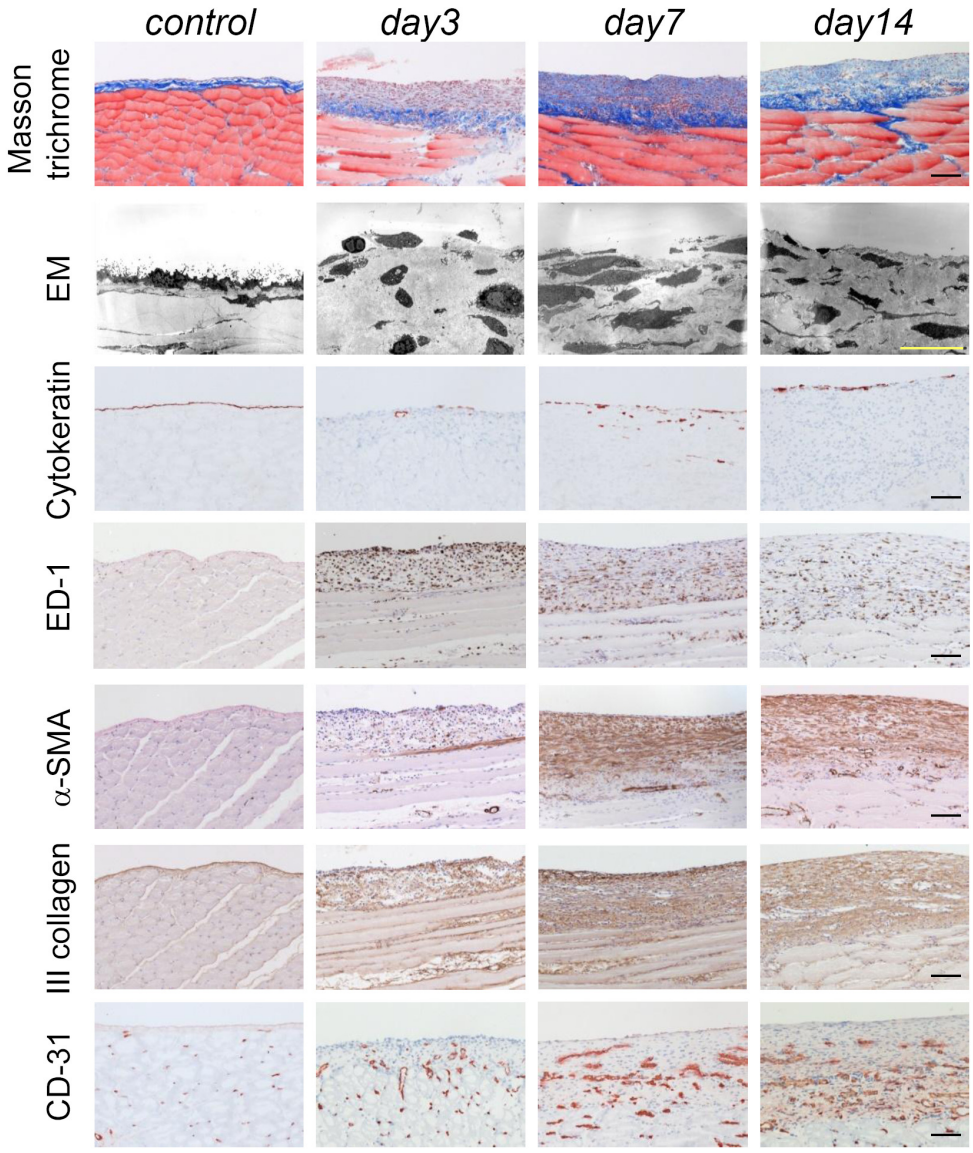

Figure 2. Pathological findings of rat scraping model. Used by permission from Am J Physiology [Ref. 38].

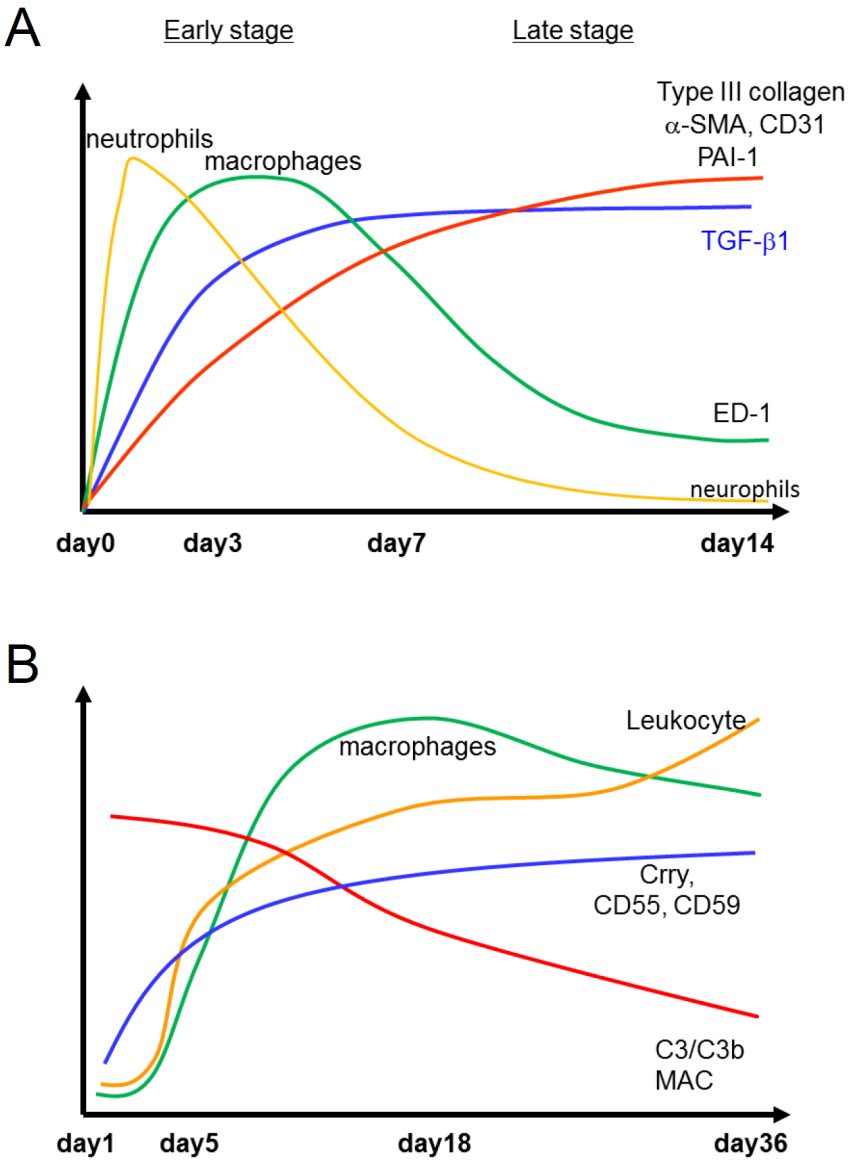

Figure 3. Time course of rat scrape model (A) and zymosan induced fungal peritonitis model (B).

3

TGF-β1 promotes lymphangiogenesis during peritoneal fibrosis

J Am Soc Nephrol. 2013;24(10):1627-42

Hiroshi Kinashi[1], Yasuhiko Ito[1], Masashi Mizuno[1], Yasuhiro Suzuki[1], Takeshi Terabayashi[1], Fumiko Nagura[1], Ryohei Hattori[2], Yoshihisa Matsukawa[2], Tomohiro Mizuno[4], Yukihiro Noda[4], Hayato Nishimura[5], Ryosuke Nishio[6], Shoichi Maruyama[1], Enyu Imai[1], Seiichi Matsuo[1], and Yoshifumi Takei[3]

[1]Departments of Nephrology and Renal Replacement Therapy, [2]Urology, and [3]Biochemistry, Nagoya University Graduate School of Medicine, Nagoya, Japan
[4]Division of Clinical Sciences and Neuropsychopharmacology, Meijyo University Graduate School of Medicine, Nagoya, Japan
[5]Department of Nephrology, Toyota Kosei Hospital, Toyota, Japan
[6]Department of Emergency Medicine, Kyoto University Hospital, Kyoto, Japan

ABSTRACT

Peritoneal fibrosis (PF) causes ultrafiltration failure (UFF) and is an important complication in long-term peritoneal dialysis (PD). We studied the roles of lymphangiogenesis and of vascular endothelial growth factor-C (VEGF-C), a potentially important mediator of lymphangiogenesis, in the relationship between PF and UFF using human dialysate effluents (n=130), human peritoneal tissues (n=75), human peritoneal mesothelial cells obtained from spent patient peritoneal dialysates (HPMC, n=29), and a PF model created by intraperitoneal injection of chlorhexidine gluconate (CG). The dialysate-to-plasma ratio of creatinine (D/P Cr), which is a measure of peritoneal transport, was positively correlated with dialysate VEGF-C concentration ($p<0.001$). Dialysate VEGF-C concentration also correlated with dialysate transforming growth factor-β (TGF-β1) concentration ($p<0.001$). The mRNA levels of VEGF-C, lymphatic endothelial hyaluronan receptor-1 (LYVE-1) and podoplanin were significantly higher in the peritoneal membranes of UFF patients than in those of patients without UFF. Lymphatic vessels increased in peritoneum with advanced fibrosis and VEGF-C was detected in the mesothelial cells and macrophages. VEGF-C expression was upregulated by TGF-β1 in cultured mesothelial cells and this upregulation was specifically suppressed by a TGF-β type I receptor (TGFβR-I) inhibitor. TGF-β1 also upregulated VEGF-C mRNA expression in cultured HPMC and this increased VEGF-C mRNA correlated with the D/P Cr of the patient from which the HPMC was derived ($p<0.001$). In the rat CG model, an increase in lymphatic vessels and VEGF-C expression was associated with fibrosis, and was significantly suppressed by TGFβR-I inhibitor treatment. These results suggest that lymphangiogenesis is associated with fibrosis via the TGF-β-VEGF-C pathway.

INTRODUCTION

The decrease in ultrafiltration capacity that is associated with the high peritoneal solute transport that is observed after prolonged peritoneal dialysis (PD) treatment is a major reason for its discontinuation[1-4]. Several studies have shown that a higher peritoneal solute transport rate is associated with reduced survival of PD patients[1, 2, 5]. The characteristic features of chronic peritoneal damage in PD treatment are associated with submesothelial fibrosis and neoangiogenesis[6, 7]. Analyses of the surface peritoneum showed no significant changes in vessel density with duration of PD[6, 8]. In addition, the vessel density in patients with ultrafiltration failure (UFF) was significantly higher than that in normal individuals or in non-PD patients, but was not higher than that in patients undergoing PD[6]. These findings suggest that factors other than increased vascular density may be involved in disease states associated with increased transport of peritoneal membranes. In addition, the relationship between peritoneal fibrosis and UFF remains obscure.

Blood capillaries have a continuous basal lamina with tight inter-endothelial junctions, and are supported by pericytes and smooth muscle cells. In contrast, lymphatic capillaries are thin-walled with a wide lumen, and do not contain pericytes or basement membrane. The structures of lymphatic vessels are suitable for the removal of tissue fluid, cells and macromolecules from the interstitium[9-11]. If lymphangiogenesis develops in the peritoneal membrane, absorption of the PD fluid could be increased and lead to UFF. An increase in the number of lymphatic vessels has recently been reported in several disease conditions including tumor metastasis[12-15], chronic respiratory inflammatory diseases[16-18], wound healing[19] and renal transplant rejection[20, 21]. We recently reported that lymphangiogenesis had developed in tubulo-interstitial fibrosis of human renal biopsy specimens[22] and we also reported the mechanisms of lymphangiogenesis in rat unilateral ureteral obstruction models[23].

The lymphatic absorption rate, which is measured by the rate at which intraperitoneally administered radioactive serum albumin or macromolecule dextran 70 disappears, is significantly higher in patients with UFF, and lymphatic reabsorption is considered to be one of the causes of UFF[24-27]. However, the results from these clinical approaches have been controversial[28, 29]. In addition, little is known about the pathology and the process of lymphangiogenesis in patients with UFF and peritonitis.

In this study, we investigated lymphangiogenesis and the expression of vascular endothelial growth factor-C (VEGF-C), which is a potentially important mediator of lymphangiogenesis, in human peritoneal tissues, peritoneal dialysis effluent and peritoneal mesothelial cells. We also explored VEGF-C induction by transforming growth factor-β1 (TGF-β1) in the human mesothelial cell line (Met-5A) and in cultured human peritoneal mesothelial cells (HPMC) from the spent PD effluent of patients with varying rates of peritoneal transport. Finally, we explored the relationship between peritoneal fibrosis and lymphangiogenesis in rats that were administered chlorhexidine gluconate (CG) into the abdominal cavity, which provide a model of chemically induced peritoneal inflammation-

fibrosis[30-32]. This is the first report to show that lymphangiogenesis is linked to the peritoneal fibrosis that is often associated with a high peritoneal transport rate.

RESULTS

VEGF-C Concentration in the Peritoneal Effluent Correlated with the Peritoneal Transport Rate

We found a positive correlation between VEGF-C concentration in the PD effluent of 4 h-dwelled samples and D/P Cr ($R = 0.663$, $P < 0.001$, Fig. 1A). We also measured dialysate TGF-β1 levels. There was a positive correlation between VEGF-C and TGF-β1 concentration in the PD effluent of 4 h-dwelled samples ($R = 0.772$, $P < 0.001$, Fig. 1B). We further assessed VEGF-C concentration in the overnight-dwelled peritoneal dialysis effluent of 83 patients; there was a positive correlation between the dialysate VEGF-C concentration and the D/P Cr ratio ($R = 0.417$, $P < 0.001$, Fig. 1C).

VEGF-C, Lymphatic Endothelial Hyaluronan Receptor-1 (LYVE-1), and Podoplanin mRNA Expression was Correlated with Peritoneal Thickness in Human Peritoneal Biopsy Samples

We next investigated the mRNA expression of lymphatic markers (LYVE-1 and podoplanin) and VEGF-C in the peritoneal membrane of human biopsy samples (Table 1). The peritoneal membrane in the pre-dialysis uremia group (160.0 ± 51.8 μm) was thicker than that in living kidney donors with normal renal function (82.0 ± 22.9 μm). The peritoneum from patients with UFF and peritonitis conditions (referred to hereafter as UFF-peritoneum and peritonitis-peritoneum) was extremely thick (295.2 ± 125.5 and 311.2 ± 169.6 μm, respectively). The mRNA expression of VEGF-C, LYVE-1, and podoplanin was significantly higher in the UFF-peritoneum than in the membranes of peritoneum from patients with normal renal function, with pre-dialysis uremia or from patients undergoing PD without UFF (Fig. 2A-C). There were correlations between VEGF-C, LYVE-1 and podoplanin mRNA expression and the thickness of the submesothelial compact zone of peritoneal membranes in all patients other than in peritonitis patients (Fig. 2D-F). Cases with peritonitis were excluded from this analysis because, as described previously, peritoneum can be thickened by acute inflammatory changes with edema[33]. Moreover, there were positive correlations between VEGF-C, LYVE-1 and podoplanin mRNA expression in peritoneal membranes (Fig. 2G-I).

Lymphatic Vessels and VEGF-C Expression Increased in UFF-human Peritoneum Analyzed by Immunohistochemistry (IHC)

We evaluated lymphatic vessels, blood vessels and the expression of VEGF-C in both UFF and pre-dialysis peritoneum by IHC. LYVE-1-positive lymphatic vessels, Pathologische Anatomie Leiden-Endothelium (PAL-E)-positive blood vessels and VEGF-C expression were widely observed in UFF-peritoneum, but, in contrast, were barely detected in pre-dialysis-peritoneum (Supplementary Fig. 1). VEGF-C was expressed in cytokeratin-

positive mesothelial cells and in CD68-positive macrophages and its expression was enhanced in UFF- and peritonitis-peritoneal membranes (Fig. 3). These findings are consistent with the quantitative PCR data (Fig. 2).

TGF-β1 Induced Upregulation of VEGF-C in Cultured Met-5A Mesothelial Cell Line and HPMCs

The time course of VEGF-C expression in response to TGF-β1 treatment was studied in both HPMC and Met-5A cells. Samples were taken after 3, 6, 12 and 24 h of exposure to TGF-β1 (5 ng/ml). In the Met-5A cells, VEGF-C protein was secreted into the culture supernatants under serum-free conditions without TGF-β1 incubation. The amount of VEGF-C protein secreted was significantly increased by TGF-β1 incubation for 6 ($P < 0.05$), 12 and 24 h ($P < 0.001$, Fig. 4A). VEGF-C mRNA induction by TGF-β1 also increased over time and peaked at 12 h (Fig. 4B). Both VEGF-C protein and mRNA induction by TGF-β1 in Met-5A cells were suppressed by a TGF-β type I receptor inhibitor (TGFβR-I inhibitor, LY364947) in a dose-dependent manner (Fig. 4C, D). Incubation of HPMC derived from 29 patients with variable peritoneal membrane transport (Table 2) with TGF-β1 increased VEGF-C protein and mRNA expression (Fig. 5A, B). VEGF-C mRNA expression peaked at 12 h in 8 of the HPMC, and at 24 h in 21 of the HPMC. Peak values for VEGF-C mRNA at 12 h or 24 h in all 29 HPMCs showed a correlation with the D/P Cr values of the patients from which they were derived ($R = 0.610$, $P < 0.001$, Fig. 5C). No significant correlation was found between the extent of the TGF-β1-induced increase in VEGF-C mRNA in the HPMC and the duration of PD treatment of the patients from which the HPMC were derived (Fig. 5D).

Lymphangiogenesis Developed in a Rat CG Model of Peritoneal Fibrosis

Immunohistochemical analysis indicated that the expression of LYVE-1-positive lymphatic vessels, whose pattern of expression is similar to that of podoplanin-positive vessels, was increased in both the parietal peritoneum and the diaphragm of CG models compared with controls (Fig. 6, Fig. 7A). Furthermore, lymphangiogenesis was more pronounced in the diaphragm than in the parietal peritoneal wall (Fig. 6A-D). TGF-β1, VEGF-C, LYVE-1 and VEGF receptor-3 (VEGFR-3) mRNA expression were also increased in both the parietal peritoneum and diaphragm in the CG model compared to controls (Fig. 6). VEGFR-3 expression, which was detected in the lymphatics, was also high in the CG model, especially in the diaphragm (Fig. 6, Supplementary Fig. 2). Double staining indicated that VEGF-C was expressed by cytokeratin-positive mesothelial cells and by ED-1-positive macrophages (Fig. 7).

TGF-β Type I Receptor Inhibitor Treatment Suppressed Lymphangiogenesis in the CG Model

We investigated the effects of a TGFβR-I inhibitor in the rat CG model (Fig. 8-10). Analysis of the parietal peritoneum indicated that the thickness of the peritoneum was

significantly reduced by TGFβR-I inhibitor treatment. Quantitative immunohistochemical assessment showed that α-smooth muscle actin (α-SMA) expression, Type III collagen deposition and the number of ED-1-positive macrophages were suppressed by TGFβR-I inhibitor treatment (Fig. 8, 9). In addition, VEGF-C expression and LYVE-1 positive areas were significantly suppressed by TGFβR-I inhibitor treatment (Fig. 8, 9). Upregulation of Type III collagen, VEGF-C, LYVE-1 and podoplanin mRNA was significantly inhibited by TGFβR-I inhibitor ($P < 0.05$, Fig. 10). Moreover, diaphragm thickness ($P < 0.01$) as well as the number of LYVE-1 positive areas ($P < 0.05$), and VEGF-C ($P < 0.001$) and LYVE-1 ($P < 0.05$) mRNA expression in the diaphragm, were all significantly suppressed by TGFβR-I inhibitor treatment (Supplementary Fig. 3).

Function of Lymphatic Vessels

We analyzed lymphatic vessel function using the modified method of lymphangiography as described previously[34]. We detected passage of fluorescein isothiocyanate (FITC)-dextran (molecular weight 2,000,000), which can only be absorbed through the lymphatic vessels in the diaphragm, by immunofluorescence microscopy (Fig. 11A) and detected positive levels of FITC in the serum, which were especially high in the rats without treatment in the CG model (Fig. 11D). The presence of FITC levels in the blood and analysis of microscopic findings including serial sections (Supplementary Fig. 4D, 5) indicated that FITC-dextran was absorbed via the lymphatic vessels and drained into the venous circulation via the lymphatic and thoracic duct. Passage through the parietal lymphatic vessels was not prominent in the parietal peritoneum in the CG rats (Supplementary Fig. 6). Inhibition of lymphangiogenesis by celecoxib[35, 36] reduced the serum FITC-dextran levels, suggesting the reduction of the absorption volume.

DISCUSSION

Ultrafiltration dysfunction often results from a combination of increased vascular surface area and decreased osmotic conductance[37, 38]. Dysfunction of the water channel aquaporine-1 (so-called ultrasmall pore[39, 40]) is an important cause of UFF, in that this water channel alters osmotic conductance. Hypopermeable peritoneum with a loss of peritoneal surface area is a rare cause of UFF. Lymphatic absorption was reported to be important in patients on short-term PD with UFF[38]. However, little is known about the pathology, process and mechanisms of lymphangiogenesis in patients with UFF and peritonitis.

In the present study, we first found that the VEGF-C content in the PD effluent of 4 h-dwelled samples and overnight-dwelled samples correlated with the peritoneal membrane transport rate. Our data are consistent with the recent report by Yang et al. that VEGF-C could possibly be a biomarker for UFF[41], although, unlike our study, they did not investigate lymphangiogenesis. Our studies of human peritoneal membranes showed that VEGF-C, LYVE-1 and podoplanin mRNA expression were higher in UFF-peritoneum than in control membranes and that the expression level of VEGF-C and the number of lymphatic vessels correlated with one another. These findings suggest that

lymphangiogenesis develops in patients with a high peritoneal transport rate. Markers of lymphatics, as well as VEGF-C mRNA levels, tended to be increased in the state of peritonitis, which is an important factor for the induction of peritoneal damage and fibrosis (Fig. 2). The extent of lymphangiogenesis may be related to the duration of infection and inflammation, which may also be the case in acute and chronic tubulo-interstitial nephritis[22]. Thus, we reported that lymphangiogenesis developed in chronic, but not in acute tubulo-interstitial nephritis, which indicates that the duration of inflammation together with fibrotic process may be important for lymphangiogenesis[22]. We propose that lymphangiogenesis is linked with the fibrotic process in the peritoneal membrane as it is in other disorders including renal fibrosis[22, 23, 42] and lung fibrosis[18]. Our experiments clearly demonstrated that TGF-β1 functions as an inducer of lymphatic growth in peritoneum as well as of inflammatory cytokines[16, 17, 43-46]. Lymphangiogenic induction by TGF-β1 may be one of the key mechanisms of the UFF that is associated with peritoneal fibrosis.

Using immunohistochemical and cell culture studies we clearly showed that mesothelial cells and macrophages expressed VEGF-C, which indicates that these cells are at least the sources of growth factors for lymphangiogenesis in the peritoneum (Fig. 3-4, 7). VEGF-C was induced by TGF-β1 in HPMCs and in a cultured mesothelial cell line; the latter induction was suppressed by the TGFβR-I inhibitor in a dose-dependent manner. In addition, we recently demonstrated that TGF-β induces VEGF-C production by macrophages[23]. These findings suggest that TGF-β1 is an important inducer of VEGF-C, leading to the lymphangiogenesis that is associated with peritoneal fibrosis in PD patients. Interestingly, TGF-β1-induced VEGF-C expression in mesothelial cells was enhanced in the mesothelial cells obtained from patients with a high peritoneal transport rate. We recently reported that connective tissue growth factor (CTGF) induction by TGF-β was higher in HPMC derived from patients with high peritoneal transport[33]. In these previous experiments, we confirmed that there was no difference in the level of TGF-β type II receptor expression on HPMC of patients with high peritoneal transport compared to those with low peritoneal transport[33] and that an imbalance of TGF-β signaling altered CTGF and bone morphogenic protein-4 expression[33]. Similar to the previous study, VEGF-C induction was also enhanced in HPMC of patients with a higher peritoneal transport rate, which suggests that the function of HPMC from patients with higher peritoneal transport rates had changed[33]. In contrast, VEGF-C is not upregulated by TGF-β1 in fibroblasts, despite the presence of basal VEGF-C expression[23]. TGF-β1 in the peritoneal dialysate was reported to be elevated in the PD effluent and to correlate with D/P Cr[47], which we confirmed in our cohort ($R=0.487$, $P<0.01$, Supplementary Fig. 7). Furthermore, we found a significant correlation between the content of TGF-β1 and VEGF-C in the PD effluent (Fig. 1B), which was consistent with the observed relationship between peritoneal thickness and the expression of VEGF-C and lymphatic vessels (Fig. 2). There are several mechanisms by which TGF-β levels can be increased in dialysate[48-51]. In this regard, prevention of TGF-β induction may reduce fibrosis and lymphangiogenesis resulting in the prevention of peritoneal membrane failure.

In the normal abdominal cavity, lymphatics in the diaphragm form a specialized system that drains fluid from the peritoneal cavity and returns it to the vascular system[52]. The net ultrafiltration volume at the end of a PD exchange equals the cumulative net transcapillary water transport minus lymphatic absorption during the exchange[53]. We demonstrated that lymphatic vessels are present in both the peritoneal and the pleural sides of the normal rat diaphragm, but are rarely detectable in the normal rat parietal peritoneum (Fig. 6). Interestingly, LYVE-1 and VEGFR-3 mRNA levels were higher in the diaphragm than in the parietal peritoneal wall. In the CG model, lymphangiogenesis developed in association with the upregulation of TGF-β1 and VEGF-C. VEGFR-3 was mainly expressed by lymphatic vessels and its expression was also increased after intraperitoneal administration of CG (Fig 6, Supplementary Fig. 2). Consistent with the human studies, VEGF-C was mainly expressed by mesothelial cells and macrophages (Fig. 7). Indeed, fibrotic processes, reflected by peritoneal thickness and α-SMA and Type III collagen expression, were suppressed by the TGFβR-I inhibitor. In addition, VEGF-C expression and lymphangiogenesis in both the parietal peritoneum and the diaphragm were also suppressed by the TGFβR-I inhibitor (Fig. 8, Supplementary Fig. 3). These findings indicate that peritoneal lymphangiogenesis is linked with TGF-β1 and VEGF-C expression. The inhibition of lymphangiogenesis by the TGFβR-I inhibitor suggests that TGF-β1 is a key mediator in the development of lymphangiogenesis in the CG rat model. The limitation in the CG model is the difficulty in assessing peritoneal permeability due to severe inflammation, as in bacterial peritonitis in humans[54]. Therefore, we performed FITC-dextran lymphangiography to evaluate the function of the lymphatic vessels, and found that these lymphatics were functional (Fig. 11). Reduction of FITC-dextran levels in the serum by inhibition of lymphangiogenesis indicates that the lymphatic vessels might be involved in the control of effluent volume in PD.

In clinical settings, TGF-β1, whose levels in dialysate are known to be increased by a glucose-based dialysis solution and by episodes of peritonitis[48-51, 55], may induce VEGF-C production by mesothelial cells and macrophages, thereby leading to lymphangiogenesis in the peritoneal membrane in PD patients, especially after long term PD treatment (Fig. 12). Future studies are required to determine whether specific inhibition of lymphatic vessels can ameliorate ultrafiltration failure in patients undergoing PD.

CONCISE METHODS

Patient Profiles

All of the studies were approved by the Ethics Committee for Human Research of the Faculty of Medicine, Nagoya University (Approval #298 - peritoneal fluid experiment; #299 - peritoneal tissue experiments), and all patients provided informed consent prior to participation in the study.

Peritoneal Transport of VEGF-C in PD Patients.

The VEGF-C concentration in peritoneal effluent was measured in overnight-dwelled (8.95 ± 1.63 h) samples collected from 83 PD patients (27 women, 56 men) who were treated

between July 2005 to April 2008 at the Department of Nephrology and Renal Replacement Therapy of Nagoya University Hospital (Nagoya, Japan) and at affiliated hospitals including Handa Municipal Hospital (Handa, Japan), Chubu Rosai Hospital (Nagoya, Japan), Yokkaichi Municipal Hospital (Yokkaichi, Japan), Kounan-Kousei Hospital (Kounan, Japan), Daiyukai-Daiichi Hospital (Ichinomiya, Japan) and Nagoya Kyoritsu Hospital (Nagoya, Japan). The mean age of all patients was 55.9 ± 13.5 (range, 28 to 89) yr and the mean duration of PD treatment was 31.9 ± 32.0 (range, 1 to 132) months. Diabetic nephropathy was the cause of end-stage renal disease in 27 PD patients (32.5%). All patients were free from peritonitis for at least one month prior to the study, and patients with other diseases, such as liver or lung diseases and malignancy, were excluded. Patients undergoing combination therapy (hemodialysis (HD) + PD) were not included in this study. Peritoneal transport was assessed based on D/P Cr and the average value was 0.67 ± 0.14 (range, 0.28 to 0.96). The correlation between VEGF-C concentration in the PD effluent and D/P Cr was analyzed. In addition, we measured VEGF-C and TGF-β1 concentration in dialysate samples at 4 h of peritoneal equilibration tests (PET) collected from 47 PD patients (16 women, 31 men) treated between November 2008 to June 2009 at the Nagoya University Hospital and Handa Municipal Hospital. Fast PET was performed using 2.27% glucose-based dialysis solutions (Dianeal-N PD-4, Baxter) as described by Twardowski ZJ et al[56]. The mean age of all patients was 52.3 ± 10.9 (range, 25 to 70) yr and the mean duration of CAPD treatment was 25.0 ± 23.7 (range, 1 to 103) months[33].

VEGF-C, LYVE-1 and Podoplanin mRNA Expression in the Human Peritoneum.

A total of 75 peritoneal tissue samples were obtained from 37 PD patients, 32 pre-dialysis chronic renal failure patients at the time of PD catheter insertion, and 6 living kidney donors with normal renal function. Among the 37 PD patients, 8 were regarded as having impaired ultrafiltration capacity (UFF), which was defined by the use of more than four hypertonic bags (2.27% glucose, 3.86% glucose or icodextrin) per 24 h to maintain fluid balance[57]; 6 patients were peritonitis positive; 23 patients (incident) had their catheters removed because of transplantation, mental disorders, severe exit site infection or difficulty in carrying out the bag exchanges (Table 1). The correlations between VEGF-C, LYVE-1 and podoplanin mRNA expression respectively, and with peritoneal membrane thickness was evaluated.

VEGF-C Production in Human Mesothelial Cells.

HPMC were isolated from spent peritoneal dialysis effluent taken from 29 clinically stable patients (Table 2) and were cultured by use of a modified method as described previously[33]. Basal and TGF-β1-induced VEGF-C mRNA expressions were studied[33].

Processing of Biopsy Samples and Morphological Analysis

Samples of parietal peritoneum were biopsied in the standard manner and processed as reported previously[6, 33, 57, 58]. The tissue samples were fixed with 10% buffered formalin overnight, routinely processed for light microscopy and embedded in paraffin. Four-μm-thick sections were cut and stained with hematoxylin and eosin (HE) and Masson's-

trichrome. Before analysis of peritoneal thickness, each specimen was assessed for size, and for the site and direction of the peritoneum. The adequacy of the samples were then judged as described by Honda K et al, in which less than 50% of the samples were considered to be appropriate[57]. It was possible to measure the thickness of 45 of 75 samples in our study. In order to assess the extent of peritoneal thickening, the submesothelial compact zone, which was the zone of peritoneal fibrosis, was defined as the zone between the basal border of the surface of the mesothelial cells and the upper border of the peritoneal adipose tissues[6, 57]. We measured peritoneal thickness at 5 random points using a Zeiss Z1 microscope and AxioVision Windows software version 4.4 (Carl Zeiss, Oberkochen, Germany), and mean thickness was calculated[33].

Cell Culture Study

A human mesothelial cell line (Met-5A) was purchased from the American Type Culture Collection (ATCC, Manassas, VA) and maintained as reported previously[33]. HPMC from spent peritoneal dialysis effluent were obtained by centrifugation of dialysis fluid taken randomly from clinically stable patients, who had a variety of peritoneal permeabilities and were undergoing nocturnal exchanges, using modified methods as described previously[33]. Cellular components were isolated using low speed (200 x g) centrifugation, washed with RPMI 1640 (Sigma, Tokyo, Japan) and then cultured in RPMI 1640 containing L-glutamine (Sigma) supplemented with 15% FBS (Sigma), insulin/transferrin/selenium A (Invitrogen, Tokyo, Japan), 10μM 2-mercaptoethanol (Wako, Osaka, Japan), 3.3 nM EGF (R&D Systems, Minneapolis, MN) and 400 μg/l hydrocortisone (Sigma) in humidified air with 5% CO2 at 37 °C. Non-adherent material was removed the next day with two brief washes with RPMI 1640 and the adherent population was incubated in fresh culture medium. The cells reached confluence in 7-10 days, and were then split two to three times and cultured. Sub-confluent HPMC and Met-5A were washed twice with PBS, and the culture medium was replaced with serum-free medium for 24 hours in order to render the cells quiescent. Subsequently, the cultures were incubated with 5 ng/ml recombinant human TGF-β1 (R&D), which was diluted in serum-free medium. Cells were harvested at 0 (basal condition), 3, 6, 12 and 24 hours (n=3 dishes of cells from each patient, at each time point). All experiments were performed during the 2nd to the 7th passage. To explore the correlation between the enhancement of VEGF-C expression by TGF-β and D/P Cr, we assessed the increase in VEGF-C mRNA after 12 or 24 h incubation with TGF-β1 as described previously[33]. TGF-β1 inhibition studies were performed by incubating Met-5A cells with 5 ng/ml TGF-β1 in combination with a selective inhibitor of TGFβR-I (Calbiochem, La Jolla, CA) for 12 h.

Animal Model

All animal studies were carried out in accordance with the Animal Experimentation Guidelines of Nagoya University Graduate School of Medicine (Nagoya, Japan). Eight-week-old male Sprague-Dawley (SD) rats (Japan SLC, Hamamatsu, Japan) that initially

weighed 240-260 g were used throughout the study. The animals were maintained under conventional laboratory conditions and were given free access to food and water. Rats were given an intraperitoneal injection of 3 ml/200 g body weight of 0.04% chlorhexidine gluconate (CG) (Wako, Japan) and 10% ethanol (Wako) dissolved in saline every other day. These rats were randomly assigned to a treatment or a saline group. The rats in the treatment group (n = 7) were given a daily intraperitoneal injection of 3 μg/ g body weight of the TGFβR-I inhibitor dissolved in saline and dimethyl sulfoxide (DMSO, 140 mg/ml) (Wako). On the day of CG injection, the rats were injected with the TGFβR-I inhibitor 2 hours prior to injection of CG. The rats in the saline group (n = 7) were given a daily intraperitoneal injection of saline and DMSO in a similar manner. Five control rats were injected daily with the same dosage of saline without CG or TGFβR-I inhibitor. All rats were sacrificed on Day 16. All injections and sacrifices were performed under anesthesia with diethyl ether (Wako). Parietal peritoneal and diaphragmatic samples were procured and the harvested samples were used for analysis of peritoneal thickness, immunohistochemical analysis of VEGF-C, VEGFR-3, LYVE-1, podoplanin, ED-1, Type III collagen,α-SMA and cytokeratin, and for analysis of the mRNA expression of VEGF-C, VEGFR-3, LYVE-1, podoplanin and Type III collagen.

Analysis of Lymphatic Vessel Function

We analyzed lymphatic vessel function using the modified method of lymphangiography as described previously[34]. We intraperitoneally administered a total of 5 ml of FITC-labeled dextran 2,000 (10 mg/ml concentration; molecular weight (MW) 2,000,000; Sigma) intraperitoneally. Twenty minutes later, blood was drawn and the animals were sacrificed. Serum samples were immediately separated from the blood and absorbance was measured at 493 nm via spectrophotometry; blood from non-administered rats was used as a normal control. The required time for all procedures by measurement with the spectrophotometer was fixed to 3 hours. The diaphragm and parietal peritoneum were harvested and snap frozen in OCT compound (Sakura Fine Technical, Tokyo, Japan). FITC-dextran was mainly taken up by the lymphatic vessels in the diaphragm and passed to the central collectors of lymphatics. The detection of the FITC signal in the blood taken from the rats administered intraperitoneally with FITC-dextran of molecular weight of 2000 KDa indicates that the FITC-dextran was absorbed via the lymphatic vessels and drained into the blood circulation through the thoracic duct[59].

Histology and Immunohistochemistry

Routine histological and immunohistological analysis of human and rat tissues were performed and analyzed as described previously[22, 23, 33, 58, 60]. VEGF-C expression was analyzed and semiquantitatively classified as follows: 0, no staining; 1, mild staining; 2, moderate staining; 3, pronounced staining. The antibodies used are listed in Supplementary Table 1.

Enzyme-Linked Immunosorbent Assays (ELISA)
VEGF-C and total (both active and latent forms) TGF-β1 protein levels in peritoneal dialysate (PD fluid) samples and in the cell culture supernatant were measured using the Human VEGF-C (IBL, Takasaki, Japan) and the TGF-β1 (R&D) ELISA kit, respectively according to the manufacturers' instructions. Samples were frozen at the time of collection and stored at -80 °C. Samples were not subjected to freeze-thaw cycles.

RNA Preparation from Peritoneal Tissues and Cultured Mesothelial Cells, and PCR Analysis
Human and rat peritoneal tissues were immersed in RNA later (Ambion, Austin, TX) for 1 day or more. RNA preparation and the synthesis of first-strand cDNA were performed as described previously[23, 33, 58]. Total RNA (1 μg) was then reverse transcribed. Real-time polymerase chain reaction analysis was performed with an Applied Biosystems Prism 7500HT sequence detection system using TaqMan gene expression assays as described previously[58]. The TaqMan Gene Expression Assays (Applied Biosystems Inc.) used are described in Supplementary Table 2. 18S ribosomal RNA was used as an endogenous control[23, 33, 58, 60].

Statistical Analyses
Values are expressed as means ± SD. Differences between two groups were analyzed by Student's t-test or by Mann-Whitney tests. Comparisons among groups were performed by one-way analysis of variance (ANOVA) followed by Dunnett's or Kruskal-Wallis multiple comparison tests. Pearson's correlation coefficient was used to analyze the correlations. Differences were considered to be statistically significant if $P<0.05$. All analyses were performed using SPSS software (SPSS, Chicago, IL).

ACKNOWLEDGEMENTS
The technical assistance of Mr. Norihiko Suzuki, Ms. Keiko Higashide, Ms. Naoko Asano and Ms. Yuriko Sawa (Department of Nephrology, Nagoya University, Nagoya, Japan) is gratefully acknowledged. We thank Drs. Isao Ito and SusumuToda (Nagoya University Hospital), Drs. Midoriko Watanabe and Makoto Mizutani (Handa Municipal Hospital, Handa, Japan), Dr. Hirotake Kasuga (Nagoya Kyoritsu Hospital, Nagoya, Japan), Dr. Masanobu Horie (Daiyukai-Daiichi Hospital, Ichinomiya, Japan) and Dr. Takeyuki Hiramatsu (Kounan-Kousei Hospital, Kounan, Japan) for collecting peritoneum from the patients.

GRANTS
This work was supported by in part by a grant-in-aid for Scientific Research from the Ministry Education, Science, and Culture, Japan (YI, # 20590972), the 2011 research grant from the Aichi Kidney Foundation (KH and YI), and the Japanese Association of Dialysis Physicians Grant 2011-13 (YI). This study was also supported in part by a Grant-in-Aid for

Progressive Renal Diseases Research, Research on Rare and Intractable Disease, from the Ministry of Health, Labor and Welfare of Japan.

DISCLOSURES

The authors declare that there are no conflicts of interest.

FIGURES

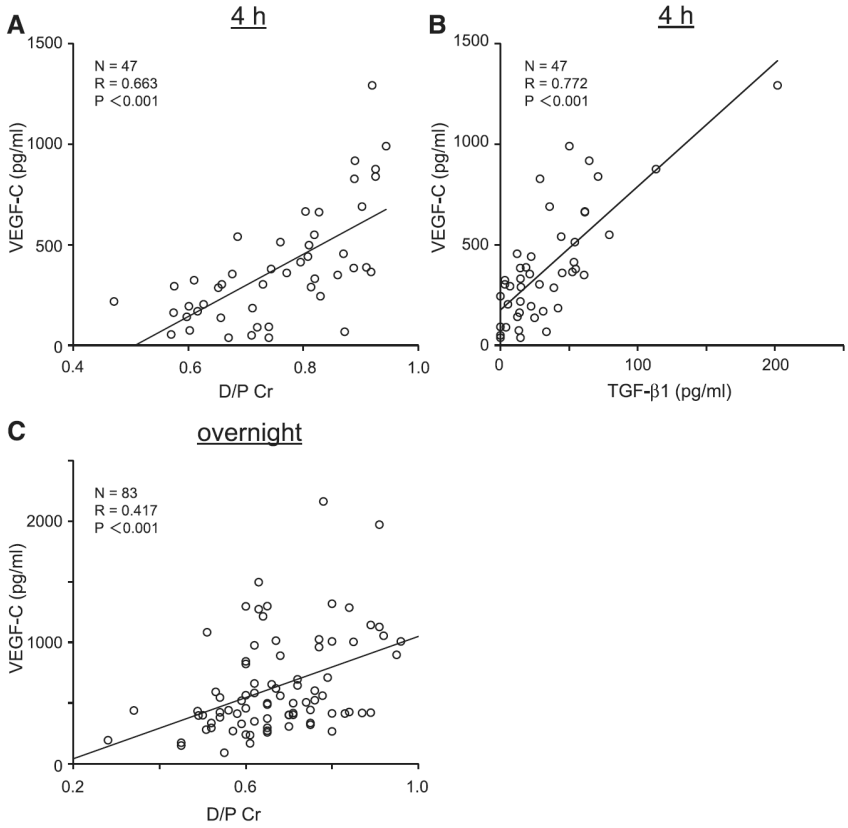

Figure 1. VEGF-C concentration in human PD effluent was correlated with TGF-β1 concentration in PD effluent, and with the peritoneal transport rate (D/P Cr).
A: Positive correlation between the VEGF-C concentration in the PD effluent of 4 h-dwelled samples and the D/P Cr.
B: Positive correlation between VEGF-C and TGF-β1 concentrations in the PD effluent of 4 h-dwelled samples.
C: Positive correlation between the VEGF-C concentration in overnight-dwelled PD effluent samples and D/P Cr.

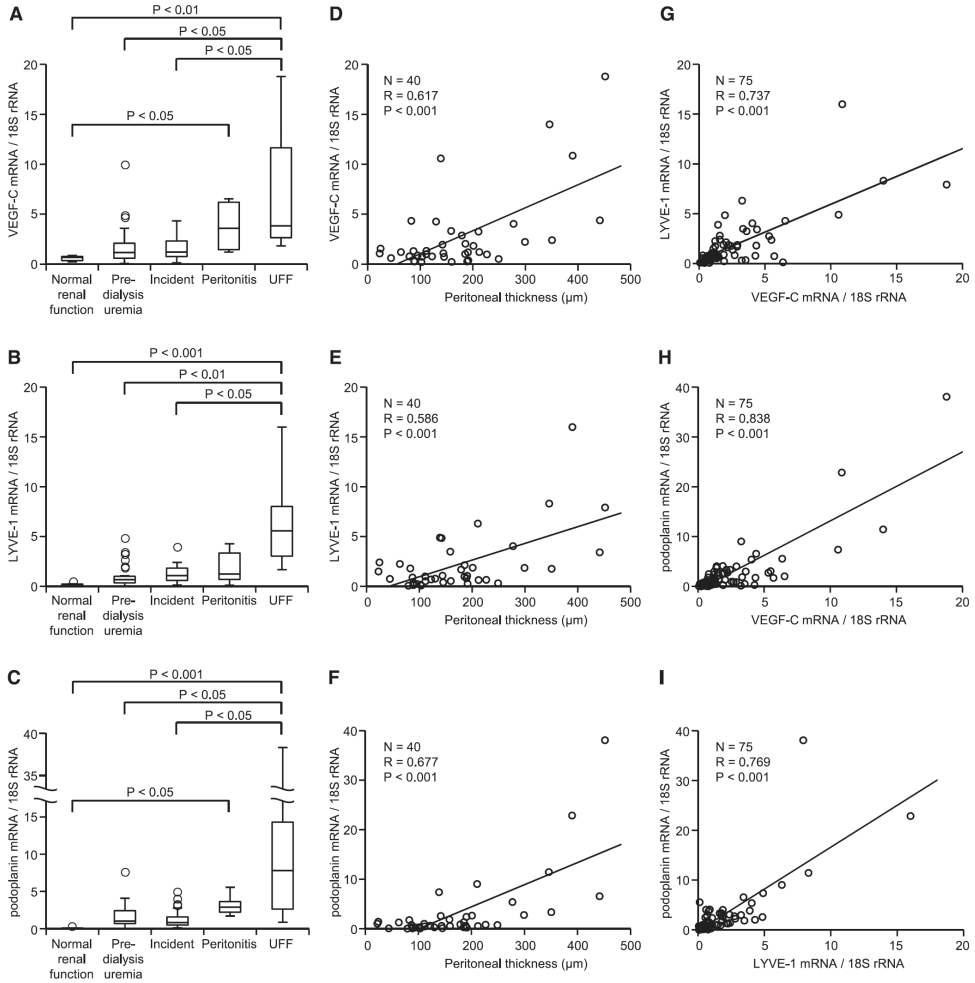

Figure 2. VEGF-C, LYVE-1, and podoplanin mRNA levels increase in UFF and correlate with the thickness of the peritoneum in human peritoneal biopsy samples. (A–C) VEGF-C, LYVE-1, and podoplanin mRNA levels were significantly higher in patients with UFF than patients with normal renal function, patients with predialysis uremia, or patients in the incident group. (D–F) The expression of VEGF-C, LYVE-1, and podoplanin mRNA significantly correlated with the thickness of the peritoneum. (G–I) Positive correlation among VEGF-C, LYVE-1, and podoplanin mRNA expression in peritoneal membranes.

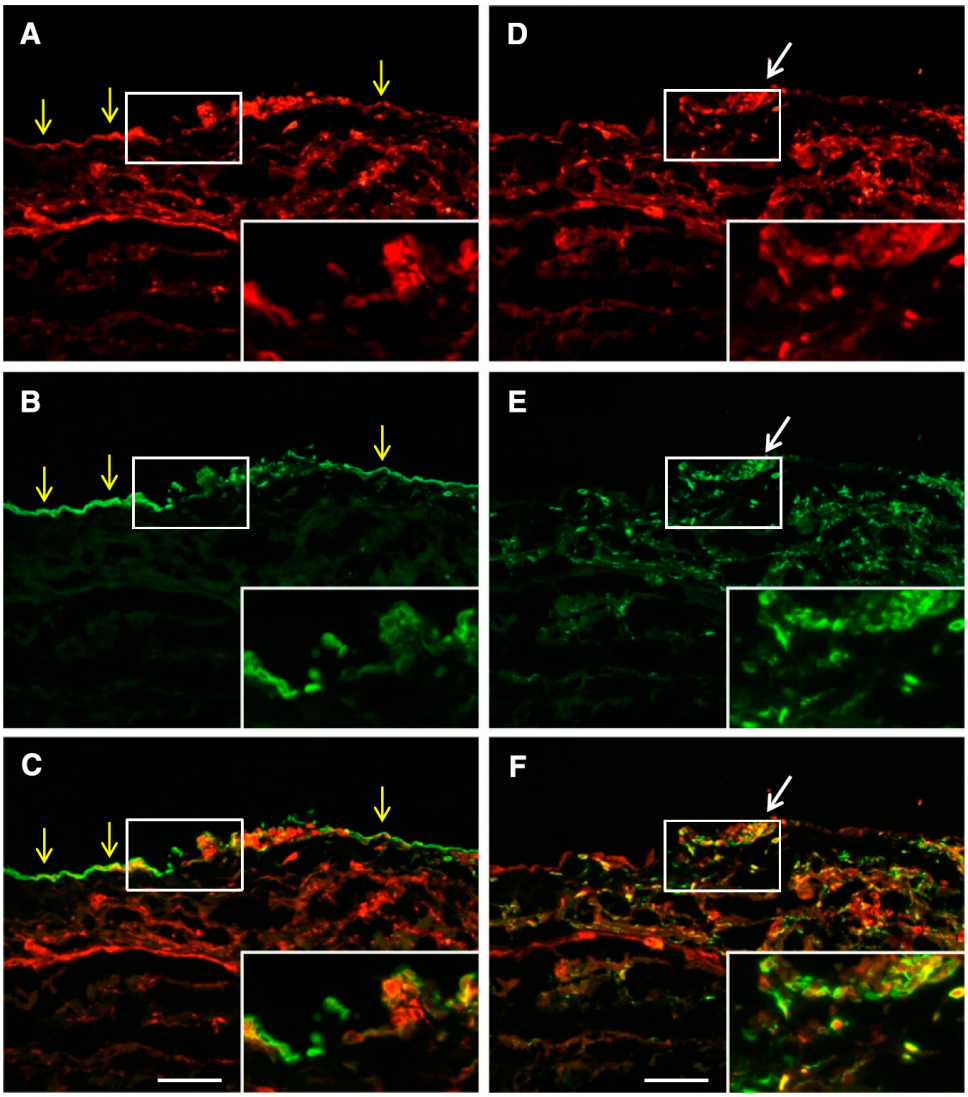

Figure 3. Double immunofluorescent analysis shows VEGF-C expression by mesothelial cells and macrophages in human peritoneal biopsy specimens of bacterial peritonitis. Biopsy specimens were (A and D) stained with VEGF-C and costained with (B) the mesothelial cell marker cytokeratin or (E) the macrophage marker CD68. Respective merged images are shown in C and F. Cytokeratin-positive mesothelial cells (yellow arrows) and CD68-positive macrophages (white arrows) both expressed VEGF-C. (Insets) Magnification of the white boxed area. Scale bars, 100μm.

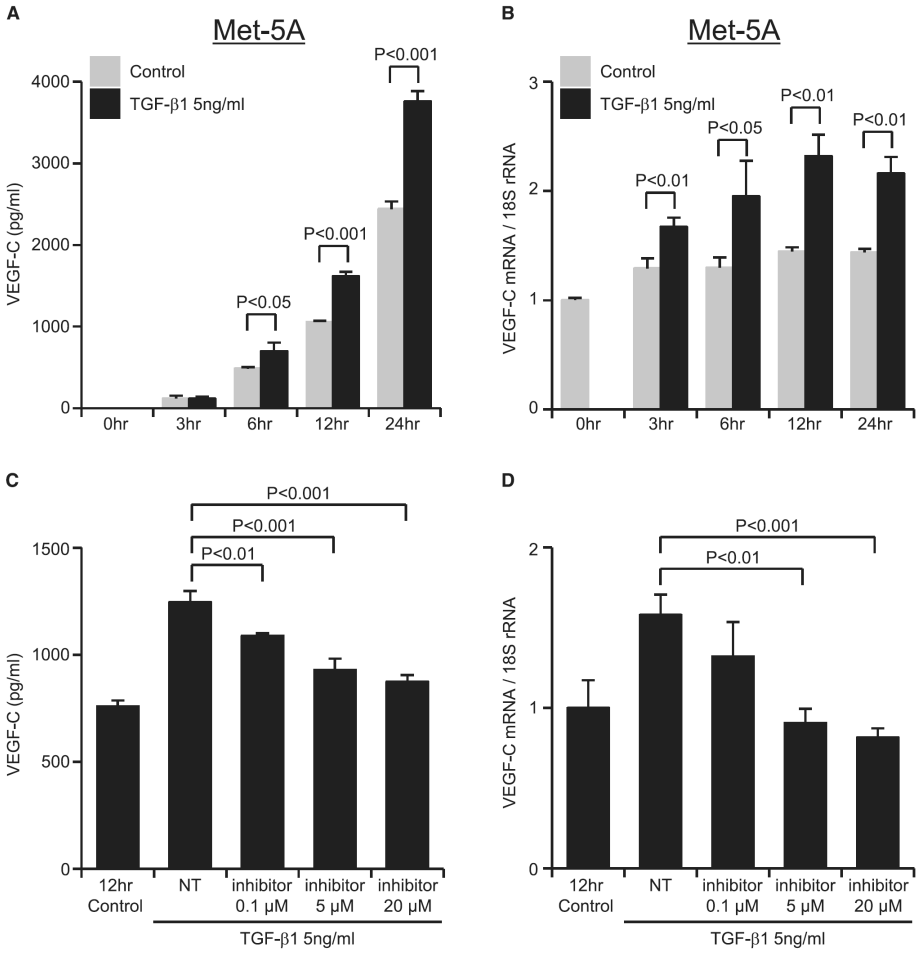

Figure 4. VEGF-C expression in a cultured mesothelial cell line (Met-5A cells) increases after treatment with TGF-β1. Met-5A cells that were preincubated for 24 hours in serum-free medium were treated with 5 ng/ml TGF-β1. (A and C) VEGF-C protein levels in the supernatant were determined by ELISA, and (B and D) VEGF-C mRNA levels were determined by real-time PCR. (A) VEGF-C protein levels were significantly increased at 6, 12, and 24 hours after incubation with TGF-β1. (B) VEGF-C mRNA expression was significantly elevated by TGF-β1 compared with the control at each time point. The effect of TGF-β inhibition on VEGF-C expression in cultured Met-5A cells was assayed by incubation of Met-5A cells with 5 ng/ml TGF-β1 in the presence or absence of the TGFβR-I inhibitor LY364947 (inhibitor) for 12 hours. (C) TGF-β–induced VEGF-C protein and (D) mRNA levels were suppressed by the inhibitor in a dose-dependent manner compared with no inhibitor treatment (NT; TGF-β1 stimulation only) at 12 hours. Results are means ± SD of three independent experiments (n=3).

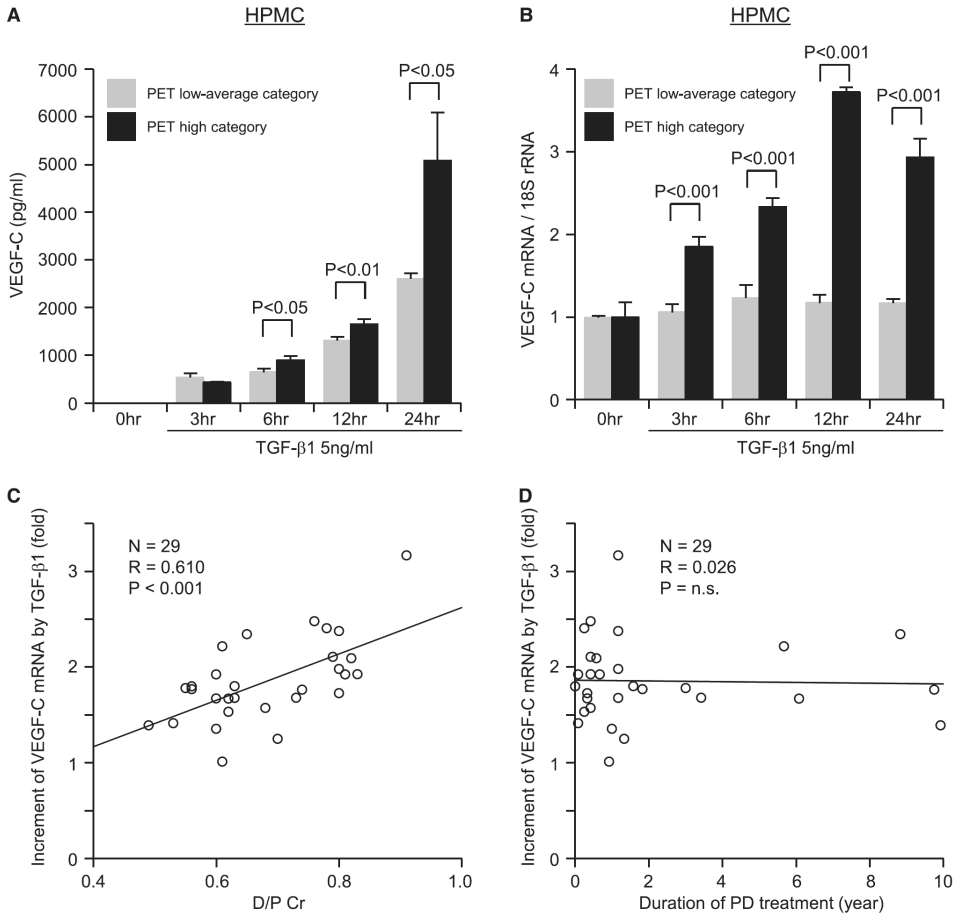

Figure 5. The increase in VEGF-C expression by TGF-β1 in HPMCs correlates with D/P Cr. HPMCs from the spent PD effluent of patients with high peritoneal permeability (PET high category) and low permeability (PET low average category) were stimulated with TGF-β1. (A) VEGF-C protein levels in the supernatant were determined by ELISA, and (B) VEGF-C mRNA levels were determined by real-time PCR. The figures show representative cases from each category. VEGF-C mRNA was increased by TGF-β1, and it peaked at 12 hours in 8 of the HPMCs and 24 hours in 21 of the HPMCs derived from 29 PD patients. (C) Positive correlation between peritoneal permeability (D/P Cr) and the peak values of enhanced VEGF-C mRNA expression at 12 or 24 hours after stimulation with TGF-β1 (5 ng/ml). (D) No significant correlation was observed between the duration of PD treatment and the peak values of increased VEGF-C mRNA expression at 12 or 24 hours after stimulation with TGF-β1 (5 ng/ml).

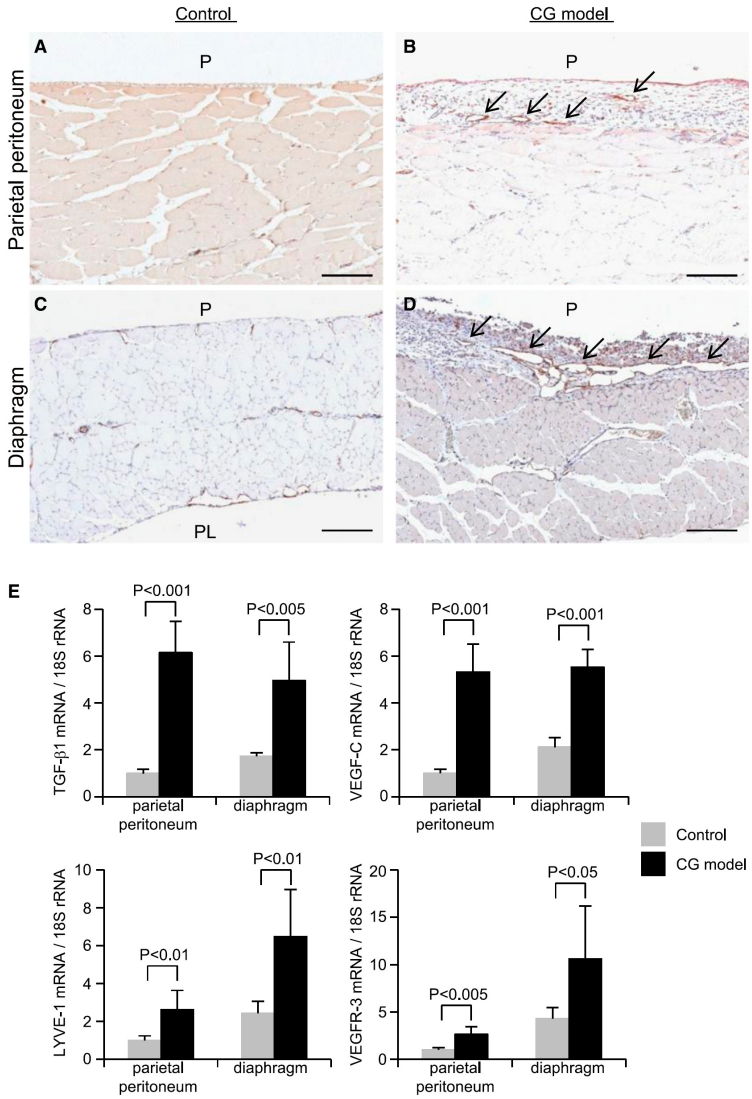

Figure 6. Expression of LYVE-1 increases in the parietal peritoneum and diaphragm of CG model rats. Staining of (A and B) the parietal peritoneum and (C and D) the diaphragm of (A and C) control and (B and D) CG model rats showed an increased expression of LYVE-1-positive lymphatic vessels (arrows) in the CG model. Strong expression of lymphatic vessels was seen in the diaphragm of the CG rats. Scale bars, 200 μm. (E) TGF-β1, VEGF-C, LYVE-1, and VEGFR-3 mRNA expressions in both the parietal peritoneum and the diaphragm were increased in the CG model compared with the control. Control, n=5; CG models, n=7 for each group. P, peritoneal side; PL, pleural side.

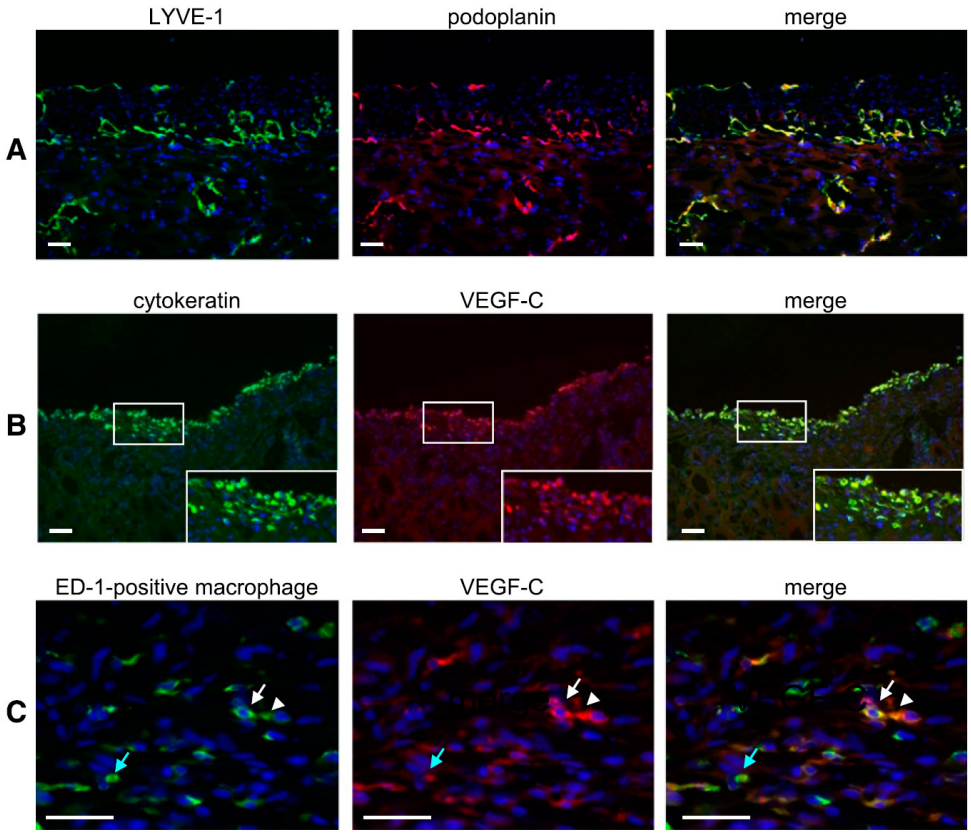

Figure 7. Double immunofluorescent staining of frozen sections of a CG rat diaphragm shows that VEGF-C is expressed by cytokeratin-positive mesothelial cells and ED-1-positive macrophages. (A) The expression pattern of LYVE-1 (green) was similar to the expression pattern of podoplanin (red). (B) VEGF-C (red) was expressed in cytokeratinpositive mesothelial cells (green). (C) VEGF-C (red) was expressed in ED-1-positive macrophages (green). Arrows and arrowheads of the same color indicate the same cells. Nuclei were counterstained with 4',6-diamino-2-phenylindole (blue). (Insets) Magnification of the white boxed area. Scale bars, 50µm.

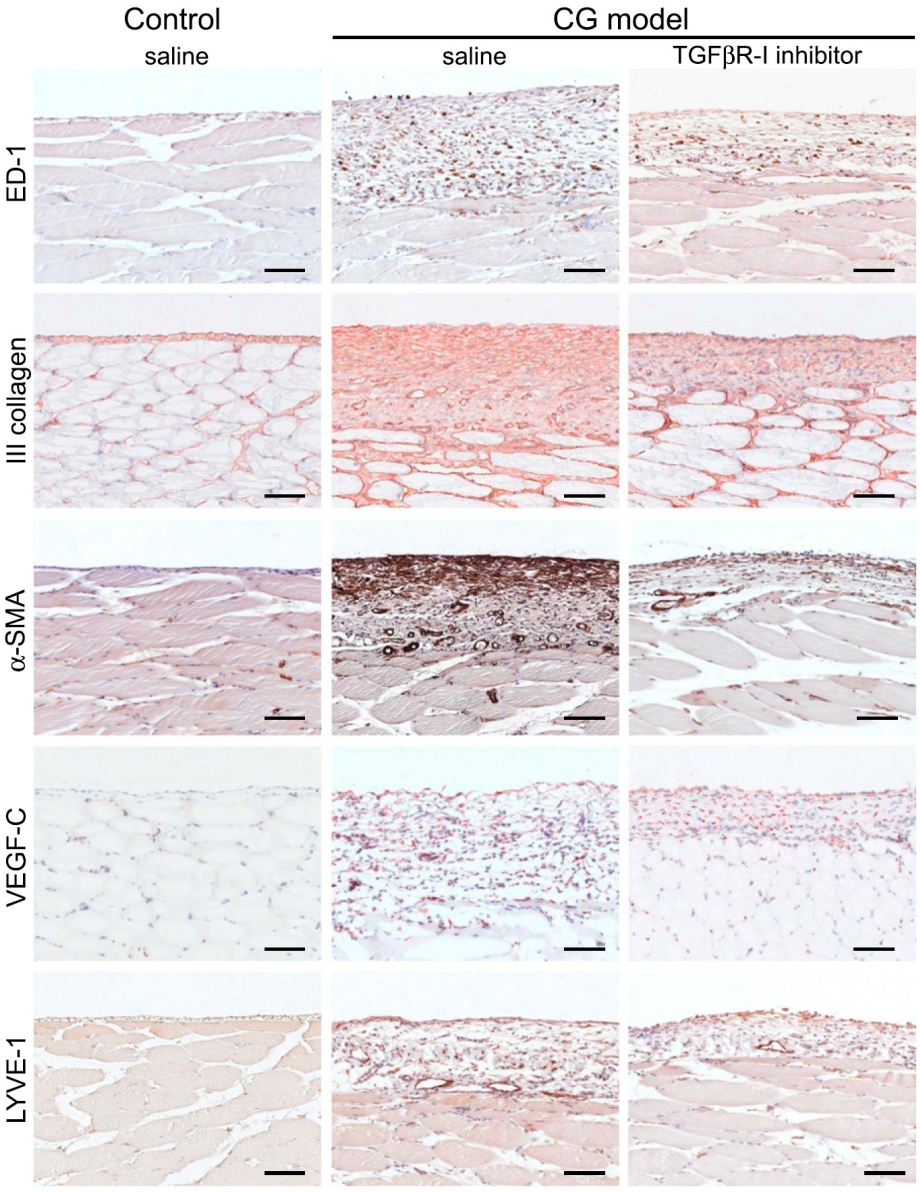

Figure 8. Under immunohistochemical analysis of the parietal peritoneum, TGFβR-I inhibitor suppresses fibrosis and lymphangiogenesis. Histochemical staining of ED-1-positive macrophages, type III collagen, α-SMA, VEGF-C, and LYVE-1 in TGFβR-I inhibitor-treated (daily intraperitoneal injection of 3μg/g body wt) and untreated CG model rats and control rats. Scale bars, 100μm.

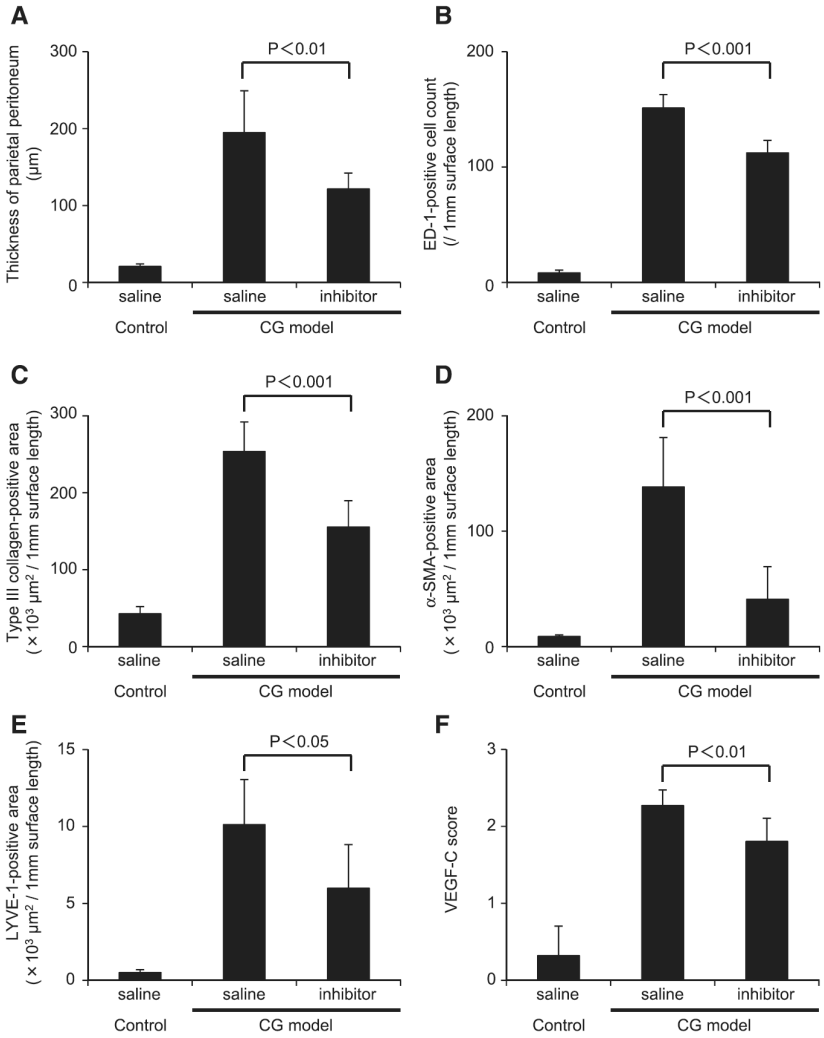

Figure 9. Quantitative immunohistochemical parameters in the rat parietal peritoneum of the CG model indicate that TGFβR-I inhibitor suppresses fibrosis and lymphangiogenesis. The histochemical parameters of the parietal peritoneum that were assayed were quantified. Compared with untreated CG rats, TGFβR-I inhibitor treatment of CG rats significantly reduced (A) the thickness of the peritoneum, (B) the number of ED-1-positive cells, (C) type III collagen deposition, (D) α-SMA expression, (E) LYVE-1-positive areas, and (F) VEGF-C expression. VEGF-C expression was analyzed and semiquantitatively scored as follows: 0, no staining; 1, mild staining; 2, moderate staining; 3, pronounced staining. Control saline treatment, n=5; CG models treated with saline or inhibitor, n=7 for each group.

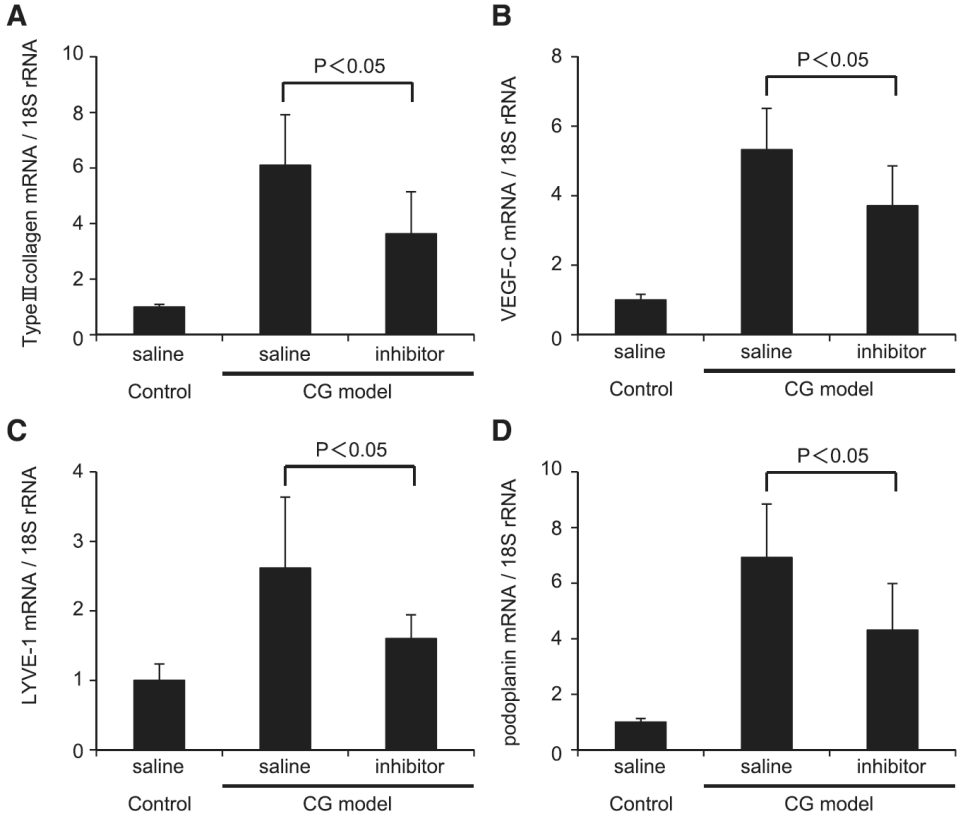

Figure 10. Quantitative real-time PCR analysis of specific mRNA expression in the rat parietal peritoneum of the CG model rat indicates that TGFβR-I inhibitor suppressed lymphangiogenesis. Real-time PCR analysis indicated that increased expression of (A) type III collagen, (B) VEGF-C, (C) LYVE-1, and (D) podoplanin mRNA was significantly suppressed in CG rats compared with controls by TGFβR-I inhibitor treatment. The mRNA expression of the indicated proteins is expressed relative to 18S ribosomal RNA. Control saline treatment, n=5; CG models treated with saline or inhibitor, n=7 for each group.

Figure 11

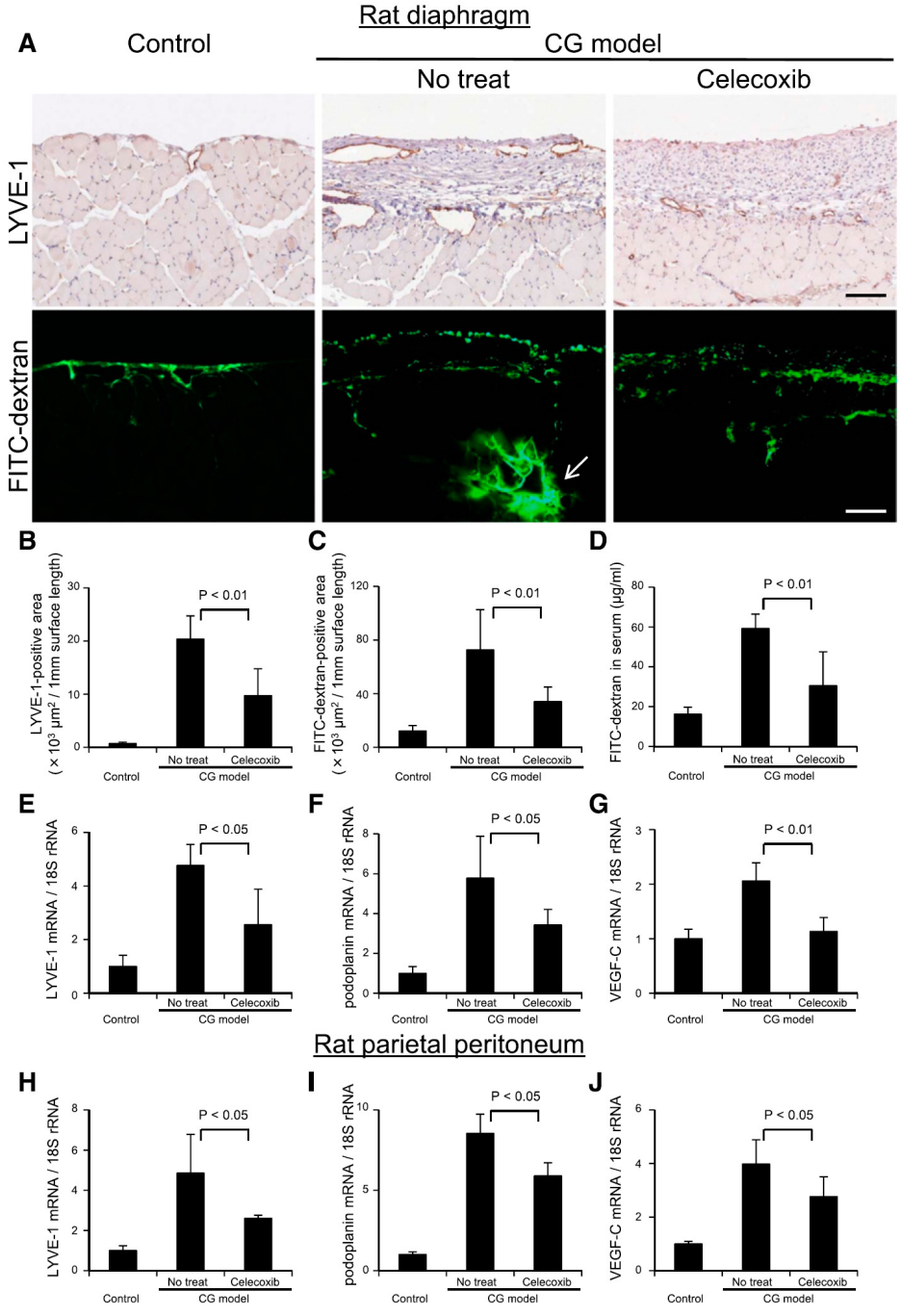
Rat diaphragm
A
Control
CG model
No treat
Celecoxib
LYVE-1
FITC-dextran
B
LYVE-1-positive area
(× 10³ μm² / 1mm surface length)
P < 0.01
C
FITC-dextran-positive area
(× 10³ μm² / 1mm surface length)
P < 0.01
D
FITC-dextran in serum (μg/ml)
P < 0.01
E
LYVE-1 mRNA / 18S rRNA
P < 0.05
F
podoplanin mRNA / 18S rRNA
P < 0.05
G
VEGF-C mRNA / 18S rRNA
P < 0.01
Rat parietal peritoneum
H
LYVE-1 mRNA / 18S rRNA
P < 0.05
I
podoplanin mRNA / 18S rRNA
P < 0.05
J
VEGF-C mRNA / 18S rRNA
P < 0.05
Control
No treat
Celecoxib
CG model

Figure 11. Drainage of FITC dextran administered into the abdominal cavity is suppressed by inhibition of lymphangiogenesis with cyclooxygenase-2 inhibitor. (A, upper panels) Immunohistochemical staining of LYVE-1 in the diaphragm of control rats, celecoxib-treated (daily oral administration of 50 mg/kg body wt) CG rats, and untreated CG rats. (A, lower panels) Rats were given intraperitoneal injections of 50 mg FITC dextran (molecular weight=2,000,000). Twenty minutes later, blood, peritoneal, and diaphragmatic samples were obtained. Immunohistochemical findings in the diaphragm of control, untreated, and celecoxib-treated rats were recorded. Scale bars, 100μm. Arrow indicates the accumulation of FITC dextran in the central collector of lymphatic vessel. Quantification of positive area determined by MetaMorph 6.3 image software (Universal Imaging, West Chester, PA) in the diaphragm for (B) LYVE-1 and (C) FITC dextran showed that celecoxib treatment significantly reduced both positive areas compared with the untreated CG rats. (D) To assess the amount of FITC dextran in blood drawn at euthanization, absorbance of serum samples was measured at 493 nm by spectrophotometry. For preparation of the standard curve, FITC dextran was reconstituted and diluted with normal rat serum. Concentrations of FITC dextran in the serum were significantly decreased in celecoxib-treated CG rats compared with untreated CG rats. Real-time PCR analysis of (E and H) LYVE-1, (F and I) podoplanin, and (G and J) VEGF-C mRNA in (E–G) the rat diaphragm and (H–J) the parietal peritoneum indicated that increased expression of LYVE-1, podoplanin, and VEGF-C mRNA in CG rats was significantly suppressed by celecoxib treatment. Control, n=5; CG models with no treat, n=6; CG models treated with celecoxib, n=6.

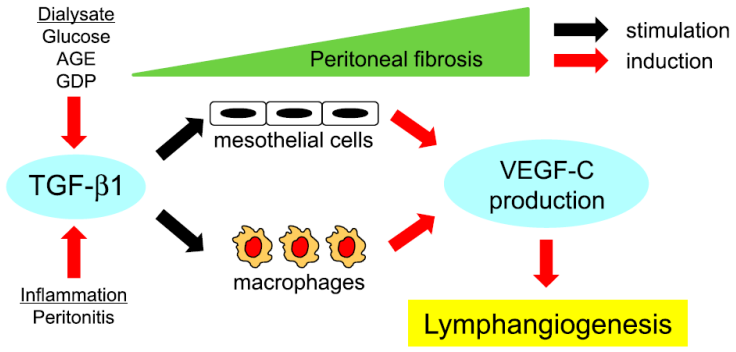

Figure 12. Lymphangiogenesis develops associated with peritoneal fibrosis through the TGF-β-VEGF-C pathway. There are several mechanisms by which TGF-β1 levels can be increased in dialysate, including exposure of the dialysate to glucose[49] or presence of advanced glycation end products,[50] glucose degradation products,[51] or bacterial peritonitis.[55] TGF-β1 induces VEGF-C expression by mesothelial cells and macrophages, leading to lymphangiogenesis in the peritoneum of the PD patients who have undergone prolonged PD treatment.

TABLES

Table 1. Peritoneal biopsy cases evaluated for VEGF-C, LYVE-1, and podoplanin mRNA expression

	Normal Renal Function	Predialysis Uremia	Incident	Peritonitis	UFF
N	6	32	23	6	8
Men	2	23	13	5	4
Women	4	9	10	1	4
Age, yr	56.5±14.1	62.3±12.4	60.8±13.2	70.8±11.1	57.8±12.0
Duration of treatment, yr	0	0	3.6±3.0	3.2±1.5	9.2±6.1
Average thickness of peritoneum, μm	82.0±22.9	160.0±51.8	155.7±93.1	311.2±169.6	295.2±125.5

Values are means ± SD. Normal renal function indicates living kidney donors with normal renal function. Predialysis uremia indicates peritoneal tissues that were taken at the time when a PD catheter was inserted because of advanced renal failure. Incident indicates that peritoneal tissues were taken when the catheter was removed because of reasons other than UFF.

Table 2. Profiles of patients from whom peritoneal mesothelial cells were isolated for culture studies

	D/P Cr	Men	Women	All Patients
Low	~0.49	10	4	14
Low average	0.5–0.64			
High average	0.65–0.8	9	6	15
High	~0.81			

D/P Cr is an index of the peritoneal transport.

REFERENCES

1. Churchill DN, Thorpe KE, Nolph KD, Keshaviah PR, Oreopoulos DG & Pagé D: Increased peritoneal membrane transport is associated with decreased patient and technique survival for continuous peritoneal dialysis patients. The Canada-USA (CANUSA) Peritoneal Dialysis Study Group. J Am Soc Nephrol 9: 1285-1292, 1998
2. Rumpsfeld M, McDonald SP & Johnson DW: Higher peritoneal transport status is associated with higher mortality and technique failure in the Australian and New Zealand peritoneal dialysis patient populations. J Am Soc Nephrol 17: 271-278, 2006
3. Kawaguchi Y, Ishizaki T, Imada A, Oohira S, Kuriyama S, Nakamoto H, Nakamoto M, Hiramatsu M, Maeda K & Ota K: Searching for the reasons for drop-out from peritoneal dialysis: A nationwide survey in Japan. Perit Dial Int 23: S175-S177, 2003
4. Mizuno M, Ito Y, Tanaka A, Suzuki Y, Hiramatsu H, Watanabe M, Tsuruta Y, Matsuoka T, Ito I, Tamai H, Shimizu H, Kurata H, Inaguma D, Hiramatsu T, Horie M, Naruse T, Maruyama S, Imai E, Yuzawa Y & Matsuo S: Peritonitis is still an important factor for withdrawal from peritoneal dialysis therapy in the Tokai area of Japan. Clin Exp Nephrol 15: 727-737, 2011
5. Brimble KS, Walker M, Margetts PJ, Kundhal KK & Rabbat CG: Meta-analysis: peritoneal membrane transport, mortality, and technique failure in peritoneal dialysis. J Am Soc Nephrol 17: 2591-2598, 2006
6. Williams JD, Craig KJ, Topley N, Von Ruhland C, Fallon M, Newman GR, Mackenzie RK, Williams GT & Peritoneal Biopsy Study Group: Morphologic changes in the peritoneal membrane of patients with renal disease. J Am Soc Nephrol 13: 470-479, 2002
7. Mateijsen MA, van der Wal AC, Hendriks PM, Zweers MM, Mulder J, Struijk DG & Krediet RT: Vascular and interstitial changes in the peritoneum of CAPD patients with peritoneal sclerosis. Perit Dial Int 19: 517-525, 1999
8. Sherif AM, Nakayama M, Maruyama Y, Yoshida H, Yamamoto H, Yokoyama K & Kawakami M: Quantitative assessment of the peritoneal vessel density and vasculopathy in CAPD patients. Nephrol Dial Transplant 21: 1675-1681, 2006
9. Tammela T & Alitalo K: Lymphangiogenesis: Molecular mechanisms and future promise. Cell 140: 460-476, 2010
10. Alitalo K, Tammela T & Petrova TV: Lymphangiogenesis in development and human disease. Nature 438: 946-953, 2005
11. Jones N, Iljin K, Dumont DJ & Alitalo K: Tie receptors: new modulators of angiogenic and lymphangiogenic responses. Nat Rev Mol Cell Biol 2: 257-267, 2001
12. Schoppmann SF, Birner P, Stöckl J, Kalt R, Ullrich R, Caucig C, Kriehuber E, Nagy K, Alitalo K & Kerjaschki D: Tumor-associated macrophages express lymphatic endothelial growth factors and are related to peritumoral lymphangiogenesis. Am J Pathol 161: 947-956, 2002
13. Kodama M, Kitadai Y, Tanaka M, Kuwai T, Tanaka S, Oue N, Yasui W & Chayama K: Vascular endotherial growth factor C stimulates progression of human gastric

cancer via both autocrine and paracrine mechanisms. Clin Cancer Res 14: 7205-7214, 2008

14. Kitadai Y, Kodama M, Cho S, Kuroda T, Ochiumi T, Kimura S, Tanaka S, Matsumura S, Yasui W & Chayama K: Quantitative analysis of lymphangiogenic markers for predicting metastasis of human gastric carcinoma to lymph nodes. Int J Cancer 115: 388-392, 2005
15. Onogawa S, Kitadai Y, Tanaka S, Kuwai T, Kimura S & Chayama K: Expression of VEGF-C and VEGF-D at the invasive edge correlates with lymph node metastasis and prognosis of patients with colorectal carcinoma. Cancer Sci 95: 32-39, 2004
16. Baluk P, Tammela T, Ator E, Lyubynska N, Achen MG, Hicklin DJ, Jeltsch M, Petrova TV, Pytowski B, Stacker SA, Ylä-Herttuala S, Jackson DG, Alitalo K & McDonald DM: Pathogenesis of persistent lymphatic vessel hyperplasia in chronic airway inflammation. J Clin Invest 115: 247-257, 2005
17. Baluk P, Yao LC, Feng J, Romano T, Jung SS, Schreiter JL, Yan L, Shealy DJ & McDonald DM: TNF-α drives remodeling of blood vessels and lymphatics in sustained airway inflammation in mice. J Clin Invest 119: 2954-2964, 2009
18. El-Chemaly S, Malide D, Zudaire E, Ikeda Y, Weinberg BA, Pacheco-Rodriguez G, Rosas IO, Aparicio M, Ren P, MacDonald SD, Wu HP, Nathan SD, Cuttitta F, McCoy JP, Gochuico BR & Moss J: Abnormal lymphangiogenesis in idiopathic pulmonary fibrosis with insights into cellular and molecular mechanisms. Proc Natl Acad Sci U S A 106: 3958-3963, 2009
19. Paavonen K, Puolakkainen P, Jussila L, Jahkola T & Alitalo K: Vascular endothelial growth factor receptor-3 in lymphangiogenesis in wound healing. Am J Pathol 156: 1499-1504, 2000
20. Kerjaschki D, Huttary N, Raab I, Regele H, Bojarski-Nagy K, Bartel G, Kröber SM, Greinix H, Rosenmaier A, Karlhofer F, Wick N & Mazal PR: Lymphatic endothelial progenitor cells contribute to de novo lymphangiogenesis in human renal transplants. Nat Med 12: 230-234, 2006
21. Kerjaschki D, Regele HM, Moosberger I, Nagy-Bojarski K, Watschinger B, Soleiman A, Birner P, Krieger S, Hovorka A, Silberhumer G, Laakkonen P, Petrova T, Langer B & Raab I: Lymphatic neoangiogenesis in human kidney transplants is associated with immunologically active lymphocytic infiltrates. J Am Soc Nephrol 15: 603-612, 2004
22. Sakamoto I, Ito Y, Mizuno M, Suzuki Y, Sawai A, Tanaka A, Maruyama S, Takei Y, Yuzawa Y & Matsuo S: Lymphatic vessels develop during tubulointerstitial fibrosis. Kidney Int 75: 828-838, 2009
23. Suzuki Y, Ito Y, Mizuno M, Kinashi H, Sawai A, Noda Y, Mizuno T, Shimizu H, Fujita Y, Matsui K, Maruyama S, Imai E, Matsuo S & Takei Y: Transforming growth factor-β induces vascular endothelial growth factor-C expression leading to lymphangiogenesis in rat unilateral ureteral obstruction. Kidney Int: 81: 865-879, 2012

24. Smit W, Schouten N, van den Berg N, Langedijk MJ, Struijk DG, Krediet RT & Netherlands Ultrafiltration Failure Study Group: Analysis of the prevalence and causes of ultrafiltration failure during long-term peritoneal dialysis: a cross-sectional study. Perit Dial Int 24: 562-570, 2004
25. Sampimon DE, Coester AM, Struijk DG & Krediet RT: The time course of peritoneal transport parameters in peritoneal dialysis patients who develop encapsulating peritoneal sclerosis. Nephrol Dial Transplant 26: 291-298, 2011
26. Heimbürger O, Waniewski J, Werynski A, Tranaeus A & Lindholm B: Peritoneal transport in CAPD patients with permanent loss of ultrafiltration capacity. Kidney Int 38: 495-506, 1990
27. Fusshöller A, zur Nieden S, Grabensee B & Plum J: Peritoneal fluid and solute transport: influence of treatment time, peritoneal dialysis modality, and peritonitis incidence. J Am Soc Nephrol 13: 1055-1060, 2002
28. Krediet RT: The effective lymphatic absorption rate is an accurate and useful concept in the physiology of peritoneal dialysis. Perit Dial Int 24: 309-313, 2004
29. Flessner M: Effective lymphatic absorption rate is not a useful or accurate term to use in the physiology of peritoneal dialysis. Perit Dial Int 24: 313-316, 2004
30. Nishino T, Miyazaki M, Abe K, Furusu A, Mishima Y, Harada T, Ozono Y, Koji T & Kohno S: Antisense oligonucleotides against collagen-binding stress protein HSP47 suppress peritoneal fibrosis in rats. Kidney Int 64: 887-896, 2003
31. Ro Y, Hamada C, Inaba M, Io H, Kaneko K & Tomino Y: Inhibitory effects of matrix metalloproteinase inhibitor ONO-4817 on morphological alterations in chlorhexidine gluconate-induced peritoneal sclerosis rats. Nephrol Dial Transplant 22: 2838-2848, 2007
32. Kushiyama T, Oda T, Yamada M, Higashi K, Yamamoto K, Oshima N, Sakurai Y, Miura S & Kumagai H: Effects of liposome-encapsulated clodronate on chlorhexidine gluconate-induced peritoneal fibrosis in rats. Nephrol Dial Transplant 26: 3143-3154, 2011
33. Mizutani M, Ito Y, Mizuno M, Nishimura H, Suzuki Y, Hattori R, Matsukawa Y, Imai M, Oliver N, Goldshmeding R, Aten J, Krediet RT, Yuzawa Y & Matsuo S: Connective tissue growth factor (CTGF/CCN2) is increased in peritoneal dialysis patients with high peritoneal solute transport rate. Am J Physiol Renal Physiol 298: F721-733, 2010
34. Tammela T, Saaristo A, Holopainen T, Lyytikkä J, Kotronen A, Pitkonen M, Abo-Ramadan U, Ylä-Herttuala S, Petrova TV & Alitalo K: Therapeutic differentiation and maturation of lymphatic vessels after lymph node dissection and transplantation. Nat Med 13: 1458-1466, 2007
35. Karnezis T, Shayan R, Caesar C, Roufail S, Harris NC, Ardipradja K, Zhang YF, Williams SP, Farnsworth RH, Chai MG, Rupasinghe TW, Tull DL, Baldwin ME, Sloan EK, Fox SB, Achen MG & Stacker SA: VEGF-D promotes tumor metastasis by

regulating prostaglandins produced by the collecting lymphatic endothelium. Cancer Cell 21: 181-195, 2012
36. Iwata C, Kano MR, Komuro A, Oka M, Kiyono K, Johansson E, Morishita Y, Yashiro M, Hirakawa K, Kaminishi M & Miyazono K: Inhibition of cyclooxygenase-2 suppresses lymph node metastasis via reduction of lymphangiogenesis. Cancer Res 67: 10181-10189, 2007
37. Kim YL: Update on mechanisms of ultrafiltration failure. Perit Dial Int 29(S2): S123-S127, 2009
38. Parikova A, Smit W, Struijk DG & Krediet RT: Analysis of fluid transport pathways and their determinants in peritoneal dialysis patients with ultrafiltration failure. Kidney Int 70: 1988-1994, 2006
39. Ni J, Verbavatz JM, Rippe A, Boisdé I, Moulin P, Rippe B, Verkman AS & Devuyst O: Aquaporin-1 plays an essential role in water permeability and ultrafiltration during peritoneal dialysis. Kidney Int 69: 1518-1525, 2006
40. de Arteaga J, Ledesma F, Garay G, Chiurchiu C, de la Fuente J, Douthat W, Massari P, Terryn S & Devuyst O: High-dose steroid treatment increases free water transport in peritoneal dialysis patients. Nephrol Dial Transplant 26: 4142-4145, 2011
41. Yang WS, Tsai TJ, Shih CL, Huang JW, Chuang HF, Chen MH & Fang CC: Intraperitoneal vascular endothelial growth factor C level is related to peritoneal dialysis ultrafiltration. Blood Purif 28: 69-74, 2009
42. Matsui K, Nagy-Bojarsky K, Laakkonen P, Krieger S, Mechtler K, Uchida S, Geleff S, Kang DH, Johnson RJ & Kerjaschki D: Lymphatic microvessels in the rat remnant kidney model of renal fibrosis: aminopeptidase p and podoplanin are discriminatory markers for endothelial cells of blood and lymphatic vessels. J Am Soc Nephrol 14: 1981-1989, 2003
43. Kerjaschki D: The crucial role of macrophages in lymphangiogenesis. J Clin Invest 115: 2316–2319, 2005
44. Kim KE, Koh YJ, Jeon BH, Jang C, Han J, Kataru RP, Schwendener RA, Kim JM & Koh GY: Role of CD11b+ macrophages in intraperitoneal lipopolysaccharide-induced aberrant lymphangiogenesis and lymphatic function in the diaphragm. Am J Pathol 175: 1733-1745, 2009
45. Maruyama K, Ii M, Cursiefen C, Jackson DG, Keino H, Tomita M, Van Rooijen N, Takenaka H, D'Amore PA, Stein-Streilein J, Losordo DW & Streilein JW: Inflammation-induced lymphangiogenesis in the cornea arises from CD11b-positive macrophages. J Clin Invest 115: 2363-2372, 2005
46. Ristimäki A, Narko K, Enholm B, Joukov V & Alitalo K: Proinflammatory Cytokines Regulate Expression of the Lymphatic Endothelial Mitogen Vascular Endothelial Growth Factor-C. J Biol Chem 273: 8413-8418, 1998
47. Lai KN, Lai KB, Szeto CC, Lam CW & Leung JC: Growth factors in continuous ambulatory peritoneal dialysis effluent. Their relation with peritoneal transport of small solutes. Am J Nephrol 19: 416-422, 1999

48. Zweers MM, de Waart DR, Smit W, Struijk DG & Krediet RT: Growth factors VEGF and TGF-beta1 in peritoneal dialysis. J Lab Clin Med 134: 124-132, 1999
49. Kang DH, Hong YS, Lim HJ, Choi JH, Han DS & Yoon KI: High glucose solution and spent dialysate stimulate the synthesis of transforming growth factor-beta1 of human peritoneal mesothelial cells: effect of cytokine costimulation. Perit Dial Int 19: 221-230, 1999
50. De Vriese AS, Tilton RG, Mortier S & Lameire NH: Myofibroblast transdifferentiation of mesothelial cells is mediated by RAGE and contributes to peritoneal fibrosis in uraemia. Nephrol Dial Transplant 21: 2549-2555, 2006
51. Leung JC, Chan LY, Tam KY, Tang SC, Lam MF, Cheng AS, Chu KM & Lai KN: Regulation of CCN2/CTGF and related cytokines in cultured peritoneal cells under conditions simulating peritoneal dialysis. Nephrol Dial Transplant 24: 458-469, 2009
52. Abu-Hijleh MF, Habbal OA & Moqattash ST: The role of the diaphragm in lymphatic absorption from the peritoneal cavity. J Anat 186: 453-467, 1995
53. Mactier RA, Khanna R, Twardowski Z, Moore H & Nolph KD: Contribution of lymphatic absorption to loss of ultrafiltration and solute clearances in continuous ambulatory peritoneal dialysis. J Clin Invest 80: 1311-1316, 1987
54. Burkart JM & Piraino B: Clinical Practice Guidelines and Clinical Practice Recommendations 2006 Updates: Peritoneal Dialysis Adequacy. Am J Kidney Dis 48(Suppl. 1): S91-S175, 2006
55. Lai KN, Lai KB, Lam CW, Chan TM, Li FK & Leung JC: Changes of cytokine profiles during peritonitis in patients on continuous ambulatory peritoneal dialysis. Am J Kidney Dis 35: 644-652, 2000
56. Twardowski ZJ: The fast peritoneal equilibration test. Semin Dial 3: 141-142, 1990
57. Honda K, Hamada C, Nakayama M, Miyazaki M, Sherif AM, Harada T, Hirano H & Peritoneal Biopsy Study Group of the Japanese Society for Peritoneal Dialysis: Impact of uremia, diabetes, and peritoneal dialysis itself on the pathogenesis of peritoneal sclerosis: a quantitative study of peritoneal membrane morphology. Clin J Am Soc Nephrol 3: 720-728, 2008
58. Nishimura H, Ito Y, Mizuno M, Tanaka A, Morita Y, Maruyama S, Yuzawa Y & Matsuo S: Mineralocorticoid receptor blockade ameliorates peritoneal fibrosis in new rat peritonitis model. Am J Physiol Renal Physiol 294: F1084-1093, 2008
59. Grimaldi A, Moriondo A, Sciacca L, Guidali ML, Tettamanti G & Negrini D: Functional arrangement of rat diaphragmatic initial lymphatic network. Am J Physiol Heart Circ Physiol 291: H876-885, 2006
60. Kato H, Mizuno T, Mizuno M, Sawai A, Suzuki Y, Kinashi H, Nagura F, Maruyama S, Noda Y, Yamada K, Matsuo S & Ito Y: Atrial natriuretic peptide ameliorates peritoneal fibrosis in rat peritonitis model. Nephrol Dial Transplant 27: 526-36, 2012

SUPPLEMENTAL

Supplementary Figure 1

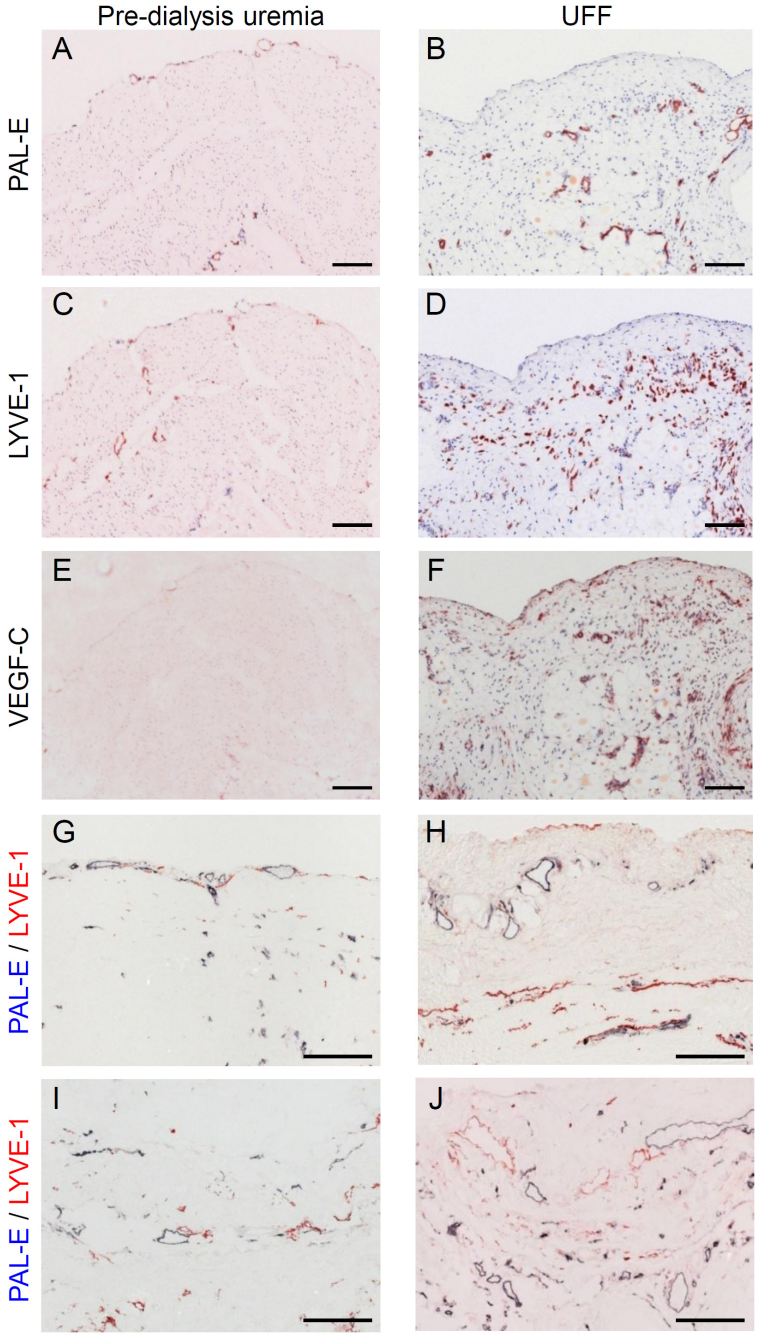

Supplementary Figure 1. The number of lymphatic vessels and VEGF-C expression were increased in UFF-peritoneum compared to pre-dialysis uremia peritoneum. Peritoneum was analyzed by immunohistochemistry. Lymphatic vessels were stained with an anti-LYVE-1 antibody. Blood vessels were stained with an anti-Pathologische Anatomie Leiden Endothelium (PAL-E) antibody. Some mononuclear cells and non-vascular structures were revealed in immunostaining of LYVE-1 (D, G-J). These cells may be derived from other cells, such as macrophages, which may potentially transform to the lymphatic vessels (Ref. 1-3). A and B: PAL-E, C and D: LYVE-1, E and F: VEGF-C, G-J: double staining of LYVE-1 (red) and PAL-E (blue). (A, C and E) and (B, D and F) were serial sections of the same patient. Scale bars, 200 μm.

References

1. El-Chemaly S, Malide D, Zudaire E, Ikeda Y, Weinberg BA, Pacheco-Rodriguez G, Rosas IO, Aparicio M, Ren P, MacDonald SD, Wu HP, Nathan SD, Cuttitta F, McCoy JP, Gochuico BR & Moss J: Abnormal lymphangiogenesis in idiopathic pulmonary fibrosis with insights into cellular and molecular mechanisms. Proc Natl Acad Sci U S A 106: 3958-3963, 2009
2. Maruyama K, Ii M, Cursiefen C, Jackson DG, Keino H, Tomita M, Van Rooijen N, Takenaka H, D'Amore PA, Stein-Streilein J, Losordo DW & Streilein JW: Inflammation-induced lymphangiogenesis in the cornea arises from CD11b-positive macrophages. J Clin Invest 115: 2363-2372, 2005
3. Kerjaschki D: The crucial role of macrophages in lymphangiogenesis. J Clin Invest 115: 2316–2319, 2005

Supplementary Figure 2

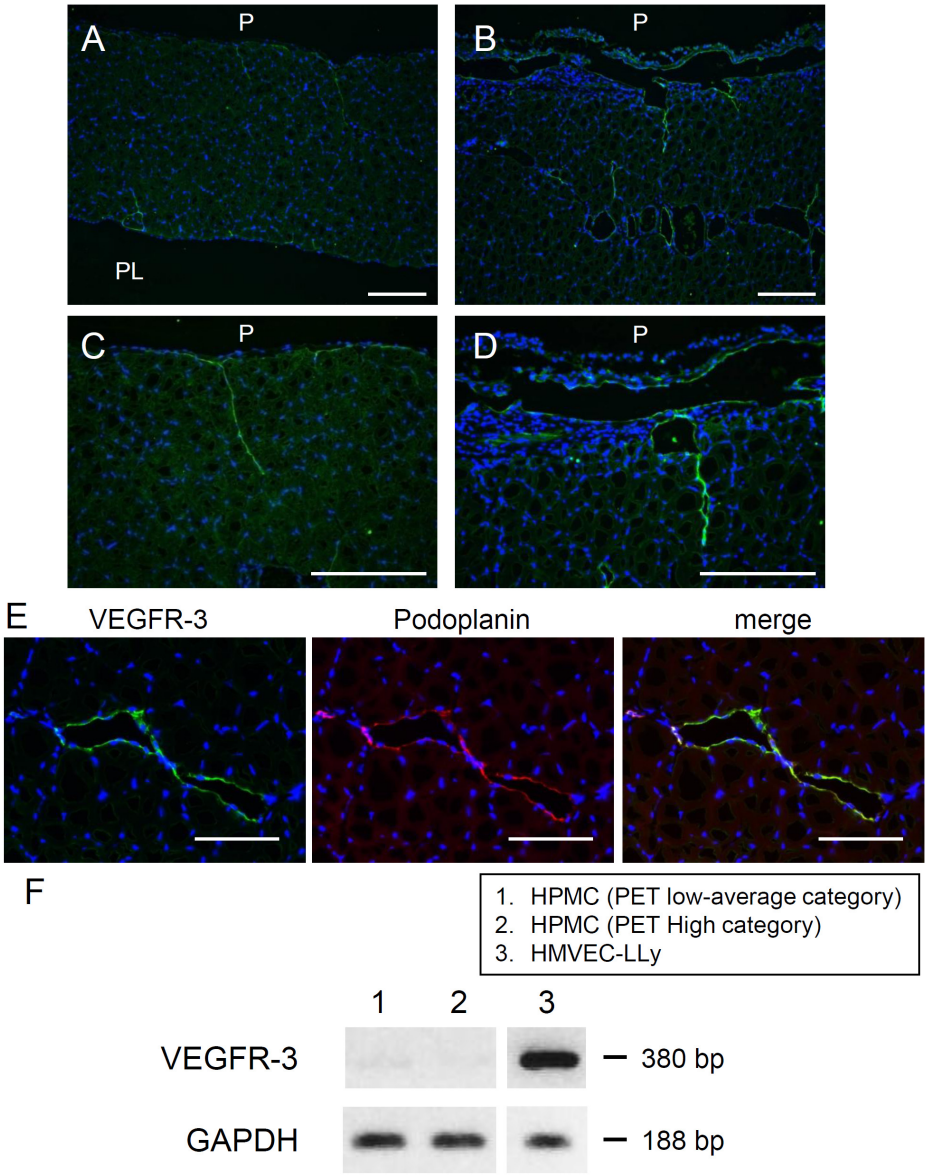

HPMC: human peritoneal mesothelial cells
HMVEC-LLy: normal human lymphatic microvasucular endothelial cells

Supplementary Figure 2. Analysis of VEGF receptor-3 (VEGFR-3) expression in the diaphragm of control and CG model rats and in human peritoneal mesothelial cells and normal human lymphatic microvascular endothelial cells. (A-E) Immunofluorescent staining of VEGFR-3 (green) in the diaphragms of representative control (A and C) and CG model (B and D) rats. Nuclei were counterstained with DAPI (blue). The level of VEGFR-3 expression, which was detected in the lymphatics, was increased in the CG model. E: Double staining of VEGFR-3 and podoplanin in the diaphragm of a CG rat. Scale bars, 200 μm. F: RT-PCR analysis of the mRNA expression of VEGFR-3, in human peritoneal mesothelial cells (HPMC) from patients with high and low peritoneal transport, and in normal human lymphatic microvascular endothelial cells (HMVEC-LLy). GAPDH was used as a loading control. VEGFR-3 mRNA was only detected in HMVEC-LLy cells.
Methods. HMVEC-LLy cells were purchased from Lonza Bioscience (Basel, Switzerland). The reverse transcription polymerase chain reaction (RT-PCR) was performed using the Hot-StarTaq PCR kit (Qiagen), as described previously (1, 2). PCR cycling conditions were as follows: initial denaturation (15 min at 94 °C) followed by 35 cycles of denaturation (1 min at 94 °C), annealing (45 s at 62 °C), and elongation (1 min at 72 °C). After the last cycle, a final extension (7 min at 72 °C) was added and thereafter the samples were kept at 4 °C. PCR products were electrophoresed on 2% agarose gels in Tris acetate EDTA buffer, followed by staining with ethidium bromide.
The sequences of the primers used were;
Human VEGFR-3 (Ref. 3)
forward: 5'-CCCACGCAGACATCAAGACG-3'
reverse: 5'-TGCAGAACTCCACGATCACC-3' (380bp)
Human GAPDH (Ref. 1)
forward: 5'-ATCATCCCTGCCTCTACTGG-3'
reverse: 5'-CCCTCCGACGCCTGCTTCAC-3' (188bp)

References

1. Takei Y, Kadomatsu K, Yuzawa Y, et al. A small interfering RNA targeting vascular endothelial growth factor as cancer therapeutics. Cancer Res 64: 3365-3370, 2004
2. Suzuki Y, Ito Y, Mizuno M , et al. Transforming growth factor-b induces vascular endothelial growth factor-C expression leading to lymphangiogenesis in rat unilateral ureteral obstruction. Kidney Int 81: 865-879, 2012
3. Gockel I, Moehler M, Frerichs K, et al. Co-expression of receptor tyrosine kinases in esophageal adenocarcinoma and squamous cell cancer. Oncol Rep 20: 845-850, 2008

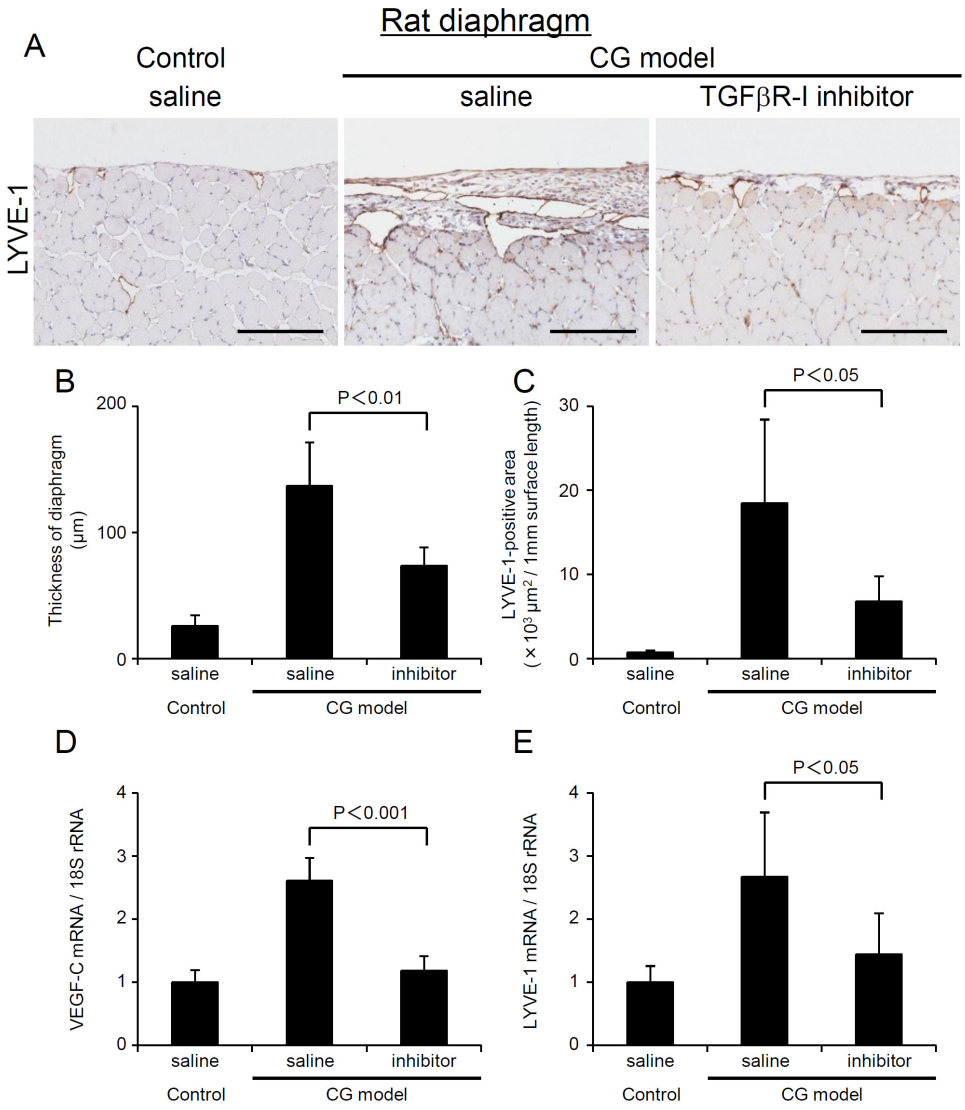

Supplementary Figure 3. Immunohistochemical analyses, and real-time PCR analyses of selected mRNAs, in the diaphragm of TGFβR-I inhibitor-treated and untreated (saline) rats. Lymphangiogenesis was suppressed by the TGFβR-I inhibitor. A: LYVE-1 staining of inhibitor-treated, untreated and control rats. Scale bars, 200 μm. B: The thickness of the diaphragm was significantly reduced by TGFβR-I inhibitor treatment of CG model rats. C: The size of the LYVE-1-positive area, as analyzed by MetaMorph, was significantly reduced by treatment with the TGFβR-I inhibitor. D and E: The increased expression of VEGF-C and LYVE-1 mRNA in the CG model rats was suppressed by TGFβR-I inhibitor treatment.

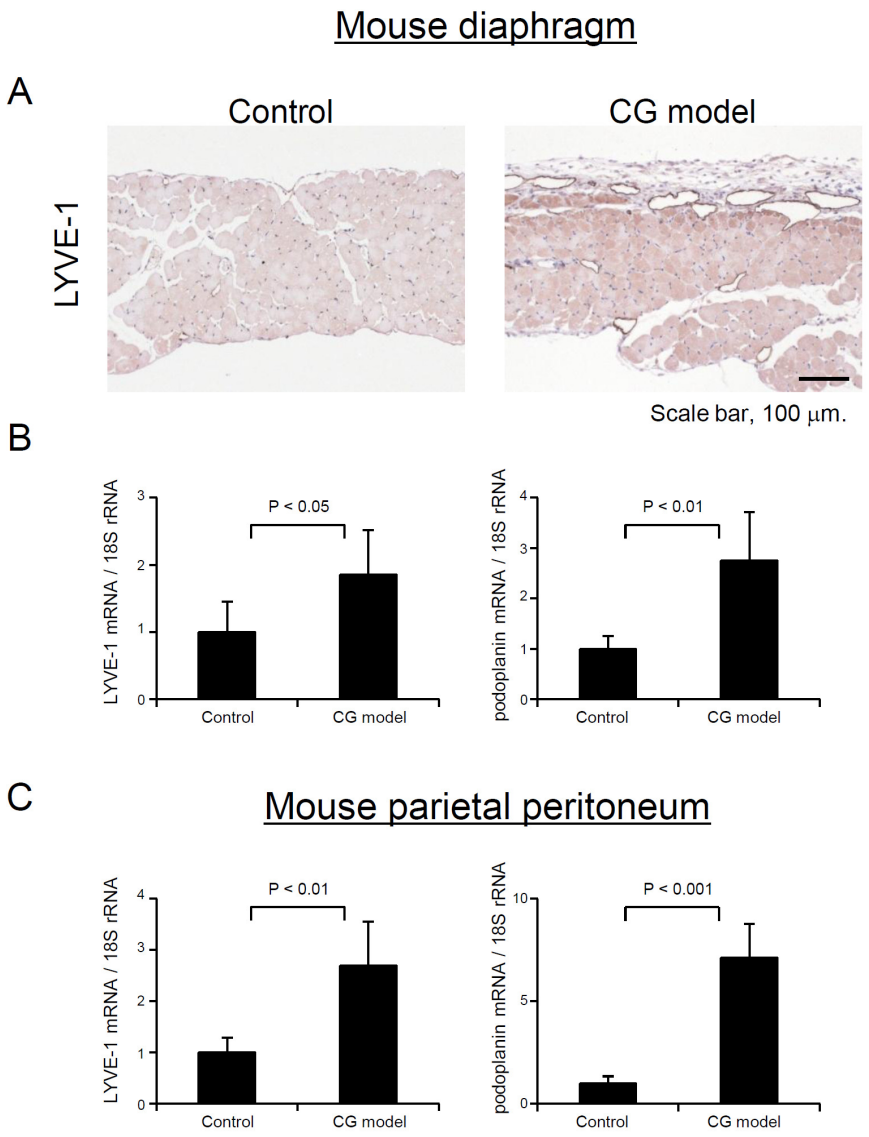

Supplementary Figure 4. The CG model in mice is similar to that in rats. Serial section analysis showed that the lymphatic vessels were connected to the central collector of the lymphatic vessels. Lymphangiogenesis developed in both the parietal peritoneum and diaphragm, which was similar to the rat CG model (A-C). Lymphatic vessels grown in the diaphragm were connected to the central collector of lymphatic vessels (D). Blue arrows in (D-4) of serial sections indicate the possible route of the passage for lymphatic fluid. (A, B) mouse diaphragm; (C) mouse parietal peritoneum.

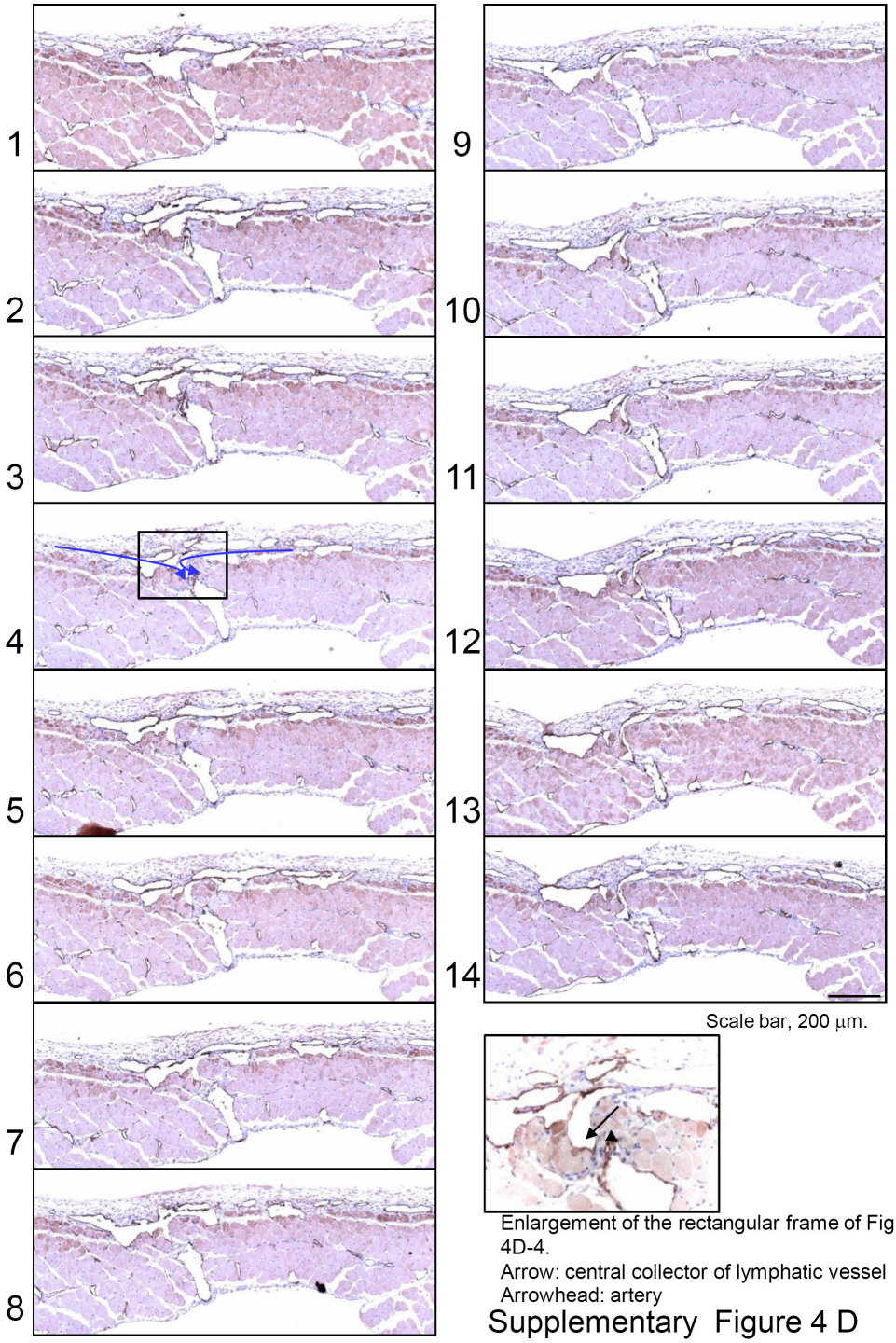

Scale bar, 200 μm.

Enlargement of the rectangular frame of Fig. 4D-4.
Arrow: central collector of lymphatic vessel
Arrowhead: artery

Supplementary Figure 4 D

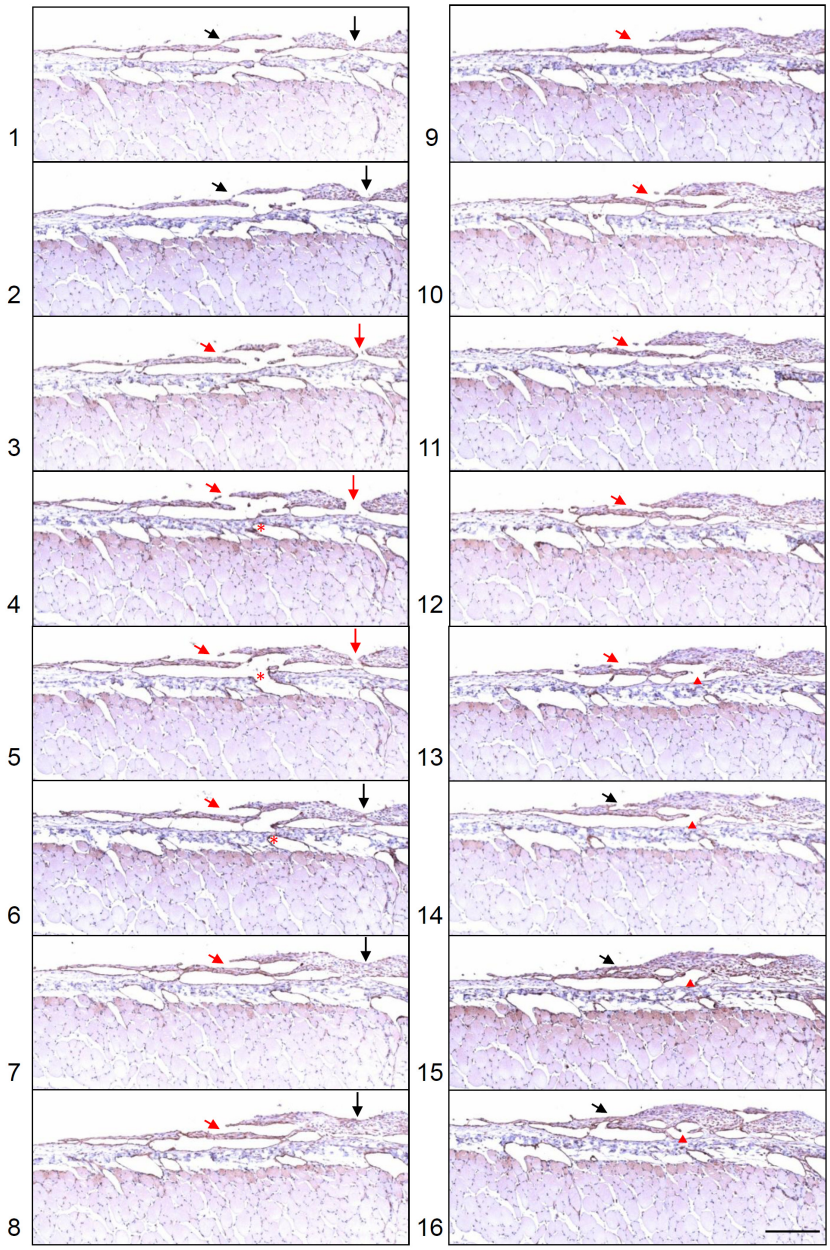

Supplementary Figure 5. Newly synthesized lymphatic vessels with entrance were revealed in the diaphragm. On analysis of the serial sections, newly synthesized lymphatic vessels with entrance (red arrows) were revealed in the fibrotic diaphragm. Black arrows indicate the edges or surroundings of the entrance of the lymphatic vessels. *(in 4-6) and ▲(in 13-16) indicate the connections of newly synthesized lymphatic vessel system. Scale bar, 200 μm.

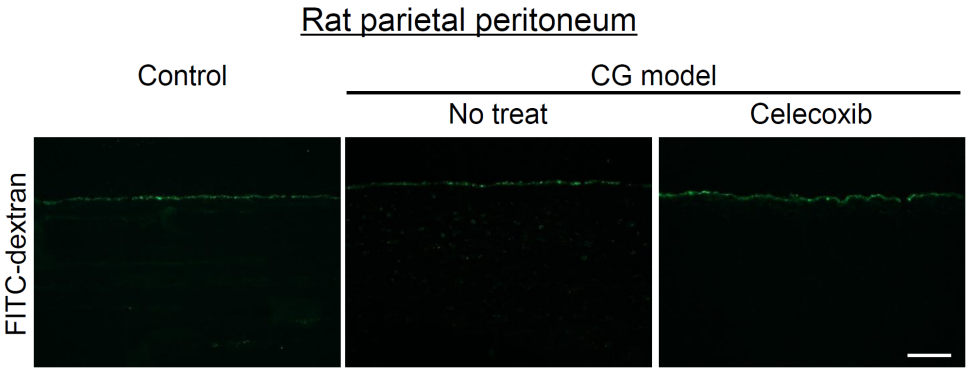

Supplementary Figure 6. There was barely detectable FITC-dextran in the parietal peritoneum, except on the surface of the peritoneum, as seen by immunofluorescence microscopy after administration of 50 mg FITC-dextran intraperitoneally. Left panel: control. Middle panel: CG model with no treatment. Right panel: CG model treated with COX-2 inhibitor, Celecoxib. Scale bar, 100 μm.

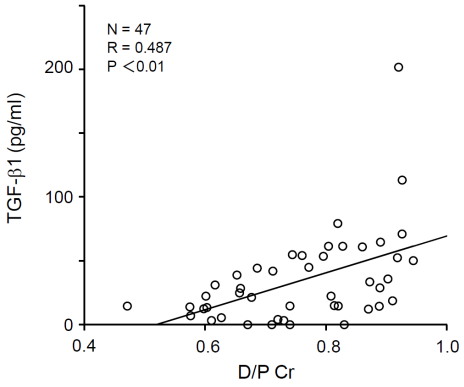

Supplementary Figure 7. The concentration of TGF-β1 protein in human PD effluent was correlated with D/P Cr. There was a positive correlation between TGF-β1 concentration in the PD effluent of 4-h-dwelled samples and D/P Cr.

Supplementary Table 1. List of the antibodies used

Antibody	company
mouse anti-PAL-E antibody	Abcam, Cambridge, UK
rabbit anti-human LYVE-1 antibody	Acris Antibodies GmbH, Hiddenhausen, Germany
rabbit anti-mouse LYVE-1 antibody	Acris Antibodies GmbH, Herford, Germany
rabbit anti-VEGF-C antibody	Zymed Laboratories, South San Francisco, CA
mouse anti-cytokeratin antibody	Dako, Glostrup, Denmark
mouse anti-CD68 antibody	Dako, Glostrup, Denmark
mouse anti-rat podoplanin antibody	Relia Tech GmbH, Braunschweig, Germany
goat anti-VEGFR3 (Flt-4) antibody	R&D System, Minneapolis, MN
mouse anti-rat monocyte/macrophage antibody (ED1)	BMA Biomedicals AG, Augst, Switzerland
rabbit anti-type III collagen antibody	LSL, Nagahama, Japan
mouse anti α-SMA antibody (1A4)	Dako, Glostrup, Denmark
rabbit anti-TGF-β1 antibody	Techne, Minneapolis, MN
FITC-labeled rabbit anti-mouse IgG	Invitrogen, Camarillo, CA
FITC-labeled goat anti-rabbit IgG	Invitrogen, Camarillo, CA
FITC-labeled rabbit anti-goat IgG	Sigma, Saint Louis, Missouri, USA
rhodamine labeled goat anti-rabbit IgG	Chemicon, Billerica, MA
rhodamine labeled rabbit anti-mouse IgG	Zymed Laboratories, Carlsbad, CA
DAPI (diamidino-2-phenylindole)	Sigma-Aldrich, St. Louis, MO

Supplementary Table 2. Primers used for real-time PCR (TaqMan Gene Expression Assays)

	Assay identification number
human VEGF-C	Hs00153458_m1
human LYVE-1	Hs00272659_m1
human podoplanin	Hs00366764_m1
rat TGF-β1	Rn00572010_m1
rat VEGF-C	Rn00586458_m1
rat LYVE-1	Rn01510422_m1
rat podoplanin	Rn00571195_m1
rat VEGFR3	Rn00586429_m1
rat type III collagen	Rn01437683_m1
18S ribosomal RNA	4319413E

4

Vascular endothelial growth factor receptor-3 is a novel target to improve net ultrafiltration in methylglyoxal-induced peritoneal injury

Lab Invest. 2015;95(9):1029-43

Takeshi Terabayashi[1], Yasuhiko Ito[1], Masashi Mizuno[1], Yasuhiro Suzuki[1], Hiroshi Kinashi[1], Fumiko Sakata[1], Takako Tomita[1], Daiki Iguchi[1], Mitsuhiro Tawada[1], Ryosuke Nishio[2], Shoichi Maruyama[1], Enyu Imai[1,3], Seiichi Matsuo[1], and Yoshifumi Takei[4]

[1]Department of Nephrology and Renal Replacement Therapy, Nagoya University Graduate School of Medicine, Nagoya, Japan
[2]Department of Emergency Medicine, Kyoto University Hospital, Kyoto, Japan
[3]Nakayamadera Imai Clinic, Takarazuka, Japan
[4]Department of Biochemistry, Nagoya University Graduate School of Medicine, Nagoya, Japan

ABSTRACT

Appropriate fluid balance is important for good clinical outcomes and survival in patients on peritoneal dialysis. We recently reported that lymphangiogenesis associated with fibrosis developed in the peritoneal cavity via the transforming growth factor-β1-vascular endothelial growth factor-C (VEGF-C) pathway. We investigated whether VEGF receptor-3 (VEGFR-3), the receptor for VEGF-C and -D, might be a new target to improve net ultrafiltration by using adenovirus-expressing soluble VEGFR-3 (Adeno-sVEGFR-3) in rodent models of peritoneal injury induced by methylglyoxal (MGO). We demonstrated that lymphangiogenesis developed in these MGO models, especially in the diaphragm, indicating that lymphangiogenesis is a common feature in the peritoneal cavity with inflammation and fibrosis. In MGO models, VEGF-D was significantly increased in the diaphragm; however, VEGF-C was not significantly upregulated. Adeno-sVEGFR-3, which was detected on day 50 after administration via tail vein injections, successfully suppressed lymphangiogenesis in the diaphragm and parietal peritoneum in mouse MGO models without significant effects on fibrosis, inflammation, or neoangiogenesis. Drained volume in the peritoneal equilibration test using a 7.5% icodextrin peritoneal dialysis solution (the 7.5% icodextrin peritoneal equilibration test) was improved by Adeno-sVEGFR-3 on day 22 ($P<0.05$) and day 50 after reduction of inflammation ($P<0.01$), indicating that the 7.5% icodextrin peritoneal equilibration test identifies changes in lymphangiogenesis. The solute transport rate was not affected by suppression of lymphangiogenesis. In human peritoneal dialysis patients, the dialysate to plasma ratio of creatinine positively correlated with the dialysate VEGF-D concentration ($P<0.001$). VEGF-D mRNA was significantly higher in the peritoneal membranes of patients with ultrafiltration failure, indicating that VEGF-D is involved in the development of lymphangiogenesis in peritoneal dialysis patients. These results indicate that VEGFR-3 is a new target to improve net ultrafiltration by suppressing lymphatic absorption and that the 7.5% icodextrin peritoneal equilibration test is useful for estimation of lymphatic absorption.

INTRODUCTION

Maintenance of optimal fluid balance is important for good clinical outcomes and survival in patients who undergo peritoneal dialysis. Overhydration states, which are often associated with higher peritoneal transport rates, are reported to be a major cause for dialysis discontinuation.[1,2] The pathological features of peritoneal membrane injury in peritoneal dialysis patients with high solute transport rates are submesothelial fibrosis, accumulation of extracellular matrix, and neoangiogenesis.[3,4]

We recently showed that lymphangiogenesis and vascular endothelial growth factor-C (VEGF-C) expression, one of the key mediators of lymphangiogenesis, were associated with fibrosis using human tissues, peritoneal dialysis effluent samples, cultured cells derived from peritoneal dialysis effluent, and rat chlorhexidine gluconate -induced peritoneal injury models.[5] In those studies, we found that the VEGF-C content in the peritoneal dialysis effluent correlated with the peritoneal membrane transport rate and transforming growth factor-beta (TGF-β) concentration, and that expression of VEGF-C and markers of lymphatics was higher in ultrafiltration failure-peritoneum.[5] In cultured mesothelial cells and macrophages, TGF-β–induced VEGF-C expression was blocked by a TGF-β type I receptor (TGFβRI) inhibitor.[5] Furthermore, VEGF-C expression and lymphangiogenesis were suppressed by the TGFβRI inhibitor or by the cyclooxygenase-2 (COX-2) inhibitor, celecoxib, in chlorhexidine gluconate-induced peritoneal injury models.[5] Thus, we proposed that lymphangiogenesis in the peritoneal membrane, similar to renal fibrosis is linked with the fibrotic process via the TGF-β–VEGF-C pathway.[6–8] The lymphatic absorption rate, which is measured by the rate at which intraperitoneally administered radioactive serum albumin or the macromolecule dextran 70 disappears, is significantly higher in patients with ultrafiltration failure, and lymphatic absorption is considered to be one of the causes of the decrease in net ultrafiltration.[9–12] However, the results from these clinical approaches have been controversial,[13,14] and there are no other methods available to assess lymphatic function.

In the present study, we investigated whether VEGF receptor-3 (VEGFR-3), the receptor for VEGF-C and -D, might be a new target to increase net ultrafiltration by suppression of lymphangiogenesis using an adenovirus-expressing soluble VEGFR-3 (Adeno-sVEGFR-3) fused with human IgG (Supplementary Figure 1) in models of murine peritoneal injury induced by methylglyoxal (MGO).[15–17] MGO is a precursor of advanced glycation end products, which accumulate in dialysis patients.[18] In addition, we proposed a new method for the peritoneal equilibration test by using a 7.5% icodextrin peritoneal dialysis solution (7.5% icodextrin peritoneal equilibration test) to assess lymphatic absorption (Supplementary Figure 1). Finally, we studied the expression of VEGF-D in lymphangiogenesis in human samples.

MATERIALS AND METHODS

MGO-Induced Peritoneal Injury Model

All animal studies were carried out in accordance with the Animal Experimentation Guidelines of Nagoya University Graduate School of Medicine (Nagoya, Japan). Ten-week-old male C57BL/6J mice (Japan SLC, Hamamatsu, Japan) initially weighing 24–29 g were used throughout the study. The animals were maintained under conventional laboratory conditions and had free access to food and water. The mice received an intraperitoneal injection of 100 ml/kg body weight of peritoneal dialysis fluid (Dianeal-N PD-4-2.5, 2.27% glucose, Baxter, Tokyo, Japan) containing 20 mmol/l MGO (MP Biomedicals LLC, Illkirch, France) for 3 weeks, 5 consecutive days per week as described previously[17] (Experiment 1, Supplementary Figure 2a). Control mice received the same dosage of peritoneal dialysis fluid without MGO. This peritoneal dialysis fluid was prepared by purification through a 0.2-μm pore-size filter and by adjustment to pH 5.0 immediately before injection every day. The mice were killed on day 22, and parietal peritoneal and diaphragmatic samples were procured. The harvested samples were used for immunohistochemical analysis of lymphatic vessel endothelial hyaluronan receptor-1 (LYVE-1), VEGFR-3, CD31, type III collagen, CD68, and VEGF-D, and for analysis of the mRNA expression of VEGF-D, VEGFR-3, LYVE-1, and CD31.

MGO Model Mice and Studies of Lymphangiogenesis Inhibition using an Adenovirus Vector

The experimental design and protocols are as follows (Supplementary Figure 2):
(a) Experiment 1: development of a MGO-induced peritoneal injury model in mice. The mice received peritoneal dialysis fluid (100ml/kg) with MGO (20mM) intraperitoneally from day 1 until day 22 (Supplementary Figure 2a).
(b) Experiment 2: inhibition studies using an adenovirus-expressing sVEGFR-3 and a control adenovirus-expressing Lac Z in a MGO-induced peritoneal injury model. Recombinant Adeno-sVEGFR-3 or β-galactosidase (Adeno-LacZ) were kindly provided by K Alitalo (the University of Helsinki, Helsinki, Finland) and were amplified and purified for use as described previously.[19–21] On day 0, prior to establishment of MGO-induced peritoneal injury as in **a**, the mice were first administered 1.0×10^9 p.f.u. of one of the adenoviral vectors intravenously through the tail vein. On day 22, the mice were assessed using a conventional peritoneal equilibration test with a 4.25% glucose-based peritoneal dialysis fluid and a peritoneal equilibration test with 7.5% icodextrin (Adeno-LacZ Day 22 group and Adeno-sVEGFR-3 Day 22 groups; Supplementary Figure 2b).
(c) Experiment 3: development of a MGO-induced peritoneal injury model with peritoneal rest from day 22 to day 50. The mice were treated as in **a** until day 22. From day 22 until their sacrifice on day 50 no dialysate was infused into the peritoneal cavity (peritoneal rest) (Supplementary Figure 2c).
(d) Experiment 4: inhibition studies using adenovirus-expressing sVEGFR-3 and control adenovirus-expressing Lac Z in a MGO model as in **b** except that the mice further underwent peritoneal lavage using a 1.5% peritoneal dialysis fluid from day 22 to day 50. For this treatment, the mice received an intraperitoneal injection of 100 ml/kg body weight

of a low concentration peritoneal dialysis fluid (Dianeal-N PD-4 1.5, 1.36% glucose) for 20 days, 5 consecutive days per week. This procedure is similar to a previously reported method.[22] In these mice, peritoneal functions were assessed on day 50 using a conventional peritoneal equilibration test with a 4.25% glucose-based peritoneal dialysis fluid and a peritoneal equilibration test with a 7.5% icodextrin peritoneal dialysis fluid (Adeno-LacZ Day 50 group and Adeno-sVEGFR-3 Day 50 group; Supplementary Figure 2d).

Tissue and blood samples were also obtained from the mice for further analysis.

Histology and Immunohistochemistry

Routine histological and immunohistological analyses of animal and human tissues were performed and assessed as we described previously.[5–7,23,24] The antibodies used are listed in Supplementary Table 1. Mast cells were evaluated using sections stained with 0.2% toluidine blue.

RNA Preparation from Peritoneal and Diaphragm Tissues, and PCR Analysis

Animal peritoneal and diaphragm tissues were immersed in RNAlater (Ambion, Austin, TX, USA) for 41 day. RNA preparation and the synthesis of first-strand cDNA were performed as described previously.[5–7,23,24] Total RNA (1 μg) was then reverse transcribed. Quantitative real-time PCR (qPCR) analysis was performed with an Applied Biosystems (South San Francisco, CA, USA) Prism 7500HT sequence detection system using TaqMan gene expression assays as described previously.[24] The TaqMan Gene Expression Assays (Applied Biosystems) used are described in Supplementary Table 2. 18S ribosomal RNA was used as an endogenous control.[5,7,23,24]

Assessment of Lymphatic Absorption

To assess absorption via the lymphatic vessels, animals that received 2000 μl of 7.5% icodextrin peritoneal dialysis solution into the peritoneal cavity were killed at 4 h after infusion. An accurate drained volume was measured.

Enzyme-Linked Immunosorbent Assays (ELISAs)

The concentration of sVEGFR-3-Ig fusion protein in the serum was determined using an ELISA kit for human IgG1 (Cayman Chemical Company, Ann Arbor, MI, USA) as described previously.[25] Levels of VEGF-D protein and prostaglandin E2 (PGE2) in the peritoneal dialysis effluent were measured using the ELISA kits for human VEGF-D (R&D Systems, Minneapolis, MN, USA) and PGE2 (Cayman Chemical Company), respectively, according to the manufacturers' instructions. The samples were frozen at the time of collection and were stored at − 80 °C. The samples were not subjected to freeze–thaw cycles.

Human Patient Studies

All of the studies were approved by the Ethics Committee for Human Research of the Faculty of Medicine, Nagoya University (Approval #298 and #299). All patients provided informed consent prior to participation in this study.

VEGF-D Concentration in the Peritoneal Effluent of Peritoneal Dialysis Patients

The VEGF-D concentrations in dialysates were measured in overnight-dwelled (8.95± 1.63 h) samples collected from 83 peritoneal dialysis patients (27 women and 56 men) who were treated between July 2005 and April 2008 in the Department of Nephrology and Renal Replacement Therapy of Nagoya University Hospital (Nagoya, Japan) and at affiliated hospitals.[5] This is the same cohort in which VEGF-C was measured in recent studies.[5] The mean age of all patients was 55.9± 13.5 (range, 28 to 89) years, and the mean duration of peritoneal dialysis treatment was 31.9± 32.0 (range, 1 to 132) months.[5] Diabetic nephropathy was the cause of end-stage renal disease in 27 peritoneal dialysis patients (32.5%). All patients were free from peritonitis for at least 1 month prior to the study, and patients with other diseases, such as liver or lung diseases and malignancy, were excluded. Patients undergoing combination therapy (hemodialysis + peritoneal dialysis) were not included in this study. Peritoneal membrane transport was assessed based on the dialysate to plasma ratio of creatinine, and the average value was 0.67± 0.14 (range, 0.28 to 0.96).[5] A fast peritoneal equilibration test was performed using a 2.27% glucose-based dialysis solution (Dianeal-N PD-4) as described by Twardowski et al (Supplementary Information 1).[26] The correlation between VEGF-D concentration in the peritoneal dialysis effluent and the dialysate to plasma ratio of creatinine was analyzed. In addition, we measured the VEGF-D concentration in peritoneal effluent samples at 4 h of the peritoneal equilibration test. These samples were collected from 40 peritoneal dialysis patients (13 women and 27 men) treated between November 2008 and June 2009 at the Handa Municipal Hospital and the Nagoya University Hospital. The mean age of all patients was 52.9 ±10.9 (range, 30 to 70) years, and the mean duration of peritoneal dialysis treatment was 26.1± 24.6 (range, 1 to 103) months.[5,23]

VEGF-D mRNA Expression in the Human Peritoneum

Fifty-four peritoneal tissue samples were obtained from 29 peritoneal dialysis patients and 25 pre-dialysis chronic renal failure patients at the time of peritoneal dialysis catheter insertion. Among the 29 peritoneal dialysis patients, 7 were regarded as having impaired ultrafiltration capacity, which was defined as described previously.[5,23,27] Twenty-two patients (incident) had their catheters removed because of transplantation, severe exit site infection, mental disorders, or difficulty in performing the bag exchanges (Table 1).

VEGF-D mRNA Expression in the Cultured Mesothelial Cells

Reverse Transcription–PCR (RT–PCR) was performed using the HotStarTaq PCR kit (Qiagen, Tokyo, Japan)[7,28] to examine whether VEGF-D mRNA was expressed in three kinds of mesothelial cells: the human mesothelial cell line Met5A,[5,23] mesothelial cells from

the peritoneal dialysis effluent of the patients on peritoneal dialysis,[5,23] and mesothelial cells derived from the omentum.[29,30] The primers according to the reported sequences of human VEGF-D and GAPDH were 5′-GTATGGACTCTCGCTCAGCAT-3′ (sense) and 5′-AGGCTCTCTTCATTGCAACAG-3′ (antisense, PCR products 225 bp);[31] and 5′-ATCATCCCTGCCTCTACTGG-3′ (sense) and 5′-CCCTCCGACGCCTGCTTCAC-3′ (antisense, PCR products 188 bp),[28] respectively.

Statistical Analyses

The Shapiro–Wilk test was applied to test normal distributions. Values are expressed as mean ± s.d. Differences between two groups were analyzed by the unpaired t-test or by the Mann–Whitney U-test. Comparisons among groups were performed by one-way analysis of variance with the Tukey's test, the Games–Howell test or the Dunnett's test, or by the Kruskal–Wallis multiple comparison test. Spearman's correlation coefficient was used to analyze correlations. Differences were considered to be statistically significant if $P<0.05$. All analyses were performed using SPSS software (SPSS, Chicago, IL, USA).

RESULTS

Lymphangiogenesis Developed in a MGO-Induced Peritoneal Injury Model

Twenty-two days after administration of MGO (Experiment 1, Supplementary Figure 2a) LYVE-1- and podoplanin-positive lymphatic vessels were increased and dilated in the diaphragm of MGO model mice compared with controls (Figure 1a,Supplementary Figure 3); however, lymphangiogenesis was not pronounced or significant in the parietal peritoneum wall (Figure 1a). In contrast, as shown in Supplementary Figure 4, in the advanced fibrotic area of the diaphragm entrances (red arrows) of newly developed lymphatic vessels were revealed in the fibrotic diaphragm. CD31-positive vessels, indicating neoangiogenesis ($P<0.05$; Figure 1b), expression of type III collagen, indicating fibrosis ($P<0.01$; Figure 1c), and CD68-positive macrophages, indicating inflammation ($P<0.05$; Figure 1d), were significantly increased in the diaphragm of the MGO models, but were not significantly increased in parietal peritoneal membranes. To confirm these immunohistochemical findings, we performed qPCR. Compared with normal mice, LYVE-1 ($P<0.01$), VEGFR-3 ($P<0.001$), and podoplanin mRNA ($P<0.001$), which are typical markers of lymphatic endothelial cells, were significantly increased in the diaphragm of the MGO model mice (Figure 2, Supplementary Figure 3). Although VEGF-D mRNA and protein expression were upregulated in the diaphragm of MGO model mice, VEGF-C mRNA and protein were not significantly increased compared with normal mice (Figure 2, Supplementary Figure 5). Neither VEGF-C nor -D were significantly elevated in parietal peritoneum, (Figure 2, Supplementary Figure 5). VEGF-C and -D proteins were undetectable in the serum and peritoneal dialysis fluid. Interestingly, expression of lymphatic vessels markers is higher in the diaphragm than in parietal peritoneum (Figure 2, Supplementary Figure 5). We also developed rat MGO models and found that lymphangiogenesis developed in the diaphragm, and that VEGF-D expression in the

diaphragm predominated over VEGF-C expression (Supplementary Figure 6). Double immunohistochemical staining indicated that the expression of LYVE-1-positive lymphatic vessels was similar to that of VEGFR-3-positive vessels (Figure 3a), and that VEGF-D was mainly expressed by CD68-positive macrophages in the MGO mouse model (Figure 3b and c), but not by mesothelial cells (data not shown). RT–PCR and ELISA using three different sources of cultured human mesothelial cells further suggested that neither VEGF-D mRNA (Figure 3d) nor protein (Figure 3e) is expressed by mesothelial cells.

sVEGFR-3 was Detected in Serum on Days 22 and 50 after Administration of the Adenovirus-Expressing sVEGFR-3

To investigate whether these occurrences of lymphangiogenesis were enhanced via VEGFR-3 activation, we performed inhibition studies using Adeno-sVEGFR-3, which traps both its VEGF-C and VEGF-D ligands. Serum sVEGFR-3 was detected on days 22 and 50 after its administration via tail vein injections, and its concentration was significantly higher on both days in mice injected with Adeno-sVEGFR-3 than in mice treated with Adeno-LacZ (Supplementary Figure 7). These results are consistent with previous reports.[19,20,32]

Adenovirus-sVEGFR3 Suppressed Lymphangiogenesis in the Diaphragm and Parietal Peritoneal Membrane of MGO Model Mice on Day 22

Expression of LYVE-1-positive lymphatic vessels in the diaphragm was significantly suppressed by Adeno-sVEGFR-3, but not by Adeno-LacZ (Figure 4a). However, there were no differences between mice treated with Adeno-sVEGFR-3 or Adeno-LacZ with respect to expression of CD31-positive vessels, type III collagen, or immune cells including CD68-positive macrophages, Ly6B-positive granulocytes, CD4 or CD8 T cells, or CD11c dendritic cells (Figure 4b–d, Supplementary Figure 8). In addition, the percentage of VEGF-D-positive macrophages was similar between the two groups (Supplementary Figure 9a). qPCR analysis indicated that, on day 22, LYVE-1 and VEGFR-3 mRNA were significantly suppressed by Adeno-sVEGFR-3 compared with Adeno-LacZ; however, neither VEGF-C nor VEGF-D mRNA or protein expression was significantly changed between the two groups (Figure 5, Supplementary Figure 9b and c). VEGF-C and -D proteins were undetectable in the serum of both groups. The extent of neoangiogenesis and fibrosis as assessed by analysis of CD31 and TGF-β1 mRNA levels was similar between the two groups (Figure 5e and f). These findings suggest that Adeno-sVEGFR-3 treatment specifically blocked the VEGFR-3 signaling pathway.

Analysis of Lymphatic Absorption on Day 22

To assess suppression of lymphangiogenesis by Adeno-sVEGFR-3, we performed a peritoneal equilibration test on day 22 using a 7.5% icodextrin peritoneal dialysis solution (Extraneal, Baxter), which is mainly absorbed via the lymphatic system.[33] In this peritoneal equilibration test (7.5% icodextrin peritoneal equilibration test), effluent volume was

recovered in mice in which lymphangiogenesis was suppressed by administration of Adeno-sVEGFR-3 (Figure 6a), although angiogenesis as assessed by CD31 analyses was similar between the Adeno-LacZ and Adeno-sVEGFR-3 groups (Figures 4b and 5e). Subsequently, we performed a conventional peritoneal equilibration test using a 4.25% glucose-based peritoneal dialysis fluid (4.25%G-peritoneal equilibration test, Dianeal) to assess peritoneal membrane transport. There was no difference in transport rates between the Adeno-LacZ and Adeno-sVEGFR-3 groups (Supplementary Figure 10a and b). On day 22, peritoneal inflammation associated with strong CD68-positive macrophage infiltration was shown (Figure 4d). It was thus considered that assessment of the peritoneal membrane function in mice was unsuitable under these conditions, as it is in human peritoneal dialysis patients with peritonitis.[34] We therefore re-assessed the peritoneal equilibration test after resolution of inflammatory changes in the peritoneal membranes. For this purpose, after development of lymphangiogenesis in MGO models on day 22, the mice were observed for 4 weeks to watch for reduction in peritoneal inflammation (Experiment 3, Supplementary Figure 2c). However, we had difficulty in performing the peritoneal equilibration test on day 50 because there were several adhesions in the peritoneal cavity due to inflammation in the peritoneum (Supplementary Figure 11a). Therefore, to prevent adhesions and to reduce the peritoneal inflammation, we administered a low concentration (1.5%) of a glucose-based peritoneal dialysis fluid into the peritoneal cavity 5 days per week from day 22 to day 50 (Experiment 4, Supplementary Figure 2d).

Analysis of Pathology and Function in the Peritoneal Membrane on Day 50 After Administration of a 1.5% Glucose-Based Solution for 4 Weeks

We found that peritoneal inflammation was successfully reduced by administration of the 1.5% glucose-based peritoneal dialysis fluid into the peritoneal cavity for 4 weeks, which enabled performance of a peritoneal equilibration test on day 50 (Supplementary Figure 11b). Leakage of PGE2 into the effluent, COX-2 mRNA expression, CD68-positive macrophages, and mast cell infiltration in the diaphragm were reduced on day 50 compared with day 22 in the Adeno-LacZ and Adeno-sVEGFR-3 groups (Figures 4d and 7). On day 50, the lymphatic vessels that were suppressed on day 22 continued to be suppressed in the Adeno-sVEGFR-3 group, and both the lymphangiogenesis and neoangiogenesis conditions were preserved from day 22 to day 50 (Figure 4a and b). Apparently, the progression of fibrosis as assessed by type III collagen expression was more advanced on day 50 compared with that on day 22; however, the extent of fibrosis was not different between the Adeno-sVEGFR-3 and Adeno-LacZ groups (Figure 4c). On day 50, we found a significant difference in fluid removal between the two groups in the 7.5% icodextrin peritoneal equilibration test (Figure 6a). This result indicates that the 7.5% icodextrin peritoneal equilibration test can assess fluid absorption via lymphatic vessels. In the 4.25%G-peritoneal equilibration test, we found a significant difference on day 22 between the control mice and the MGO model mice in the ratio of dialysate glucose at 2 h dwell time to dialysate glucose at 0 h dwell time; however, there was no difference on day 50, suggesting

that the low levels on day 22 may be due to vascular permeability with strong inflammation (Figure 7 and Supplementary Figure 10a). In addition, there was no difference in the ratio of dialysate glucose at 2 h dwell time to dialysate glucose at 0 h or in the dialysate to plasma ratio of creatinine between the groups (Supplementary Figure 10a and b), indicating that lymphatic vessels are not involved in the function of solute transport. Similar tendencies in pathological findings were observed in the parietal peritoneal membrane by treatment with Adeno-sVEGFR-3 and Adeno-LacZ (Supplementary Figure 12). Amylase concentration in the effluent was not different between the two groups on day 22 or day 50 (Figure 6b).

VEGF-D Concentration in Human Peritoneal Effluent Correlated with the Peritoneal Membrane Transport Rate. VEGF-D and VEGFR-3 mRNA Expression was Increased in Human Peritoneal Biopsy Samples of Ultrafiltration Failure

In human peritoneal dialysis patients, VEGF-D concentration was correlated with the dialysate to plasma ratio of creatinine in the peritoneal dialysis effluent of samples dwelled for 4 h ($R = 0.622$, $P<0.001$, Figure 8a). We further measured VEGF-D concentration in the overnight-dwelled peritoneal dialysis effluent of 83 patients; we found a positive correlation between the dialysate VEGF-D concentration and the dialysate to plasma ratio of creatinine ($R= 0.516$, $P<0.001$, Figure 8b). We assessed the VEGF-D mRNA expression in the peritoneal membrane of human biopsy samples (Table 1). VEGF-D mRNA was significantly higher in the peritoneum of ultrafiltration failure patients than in the peritoneal membrane from patients on peritoneal dialysis without ultrafiltration failure or from patients with pre-dialysis uremia (Figure 8c). In ultrafiltration failure, VEGFR-3 and LYVE-1 mRNA expression was elevated compared with the other patients (Figure 8d and Supplementary Figure 13). VEGF-D was mainly detected in CD68-positive macrophages of peritoneal biopsy samples of ultrafiltration failure patients (Figure 8e), which was similar to observations in the animal models (Figure 3b and c).

DISCUSSION

In the majority of organs, one of the main functions of lymphatic vessels is to return fluid and macromolecules to the vascular system.[35,36] In peritoneal dialysis, the net ultrafiltration volume at the end of an exchange equals the cumulative net transcapillary water transport minus the lymphatic absorption during the exchange;[37] therefore, control of lymphatic absorption is important to obtain higher drained volume. In a previous study using human materials and rat chlorhexidine gluconate models, we showed that lymphangiogenesis developed in the peritoneal cavity.[5] In the present study, we demonstrated that lymphangiogenesis developed in rodent MGO models and found that lymphatic vessels grow in association with inflammatory changes, especially in the diaphragm. These findings and our previous studies[5] indicate that lymphangiogenesis is a common feature in the peritoneal cavity, together with inflammation and fibrosis, and that lymphangiogenesis is more predominant in the diaphragm compared with that in the parietal peritoneal

membrane. Interestingly, in the MGO model animals on day 22, VEGF-D was significantly increased in the diaphragms of mice ($P<0.01$, Figure 2, $P<0.05$, Supplementary Figure 5) and rats ($P<0.05$, Supplementary Figure 6); however, VEGF-C was not significantly upregulated (Figure 2, Supplementary Figures 5 and 6). This situation was different from that of the chlorhexidine gluconate models.[5] In the chlorhexidine gluconate models of our previous studies, lymphangiogenesis was suppressed by COX-2 inhibitors; however, these drugs are not suitable for peritoneal dialysis patients in terms of preservation of residual renal function and are not suitable as specific inhibitors of lymphangiogenesis.[5] VEGFR-3, a receptor for both VEGF-C and -D, is expressed by lymphatic endothelial cells and is upregulated in both MGO (Figure 2, Supplementary Figure 6) and chlorhexidine gluconate models;[5] we therefore considered that VEGFR-3 is suitable as a target molecule to suppress lymphangiogenesis in the peritoneal cavity. The effect of sVEGFR-3 on inhibition of VEGFR-3 activation was similar to that of the VEGFR-3 kinase inhibitor in cultured human lymphatic endothelial cells stimulated with recombinant VEGF-D (Supplementary Figures 1 and 14).

In our previous studies,[5] we used immunofluorescence microscopy to detect the passage of fluorescein isothiocyanate (FITC)-dextran (molecular weight 2 000 000), which can only be absorbed through the lymphatic vessels in the diaphragm, and detected high FITC-dextran levels in the serum of the chlorhexidine gluconate models.[5] However, these methods are not appropriate for peritoneal dialysis patients. Therefore, we tried to develop practical methods using a 7.5% icodextrin peritoneal dialysis solution, which reflects lymphatic functions. Icodextrin is a glucose polymer osmotic agent that is used to promote sustained ultrafiltration during long peritoneal dialysis dwells.[33,38] The disappearance of icodextrin from the peritoneal cavity was reported to be consistent with a constant rate of fluid transport from the peritoneal cavity, mainly via the lymphatics.[33] In our experiments, the drained volume of the 7.5% icodextrin peritoneal equilibration test identified the upregulation and suppression of lymphangiogenesis, even in the presence of inflammation on day 22 (Figure 6a). It has been reported that protein and solutions pass into the lymphatic capillaries without sieving[14] because they have anatomically discontinuous basal lamina and have gaps between the lymphatic endothelial cells.[6,35] This finding is in agreement with there being no difference in glucose and creatinine transport rates between the conditions of suppression and lack of suppression of lymphangiogenesis (Supplementary Figure 10). In the 4.25% G-peritoneal equilibration test, the drained volume tended to be increased in the Adeno-sVEGFR-3 groups, but the difference versus the volume in the Adeno-LacZ group was not statistically significant (Supplementary Figure 10c). This result suggests that the 4.25% G-peritoneal equilibration test may be unsuitable for identifying the different states of lymphatic absorption. In the use of icodextrin solution in rodents, the reduction in recovery volume was shown to result from degradation of icodextrin by 10- to 25-fold higher levels of amylase compared with humans.[39,40] The low drained volume in the 7.5% icodextrin peritoneal equilibration test on day 22 was probably therefore due to high amylase concentrations (Figure 6). We did not

find any differences in amylase concentrations in peritoneal dialysis effluent between the Adeno-sVEGFR-3 and Adeno-LacZ groups (Figure 6b). We performed the 7.5% icodextrin peritoneal equilibration test for a short duration of 4 h, under which condition the removal of fluid from the circulation by the oncotic pressure of icodextrin solution may not be strongly affected. However, to determine whether these methods might be available for peritoneal dialysis patients, future detailed studies, including studies of optimal conditions, are necessary.

We successfully evaluated peritoneal membrane function after peritoneal rest with lavage for reduction of inflammation. These results suggest that peritoneal lavage before removal of the peritoneal dialysis catheter after prolonged peritoneal dialysis treatment[41] may be useful to prevent adhesions that could lead to encapsulating peritoneal sclerosis.

In MGO model animals, VEGF-D that is expressed mainly by macrophages is a key growth factor for lymphangiogenesis in the peritoneal cavity, especially in the diaphragm (Figures 2b and 3b, c and Supplementary Figure 6). In cultured macrophages and fibroblasts, VEGF-D has been reported to be increased by PGE2,[42] which was elevated in the effluent of MGO model mice (Figure 7), and by inflammatory cytokines.[43] In contrast to VEGF-C, VEGF-D was downregulated by TGF-β.[44] We have reported that mesothelial cells strongly express VEGF-C;[5] however, VEGF-D was not expressed by mesothelial cells in the MGO model mice or in cultured human mesothelial cells (Figure 3d and e). These instances of expression and regulation of VEGF-D are different from those of VEGF-C. We are the first to report that VEGF-D is increased in the human peritoneal membrane and in the peritoneal dialysis effluent with ultrafiltration failure (Figure 8). These data indicate that VEGF-D is involved in lymphangiogenesis in human peritoneal dialysis patients.

In summary, lymphatic absorption is a common feature associated with peritoneal inflammation and fibrosis, and VEGF-D is involved in the development of lymphangiogenesis. VEGFR-3 is a new target to increase net ultrafiltration by suppressing lymphatic absorption.

ACKNOWLEDGMENTS

We express our gratitude to Mr Norihiko Suzuki, Ms Naoko Asano, Ms Keiko Higashide, and Ms Yuriko Sawa (Department of Nephrology and Renal Replacement Therapy, Nagoya University, Nagoya, Japan) for their technical assistance. We also thank Dr Makoto Mizutani (Handa Municipal Hospital, Handa, Japan), Dr Isao Ito (Yokkaichi Municipal Hospital, Yokkaichi, Japan), Dr Hirotake Kasuga (Nagoya Kyoritsu Hospital, Nagoya, Japan), Dr Takeyuki Hiramatsu (Kounan-Kousei Hospital, Kounan, Japan), and Dr Masanobu Horie (Daiyukai-Daiichi Hospital, Ichinomiya, Japan) for collecting peritoneum samples from the peritoneal dialysis patients. We also express our gratitude to Professor Kari Alitalo (University of Helsinki, Helsinki, Finland) and Dr Hajime Kubo (Kyoto University, Kyoto, Japan, currently working at Tanabe Mitsubishi Pharma Corporation, Osaka, Japan), and Vegenics Pty Limited (a subisidialy of Circadian Technologies Limited, Australia) for providing Adeno-VEGFR-3, and also Professor Alitalo and Dr Kubo for

discussing the Adeno-sVEGFR-3 treatment and this manuscript. This work was supported in part by a Grant-in-Aid for Scientific Research from the Ministry of Education, Science, and Culture, Japan (YI # 20590972), the 2013 research grant from the Aichi Kidney Foundation (T Terabayashi and YI), and the Japanese Association of Dialysis Physicians, Grant 2013-15 (YI). This study was also supported in part by a Grant-in-Aid for Progressive Renal Diseases Research, Research on Rare and Intractable Disease, from the Ministry of Health, Labor and Welfare of Japan.

TABLE1 Profiles of peritoneal biopsy cases evaluated for VEGF-D mRNA expression

	Pre-dialysis uremia	Incident	UFF
N	25	22	7
Male	16	13	4
Female	9	9	3
Age, years	63.2 ± 10.4	58.5 ± 14.1	60.4 ± 10.0
Duration of treatment, years	0	3.7 ± 3.0	10.1 ± 5.1
Average thickness of peritoneum, μm	131.3 ± 38.9	148.1 ± 90.5	317.1 ± 118.0

FIGURES

Figure 1

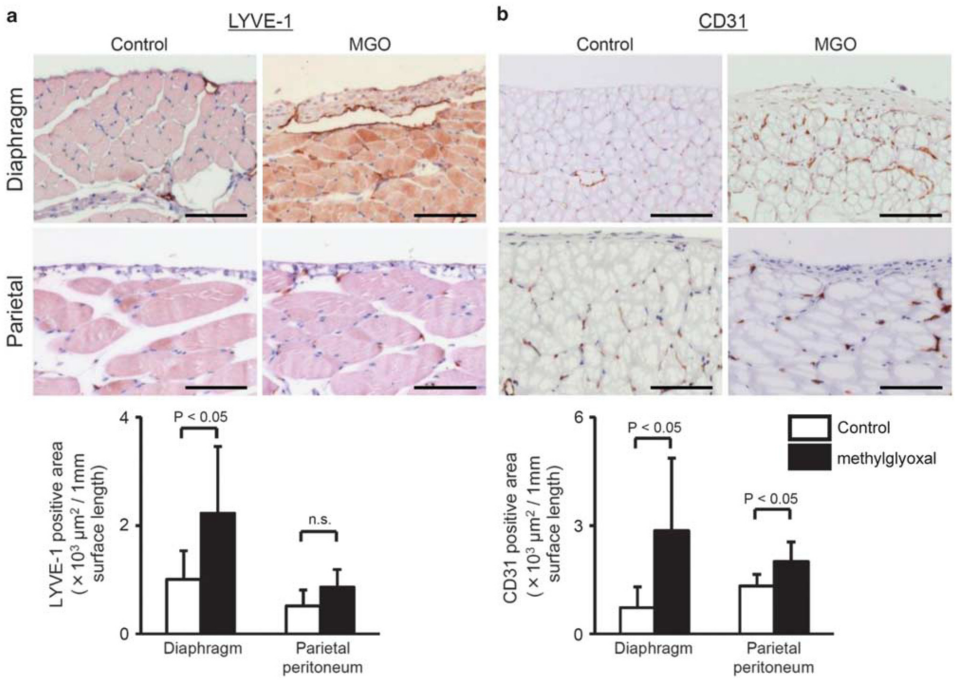

Figure 1 continued

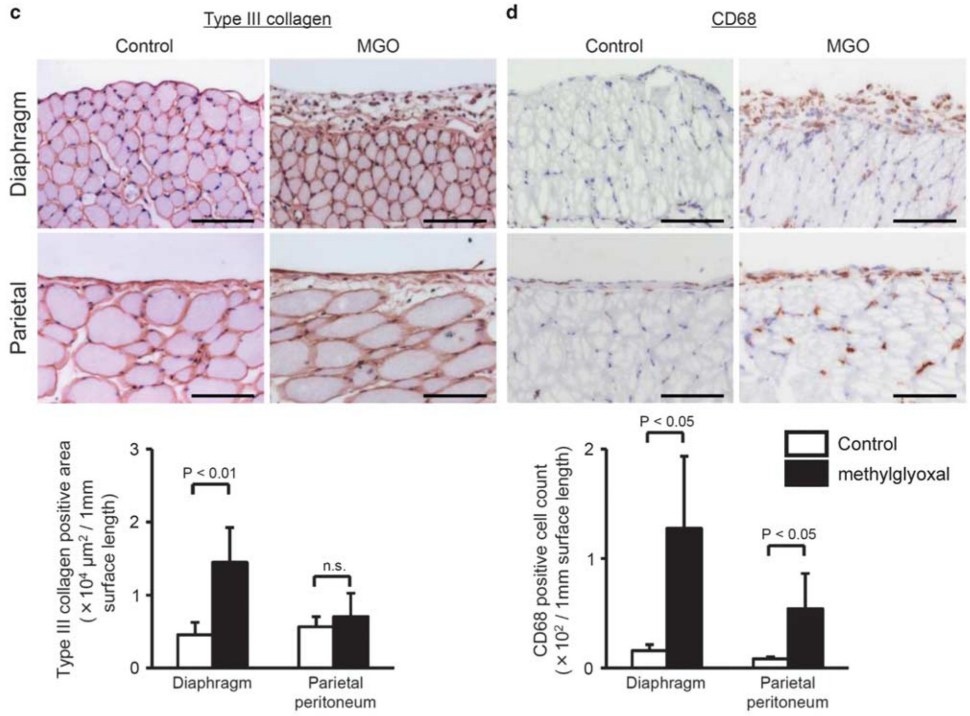

Figure 1. LYVE-1-positive lymphatic vessels were increased and dilated in the diaphragm of methylglyoxal mouse models compared with controls. Expression of lymphatic vessels was predominant in the diaphragm compared with that of control mice. Quantification of immunohistochemical parameters indicated the following: (a) LYVE-1-positive lymphatic vessels were significantly increased in the diaphragm, but not in the parietal peritoneal membrane; CD31-positive vessels (b), expression of type III collagen (c), and CD68-positive macrophages (d) were significantly increased in the diaphragm of methylglyoxal model mice compared with normal control mice. (each group, n = 6). Scale bars, 100 μm. LYVE-1, lymphatic vessel endothelial hyaluronan receptor-1; NS, not significant.

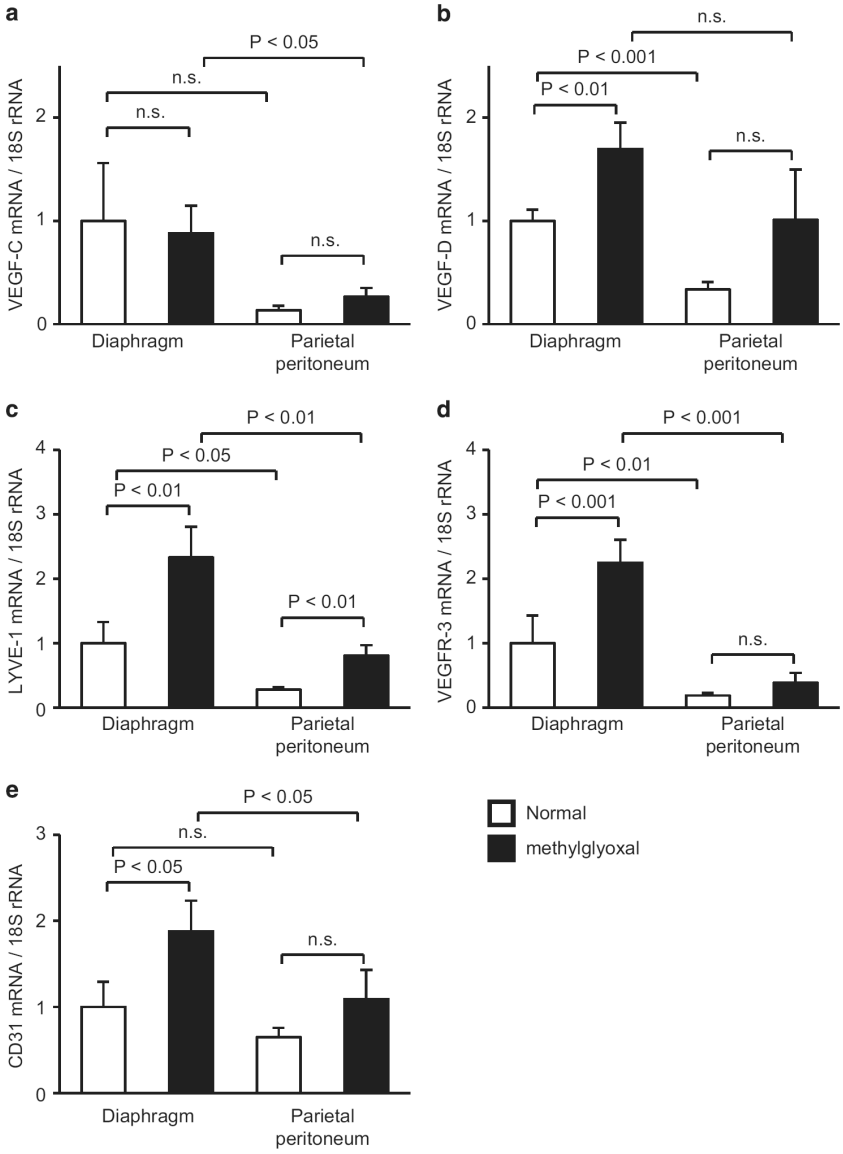

Figure 2. Quantitative PCR analyses of specific mRNA expression in the diaphragm and parietal peritoneum of methylglyoxal model mice. VEGF-C mRNA expression was not significantly increased in the diaphragm (a). VEGF-D (b), LYVE-1 (c), VEGFR-3 (d), and CD31 (e) mRNA expression were increased in the diaphragm in the methylglyoxal model mice compared with normal controls. (each group, n = 6). NS, not significant; VEGF, vascular endothelial growth factor.

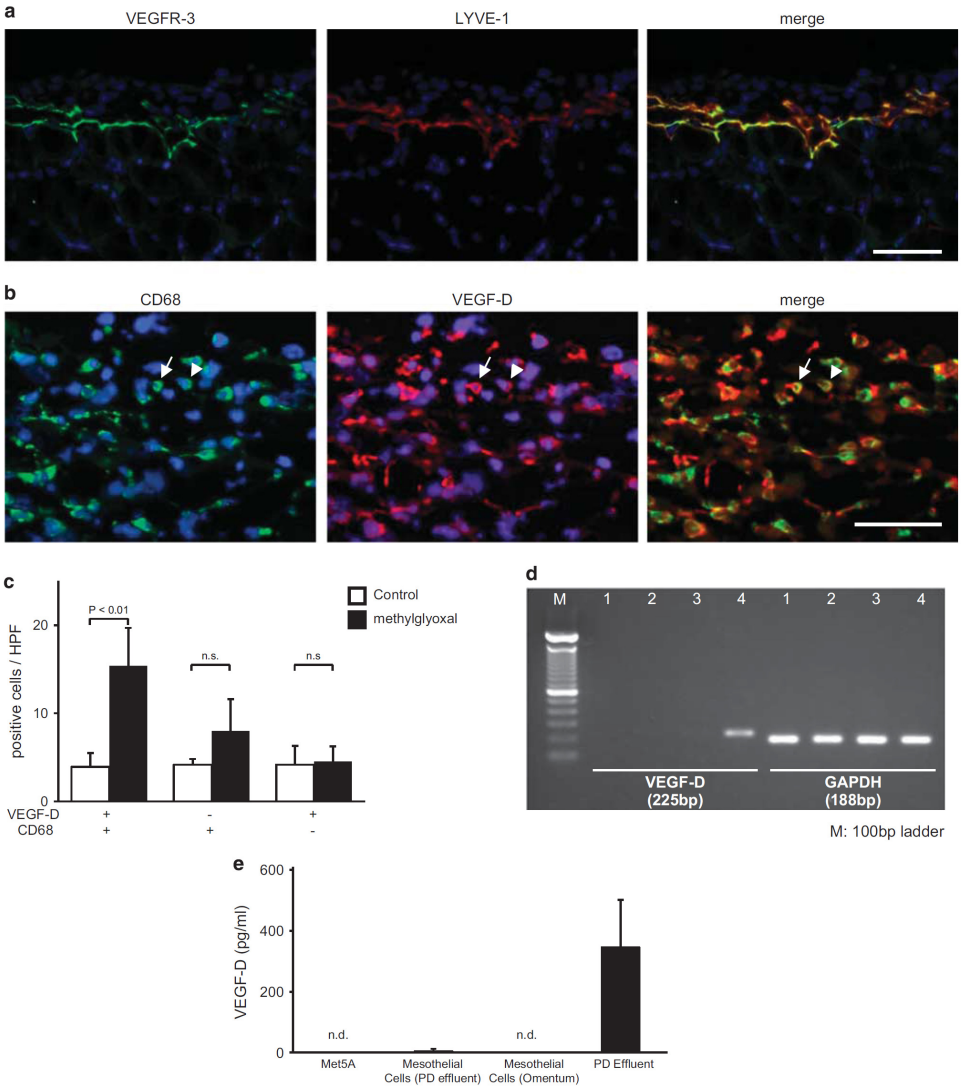

Figure 3. Analysis of VEGF-D expression. (a–c) Representative double immunofluorescent staining for VEGFR-3 and LYVE-1 (a), and for CD68 and VEGF-D (b) in the diaphragm of a methylglyoxal mouse is shown. Arrows and arrowheads of the same color indicate the same cells. Scale bars, 50 μm. Quantification of CD68- and VEGF-D-stained cells (number of labeled cells per high power field (HPF)) in control and methylglyoxal mouse models is shown in (c). VEGF-D was mainly expressed by CD68-positive macrophages in the methylglyoxal mouse model (c). n = 6 in both control and methylglyoxal models. (d and e) VEGF-D mRNA (d) and protein (e) expression analyzed using RT–PCR and ELISA,

respectively, were not detected in the human mesothelial cell line Met5A (d, lane 1) (e), in mesothelial cells derived from the peritoneal dialysis effluent of the patients on peritoneal dialysis (d, lane 2) (e), or in mesothelial cells from the omentum (d, lane 3) (e). In contrast, VEGF-D mRNA was detected in peritoneal tissues (d, lane 4) and VEGF-D protein was detected in peritoneal dialysis effluent (e) from patients with ultrafiltration failure (Table 1). (d) GAPDH was used as a loading control. PD, peritoneal dialysis, ND, not detected.

Figure 4

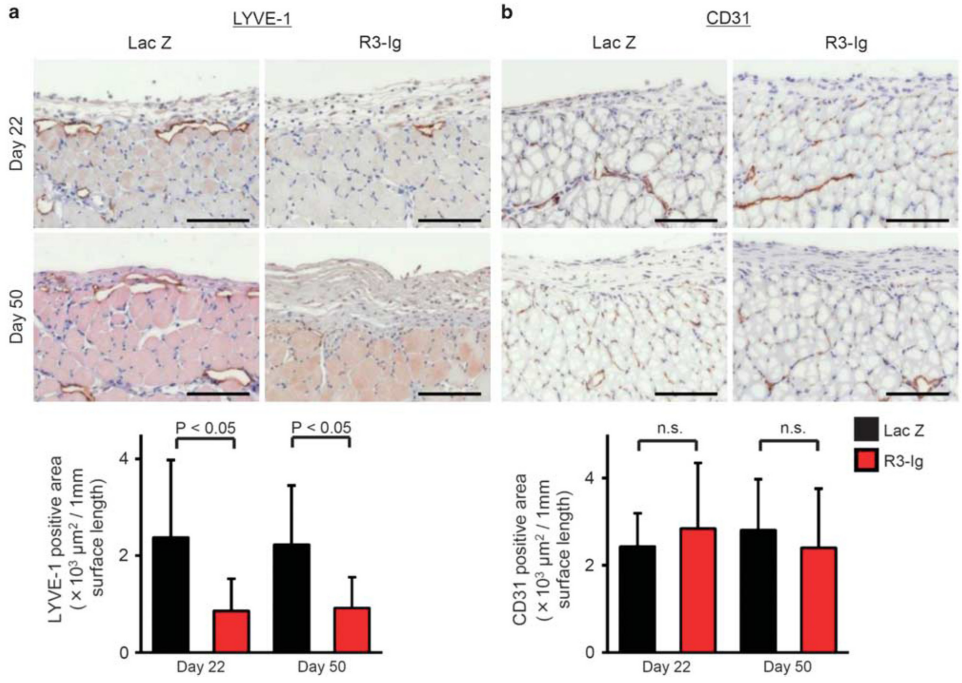

Figure 4 continued

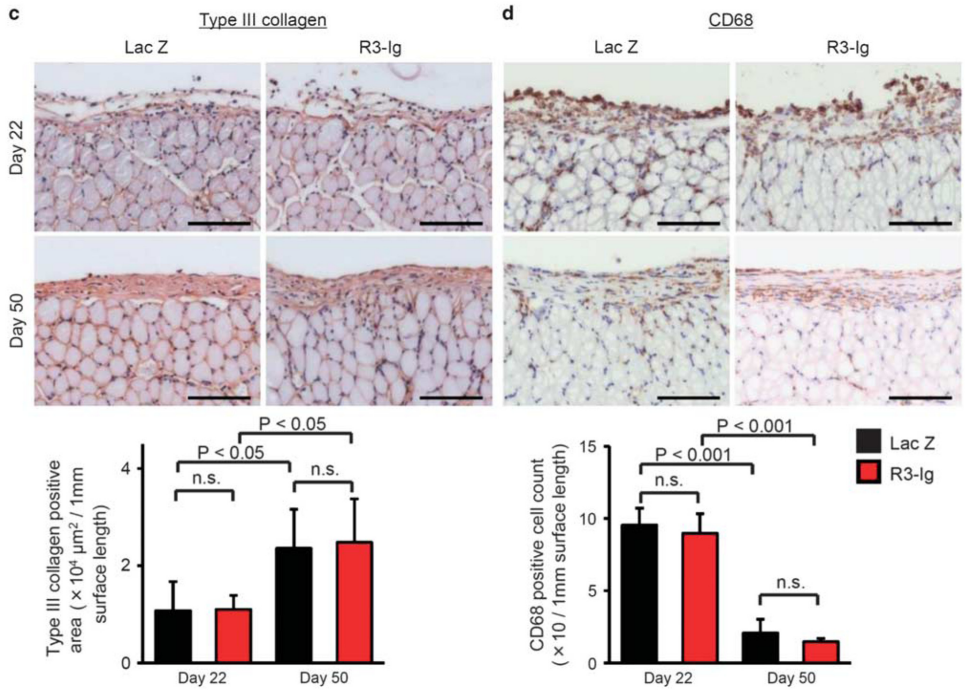

Figure 4. In immunohistochemical analyses of the diaphragm, adenovirus-expressing sVEGFR-3 suppressed LYVE-1–positive lymphatic vessels but not expression of CD31-positive vessels, type III collagen or CD68-positive cells. The diaphragm of mice treated with Adeno-Lac Z (Lac Z) or with AdenosVEGFR-3-Ig (R3-Ig) was immunohistochemically analyzed for: (a) LYVE-1-positive lymphatic vessels, (b) CD31-positive vessels, (c) deposition of type III collagen, and (d) CD68-positive macrophages. (each group, n = 6). Scale bars, 100 μm. Lac Z: treatment with Adeno-LacZ, R3-Ig: treatment with AdenosVEGFR-3-Ig. LYVE-1, lymphatic vessel endothelial hyaluronan receptor-1; ND, not detected; NS, not significant; PD, peritoneal dialysis; RT–PCR, reverse transcription–PCR; sVEGFR-3, soluble vascular endothelial growth factor receptor-3.

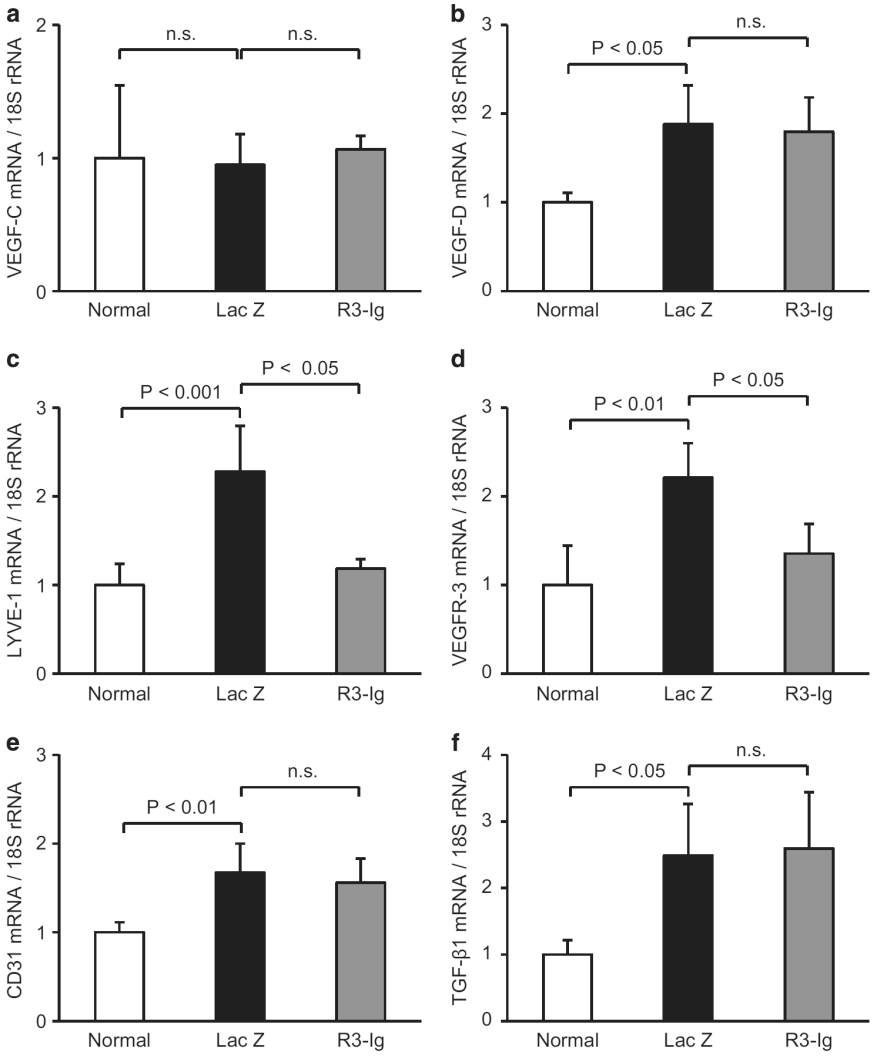

Figure 5. Quantitative PCR analysis of specific mRNA expression in the diaphragm of methylglyoxal mouse models indicated that adenovirus-sVEGFR-3 treatment suppressed lymphangiogenesis as assessed by LYVE-1 and VEGFR-3 mRNA expression; however, there was no difference between the AdenosVEGFR-3 and Adeno-LacZ groups in the expression of VEGF-C, -D, CD31, and TGF-β1 mRNA (Day 22). (a) VEGF-C, (b) VEGF-D, (c) LYVE-1, (d) VEGFR-3, (e) CD31, and (f) TGF-β1 mRNA expression in the diaphragms of the indicated mice. (each group, n = 6). Lac Z, treatment with Adeno-LacZ; LYVE-1, lymphatic vessel endothelial hyaluronan receptor-1; NS, not significant; R3-Ig, treatment with Adeno-sVEGFR-3-Ig; sVEGFR-3, soluble vascular endothelial growth factor receptor-3; TGF-β, transforming growth factor-beta; VEGFR, vascular endothelial growth factor receptor.

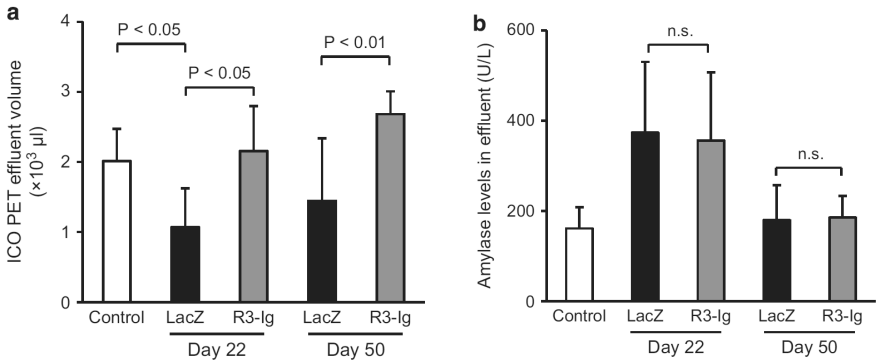

Figure 6. Analyses of peritoneal functions. Peritoneal equilibration test with a 7.5% icodextrin peritoneal dialysis fluid can identify the upregulation and suppression of lymphangiogenesis. Peritoneal dialysis fluid containing 7.5% icodextrin (2000 μl) was intraperitoneally injected into control, Adeno-Lac Z, or Adeno-sVEGFR-3-Ig mice. Drained dialysate was collected 4 h after administration. (a) There was a difference in effluent volume between groups as detected by the 7.5% icodextrin peritoneal equilibration test, indicating that the 7.5% icodextrin peritoneal equilibration test can identify the suppression of lymphangiogenesis. (b) Amylase levels in the effluent were significantly increased on day 22; however, there was no difference between the groups on days 22 and 50. (each group, n = 6). ICO PET, icodextrin peritoneal equilibration test; Lac Z, treatment with Adeno-LacZ; NS, not significant; R3-Ig, treatment with Adeno-sVEGFR-3-Ig; sVEGFR-3, soluble vascular endothelial growth factor receptor-3.

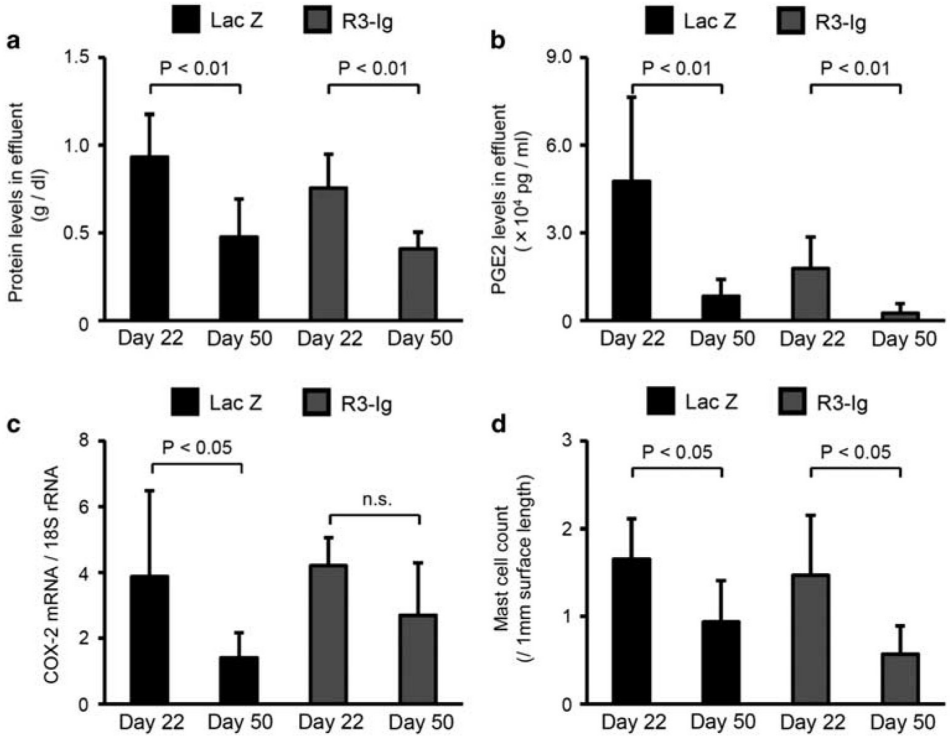

Figure 7. Peritoneal inflammation associated with protein and PGE2 leakage into peritoneal fluid. Increased expression of COX-2 mRNA and mast cells in diaphragms on day 22 was decreased on day 50 after peritoneal lavage. (a) Protein leakage into and (b) prostaglandin E2 (PGE2) in the peritoneal dialysis fluid. (c) COX-2 mRNA expression, and (d) the number of mast cells in the diaphragm. (each group, n = 6). Lac Z, treatment with Adeno-LacZ; NS, not significant; R3-Ig, treatment with Adeno-sVEGFR-3-Ig.

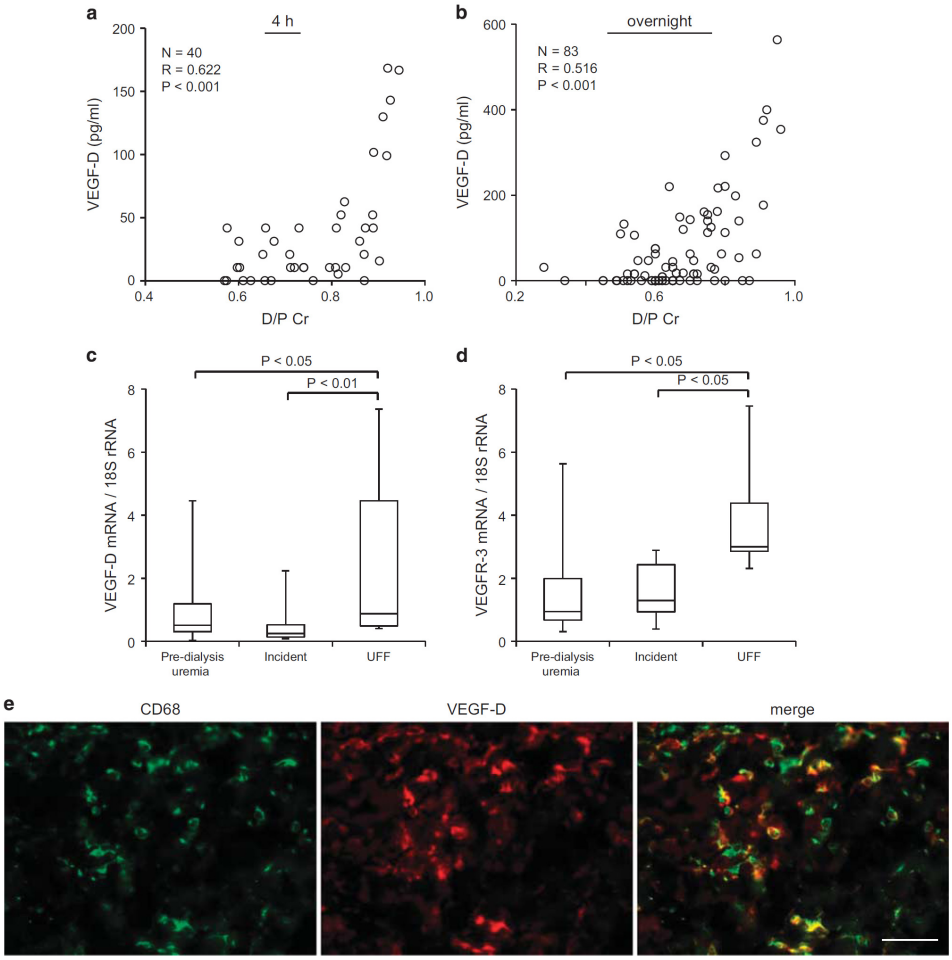

Figure 8. VEGF-D concentration in human peritoneal dialysis effluent correlated with the peritoneal transport rate (dialysate to plasma ratio of creatinine, D/P Cr). VEGF-D and VEGFR-3 mRNA levels were increased in ultrafiltration failure in human peritoneal biopsy samples. (a) Positive correlation between the VEGF-D concentration in the peritoneal dialysis effluent of samples dwelled for 4 h and the dialysate to plasma ratio of creatinine (D/P Cr). (b) Positive correlation between VEGF-D concentration in overnight-dwelled peritoneal dialysis effluent samples and the dialysate to plasma ratio of creatinine. VEGF-D (c) and VEGFR-3 (d) mRNA levels, as assessed using qRT–PCR, were significantly higher in patients with ultrafiltration failure than in patients with pre-dialysis uremia, or in patients in the incident group. (e) Double immunofluorescent analysis showed that VEGF-D is mainly expressed by macrophages in human peritoneal biopsy specimens of bacterial peritonitis. Scale bar, 50 μm. qRT–PCR, quantitative reverse transcription–PCR; UFF, ultrafiltration failure; VEGF, vascular endothelial growth factor.

REFERENCES

1. Mizuno M, Ito Y, Tanaka A et al. Peritonitis is still an important factor for withdrawal from peritoneal dialysis therapy in the Tokai area of Japan. Clin Exp Nephrol 2011;15:727–737.
2. Kawaguchi Y, Ishizaki T, Imada A et al. Searching for the reasons for drop-out from peritoneal dialysis: a nationwide survey in Japan. Perit Dial Int 2003;23 Suppl 2:S175–S177.
3. Williams JD, Craig KJ, Topley N et al. Morphologic changes in the peritoneal membrane of patients with renal disease. J Am Soc Nephrol 2002;13:470–479.
4. Mateijsen MA, van der Wal AC, Hendriks PM et al. Vascular and interstitial changes in the peritoneum of CAPD patients with peritoneal sclerosis. Perit Dial Int 1999;19:517–525.
5. Kinashi H, Ito Y, Mizuno M et al. TGF-beta1 promotes lymphangiogenesis during peritoneal fibrosis. J Am Soc Nephrol 2013;24:1627–1642.
6. Sakamoto I, Ito Y, Mizuno M et al. Lymphatic vessels develop during tubulointerstitial fibrosis. Kidney Int 2009;75:828–838.
7. Suzuki Y, Ito Y, Mizuno M et al. Transforming growth factor-beta induces vascular endothelial growth factor-C expression leading to lymphangiogenesis in rat unilateral ureteral obstruction. Kidney Int 2012;81:865–879.
8. Lee AS, Lee JE, Jung YJ et al. Vascular endothelial growth factor-C and -D are involved in lymphangiogenesis in mouse unilateral ureteral obstruction. Kidney Int 2013;83:50–62.
9. Smit W, Schouten N, van den Berg N et al. Analysis of the prevalence and causes of ultrafiltration failure during long-term peritoneal dialysis: a cross-sectional study. Perit Dial Int 2004;24:562–570.
10. Sampimon DE, Coester AM, Struijk DG et al. The time course of peritoneal transport parameters in peritoneal dialysis patients who develop encapsulating peritoneal sclerosis. Nephrol Dial Transplant 2011;26:291–298.
11. Heimburger O, Waniewski J, Werynski A et al. Peritoneal transport in CAPD patients with permanent loss of ultrafiltration capacity. Kidney Int 1990;38:495–506.
12. Fussholler A, zur Nieden S, Grabensee B et al. Peritoneal fluid and solute transport: influence of treatment time, peritoneal dialysis modality, and peritonitis incidence. J Am Soc Nephrol 2002;13:1055–1060.
13. Krediet RT. The effective lymphatic absorption rate is an accurate and useful concept in the physiology of peritoneal dialysis. Perit Dial Int 2004;24:309–313 discussion 316-307.
14. Flessner M. Effective lymphatic absorption rate is not a useful or accurate term to use in the physiology of peritoneal dialysis. Perit Dial Int 2004;24:313–316.
15. Hirahara I, Kusano E, Yanagiba S et al. Peritoneal injury by methylglyoxal in peritoneal dialysis. Perit Dial Int 2006;26:380–392.

16. Hirahara I, Ishibashi Y, Kaname S et al. Methylglyoxal induces peritoneal thickening by mesenchymal-like mesothelial cells in rats. Nephrol Dial Transplant 2009;24:437–447.
17. Kitamura M, Nishino T, Obata Y et al. Epigallocatechin gallate suppresses peritoneal fibrosis in mice. Chem Biol Interact 2012;195:95–104.
18. Nakayama K, Nakayama M, Iwabuchi M et al. Plasma alpha-oxoaldehyde levels in diabetic and nondiabetic chronic kidney disease patients. Am J Nephrol 2008;28:871–878.
19. He Y, Kozaki K, Karpanen T et al. Suppression of tumor lymphangiogenesis and lymph node metastasis by blocking vascular endothelial growth factor receptor 3 signaling. J Natl Cancer Inst 2002;94:819–825.
20. He Y, Rajantie I, Pajusola K et al. Vascular endothelial cell growth factor receptor 3-mediated activation of lymphatic endothelium is crucial for tumor cell entry and spread via lymphatic vessels. Cancer Res 2005;65:4739–4746.
21. Yang H, Kim C, Kim MJ et al. Soluble vascular endothelial growth factor receptor-3 suppresses lymphangiogenesis and lymphatic metastasis in bladder cancer. Mol Cancer 2011;10:36.
22. Kim YL, Kim SH, Kim JH et al. Effects of peritoneal rest on peritoneal transport and peritoneal membrane thickening in continuous ambulatory peritoneal dialysis rats. Perit Dial Int 1999;19(Suppl 2):S384–S387.
23. Mizutani M, Ito Y, Mizuno M et al. Connective tissue growth factor (CTGF/CCN2) is increased in peritoneal dialysis patients with high peritoneal solute transport rate. Am J Physiol Renal Physiol 2010;298:F721–F733.
24. Nishimura H, Ito Y, Mizuno M et al. Mineralocorticoid receptor blockade ameliorates peritoneal fibrosis in new rat peritonitis model. Am J Physiol Renal Physiol 2008;294:F1084–F1093.
25. Makinen T, Jussila L, Veikkola T et al. Inhibition of lymphangiogenesis with resulting lymphedema in transgenic mice expressing soluble VEGF receptor-3. Nat Med 2001;7:199–205.
26. Twardowski ZJ. The fast peritoneal equilibration test. Semin Dial 1990;3:141–142.
27. Honda K, Hamada C, Nakayama M et al. Impact of uremia, diabetes, and peritoneal dialysis itself on the pathogenesis of peritoneal sclerosis: a quantitative study of peritoneal membrane morphology. Clin J Am Soc Nephrol 2008;3:720–728.
28. Takei Y, Kadomatsu K, Yuzawa Y et al. A small interfering RNA targeting vascular endothelial growth factor as cancer therapeutics. Cancer Res 2004;64:3365–3370.
29. Yung S, Li FK, TM C. Peritoneal mesothelial cell culture and biology. Perit Dial Int 2006;26:162–173.
30. Stylianou E, Jenner LA, Davies M et al. Isolation, culture and characterization of human peritoneal mesothelial cells. Kidney Int 1990;37:1563–1570.

31. Onogawa S, Kitadai Y, Tanaka S et al. Expression of VEGF-C and VEGF-D at the invasive edge correlates with lymph node metastasis and prognosis of patients with colorectal carcinoma. Cancer Sci 2004;95:32–39.
32. Nykanen AI, Sandelin H, Krebs R et al. Targeting lymphatic vessel activation and CCL21 production by vascular endothelial growth factor receptor-3 inhibition has novel immunomodulatory and antiarteriosclerotic effects in cardiac allografts. Circulation 2010;121:1413–1422.
33. Moberly JB, Mujais S, Gehr T et al. Pharmacokinetics of icodextrin in peritoneal dialysis patients. Kidney Int 2002;62:S23–S33.
34. Peritoneal Dialysis Adequacy 2006 Work Group. Clinical practice guidelines for peritoneal adequacy, update 2006. Am J Kidney Dis 2006;48:S91–S175.
35. Tammela T, Alitalo K. Lymphangiogenesis: Molecular mechanisms and future promise. Cell 2010;140:460–476.
36. Alitalo K, Tammela T, Petrova TV. Lymphangiogenesis in development and human disease. Nature 2005;438:946–953.
37. Mactier RA, Khanna R, Twardowski Z et al. Contribution of lymphatic absorption to loss of ultrafiltration and solute clearances in continuous ambulatory peritoneal dialysis. J Clin Invest 1987;80:1311–1316.
38. Johnson DW, Agar J, Collins J et al. Recommendations for the use of icodextrin in peritoneal dialysis patients. Nephrology (Carlton) 2003;8:1–7.
39. Garcia-Lopez E, Pawlaczyk K, Anderstam B et al. Icodextrin metabolism and alpha-amylase activity in nonuremic rats undergoing chronic peritoneal dialysis. Perit Dial Int 2007;27:415–423.
40. Pawlaczyk K, Garcia-Lopez E, Kuzlan-Pawlaczyk M et al. The effect of icodextrin-based solutions on peritoneal transport in rats undergoing chronic peritoneal dialysis. Perit Dial Int 2001;21(Suppl 3):S359–S361.
41. Yamamoto T, Nagasue K, Okuno S et al. The role of peritoneal lavage and the prognostic significance of mesothelial cell area in preventing encapsulating peritoneal sclerosis. Perit Dial Int 2010;30:343–352.
42. Hosono K, Suzuki T, Tamaki H et al. Roles of prostaglandin E2-EP3/EP4 receptor signaling in the enhancement of lymphangiogenesis during fibroblast growth factor-2-induced granulation formation. Arterioscler Thromb Vasc Biol 2011;31:1049–1058.
43. Watari K, Nakao S, Fotovati A et al. Role of macrophages in inflammatory lymphangiogenesis: Enhanced production of vascular endothelial growth factor C and D through NF-kappaB activation. Biochem Biophys Res Commun 2008;377:826–831.
44. Cui Y, Osorio JC, Risquez C et al. Transforming growth factor-β1 downregulates vascular endothelial growth factor-D expression in human lung fibroblasts via JNK signaling pathway. Mol Med 2014;20: 120–134.

SUPPLEMENTAL

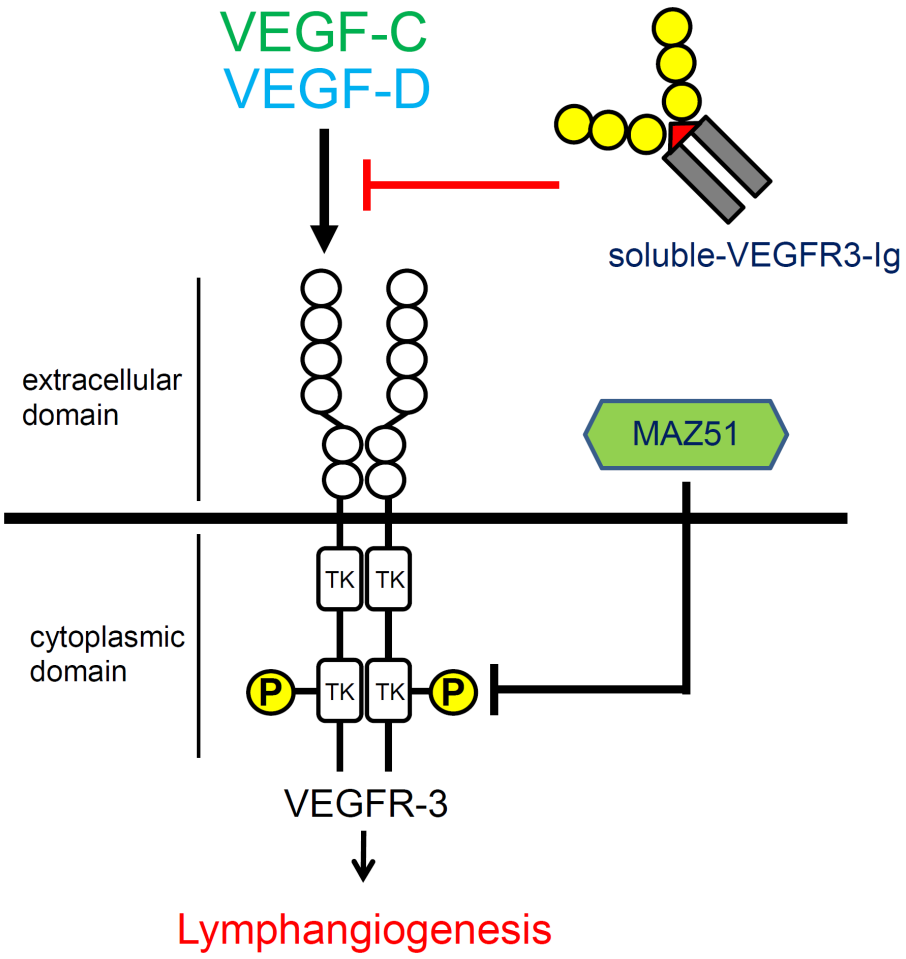

Supplementary Figure 1. Schematic diagram of the inhibition of VEGFR-3 activation by soluble VEGFR-3 or by a VEGFR-3 kinase inhibitor. A schematic diagram showing two different mechanisms of inhibition of VEGFR-3 activation. A soluble VEGFR-3-immunoglobulin (Ig) G Fc-domain fusion protein acts as a decoy receptor and traps VEGF-C/-D that bind to the extracellular domain of VEGFR-3 (Tammela T et al., Cell 2010; 140: 460-476). The VEGFR-3 kinase inhibitor, 4-dimethylamino-naphthalene-1-carbaldehyde (MAZ51), has been reported to specifically inhibit VEGF-C/-D induced VEGFR-3 auto-phosphorylation (Kirkin V et al., Eur J Biochem 2001; 268: 5530-40). TK: tyrosine kinase domain.

Supplementary Figure 2

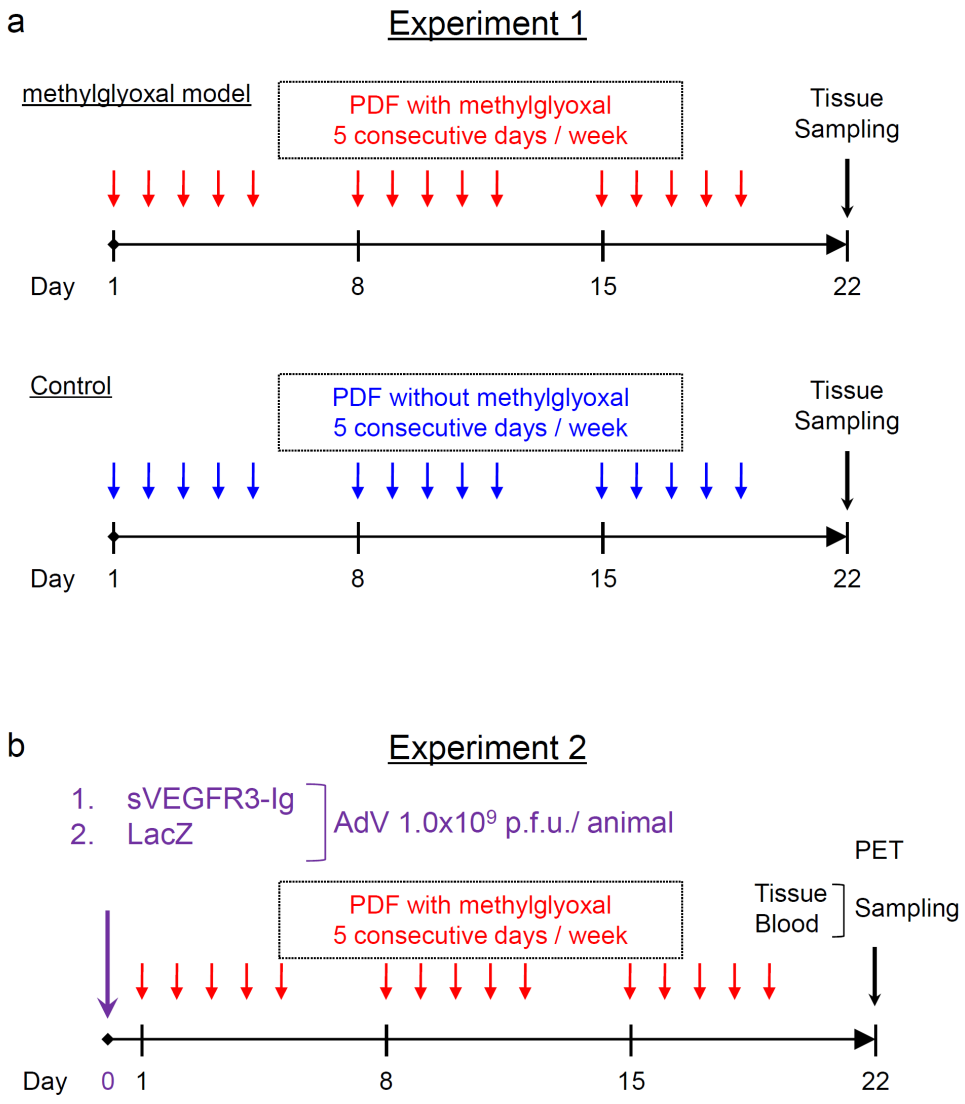

PDF: peritoneal dialysis fluid
PET: peritoneal equilibration test

Supplementary Figure 2 Continued

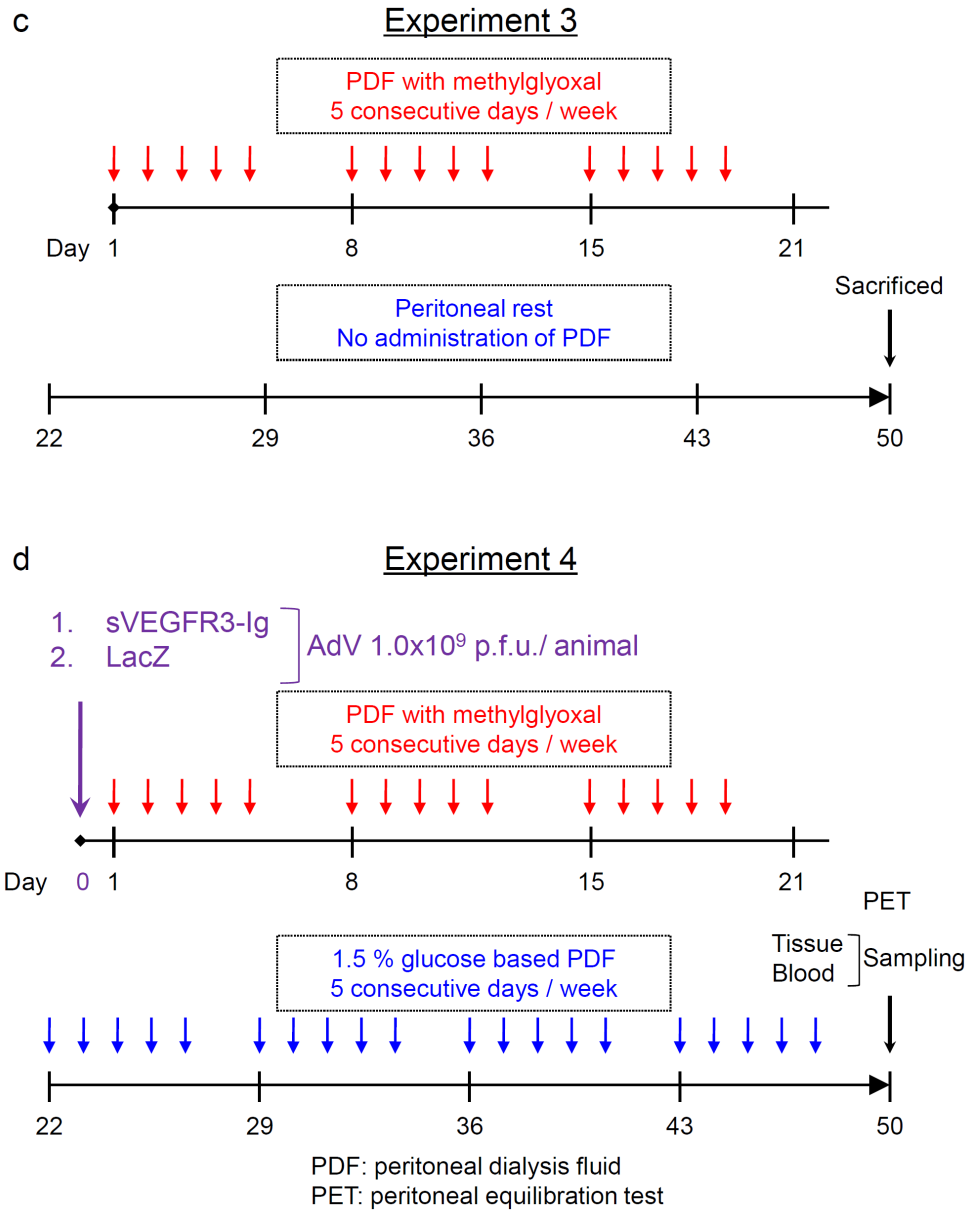

Supplementary Figure 2. Experimental design and protocols.
a: Experiment 1. Development of methylglyoxal induced peritoneal injury model in mice
b: Experiment 2. Inhibition studies using an adenovirus expressing sVEGFR-3 and a control adenovirus expressing Lac Z in methylglyoxal-induced peritoneal injury models. The models were assessed using a traditional peritoneal equilibration test with a 4.25% glucose-based peritoneal dialysis fluid and a peritoneal equilibration test with 7.5% icodextrin on day 22.
c: Experiment 3. Development of a methylglyoxal-induced peritoneal injury model with peritoneal rest from day 22 to day 50. In these mice, dialysate was not infused into the peritoneal cavity during the peritoneal rest.
d: Experiment 4. Inhibition studies using adenovirus expressing sVEGFR-3 and control adenovirus expressing Lac Z, in a methylglyoxal model as in (b) except that the mice further underwent peritoneal lavage using a 1.5% peritoneal dialysis fluid from day 22 to day 50. In these mice, peritoneal functions were assessed on day 50 using a traditional peritoneal equilibration test with a 4.25% glucose-based peritoneal dialysis fluid and a peritoneal equilibration test with 7.5% icodextrin peritoneal dialysis fluid.

Supplementary Figure 3. Expression of podoplanin-positive lymphatic vessels in the murine diaphragm and parietal peritoneum.
Expression of podoplanin-positive lymphatic vessels and podoplanin mRNA were increased mainly in the diaphragm of murine methylglyoxal model similar to other lymphatic endothelial cell markers. (a) Immunohistochemistry for podoplanin of methylglyoxal model mice. Podoplanin has been reported to be expressed by mesothelial cells (Braun N et al., Nephrol Dial Transplant 2011; 26: 1033–1041). Arrows and arrowheads indicate podoplanin-positive lymphatic vessels and mesothelial cells, respectively. scale bars, 100 μm. (b) Quantification of immunohistochemical analyses of podoplanin-positive lymphatic vessels (each group, n=6). (c) Double immunofluorescent staining for podoplanin and LYVE-1 in the diaphragm of a representative methylglyoxal model mouse. scale bars, 50 μm. (d) Podoplanin mRNA expression analyzed by quantitative RT-PCR analyses. n.s., not significant.

Supplementary Figure 3.

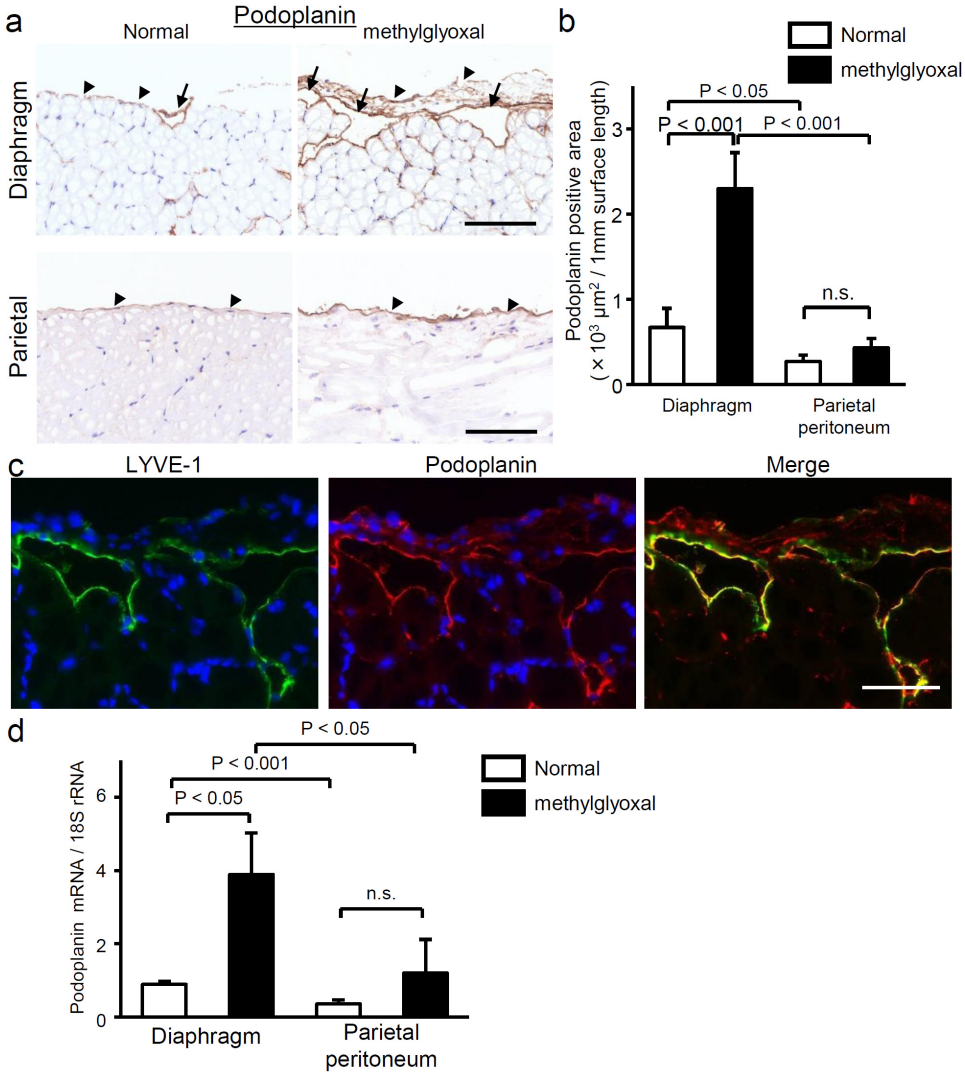

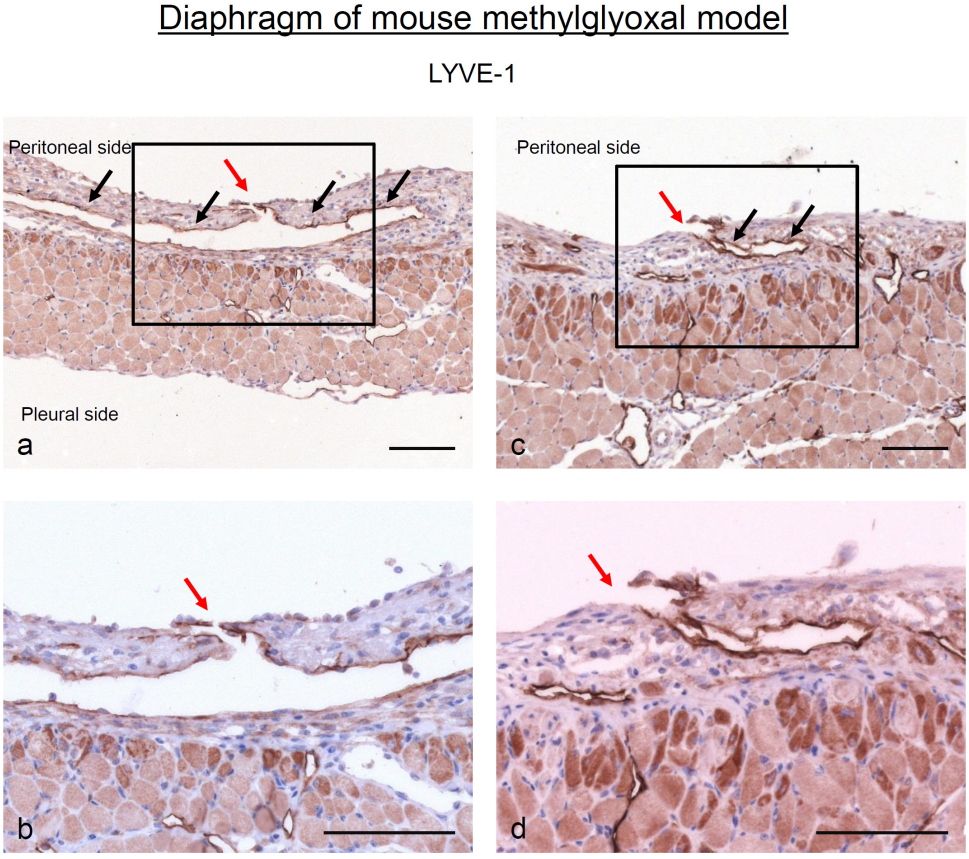

Supplementary Figure 4.
Lymphatic vessels in the diaphragm in the mouse methylglyoxal models on day 22. Immunohistochemical analysis identified LYVE-1–positive dilated lymphatic vessels (black arrows) in the thickened diaphragm. In the advanced fibrotic area of the diaphragm, entrances of newly developed lymphatic vessels (red arrows) were revealed in the fibrotic diaphragm. Figs. (b) and (d) are larger magnifications of the boxed areas in Figs. (a) and (c), respectively. Scale bars, 100 μm.

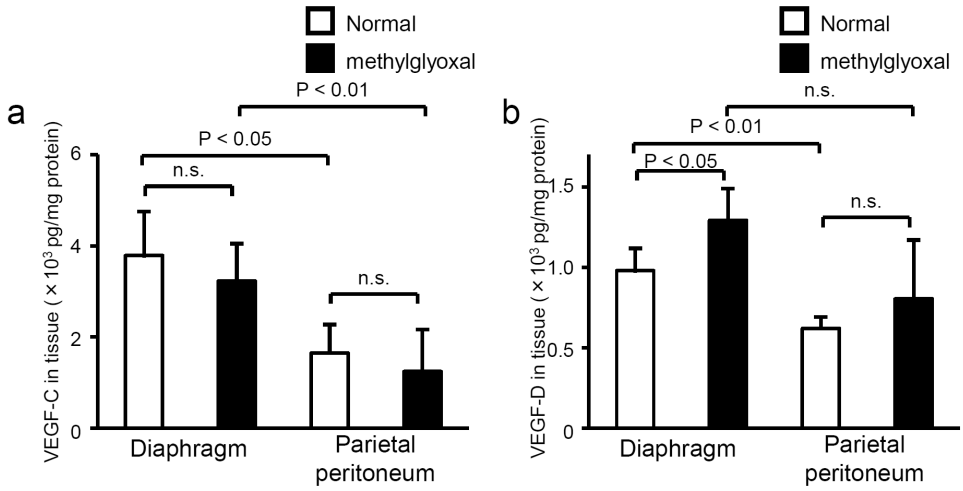

Supplementary Figure 5. VEGF-C and VEGF-D protein expression in the diaphragm and parietal peritoneum of the methylglyoxal model mice.
VEGF-C (a) and VEGF-D (b) proteins in the diaphragm and parietal peritoneum of control and methylglyoxal model mice were measured using a mouse VEGF-C ELISA kit (Cloud-Clone Corp., Houston, TX, USA) and a mouse VEGF-D ELISA kit (Biomatik Corporation, Cambridge, Ontario, Canada), respectively. VEGF-D was significantly elevated in the diaphragm of the methylglyoxal model mouse compared to control. In contrast an increase in VEGF-C in the diaphragm or parietal peritoneum could not be detected. These findings were similar to those of VEGF-C and -D mRNA levels. a and b: each group, n=6.

Supplementary Figure 6. Immunohistochemical analyses and qPCR analyses of selected mRNAs in the diaphragm and parietal peritoneal membrane of methylglyoxal-induced peritoneal injury rats. The methylglyoxal model in rats is similar to that in mice. Methylglyoxal model rats were generated in a similar fashion to the mouse methylglyoxal models. Eight-week-old male Sprague–Dawley rats (Japan SLC, Hamamatsu, Japan), initially weighing 240–260 g, were used in this study. Briefly, 100 mL/kg body weight of 2.5% peritoneal dialysis fluid (Dianeal-N PD-4-2.5) containing 20 mmol/L methylglyoxal (MP Biomedicals LLC) was administered intraperitoneally for 3 weeks. Immunohistochemical analysis indicated that LYVE-1–positive lymphatic vessels (black arrows) were increased and dilated in the diaphragm of the rat methylglyoxal models (b, d) compared with controls (a, c); however, lymphangiogenesis was predominant in the diaphragm (b). (e) Quantitative RT-PCR analysis indicated that the mRNA expression of LYVE-1 and VEGFR-3, which are markers of lymphatic endothelial cells, and VEGF-D mRNA expression were increased in the diaphragm of the methylglyoxal models compared to normal controls. However, VEGF-C mRNA expression was not significantly increased in the diaphragm. (each group, n=5). n.s., not significant. Scale bars, 200 μm.

Supplementary Figure 6.

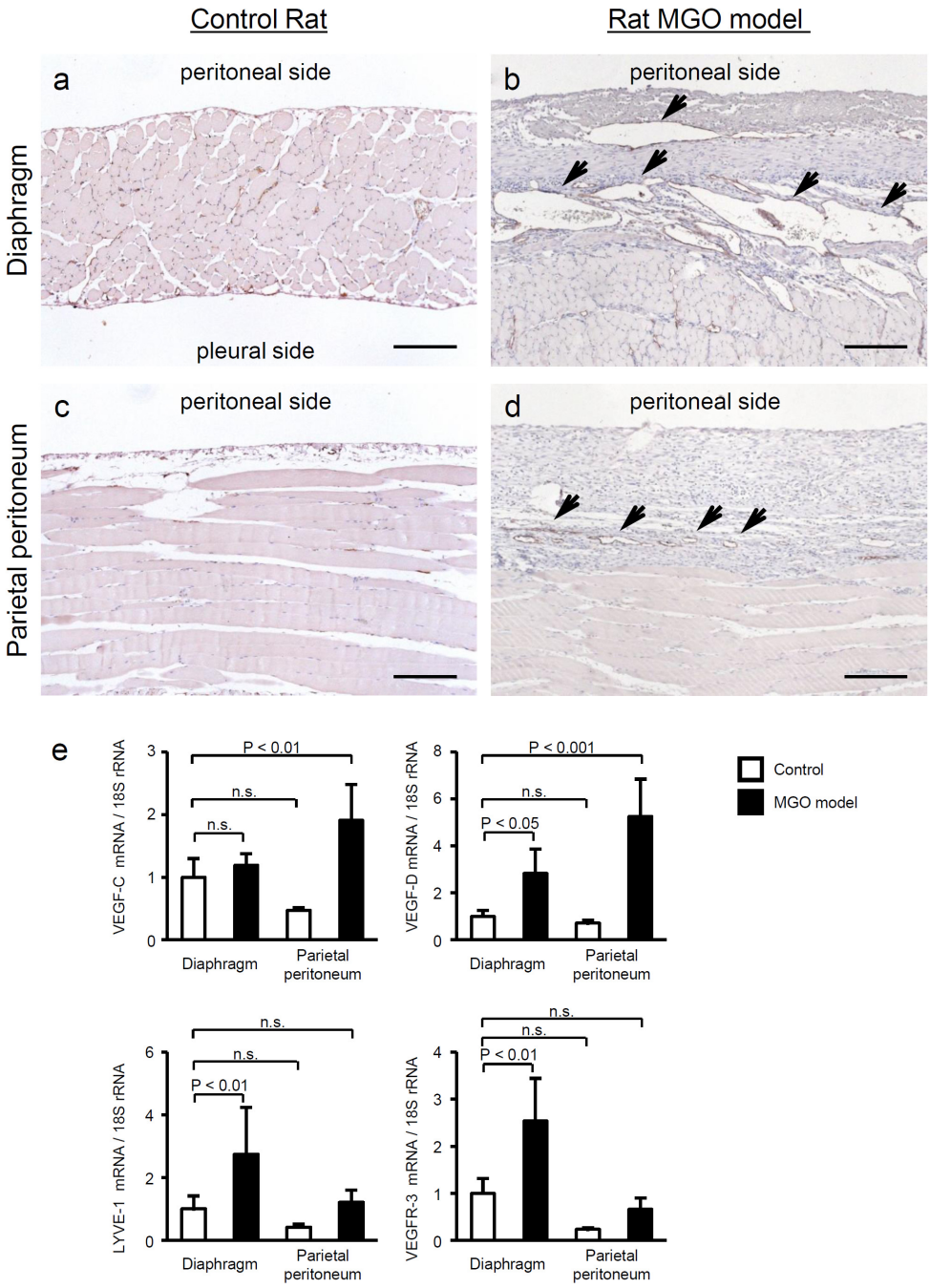

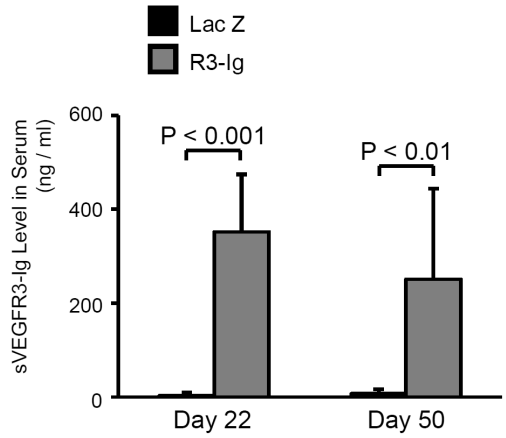

Supplementary Figure 7. The serum concentration of soluble-VEGFR-3 protein was significantly higher on day 22 and day 50 in mice treated with an adenovirus expressing sVEGFR-3 than in mice administered an adenovirus expressing Lac Z.
Serum soluble-VEGFR-3-Ig was assayed using an ELISA kit for human IgG1.
Lac Z: treatment with Adeno-LacZ, R3-Ig: treatment with Adeno-sVEGFR-3-Ig. (each group, n=6)

Supplementary Figure 8. Immunohistochemical analyses of the diaphragm of control and methylglyoxal model mice. Treatment with soluble VEGFR-3 did not affect the infiltration of immune cells. Scale bars, 50 μm.
Immunohistochemical analysis of the indicated immune cells in the diaphragm of control, Lac Z and R3-Ig-treated methylglyoxal model mice. The number of positively labeled cells per high power field (HPF) was counted. Arrows indicate positive staining of the immune cells. Lac Z: treatment with Adeno-LacZ, R3-Ig: treatment with Adeno-sVEGFR-3-Ig.

Supplementary Figure 8.

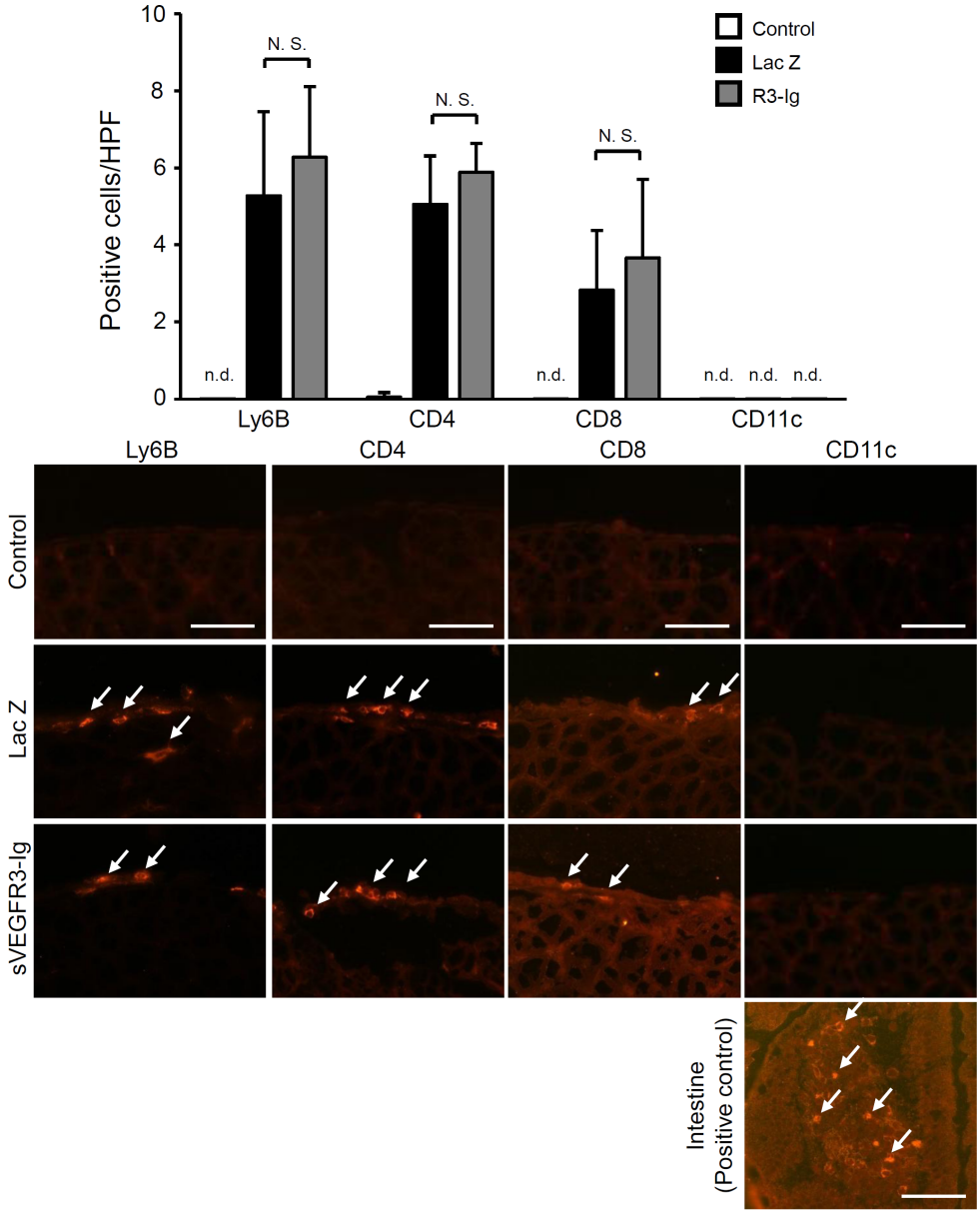

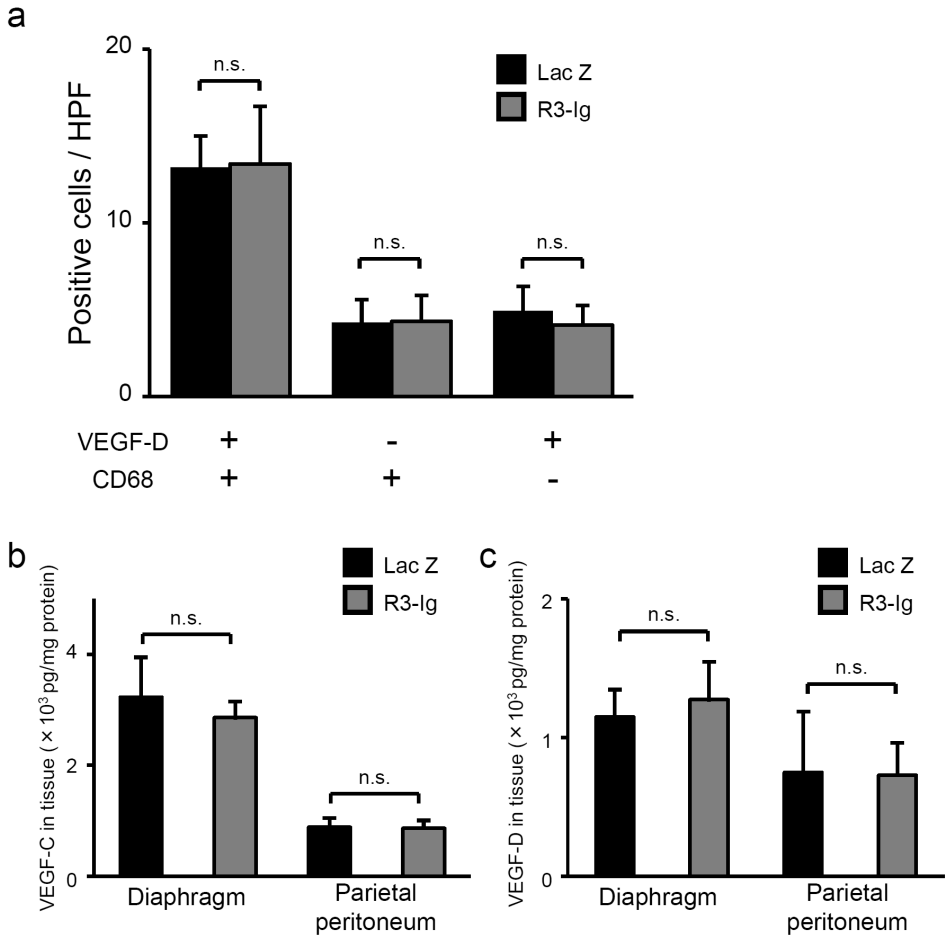

Supplementary Figure 9. There was no difference in the percentage of VEGF-D positive cells or in the level of tissue VEGF-C or -D protein expression between the Adeno-Lac Z or Adeno-sVEGFR-3-Ig –treated methylglyoxal mouse groups.
(a) Quantification of VEGF-D and/or CD68 positive cells in the double immunofluorescent staining of the diaphragm in the adenovirus treated methylglyoxal models. each group, n=6. (b) VEGF-C and (c) VEGF-D protein expression in the tissues of methylglyoxal models as assessed using ELISA. each group, n=5. ns., not significant
Lac Z: treatment with Adeno-LacZ, R3-Ig: treatment with Adeno-sVEGFR-3-Ig.

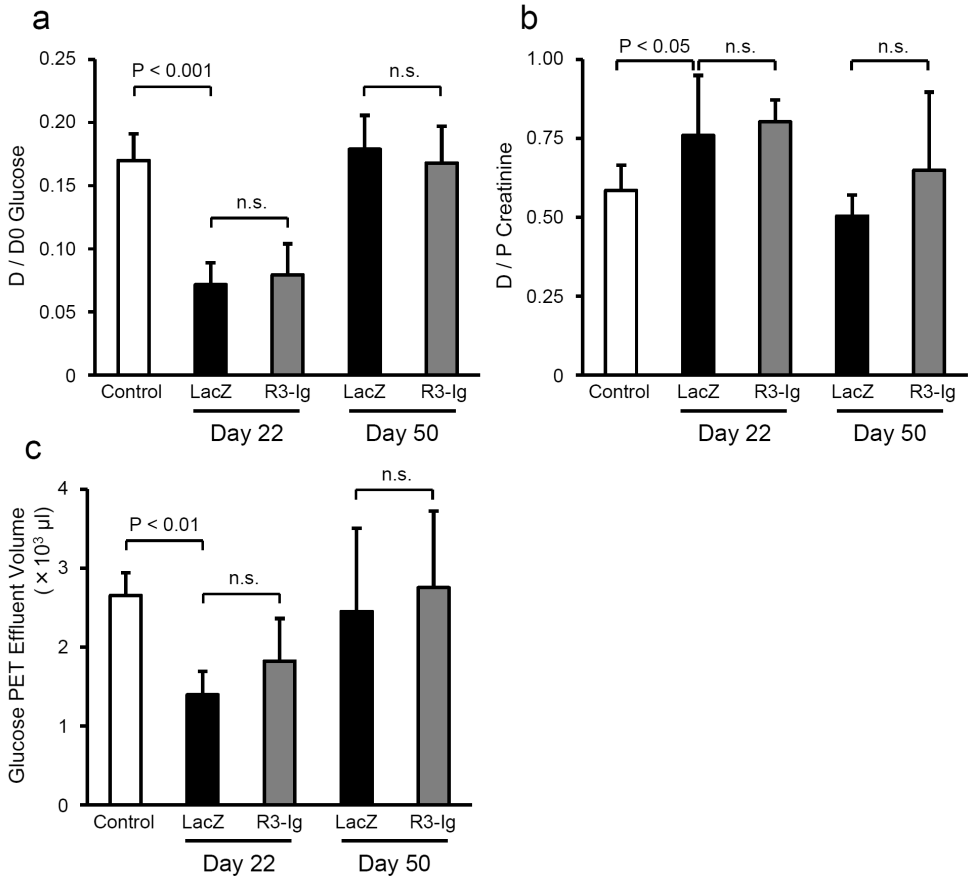

Supplementary Figure 10. Lymphatic vessels are not involved in the function of solute transport. The mice described in Supplementary Figs. 2b, d were sacrificed on day 22 or day 50 for assessment of ultrafiltration and membrane transport. The animals that received 2,000 µL of a 4.25% glucose-based peritoneal dialysis fluid (Dianeal PD-2-4.25, 3.86% glucose, Baxter) were sacrificed at 2 h after intraperitoneal infusion (Ni J et al. Kidney Int 2005; 67:2021-31). An accurate ultrafiltration volume was measured, and blood samples were obtained. Creatinine, blood urea nitrogen, glucose, and total protein were measured in the plasma and peritoneal dialysis effluent. (a, b) There was no difference between the indicated groups in the ratio of dialysate glucose at 2 h dwell time to dialysate glucose at 0 h (D / D0 glucose) or in the dialysate to plasma ratio (D / P) of creatinine in the 4.25%G-peritoneal equilibration test. The ratio of dialysate glucose at 2 h dwell time to dialysate glucose at 0 h was improved on day 50 by reduction of inflammation. (c) In the 4.25%G-peritoneal equilibration test, the drained volume tended to be increased in the Adeno-sVEGFR-3 group versus the Lac Z group, but this increase was not statistically significant. (each group, n=6). n.s., not significant. Lac Z: treatment with Adeno-LacZ, R3-Ig: treatment with Adeno-sVEGFR-3-Ig. G: glucose based peritoneal dialysis fluid. PET: peritoneal equilibration test.

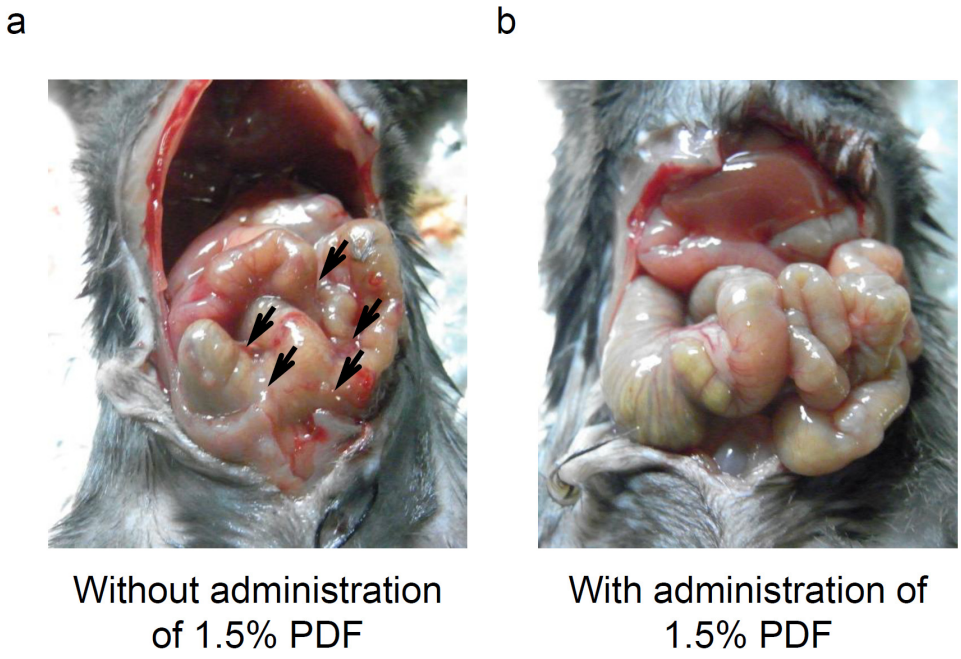

Supplementary Figure 11. Macroscopic observations of the abdominal cavity of methylglyoxal model mice on day 50 in Experiment 3 (without peritoneal lavage from day 22 to day 50) and Experiment 4 (with peritoneal lavage from day 22 to day 50)
(a) In Experiment 3 (without peritoneal lavage with 1.5% peritoneal dialysis fluid (PDF) from day 22 to day 50), it was difficult to perform the peritoneal equilibration test because of severe adhesions in the peritoneal cavity. Arrows indicate adhesion sites.
(b) In Experiment 4 (with peritoneal lavage using 1.5% peritoneal dialysis fluid from day 22 to day 50), no peritoneal adhesions were found.

Supplementary Figure 12.

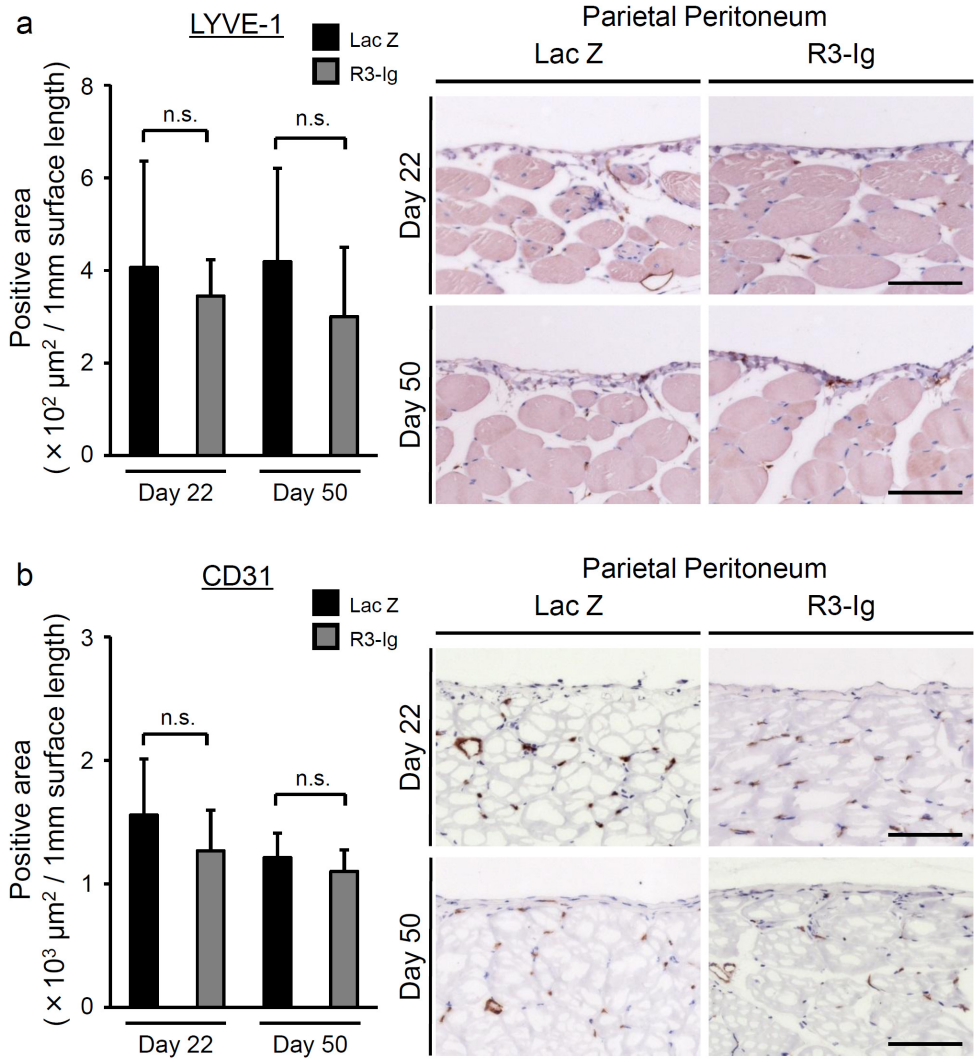

Supplementary Figure 12. Continued

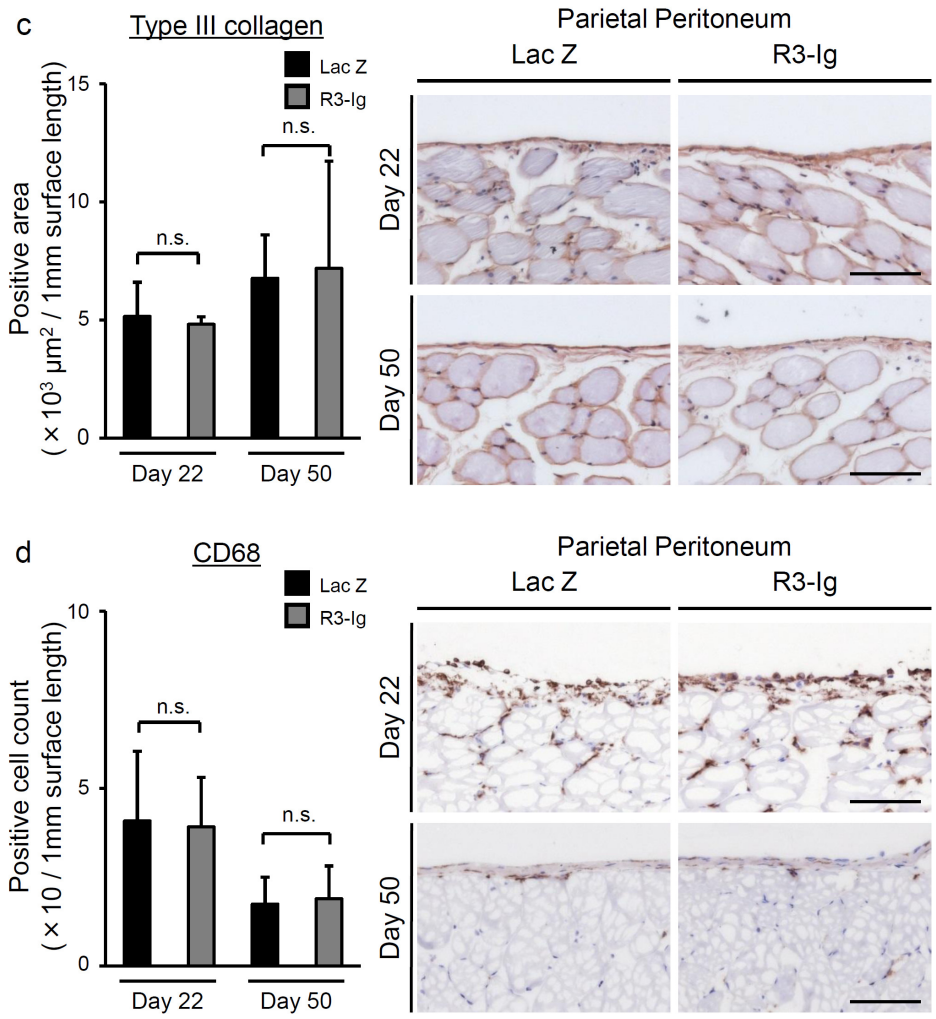

Supplementary Figure 12. Pathological findings and immunohistochemical analyses of murine parietal peritoneum of methylglyoxal model mice treated with an adenovirus expressing sVEGFR-3 or an adenovirus encoding Lac Z

Similar pathological findings were observed in the parietal peritoneal membrane by treatment with Adeno-sVEGFR-3 and Adeno-LacZ on day 22 and day 50; however, these findings were weaker than those in the diaphragm.

Immunohistochemical analysis and quantification of (a) LYVE-1 positive lymphatic vessels, (b) CD31-positive vessels, (c) expression of type III collagen, and (d) CD68-positive macrophages on day 22 and day 50 in murine parietal peritoneal membrane of mice treated with Adeno-sVEGFR-3 or Adeno-LacZ. (each group, n=6). n.s., not significant. Scale bars, 100 μm. Lac Z: treatment with Adeno-LacZ, R3-Ig: treatment with Adeno-sVEGFR-3-Ig.

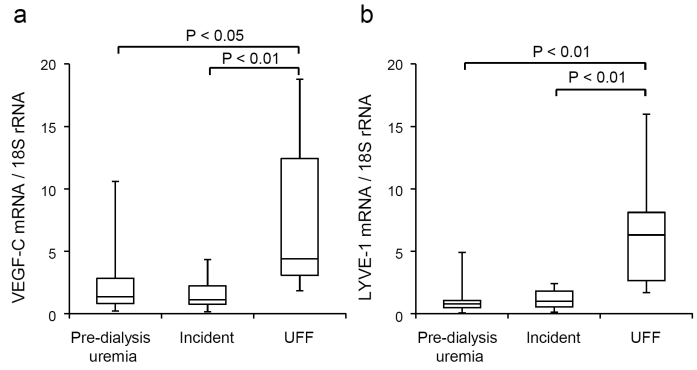

Supplementary Figure 13. VEGF-C and LYVE-1 mRNA levels were increased in ultrafiltration failure (UFF) of human peritoneal biopsy samples.
Some of these samples were used and evaluated for VEGF-C and LYVE-1 mRNA expression in our previous study (Kinashi H et al., J Am Soc Nephrol 2013; 24: 1627-1642).
UFF: ultrafiltration failure.

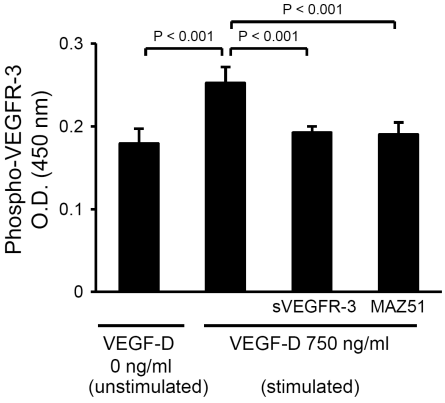

Supplementary Figure 14. Soluble VEGFR-3 inhibits VEGF-D induced VEGFR-3 phosphorylation.
Lymphatic endothelial cells (HMVEC-dLy Neo, Lonza Japan, Tokyo, Japan) were seeded onto 60 mm culture dishes and were then starved for 48 h. Starved cells were stimulated with 750 ng/ml recombinant human VEGF-D (R&D) for 30 minutes, in the absence or presence of sVEGFR-3 (115 nM) or the VEGFR-3 kinase inhibitor, 4-dimethylamino-naphthalene-1-carbaldehyde (MAZ51, 50 μM) (Merck Millipore, Darmstadt, Germany). The cells were lysed in lysis buffer and the cell extracts were examined for VEGFR-3 phosphorylation levels using a Human Phospho-VEGF R3/Flt-4 ELISA kit (R&D). Control group, n=4, other groups, n=5 each group.

Supplementary Table 1. List of antibodies used

Antibody	Company
rabbit anti-mouse LYVE-1 antibody	Acris Antibodies GmbH, Herford, Germany
rat anti-mouse CD31 antibody	EMD Millipore, Temeculo, CA
rabbit anti-type III collagen antibody	LSL, Nagahama, Japan
rat anti-mouse CD68 antibody	AbD Serotec, Oxfordshire, UK
rat anti-mouse Ly-6B antibody	AbD Serotec, Oxfordshire, UK
rat anti-mouse CD4 antibody	abcam, Cambridge, UK
rat anti-mouse CD8 antibody	abcam, Cambridge, UK
hamster anti-mouse CD11c antibody	abcam, Cambridge, UK
gout anti-mouse VEGFR3 (Flt-4) antibody	R&D, Minneapolis, Minn.
gout anti-mouse podoplanion antibody	R&D, Minneapolis, Minn.
rabbit anti-rat VEGF-D antibody	Cell Sciences, Canton, MA
mouse anti-human CD68 antibody	Dako, Glostrup, Denmark
rabbit anti-human VEGF-D antibody	Santa Cruz Biotechnology, Santa Cruz, CA
FITC-labbeled donkey anti-gout IgG	abcam, Cambridge, UK
FITC-labbeled gout anti-rat IgG F(ab')2	AbD Serotec, Oxfordshire, UK
FITC-labeled gout anti-rabbit IgG	Jackson Immuno Research, West Grove, PA
Alexa488-labeled gout anti-mouse IgG F(ab')2	Life Technologies, Carlsbad, CA
Alexa555-labeled gout anti-rabbit IgG F(ab')2	Life Technologies, Carlsbad, CA
Alexa555-labeled gout anti-rat IgG	Life Technologies, Carlsbad, CA
Alexa555-labeled donkey anti-gout IgG	Life Technologies, Carlsbad, CA
DAPI (diamidino-2-phenylindole)	Sigma-Aldrich, St. Louis, MO

Supplementary Table 2.
Primers used for real-time PCR (TaqMan Gene Expression Assays)

	Assay identification number
mouse VEGF-C	Mm 00437313_m1
mouse VEGF-D	Mm 00438965_m1
mouse LYVE-1	Mm 00475056_m1
mouse VEGFR3	Mm 01292604_m1
mouse PECAM-1	Mm 01242584_m1
mouse podoplanin	Mm 00494716_m1
mouse Cox2 (ptgs2)	Mm 00478372_m1
rat VEGF-C	Rn 00586458_m1
rat VEGF-D	Rn 00582193_m1
rat LYVE-1	Rn 01510422_m1
rat VEGFR3	Rn 00586429_m1
human VEGF-D	Hs 00189521_m1
18S ribosomal RNA	4319413E

Supplementary Information 1.

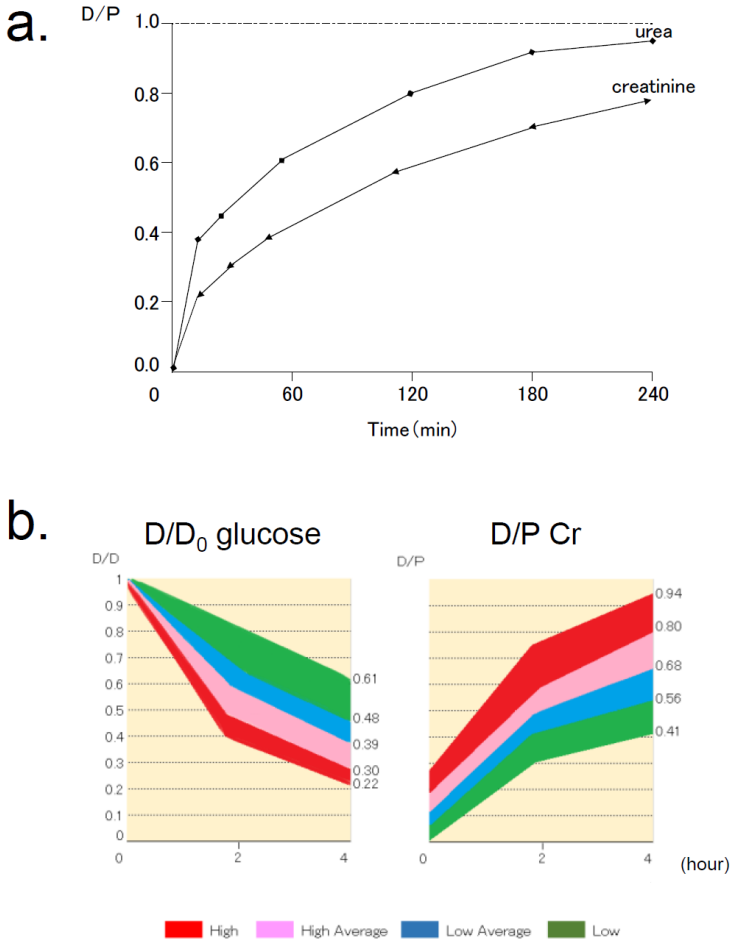

Human Conventional Peritoneal Equilibration Test (PET) Diffusion is quantitatively the most important transport mechanism for low-molecular-weight solutes, such as urea and creatinine (Supplementary information 1a). The Peritoneal Equilibration Test is a common method to determine how rapidly two small solutes (creatinine and glucose) cross the peritoneal membrane and to assess peritoneal transport. In this test, after dwelling of a peritoneal dialysate of 2.27% glucose-based dialysis solutions for 4 h, the volume (mL) of effluent in the drain bag is measured and recorded. The 4 h peritoneal effluent sample is collected and the creatinine concentration and glucose concentration are measured. The dialysate/Plasma (D/P) ratio after a 4-h dwell is the most often used evaluation of creatinine in clinical practice and is calculated as follows: A 4-hour dialysate (D) to plasma (P) ratio of creatinine (D/P creatinine) = the creatinine concentration of 4 h effluent samples/serum concentration of creatinine. For evaluation of glucose, which is absorbed from the dialysate to blood very quickly, the following evaluation is used: 4-hour D/D0 glucose = the glucose concentration of 4 h effluent samples/ the glucose concentration of 0 h effluent samples. The results are classified into 4 categories as shown in Supplementary information 1b and are useful for deciding the treatment with peritoneal dialysis solutions. (Rodrigues AS Blood Purif. 2007;25:497-504 , Twardowski ZJ. Contrib Nephrol. 2006;150:13-9, Twardowski ZJ. Semin Dial 1990; 3: 141-42)

5

Connective tissue growth factor is correlated with lymphangiogenesis in peritoneal fibrosis

Manuscript in preparation

Hiroshi Kinashi[1,2], Tri Q. Nguyen[1], Roel Broekhuizen[1], Roel Goldschmeding[1], and Yasuhiko Ito[2]

[1]Department of Pathology, University Medical Center Utrecht, Utrecht, the Netherlands
[2]Department of Nephrology and Renal Replacement Therapy, Nagoya University Graduate School of Medicine, Nagoya, Japan

ABSTRACT

Background. Lymphatic absorption in peritoneal cavity may contribute to ultrafiltration failure in peritoneal dialysis (PD). Lymphatic vessels develop during PD-related peritoneal fibrosis. Connective tissue growth factor (CTGF, CCN2) is an important determinant of fibrotic tissue remodeling, but its possible involvement in lymphangiogenesis has not been explored. We studied the relationship between CTGF and lymphangiogenesis in association with PD.

Methods. Protein levels of CTGF and vascular endothelial growth factor-C (VEGF-C), a major lymphangiogenic factor, in human PD effluents were measured by enzyme-linked immunosorbent assay. Messenger RNA (mRNA) expression of CTGF, lymphatic markers (lymphatic endothelial hyaluronan receptor-1 [LYVE-1] and podoplanin), and VEGF-C in human peritoneal biopsies was analyzed by quantitative real-time polymerase chain reaction (qPCR). CTGF and VEGF-C mRNA were assessed in human peritoneal mesothelial cells (HPMC) treated with transforming growth factor-β1 (TGF-β1). Expression of CTGF, VEGF-C, and lymphatics in a rat peritoneal fibrosis model induced by chlorhexidine gluconate (CG) was analyzed by immunohistochemistry (IHC) and qPCR.

Results. A positive correlation was observed between CTGF and VEGF-C concentration in human PD effluents. CTGF mRNA positively correlated with VEGF-C, LYVE-1, and podoplanin mRNA in human peritoneal biopsies. There was a positive relationship between CTGF and VEGF-C mRNA fold-increase in HPMC at 12 and 24 h after TGF-β1 treatment. The expression of CTGF, VEGF-C, and lymphatic vessels was increased in the rat diaphragm of CG model compared to control rats. Moreover, CTGF expression positively correlated with expression of VEGF-C and LYVE-1-positive lymphatic vessels in CG model.

Conclusions. Our results suggest a close relationship between CTGF and peritoneal fibrosis-associated lymphangiogenesis.

INTRODUCTION

Ultrafiltration failure (UFF) accompanied with high peritoneal solute transport is an important complication seen after prolonged peritoneal dialysis (PD). UFF is a major reason for the discontinuation of PD treatment, and is also associated with poor survival rate of PD patients.[1-4] The characteristic features of chronic peritoneal damage in PD treatment are submesothelial fibrosis and neoangiogenesis.[5,6] However, the relationship between peritoneal fibrosis and UFF remains obscure. One potential mechanism focuses on lymphangiogenesis.

Lymphatic vessels normally drain fluid from the peritoneal cavity and return it to the vascular system.[7] Several clinical studies have shown that higher lymphatic absorption resulted in lower effective ultrafiltration.[8,9] However, the results from these clinical approaches have been controversial,[10,11] and the process of lymphangiogenesis have remained poorly understood. We therefore investigated whether lymphangiogenesis is associated with peritoneal fibrosis.[12] Signaling via vascular endothelial growth factor (VEGF)-C/D and VEGF receptor (VEGFR)-3 is central to lymphangiogenesis.[13,14] During peritoneal fibrosis, transforming growth factor–β (TGF-β) promotes VEGF-C expression, which leads to lymphangiogenesis.[12] Furthermore, blocking of lymphangiogenesis by soluble VEGFR-3 improved impaired ultrafiltration in a mouse peritoneal fibrosis model.[15]

Connective tissue growth factor (CTGF) is a member of the CCN (CTGF/Cyr61/Nov) family and an important player in the pathogenesis of fibrotic disorders. CTGF is increased in human PD effluents and human peritoneal biopsy samples in association with high peritoneal solute transport rate.[16] CTGF production by human peritoneal mesothelial cells (HPMC) is regulated by advanced glycation end products, glucose degradation products, and TGF-β.[16-18] Besides the major regulatory role during fibrosis, CTGF is an important regulator of angiogenesis.[19] However, nothing is known about the possible association of CTGF also with lymphangiogenesis.

In this study, we investigated the relationship between CTGF and VEGF-C expression in human PD effluents. We also explored the association of CTGF with VEGF-C and lymphatic vessels in human peritoneal biopsy samples. In vitro, we analyzed TGF-β1-induced CTGF and VEGF-C upregulation in HPMC collected from spent PD effluents. In addition, we analysed lymphangiogenesis in the diaphragm, which we previously showed to play a central role in peritoneal lymphatic absorption.[12,15] This was done in the chlorhexidine gluconate (CG)-induced rat peritoneal fibrosis model.[12,20]

SUBJECTS AND METHODS

Patient profiles

All of the human studies were approved by the Ethics Committee for Human Research of the Faculty of Medicine, Nagoya University (approval no. 298: peritoneal fluid experiment; approval no. 299: peritoneal tissue experiments), and all patients provided informed consent before participation in the study.

CTGF and VEGF-C concentration in peritoneal effluent were measured in overnight dwelled (8.97±1.62 h) samples collected from 77 PD patients (24 women and 53 men) who were treated between July of 2005 and April of 2008 at the Department of Nephrology and Renal Replacement Therapy of Nagoya University Hospital (Nagoya, Japan) and affiliated hospitals.[12,16] The mean age of all patients was 54.7±13.0 (range=28-84) years, and the mean duration of PD treatment was 32.1±32.6 (range=1-132) months. Diabetic nephropathy was the cause of ESRD in 26 PD patients (33.8%). All patients were free from peritonitis for at least 1 month before the study, and patients with other diseases, such as liver or lung diseases and malignancy, were excluded. Patients undergoing combination therapy (hemodialysis + PD) were excluded in this study. Peritoneal transport was assessed based on D/P Cr, and the average value was 0.68±0.13 (range=0.28-0.96).[12,16]

A total of 56 peritoneal tissue samples were obtained from 26 pre-dialysis chronic renal failure patients at the time of PD catheter insertion and 30 PD patients. The mean age of pre-dialysis uremia patients (9 women and 17 men) was 62.0±12.8 years and the average peritoneal thickness was 157.9±62.1 μm. Among 30 PD patients, 7 patients (4 women and 3 men) were regarded as having impaired UFF, which was defined by the use of more than four hypertonic bags (2.27% glucose and 3.86% glucose or icodextrin) per 24 hours to maintain fluid balance.[21] The mean age of UFF patients was 55.9±11.6 years, the mean duration of PD treatment was 9.4±6.6 years, and the average peritoneal thickness was 308.6±129.2 μm. 23 patients (10 women and 13 men) had their catheters removal because of transplantation, mental disorders, severe exit site infection, or difficulty in carrying out the bag exchanges. The mean age of 23 PD patients without UFF was 60.8±13.2 years, the mean duration of PD treatment was 3.7±3.0 years, and the average peritoneal thickness was 155.7±93.1 μm. Correlation between CTGF and lymphatic endothelial hyaluronan receptor-1 (LYVE-1), podoplanin, and VEGF-C mRNA expression was evaluated.[12,16]

Cell culture study

HPMCs from spent PD effluent were obtained by centrifugation of dialysis fluid taken randomly from clinically stable 21 patients who had a variety of peritoneal transport (Table 1) and were undergoing nocturnal exchanges using modified methods as described previously.[12,16] Cellular components were isolated using low-speed (200×g) centrifugation, washed with RPMI 1640 (Sigma, Tokyo, Japan), and then cultured in RPMI 1640 containing L-glutamine (Sigma) supplemented with 15% FBS (Sigma), insulin/transferrin/selenium A (Invitrogen, Tokyo, Japan), 10 μM 2-mercaptoethanol (Wako, Osaka, Japan), 3.3 nM EGF (R&D Systems, Minneapolis, MN), and 400 μg/L hydrocortisone (Sigma) in humidified air with 5% CO2 at 37°C. Nonadherent material was removed the next day with two brief washes with RPMI 1640, and the adherent population was incubated in fresh culture medium. The cells reached confluence in 7-10 days, and they were then split two to three times and cultured. Subconfluent HPMCs were rinsed twice with PBS, and the culture medium was replaced with serum-free medium for 24 h to render the cells quiescent. Subsequently, the cultures were incubated with or without 5 ng/ml

recombinant human TGF-β1 (R&D Systems), which was diluted in serum-free medium. Cells were harvested at 12 and 24 h (n=3 dishes of cells from each patient at each time point). All experiments were performed during 3rd to 4th passage. To explore the correlation between the enhancement of CTGF and VEGF-C expression by TGF-β1, we assessed the fold-increase of CTGF and VEGF-C mRNA after 12 and 24 h incubation with TGF-β1 compared to control mRNA expression without TGF-β1 treatment.

Animal model

All animal studies were carried out in accordance with the Animal Experimentation Guidelines of Nagoya University Graduate School of Medicine (Nagoya, Japan). Eight-week old male Sprague-Dawley rats (Japan SLC, Hamamatsu, Japan) that initially weighed 240-260 g were used throughout the study. The animals were maintained under conventional laboratory conditions and given free access to food and water. Nine rats were given an intraperitoneal injection of 3 ml/200 g body wt of 0.04% chlorhexidine gluconate (CG) (Wako, Japan) and 10% ethanol (Wako) dissolved in saline every other day. Five control rats were injected with the same dosage of saline without CG. All rats were euthanized on day 16, and diaphragmatic samples were procured. All injections and euthanizations were performed under anesthesia with diethyl ether (Wako). The harvested samples were analyzed by immunohistochemistry (IHC) and quantitative real-time polymerase chain reaction (qPCR).

ELISA

CTGF protein was measured in human peritoneal dialysate samples by a sandwich enzyme-linked immunosorbent assay (ELISA). Microtiter plates were coated overnight at 4°C with a mouse monoclonal antibody (FG-3145, Fibrogen, South San Francisco, CA) that binds distinct epitopes in domain 2 of CTGF. Wells were rinsed and blocked with 1% BSA overnight at 4°C. After washing, the NH2-terminal fragment of human recombinant CTGF (Fibrogen) which was used for the calibration curve and samples were added and incubated with alkaline phosphatase-conjugated antibody against CTGF (Leinco Technologies, Fenton, MO) overnight at 4°C. Plates were washed and substrate solution containing p-nitrophenyl phosphate was added. Absorbance was read at 405 nm. VEGF-C protein levels in human PD fluid samples were measured using the Human VEGF-C Assay Kit (IBL, Takasaki, Japan) according to the manufacture's instruction.

Quantitative PCR

Human and rat tissue were immersed in RNA later (Ambion, Austin, TX) for at least 1 day. Total RNA was extracted from tissue and cultured cells using RNeasy columns (Qiagen, Hilden, Germany). After cDNA synthesis, samples were mixed with TaqMan Gene Expression Assays (CTGF, Hs00170014_m1, Rn01537279_g1; VEGF-C, Hs00153458_m1, Rn00586458_m1; LYVE-1, Hs00272659_m1, Rn01510422_m1; podoplanin, Hs00366764_m1, Rn00571195_m1; Applied Biosystems, Foster City, CA) and run on

Applied Biosystems Prism 7500HT. 18S ribosomal RNA (4319413E) was used as an internal reference.

Immunohistochemistry

For IHC in rat diaphragmatic specimens, 4μm formalin-fixed paraffin sections were deparaffinized and rehydrated. After blocking endogenous peroxidase activity, heat-based antigen retrieval was performed in citrate buffer (pH=6) for CTGF and LYVE-1 or EDTA buffer (pH=9) for VEGF-C. Slides were incubated with goat anti-CTGF antibody (Santa Cruz Biotechnology, sc-14939, Santa Cruz, CA), followed by incubation with rabbit anti-goat IgG (Dako, Glostrup, Denmark) and Brightvision Poly-horseradish peroxidase (HRP)-anti-rabbit IgG (Immunologic BV, Duiven, Netherlands), or rabbit anti-mouse LYVE-1 antibody (Acris Antibodies GmbH, Herford, Germany) and rabbit anti-VEGF-C antibody (Zymed Laboratories, South San Francisco, CA), followed by incubation with Brightvision Poly-HRP-anti-rabbit IgG. Bound antibody was visualized with 3,3'-diaminobenzidine or NovaRed (Vector Laboratories, Burlingame, CA), and sections were counterstained with hematoxylin. To determine positive area of stained slides, 10 random fields per section were chosen and photographed. LYVE-1-positive area of the submesothelial compact zone was quantitated using MetaMorph 6.3 image analysis software (Universal Imaging Co., West Chester, PA). CTGF and VEGF-C expression was analyzed and semiquantitatively classified as follows: 0, no staining; 1, mild staining; 2, moderate staining; 3, pronounced staining.[12,22]

Statistical analysis

Values are expressed as mean ± SD. Differences between two groups were analyzed by Mann-Whitney U-test. Variables of mRNA expression in human peritoneal biopsies were transformed into the logarithmic scale for a parametric test. Ordinal CTGF and VEGF-C data in CG model was compared using Spearman rank correlation. Pearson correlation was used for the other variables. Differences were considered to be statistically significant if $P<0.05$. All analyses were performed using SPSS software (SPSS, Chicago, IL).

RESULTS

Positive correlation between CTGF and VEGF-C concentration in human PD effluent

In order to explore the involvement of CTGF in peritoneal lymphangiogenesis, we measured CTGF and VEGF-C concentration in the overnight dwelled PD effluents derived from 77 patients. The mean CTGF concentration was 0.79±0.63 (range=0.16-2.95) nM. The mean VEGF-C concentration was 643±407 (range=89.3-2161) pg/ml. There was a positive correlation between CTGF and VEGF-C concentration in the PD effluents ($R=0.428$, $P<0.001$, Figure 1).

CTGF mRNA expression was correlated with LYVE-1, podoplanin, and VEGF-C mRNA expression in human peritoneal biopsy samples

Second, we analyzed the mRNA expression of CTGF, VEGF-C, and lymphatic markers (LYVE-1 and podoplanin) in 56 human peritoneal biopsy samples derived from pre-dialysis uremic patients and PD patients with or without UFF. CTGF mRNA expression positively correlated with LYVE-1 ($R=0.638$, $P<0.001$, Figure 2A), podoplanin ($R=0.592$, $P<0.001$, Figure 2B), and VEGF-C ($R=0.670$, $P<0.001$, Figure 2C) mRNA expression in the human peritoneal membranes.

Increment of CTGF mRNA expression correlated with increment of VEGF-C mRNA expression in HPMCs treated with TGF-β1

Next, we assessed CTGF and VEGF-C mRNA expression in HPMC derived from 21 PD patients with variable peritoneal membrane transport (Table 1). Cells were cultured with or without TGF-β1 (5 ng/ml) and harvested at 12 and 24 h. CTGF and VEGF-C mRNA expression were increased to varying degrees by TGF-β1 treatment. There were positive correlations between CTGF and VEGF-C mRNA fold-increase at 12 ($R=0.722$, $P<0.001$, Figure 3A) and 24 h ($R=0.532$, $P<0.01$, Figure 3B) after TGF-β1 treatment.

CTGF expression was correlated with expression of VEGF-C and lymphatic vessels in the diaphragm in the rat CG model of peritoneal fibrosis

IHC analysis indicated that expression of CTGF ($P<0.01$), VEGF-C ($P<0.01$), and LYVE-1-positive lymphatic vessels ($P<0.01$) was increased in the diaphragm in rats i.p. injected with CG (Figure 4A, B). qPCR analysis showed that mRNA expression of CTGF, VEGF-C, LYVE-1, and podoplanin was increased to 4.8- ($P < 0.01$), 2.2- ($P < 0.01$), 2.3- ($P < 0.01$), and 3.3-fold ($P < 0.01$), respectively in CG injected rats compared to controls (Figure 4C). Quantification of IHC showed that CTGF expression positively correlated with expression of VEGF-C ($R=0.952$, $P<0.001$, Figure 4D) and LYVE-1-positive lymphatic vessels ($R=0.775$, $P<0.05$, Figure 4E) in the rats injected with CG. Moreover, there was a positive correlation between VEGF-C and LYVE-1 expression in these rats ($R=0.704$, $P<0.05$, Figure 4F).

DISCUSSION

Involvement of lymphatic absorption in the physiology of PD was noticed three decades ago.[23] Several clinical studies showed that higher lymphatic absorption was associated with PD duration and UFF.[8,24] However, effective lymphatic absorption rate which was estimated by the disappearance of intraperitoneally administered macromolecules, such as radioactive iodinated serum albumin or dextran caused controversy.[10,11] Since then, lymphatics in PD have been less studied in the recent decade. In contrast, owing to recent discovery of several useful lymphatic markers and key molecular mechanism, lymphangiogenesis has been studied in a variety of diseases, such as tumor metastasis,[25] inflammatory disease,[26] heart disease,[27] and transplant rejection.[28] We observed lymphangiogenesis in various kinds of human kidney diseases, and demonstrated that the number of lymphatic vessels was correlated with the degree of renal interstitial fibrosis.[29]

Lymphangiogenesis was also associated with human peritoneal fibrosis, and patients with UFF showed a high expression of lymphatic vessels in peritoneum compared to other PD patients without UFF.[12] Interestingly, the rat remnant kidney model recently revealed that chronic kidney disease itself can induce peritoneal fibrosis, lymphangiogenesis, and high lymphatic absorption rate, independent of exposure to PD solution.[30] Two major mechanisms, i.e. neoangiogenesis accompanied with high vascular permeability, and reduction of osmotic gradient by tissue fibrosis are highlighted in the context of UFF in peritoneal fibrosis.[31] However, fibrosis-associated lymphangiogenesis additionally suggests a possible involvement of lymphatic absorption in the UFF mechanism of progressive peritoneal membrane injury.

In this study, we first explored whether CTGF concentration positively correlated with VEGF-C concentration in human PD effluents. Both CTGF and VEGF-C protein in human dialysate have been reported to correlate with the peritoneal membrane transport rate,[12,16,32] suggesting that both could be a biomarker and therapeutic target for UFF. The dialysate protein level is affected by the peritoneal local production and the transfer from blood circulation, which is also dependent on several factors including plasma level,[33] peritoneal protein clearance,[34] molecular weight with degradation,[16] and protein charge.[35] Although the data includes complicated factors, our findings would be compatible with role of CTGF in lymphangiogenesis in the peritoneum.

It has been reported that CTGF was detected and increased in mesothelial cells and fibroblasts in human fibrotic peritoneal membranes in relation to UFF.[16] Previous reports showed that mRNA expression of CTGF, VEGF-C, and lymphatic markers in peritoneum was higher in UFF patients than in pre-dialysis uremia patients, and was correlated with peritoneal thickness.[12,16] Interestingly, there was no correlation between CTGF mRNA expression and the density of blood vessels in human peritoneal biopsies.[16] Unlike the blood vessel analysis, however, this study showed that CTGF mRNA expression was positively correlated with VEGF-C, LYVE-1, and podoplanin mRNA expression in human peritoneal biopsies. Our results indicate that the local CTGF expression in the context of peritoneal fibrosis is closely linked to lymphangiogenesis.

Mesothelial cells that line the surface of the peritoneal cavity predominantly regulate intraperitoneal homeostasis including the synthesis of cytokines, growth factors, and matrix proteins.[36] In parallel with the enhancement of profibrotic activity by CTGF production, mesothelial cells also play an important role in lymphangiogenesis by producing VEGF-C. We treated HPMC from spent PD effluent with TGF-β1 which can be elevated in the peritoneal cavity by several mechanisms, such as exposure to dialysate glucose,[37] advanced glycation end products,[38] glucose degradation products,[18] and presence of bacterial peritonitis.[39] Our results demonstrated that both CTGF and VEGF-C production was increased by TGF-β1 to varying degrees in HPMC cultures from individuals, and that their enhancement showed a positive correlation. This is in accordance with the findings in PD effluent and peritoneal biopsy analyses.

The diaphragm contains a specialized form of lymphatic absorption system including lymphatic lacunae and mesothelial stomata.[7] This aspect of UFF and lymphangiogenesis could be studied only in animal experiments. IHC of diaphragm sections from the rat CG model showed that CTGF was mainly increased in peritoneal mesothelial cells and fibroblast-like cells, and VEGF-C was increased in mesothelial cells and mononuclear infiltrates, consistent with the observations in parietal peritoneum.[12,16,22] CTGF expression in the diaphragm was significantly correlated with expression of VEGF-C and LYVE-1-positive lymphatic vessels, supporting the concept of involvement of CTGF also in diaphragmatic lymphangiogenesis.

Several animal experiments demonstrated that CTGF inhibition ameliorated fibrotic development in obstructive nephropathy,[40] diabetic nephropathy,[41] allograft nephropathy,[42] and the remnant kidney model.[43]

In conclusion, we have identified a close association of CTGF expression with lymphangiogenesis in peritoneal fibrosis. Studies are underway to clarify possible benefit of targeting CTGF to prevent lymphangiogenesis, UFF and peritoneal fibrosis in the course of PD therapy.

DISCLOSURE

R.G. has received research supports from FibroGen.

ACKNOWLEDGEMENTS

We are grateful for the technical assistance of Keiko Higashide and Yuriko Sawa (Department of Nephrology, Nagoya University, Nagoya, Japan).

This work was supported in part by Ministry Education, Science, and Culture, Japan Grant-in-Aid for Scientific Research 20590972, the research grant from the Aichi Kidney Foundation in 2007 and 2011, Baxter Japan PD Grant 2009, and the Japanese Association of Dialysis Physicians Grant 2011-13.

TABLE 1. Patient profiles of the cell culture study

D/P Cr	Men/Women	All
0.65～	6/6	12
～0.64	5/4	9

D/P Cr, ratio of creatinine concentrations in dialysate and plasma, an index of the peritoneal transport.

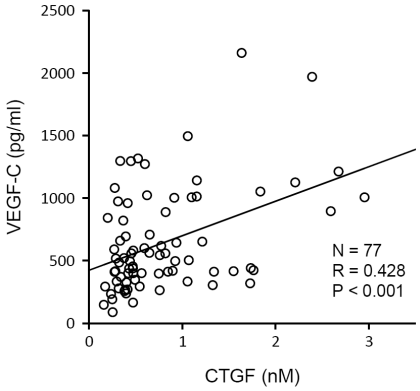

Figure 1. Connective tissue growth factor (CTGF) concentration was positively correlated with vascular endothelial growth factor-C (VEGF-C) concentration in overnight dwelled human peritoneal dialysis effluent samples.

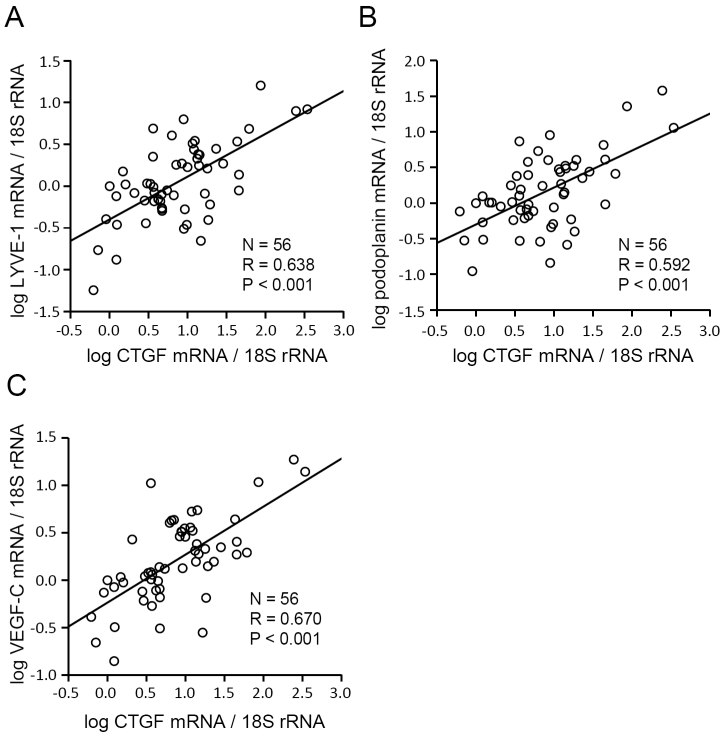

Figure 2. Positive correlation was observed between connective tissue growth factor (CTGF) messenger RNA (mRNA) expression and lymphatic endothelial hyaluronan receptor-1 (LYVE-1) (A), podoplanin (B), and vascular endothelial growth factor-C (VEGF-C) (C) mRNA expression in human peritoneal biopsy samples.

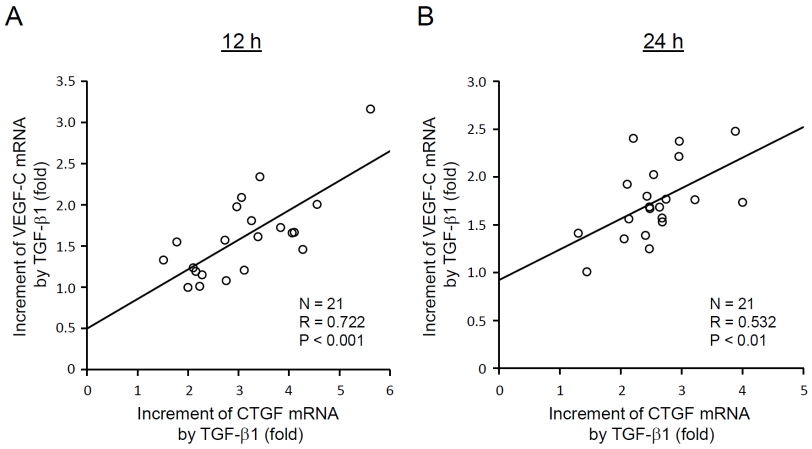

Figure 3. Human peritoneal mesothelial cells from the spent peritoneal dialysis effluent were cultured and stimulated with transforming growth factor-β1 (TGF-β1). Positive correlation was observed between connective tissue growth factor (CTGF) and vascular endothelial growth factor-C (VEGF-C) messenger RNA (mRNA) amplification at 12 (A) and 24 (B) hours after TGF-β1 treatment.

Figure 4

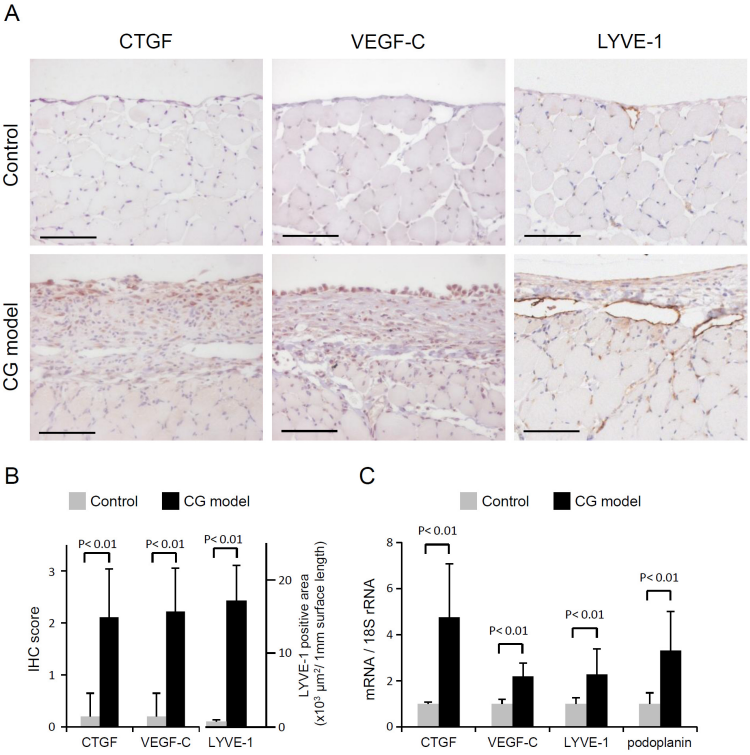

Figure 4 Continued

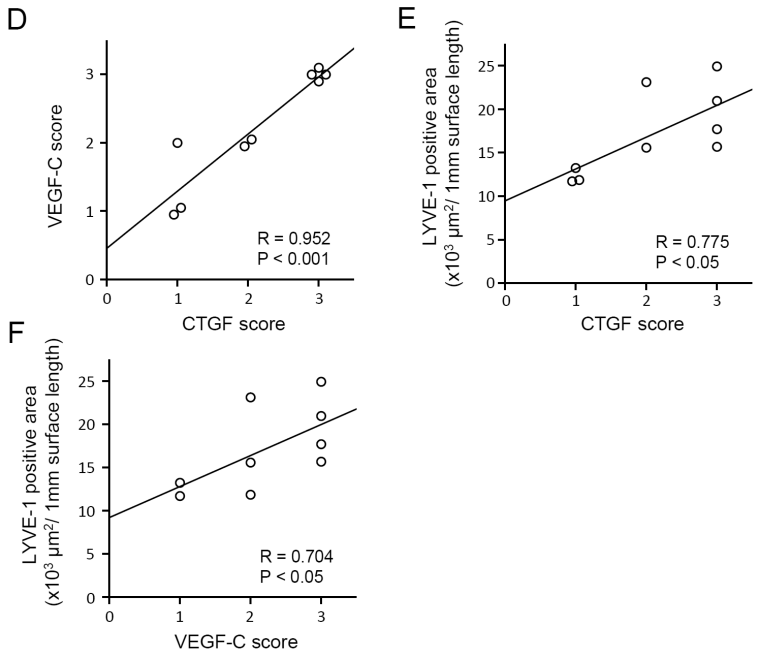

Figure 4. Immunohistochemistry (IHC) in the rat diaphragm showed an increased expression of connective tissue growth factor (CTGF), vascular endothelial growth factor-C (VEGF-C), and lymphatic endothelial hyaluronan receptor-1 (LYVE-1) in CG model (A and B). CTGF, VEGF-C, LYVE-1, and podoplanin messenger RNA (mRNA) expression were increased in CG model (C). IHC analysis showed positive correlations among CTGF, VEGF-C, and LYVE-1 expression in CG model (D-F). Scale bars; 100μm.

REFERENCES

1. Ateş K, Nergizoğlu G, Keven K et al. Effect of fluid and sodium removal on mortality in peritoneal dialysis patients. Kidney Int 2001; 60: 767-776
2. Rumpsfeld M, McDonald SP, Johnson DW. Higher peritoneal transport status is associated with higher mortality and technique failure in the Australian and New Zealand peritoneal dialysis patient populations. J Am Soc Nephrol 2006; 17: 271-278
3. Brimble KS, Walker M, Margetts PJ et al. Meta-analysis: peritoneal membrane transport, mortality, and technique failure in peritoneal dialysis. J Am Soc Nephrol 2006; 17: 2591-2598
4. Mizuno M, Ito Y, Suzuki Y et al. Recent analysis of status and outcomes of peritoneal dialysis in the Tokai area of Japan: the second report of the Tokai peritoneal dialysis registry. Clin Exp Nephrol 2016; DOI: 10.1007/s10157-016-1249-9
5. Williams JD, Craig KJ, Topley N et al. Morphologic changes in the peritoneal membrane of patients with renal disease. J Am Soc Nephrol 2002; 13: 470-479
6. Mateijsen MA, van der Wal AC, Hendriks PM et al. Vascular and interstitial changes in the peritoneum of CAPD patients with peritoneal sclerosis. Perit Dial Int 1999; 19: 517-525
7. Abu-Hijleh MF, Habbal OA, Moqattash ST. The role of the diaphragm in lymphatic absorption from the peritoneal cavity. J Anat 1995; 186: 453-467
8. Fusshöller A, zur Nieden S, Grabensee B et al. Peritoneal fluid and solute transport: influence of treatment time, peritoneal dialysis modality, and peritonitis incidence. J Am Soc Nephrol 2002; 13: 1055-1060
9. Parikova A, Smit W, Struijk DG et al. Analysis of fluid transport pathways and their determinants in peritoneal dialysis patients with ultrafiltration failure. Kidney Int 2006; 70: 1988-1994
10. Krediet RT. The effective lymphatic absorption rate is an accurate and useful concept in the physiology of peritoneal dialysis. Perit Dial Int 2004; 24: 309-313
11. Flessner M. Effective lymphatic absorption rate is not a useful or accurate term to use in the physiology of peritoneal dialysis. Perit Dial Int 2004; 24: 313-316
12. Kinashi H, Ito Y, Mizuno M et al. TGF-β1 promotes lymphangiogenesis during peritoneal fibrosis. J Am Soc Nephrol 2013; 24: 1627-1642
13. Zheng W, Aspelund A, Alitalo K. Lymphangiogenic factors, mechanisms, and applications. J Clin Invest 2014; 124: 878-887
14. Coso S, Bovay E, Petrova TV. Pressing the right buttons: signaling in lymphangiogenesis. Blood 2014; 123: 2614-2624
15. Terabayashi T, Ito Y, Mizuno M et al. Vascular endothelial growth factor receptor-3 is a novel target to improve net ultrafiltration in methylglyoxal-induced peritoneal injury. Lab Invest 2015; 95: 1029-1043
16. Mizutani M, Ito Y, Mizuno M et al. Connective tissue growth factor (CTGF/CCN2) is increased in peritoneal dialysis patients with high peritoneal solute transport rate. Am J Physiol Renal Physiol 2010; 298: F721-F733

17. Zarrinkalam KH, Stanley JM, Gray J et al. Connective tissue growth factor and its regulation in the peritoneal cavity of peritoneal dialysis patients. Kidney Int 2003; 64: 331-338
18. Leung JC, Chan LY, Tam KY et al. Regulation of CCN2/CTGF and related cytokines in cultured peritoneal cells under conditions simulating peritoneal dialysis. Nephrol Dial Transplant 2009; 24: 458-469
19. Pi L, Shenoy AK, Liu J et al. CCN2/CTGF regulates neovessel formation via targeting structurally conserved cystine knot motifs in multiple angiogenic regulators. FASEB J 2012; 26: 3365-3379
20. Ueno T, Nakashima A, Doi S et al. Mesenchymal stem cells ameliorate experimental peritoneal fibrosis by suppressing inflammation and inhibiting TGF-β1 signaling. Kidney Int 2013; 84: 297-307
21. Honda K, Hamada C, Nakayama M et al. Impact of uremia, diabetes, and peritoneal dialysis itself on the pathogenesis of peritoneal sclerosis: a quantitative study of peritoneal membrane morphology. Clin J Am Soc Nephrol 2008; 3: 720-728
22. Kato H, Mizuno T, Mizuno M et al. Atrial natriuretic peptide ameliorates peritoneal fibrosis in rat peritonitis model. Nephrol Dial Transplant 2012; 27: 526-536
23. Mactier RA, Khanna R, Twardowski Z et al. Contribution of lymphatic absorption to loss of ultrafiltration and solute clearances in continuous ambulatory peritoneal dialysis. J Clin Invest 1987; 80: 1311-1316
24. Smit W, Schouten N, van den Berg N et al. Analysis of the prevalence and causes of ultrafiltration failure during long-term peritoneal dialysis: a cross-sectional study. Perit Dial Int 2004; 24: 562-570
25. Alitalo A, Detmar M. Interaction of tumor cells and lymphatic vessels in cancer progression. Oncogene 2012; 31: 4499-4508
26. Kim H, Kataru RP, Koh GY. Inflammation-associated lymphangiogenesis: a double-edged sword? J Clin Invest 2014; 124: 936-942
27. Dashkevich A, Hagl C, Beyersdorf F et al. VEGF Pathways in the Lymphatics of Healthy and Diseased Heart. Microcirculation 2016; 23: 5-14
28. Cui Y, Liu K, Monzon-Medina ME et al. Therapeutic lymphangiogenesis ameliorates established acute lung allograft rejection. J Clin Invest 2015; 125: 4255-4268
29. Sakamoto I, Ito Y, Mizuno M et al. Lymphatic vessels develop during tubulointerstitial fibrosis. Kidney Int 2009; 75: 828-838
30. Vlahu CA, de Graaff M, Aten J et al. Lymphangiogenesis and Lymphatic Absorption Are Related and Increased in Chronic Kidney Failure, Independent of Exposure to Dialysis Solutions. Adv Perit Dial 2015; 31: 21-25
31. Davies SJ. Unraveling the mechanisms of progressive peritoneal membrane fibrosis. Kidney Int 2016; 89: 1185-1187
32. Yang WS, Tsai TJ, Shih CL et al. Intraperitoneal vascular endothelial growth factor C level is related to peritoneal dialysis ultrafiltration. Blood Purif 2009; 28: 69-74

33. Gerritsen KG, Abrahams AC, Peters HP et al. Effect of GFR on plasma N-terminal connective tissue growth factor (CTGF) concentrations. Am J Kidney Dis 2012; 59: 619-627
34. Yu Z, Lambie M, Davies SJ. Longitudinal study of small solute transport and peritoneal protein clearance in peritoneal dialysis patients. Clin J Am Soc Nephrol 2014; 9: 326-334
35. Rippe B, Davies S. Permeability of peritoneal and glomerular capillaries: what are the differences according to pore theory? Perit Dial Int 2011; 31: 249-258
36. Yung S, Chan TM. Intrinsic cells: mesothelial cells -- central players in regulating inflammation and resolution. Perit Dial Int 2009; 29: S21-S27
37. Kang DH, Hong YS, Lim HJ et al. High glucose solution and spent dialysate stimulate the synthesis of transforming growth factor-beta1 of human peritoneal mesothelial cells: effect of cytokine costimulation. Perit Dial Int 1999; 19: 221-230
38. De Vriese AS, Tilton RG, Mortier S et al. Myofibroblast transdifferentiation of mesothelial cells is mediated by RAGE and contributes to peritoneal fibrosis in uraemia. Nephrol Dial Transplant 2006; 21: 2549-2555
39. Lai KN, Lai KB, Lam CW et al. Changes of cytokine profiles during peritonitis in patients on continuous ambulatory peritoneal dialysis. Am J Kidney Dis 2000; 35: 644-652
40. Yokoi H, Mukoyama M, Nagae T et al. Reduction in connective tissue growth factor by antisense treatment ameliorates renal tubulointerstitial fibrosis. J Am Soc Nephrol 2004; 15: 1430-1440
41. Guha M, Xu ZG, Tung D et al. Specific down-regulation of connective tissue growth factor attenuates progression of nephropathy in mouse models of type 1 and type 2 diabetes. FASEB J 2007; 21: 3355-3368
42. Luo GH, Lu YP, Song J et al. Inhibition of connective tissue growth factor by small interfering RNA prevents renal fibrosis in rats undergoing chronic allograft nephropathy. Transplant Proc 2008; 40: 2365-2369
43. Okada H, Kikuta T, Kobayashi T et al. Connective tissue growth factor expressed in tubular epithelium plays a pivotal role in renal fibrogenesis. J Am Soc Nephrol 2005; 16: 133-143

6

Transforming growth factor-β induces vascular endothelial growth factor-C expression leading to lymphangiogenesis in rat unilateral ureteral obstruction

Kidney Int. 2012;81(9):865-79

Yasuhiro Suzuki[1], Yasuhiko Ito[1], Masashi Mizuno[1], Hiroshi Kinashi[1], Akiho Sawai[1], Yukihiro Noda[2], Tomohiro Mizuno[3], Hideaki Shimizu[4], Yoshiro Fujita[4], Katsuyuki Matsui[5], Shoichi Maruyama[1], Enyu Imai[1], Seiichi Matsuo[1], and Yoshifumi Takei[6]

[1]Department of Nephrology and Renal Replacement Therapy, Nagoya University Graduate School of Medicine, Nagoya, Japan
[2]Division of Clinical Sciences and Neurosychopharmacology, Meijyo University Graduate School of Medicine, Nagoya, Japan
[3]Department of Neurosychopharmacology and Hospital Pharmacy, Nagoya University Graduate School of Medicine, Nagoya, Japan
[4]Department of Nephrology, Chubu Rosai General Hospital, Nagoya, Japan
[5]Department of Internal Medicine IV, Teikyo University, Kawasaki, Japan
[6]Department of Biochemistry, Nagoya University Graduate School of Medicine, Nagoya, Japan

ABSTRACT

Inflammation is recognized as an important contributor to lymphangiogenesis; however, in tubulointerstitial lesions in human chronic kidney diseases, this process is better correlated with the presence of myofibroblasts rather than macrophages. As little is known about the interaction between lymphangiogenesis and renal fibrosis, we utilized the rat unilateral ureteral obstruction model to analyze inflammation, fibrosis, lymphangiogenesis, and growth factor expression. Additionally, we determined the relationship between vascular endothelial growth factor-C (VEGF-C), an inducer of lymphangiogenesis, and the profibrotic factor, transforming growth factor-β1 (TGF-β1). The expression of both TGF-β1 and VEGFC was detected in tubular epithelial and mononuclear cells, and gradually increased, peaking 14 days after ureteral obstruction. The kinetics and localization of VEGF-C were similar to those of TGF-β1, and the expression of these growth factors and lymphangiogenesis were linked with the progression of fibrosis. VEGF-C expression was upregulated by TGF-β1 in cultured proximal tubular epithelial cells, collecting duct cells, and macrophages. Both in vitro and in vivo, the induction of VEGF-C along with the overall appearance of lymphatics in vivo was specifically suppressed by the TGF-β type I receptor inhibitor LY364947. Thus, TGF-β1 induces VEGF-C expression, which leads to lymphangiogenesis.

INTRODUCTION

Blood vessels have a continuous basal lamina with tight inter-endothelial junctions and are supported by pericytes and smooth muscle cells. In contrast, lymphatic endothelial cells have a thin discontinuous basement membrane and have gaps between the cells that open to the adjacent connective tissues.[1] In edematous tissue, the lymphatic endothelial cells are pulled by anchoring filaments and bileaflet valves to prevent the backflow of lymphatic fluid.[2] These structures remove tissue fluid from the interstitium and transfer extravasated plasma protein and cells back into circulation. In this respect, lymphatic vessels are essential for body fluid balance and immunological surveillance.[3]

Increases in lymphatic vessels have recently been reported in several disease conditions, including tumor metastasis,[4–7] chronic respiratory inflammatory diseases,[8] wound healing,[9] renal transplant rejection,[10,11] and granulation tissues in myocardial infarction.[12] Inflammation is recognized as an important contributor to lymphangiogenesis in human diseases[10,13] and in animal models.[14,15] In particular, macrophages are involved in lymphangiogenesis in the production of vascular endothelial growth factor (VEGF)-C and -D, which are recognized as potentially important mediators for lymphangiogenesis.[16] Interleukin-1β and tumor necrosis factor-α have been shown to induce the upregulation of VEGF-C.[17] In addition, CD11b+ macrophages may form lymphatic-like vessels in vitro.[14,18] A recent report showed that inflammation induced lymphangiogenesis through the upregulation of VEGF receptor-3 mediated by nuclear factorkappa-B and prospero-related homeobox 1.[19]

In chronic kidney disease, we recently reported an increase in the number of lymphatics observed at the site of tubulointerstitial lesions and this increase was correlated with degree of tissue damage. In addition, lymphangiogenesis was more strongly correlated with fibrosis than inflammation on analysis of human glomerular diseases and acute and chronic tubulo-interstitial nephritis.[20] We also demonstrated strong expression of VEGF-C in the proximal tubules.[20] Our results indicated that lymphangiogenesis is a common feature in the progression of tubulo-interstitial fibrosis, and the fibrotic process may play a role in the development of lymphatics.[20] However, there has been little focus on the role of transforming growth factor (TGF)- β, one of the most important mediators for tissue fibrosis, in lymphangiogenesis to date.

In this study, we investigated the roles of TGF-β and VEGF-C in the development of lymphangiogenesis in the unilateral ureteral obstruction (UUO) model. In addition, we studied the relationship between TGF-β and VEGF-C in cultured proximal and collecting tubules, macrophages and fibroblasts, which are involved in tubulo-interstitial fibrosis. This is the first report to examine the mechanisms and roles of TGF-β in lymphangiogenesis.

RESULTS

Basic characteristics of the rat UUO model

Three days after ligation, dilation of the tubules and infiltration of inflammatory cells were seen in both the cortex and the medulla. On day 14, tubular degeneration, dilation, and

atrophy became severe and intense interstitial fibrosis was also observed (Figure 1). Morphological analysis demonstrated strong infiltration of CD68 (ED-1)-positive macrophages in both the cortex and medulla on day 3 that was more prominent than the expression of α-smooth muscle actin (α-SMA)-positive fibroblasts (Figure 2a and b). Expression of α-SMA-positive fibroblasts and type III collagen deposition in the tubulo-interstitial area became conspicuous and peaked on day 14 (Figure 2).

Lymphatic vessels in control and UUO model

In the control kidney, podoplanin-positive and lymphatic endothelial hyaluronan receptor-1 (LYVE-1)-positive lymphatic vessels were not encountered in the normal cortical tubulo-interstitial area and were observed only adjacent to the large and intermediate-sized vessels (Figures 3a, b, and 4). In the glomeruli, podoplanin was expressed in the podocytes and parietal epithelial cells. In contrast, LYVE-1 was expressed in the glomerular endothelial cells detected by anti-aminopeptidase P antibody, a marker of rat endothelial cells,[21] on serial sections and double staining (Figure 3a–c, Supplementary Figure S1a–c online). In the kidney with ureteral obstruction, podoplanin- and LYVE-1-positive lymphatic vessels grew with time and peaked on day 14 in both the medullary and cortical areas (Figures 3d–g and 4). On serial sections of the medulla on day 14, a number of podoplanin- and LYVE-1-positive lymphatic vessels that were negative for aminopeptidase P were observed, and the entry of the lymphatics was confirmed in the renal pelvis (red and blue arrows in Figure 3h–j). On the other hand, endothelial cells of the blood vessels were negative for podoplanin and LYVE-1 (Figure 3h–j). The expression pattern of podoplanin in the interstitial area was similar to that of LYVE-1 (Supplementary Figure S1d–i). The expression pattern in the glomeruli of these three markers (Figure 3h–j) was the same as those in control kidneys (Figure 3a–g).

Expression of VEGF-C and TGF-b, and lymphangiogenesis during UUO

Because TGF-β is known to have an important role in the pathogenesis of tubulo-interstitial fibrosis,[22] expression of TGF-β was compared with that of VEGF-C in this model. On immunohistochemistry, expression of TGF-β protein detected by anti-TGF-β 1, 2 and 3 antibodies was seen to increase gradually, peaking on day 14 (Figure 4); this expression was primarily seen in the tubular epithelial cells, and was partly seen in the inflammatory cells. TGF-β expression in the glomeruli was not elevated. In the control kidney, VEGFC was weakly detected in the tubular epithelial cells (day 0, Figure 4). VEGF-C expression was also gradually upregulated, mainly in the enlarged tubular epithelial cells in both the cortex and medulla after disease induction. Although we were able to detect VEGF-C in the infiltrating cells in the tubulo-interstitial area on days 9 and 14, expression was more marked in the tubules than in the inflammatory cells (Figure 4, Supplementary Figures S2–4 online). Morphometric analysis demonstrated that TGF-β and VEGF-C expression paralleled lymphangiogenesis (Figure 5).

Localization of VEGF-C and TGF-β protein in UUO (day 14)

To identify the segments of tubules that expressed VEGF-C and TGF-β, serial sections were stained with aquaporin-1 and aquaporin-2. VEGF-C and TGF-β were expressed by the aquaporin-1-positive proximal tubules and aquaporin-2-positive collecting tubules in the injured tubulo-interstitial areas of the cortex and the medulla (Figure 6). Interestingly, localization of VEGF-C was similar, and often showed co-localization with TGF-β (Figure 6, Supplementary Figure S3 online).

VEGF-C, TGF-β, podoplanin, and LYVE-1 messenger RNA (mRNA) expression analyzed by real-time polymerase chain reaction (PCR) in UUO

All isoforms of TGF-β and VEGF-C mRNA increased with time, and peaked on day 14 in both the cortex and medulla (Figure 7a–d). mRNA expression of LYVE-1, podoplanin, and vascular endothelial growth factor receptor-3, markers of lymphangiogenesis, increased over time and peaked on day 14 (Figure 7e–h, Supplementary Figure S5a and b online). These kinetics were similar to those of TGF-β and VEGF-C mRNA and protein (Figures 5a, b, and 7a–d). These expression patterns were also comparable to the expression of α-SMA and type III collagen, but not ED-1-positive macrophages (Figure 2). These findings indicate that lymphangiogenesis developed in association with the fibrotic process. In contrast, the expression of VEGF-A mRNA, the most potent mediator of neoangiogenesis, was slightly lower on day 3, but was not significantly altered during the observation period (Supplementary Figure S6 online).

VEGF-C induction by TGF-β1 in cultured proximal tubular epithelial (HK-2) cells, collecting duct (M-1) cells, macrophages (RAW264.7) and fibroblasts (NRK-49F)

To explore the roles of TGF-β in lymphangiogenesis, we investigated VEGF-C induction by TGF-β1 in cultured proximal tubular epithelial cells, collecting duct cells, macrophages and fibroblasts, which are involved in the development of tubulo-interstitial injury of UUO (Figure 8).

In human kidney-2 (HK-2, human proximal tubular epithelial cells), dose–response studies were conducted using incubation for 24 h with recombinant TGF-β1 at 0, 1, 5, or 20 ng/ml. TGF-β1 induced significant upregulation of VEGF-C protein ($P<0.001$), determined by an enzymelinked immunosorbent assay and VEGF-C mRNA expression ($P<0.001$), determined by real-time PCR (Figure 8a and c). On the basis of these experiments, time-course studies were performed using 5 ng/ml TGF-β1. VEGF-C mRNA/18S ribosomal RNA increased by about a 2- to 2.5-fold and peaked at 12 h. VEGF-C protein was secreted into supernatants under serum-free conditions and without TGF-β incubation. TGF-β1 significantly induced VEGF-C protein secretion at 24 h ($P<0.001$, Figure 8b).

In the M-1 mouse cortical collecting duct cell line, TGF-β1 induced the upregulation of VEGF-C mRNA expression. VEGF-C mRNA/18S ribosomal RNA increased and peaked 24 h after incubation with 5 ng/ml TGF-β1 (Figure 8e and f).

In mouse macrophages (RAW264.7), concentrations above 5 ng/ml TGF-β1 significantly increased VEGF-C mRNA expression ($P<0.05$, Figure 8g). VEGF-C mRNA/18S ribosomal RNA was elevated and peaked at 12 h after incubation with 5 ng/ml TGF-β1 (Figure 8h). VEGF-C induction by TGF-β1 in these cells was suppressed by TGF-β type I receptor inhibitor LY364947 (LY) in a dose-dependent manner (Figure 9).

On the other hand, in the NRK-49F rat renal fibroblast cell line, VEGF-C mRNA was not upregulated in dose–response experiments (0, 1, 5 or 20 ng/ml) or by 5 ng/ml TGF-β1 at any time points (data not shown).

Effects of TGF-β type I receptor inhibitor (LY364947) on lymphangiogenesis in UUO

To investigate the effects of the TGF-β–VEGF-C pathway on lymphangiogenesis in UUO, we administered LY364947 into the obstructed kidney via the aorta. LY364947 suppressed type III collagen, VEGF-C and LYVE-1 mRNA expression resulting in a reduction in the number of lymphatics (Figure 10).

DISCUSSION

Sustained injury by persistence of the initiating events, such as immunologically mediated glomerulonephritis and tubulo-interstitial nephritis, hemodynamic disorders, and metabolic diseases, may lead to a chronic and fibrogenic inflammatory response involving macrophage infiltration, fibroblast proliferation and accumulation of extracellular matrix.[23–25] Inflammation is thought to have an important role in lymphatic development in several disease conditions, and macrophages have been suggested to stimulate lymphangiogenesis by acting as a source of lymphatic endothelial progenitor cells and by providing a crucial source of pro-lymphangiogenic growth factors.[10,11,13–15,17,18,26,27]

In our recent reports on human renal diseases, we found that lymphangiogenesis was affected by the duration of inflammation and progression of fibrosis, rather than by acute inflammation.[20] Tubulo-interstitial fibrosis in a rat remnant kidney model was also reported to be associated with newly formed lymphatic vessels.[21] In other organs, lymphatic proliferation was confirmed in human idiopathic pulmonary fibrosis and bleomycin-induced pulmonary fibrosis in rats.[18,28] However, conflicting data between tissue fibrosis and lymphangiogenesis have recently been reported.[29–31] TGF-β was reported to directly inhibit growth of lymphatic endothelial cells.[29–31] In addition, TGF-β type I receptor inhibitor enhanced their proliferation.[29] To address the different aspects of lymphatic proliferation in tubulo-interstitial fibrosis on the human biopsy specimens,[20] we investigated the roles of TGF-β and VEGF-C on lymphangiogenesis in UUO. In our analysis of a UUO model on day 3, numerous infiltrating macrophages had already appeared, but only weak upregulation of VEGF-C and slight lymphatic proliferation were confirmed (Figures 2, 5, and 7). From days 9 to 14 in rat UUO, we observed that lymphangiogenesis was associated with tubulo-interstitial fibrosis and chronic inflammation. In addition, VEGF-C expression was elevated in both the cortex and medulla with time after ureteral ligation, and paralleled TGF-β expression (Figures 4, 5, and 7).

These findings suggest that the fibrotic process with chronic inflammation may be linked with lymphangiogenesis rather than acute inflammation.

VEGF-C is known to be one of the most important mediators of lymphangiogenesis.[16,32] VEGF-C has been shown to be required for the normal development of lymphatic vessels, particularly those sprouting from the embryonic veins.[3] To clarify the roles of TGF-β in lymphangiogenesis, we investigated VEGF-C induction by TGF-β1 in cultured proximal tubular epithelial cells (HK-2), collecting duct cells (M-1), macrophages (RAW264.7), and fibroblasts (NRK-49F) (Figure 8). We detected basal VEGF-C expression in all cell lines. Notably, significant increases in VEGF-C expression in response to TGF-β1 were seen in cultured proximal tubular epithelial cells, collecting duct cells and macrophages, but not in fibroblasts. In UUO, TGF-β expression increased over time and was preferentially increased in tubular epithelial cells and to a lesser degree in infiltrating macrophages (Figure 4, Supplementary Figures S2–4 online), which is consistent with previous reports of precise studies by in situ hybridization, competitive PCR and immunohistochemistry.[33,34] Tubular epithelial cell injury induced by UUO may also affect TGF-β and VEGF-C expression. The strong expression of VEGF-C in aquaporin-1- and -2-positive tubular epithelial cells in vivo (Figure 6) and in culture studies suggests that tubular epithelial cells are an important source of VEGF-C in UUO (Figure 8). On reverse transcription–PCR, we were not able to detect vascular endothelial growth factor receptor-2 and -3 in cultured proximal tubular epithelial cells, collecting duct cells, fibroblasts, and macrophages (Supplementary Figure S7 online), which suggests that VEGF-C does not act in an autocrine manner. Vascular endothelial growth factor receptor-3 was only detected in the lymphatics in vivo (Supplementary Figure S5e–g online). These findings suggest that TGF-β1 is the central inducer of VEGF-C leading to lymphangiogenesis in tubulo-interstitial fibrosis of UUO. In the human chronic glomerular diseases associated with tubulo-interstitial injury, VEGF-C expression was also observed in the tubular epithelial cells.[20] Recent reports have indicated that TGF-β directly inhibits lymphatic endothelial cell proliferation and migration.[29–31] In the cultured NRK-49F fibroblasts of our study, VEGF-C induction by TGF-β1 was not significant, despite the presence of basal expression (Figure 11). These findings suggest that fibroblasts do not directly enhance lymphangiogenesis. However, in the kidney, VEGF-C production by tubular epithelial cells may have a crucial role in the growth of lymphatics, in contrast to the situation in other organs. In the process of lymphatic growth, the effects of VEGF-C produced by these cells may exceed the direct effects by TGF-β on the lymphatic endothelial cells, and the balance between these two factors may control the extent of lymphangiogenesis. The limitation in in vivo experiments is the difficulty of systemic administration of TGF-β receptor I inhibitor in UUO. Low doses (1 mg/body g/day intraperitoneally) of LY364947 did not reduce the collagen expression, and rats cannot tolerate high doses (3 mg/body g/day intravenously). Therefore, we administered LY364947 to obstructed kidney via the aorta, which resulted in inhibition of TGF-β, VEGF-C and LYVE-1 (Figure 10). Although it remains unclear whether fibrosis with collagen deposition can modulate lymphangiogenesis, at least TGF-β upregulated

VEGF-C in renal cells leading to lymphangiogenesis in UUO. Thus, our data indicate that TGF-β is a critical regulator of VEGF-C, and lymphatic proliferation is likely to depend on the TGF-β–VEGF-C pathway in UUO (Figure 11). Conversely, VEGF-A mRNA expression was not significantly affected (Supplementary Figure S5 online), which is consistent with previous reports. In contrast to the proliferation of lymphatics, peritubular capillary density was shown to decrease in areas of tubulo-interstitial scarring.[35]

In our studies, we used three markers to discriminate between lymphatics and blood vessels. Podoplanin, a transmembrane glycoprotein, is expressed by lymphatic endothelial cells, but not by blood endothelial cells.[10,11] However, it has been reported that podoplanin is expressed in keratinocytes, type I epithelial cells of the lung, mesothelial cells, myoepithelial cells, and glomerular podocytes.[21,26] LYVE-1 was first identified as a CD44 homolog and is used as a specific marker of lymphatic endothelial cells.[26,36–38] LYVE-1 is also known to be expressed by liver sinusoids with fenestration, pulmonary capillaries, and some macrophages.[26,39] We found that glomerular endothelial cells, which have a fenestration structure, are extra sites that express LYVE-1 (Figure 3). This was confirmed by double staining with aminopeptidase P, which is a specific marker of endothelial cells in rat blood vessels (Figure 3).[21] In this respect, both markers have limitations as specific markers for lymphatic endothelial cells. We successfully identified the entry of the lymphatic vessels, which were positive for podoplanin and LYVE-1, and negative for aminopeptidase P, into the renal pelvis (Figure 3h–j). A previous study revealed that obstruction of the ureter resulted in a marked increase in thoracic duct lymph flow and pressure in UUO.[40] In addition, lymphatic ligation leads to an increase in renal interstitial pressure.[41,42] In a clinical case of chyluria due to filariasis, occlusion of the thoracic duct was demonstrated by pedal lymphangiography (Supplementary Figure S8a). Enhancement with contrast media on a computed tomography scan of the renal pelvis strongly suggested an interconnection between lymphatics and the urinary excretion system in chyluria (Supplementary Figure S8c online). These findings indicate that there is a connection between pelvic and systemic lymphatic circulation, which may reduce pelvic pressure.

In summary, we demonstrated that lymphatic vessels proliferate and show a correlation with TGF-β expression in UUO. Thus, TGF-β has an important role in the progression of lymphangiogenesis. Tubular epithelial cells and macrophages are involved in the progression of lymphangiogenesis in UUO, and the TGF-β–VEGF-C pathway might have a crucial role. Knowledge regarding the effects of TGF-β on VEGF-C in renal cells may enhance our understanding of the underlying mechanisms and may lead to strategies for modulating lymphatics in chronic renal diseases. Stimulation of lymphatic growth was recently considered as a new target in some disease states. The relative importance of lymphangiogenesis will have to be established by manipulation of VEGF-C levels in chronic renal injury models in the future.

MATERIALS AND METHODS

Animals and experimental design

All animal studies were carried out in accordance with the animal experimentation guidelines of Nagoya University Graduate School of Medicine (Nagoya, Japan). Seven-week-old male Sprague-Dawley rats (Japan SLC, Hamamatsu, Japan) initially weighing 210–230 g were used. After induction of anesthesia, the left flank was opened through a small incision and the left ureter was completely ligated with 2-0 suture at two points and cut between the ligatures to prevent retrograde infection. Rats were killed on days 0, 3, 9, and 14 after UUO (n=5 for each time point), and both the obstructed kidney and contralateral kidney were collected. To investigate the TGF-β–VEGF-C pathway on lymphangiogenesis in UUO, we administered TGF-β type I receptor inhibitor LY364947 (2μg/body g in saline; Calbiochem, La Jolla, CA) or saline alone into the obstructed kidney via the aorta with a 28-gauge needle while clamping the aorta just above the left renal artery on 3 consectutive days from days 2 to 4. Rats were killed and evaluated on day 5. The left kidney was processed for routine histology, immunohistochemistry, and total RNA isolation. Kidney specimens were cut into transverse fragments. One part was fixed for 16 h in 10% buffered formalin and embedded in paraffin by conventional techniques. Sections were stained with periodic acid–Schiff 's stain and Masson's trichrome. Formalin-fixed tissue was also used for immunohistochemistry as detailed below. A second part was snap-frozen in liquid nitrogen. Sections (4μm) were cut with a cryostat and used for immunohistochemistry. A third part of the excised left kidney was cut and divided into the cortex and medulla, which were immersed in RNAlater (Ambion, Austin, TX) for total RNA isolation. To preserve the integrity and stability of total RNA, all steps were performed at 4 °C under sterile conditions.

Histology and immunohistochemistry

Immunostaining for type III collagen, α-SMA, monocytes/macrophages (ED-1), podoplanin, LYVE-1 and aminopeptidase P was performed on buffered formalin-fixed tissues, and for VEGF-C, TGF-β, and LYVE-1 staining, immunostaining was performed using 4-μm cryostat sections, as described previously (Supplementary Table S1 online).[20,24,43]

Morphological analysis

To assess the relationship between lymphangiogenesis and tubulointerstitial injury, morphological analysis was separately performed in both the cortex and medulla. Tubulo-interstitial injury was assessed by inflammation (ED-1-positive cells) and by fibrotic processes (α-SMA-positive cells and type III collagen). ED-1-positive macrophages and LYVE-1-positive lymphatic vessels were identified and counted in the cortex and medulla using Zeiss Z1 image microscopy and Axiovision Windows software version 4.4 (Carl Zeiss, Oberkochen, Germany). These were counted in 10 random 750×500-μm areas of both the cortex and the medulla at ×200 magnification, and are expressed in terms of counts per square millimeter. Areas positive for a-SMA, type III collagen, TGF-β 1, 2, and 3, and VEGF-C were assessed in 10 random high-powered fields (×200) of both the cortex and the

medulla using MetaMorph 6.3 image analysis software (Universal Imaging, West Chester, PA).

Cell culture study

Human HK-2 proximal tubular cell lines were purchased from the American Type Culture Collection (ATCC, Manassas, VA) and were maintained in medium containing Dulbecco's modified Eagle's medium and Ham's F-12 medium (Sigma, Tokyo, Japan) supplemented with 10% fetal bovine serum (FBS; Hyclone, Yokohama, Japan).[44] M-1 cells derived from the mouse cortical collecting duct were purchased from the European Collection of Cell Cultures (ECACC, No. 95092201; Salisbury, UK) and were grown in medium containing a 1:1 mixture of Ham's F-12 medium, Dulbecco's modified Eagle's medium, 5μmol/l dexamethasone and 5% FBS. RAW 264.7 cells derived from murine macrophages were purchased from ATCC, and were cultured in Dulbecco's modified Eagle's Medium (Sigma) containing 10% FBS. A rat renal fibroblast cell line (NRK-49F) was purchased from ATCC, and was grown in medium containing Dulbecco's modified Eagle's medium supplemented with 5% FBS. All cells were cultured in humidified air with 5% CO2 at 37 °C. All experiments were performed between passages two and six.

All cells were plated at a density of 2×10^5 cells in 6-cm dishes and grown. Under subconfluent conditions, cells were washed twice with phosphate-buffered saline, and culture medium was replaced with serum-free medium for 24 h to render cells quiescent. Subsequently, cultures were incubated with 5 ng/ml recombinant human TGF-β1 (R&D System, Minneapolis, MN) diluted in serum-free medium. Cells were collected at 0, 6, 12, and 24 h after incubation, and all conditioned media were collected for enzyme-linked immunosorbent assay. For determination of dose response to TGF-β1 stimulation, cells were cultured for 24 h in media supplemented with 0, 1, 5, or 20 ng/ml TGF-β1 after starvation for 24 h. In inhibition studies, cells were incubated with 5 ng/ml TGF-β1 in combination with a selective inhibitor of TGF-β receptor I (LY364947) for 24 h.

Total RNA isolation from rat kidney tissues and cultures cells

Total RNA was extracted from rat kidney tissues and cultured cells using the RNeasy Mini Kit (Qiagen, Hilden, Germany). Total RNA concentrations were estimated using a spectrophotometer (Ultrospec 3300 pro; Amersham Biosciences, Tokyo, Japan). Rat kidney tissues were immersed in RNAlater (Ambion, Austin, TX) for 1 day. The mixture was ground for 2 min with 5-mm tungsten carbide beads at a frequency of 27 Hz using a mixer-mill grinder according to the manufacturer's instructions (Tissuelyser; Qiagen).

Polymerase chain reaction

For both animal samples and cultured cells, first-strand cDNA was synthesized using the QuantiTect Reverse Transcription Kit (Qiagen) for animal samples or High Capacity Reverse Transcription Kit (Applied Biosystems, Foster City, CA) for cultured cells, according to the manufacturers' instructions. Total RNA (1μg) was then reverse transcribed.

Real-time PCR analysis was performed with an Applied Biosystems Prism 7500HT sequence detection system using TaqMan gene expression assays, as described previously.[45] TaqMan gene expression assays (Applied Biosystems) were used (Supplementary Table S2 online). 18S ribosomal RNA was used as an endogenous control.

VEGF-C enzyme-linked immunosorbent assay

Secretion of VEGF-C into culture supernatants was determined using the Human VEGF-C Assay kit (IBL, Takasaki, Japan), according to the manufacturer's instructions.

Statistical analysis

Values are expressed as means ± s.e. Comparisons among groups were performed by one-way analysis of variance followed by Dunnett's or Tukey's HSD (honestly significant difference) multiple comparison test. Comparisons between LY364947 and saline groups in in vivo experiments were assessed by Mann–Whitney U-test. Differences were considered to be statistically significant at $P<0.05$. All analyses were performed using SPSS software (SPSS, Chicago, IL).

DISCLOSURE

All the authors declared no competing interests.

ACKNOWLEDGMENTS

Grant numbers and sources of support: This work was supported by a Grant-in-Aid for Scientific Research from the Ministry Education, Science, and Culture, Japan (# 20590972), and a 2008 research grant from the Aichi Kidney Foundation, Japan. Financial supports: none. We are grateful for the technical assistance of Mr Norihiko Suzuki, Ms Keiko Higashide, Ms Naoko Asano and Ms Yuriko Sawa (Department of Nephrology, Nagoya University, Nagoya, Japan).

FIGURES

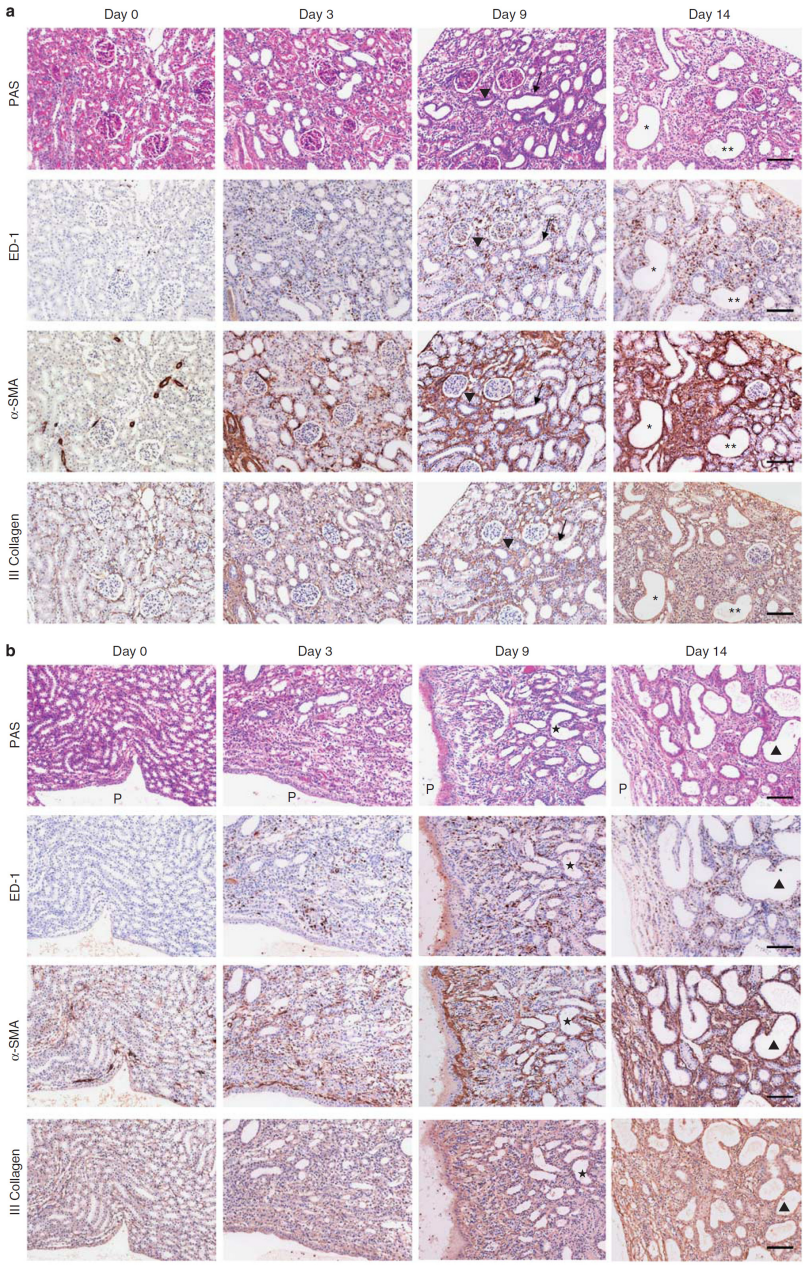

Figure 1 | Rat unilateral ureteral obstruction (UUO) model. (a) Renal cortex of rat UUO model. (b) Renal medulla of rat UUO model. Arrows, arrowheads, asterisks, triangles, and stars indicate the same dilated tubules. Bar = 100μm. ED-1, CD68; P, renal pelvis; PAS, periodic acid–Schiff; α-SMA, α-smooth muscle actin.

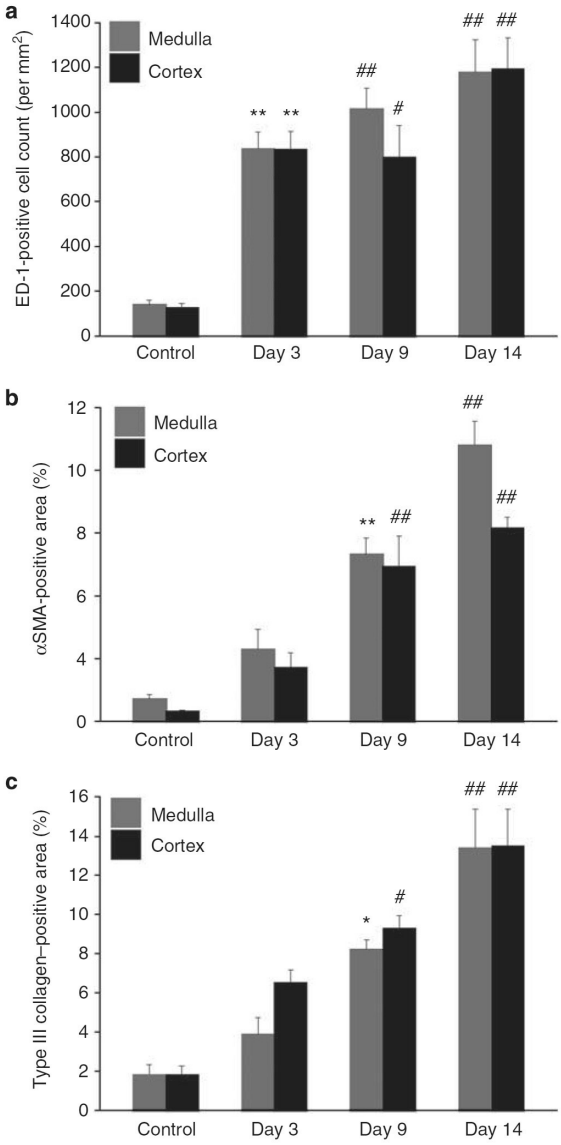

Figure 2 | Quantification of morphological analysis by immunohistochemistry in rat unilateral ureteral obstruction. CD68 (ED-1)-positive macrophage infiltration (a) increased significantly on day 3 and continued to increase until day 14. Areas positive for α-smooth muscle actin (α-SMA) (b) and type III collagen (c) increased with time and peaked on day 14. Values are means ± s.e. (N=5). *P<0.05; **P<0.005; #P<0.01; ##P<0.001 vs. control.

Figure 3

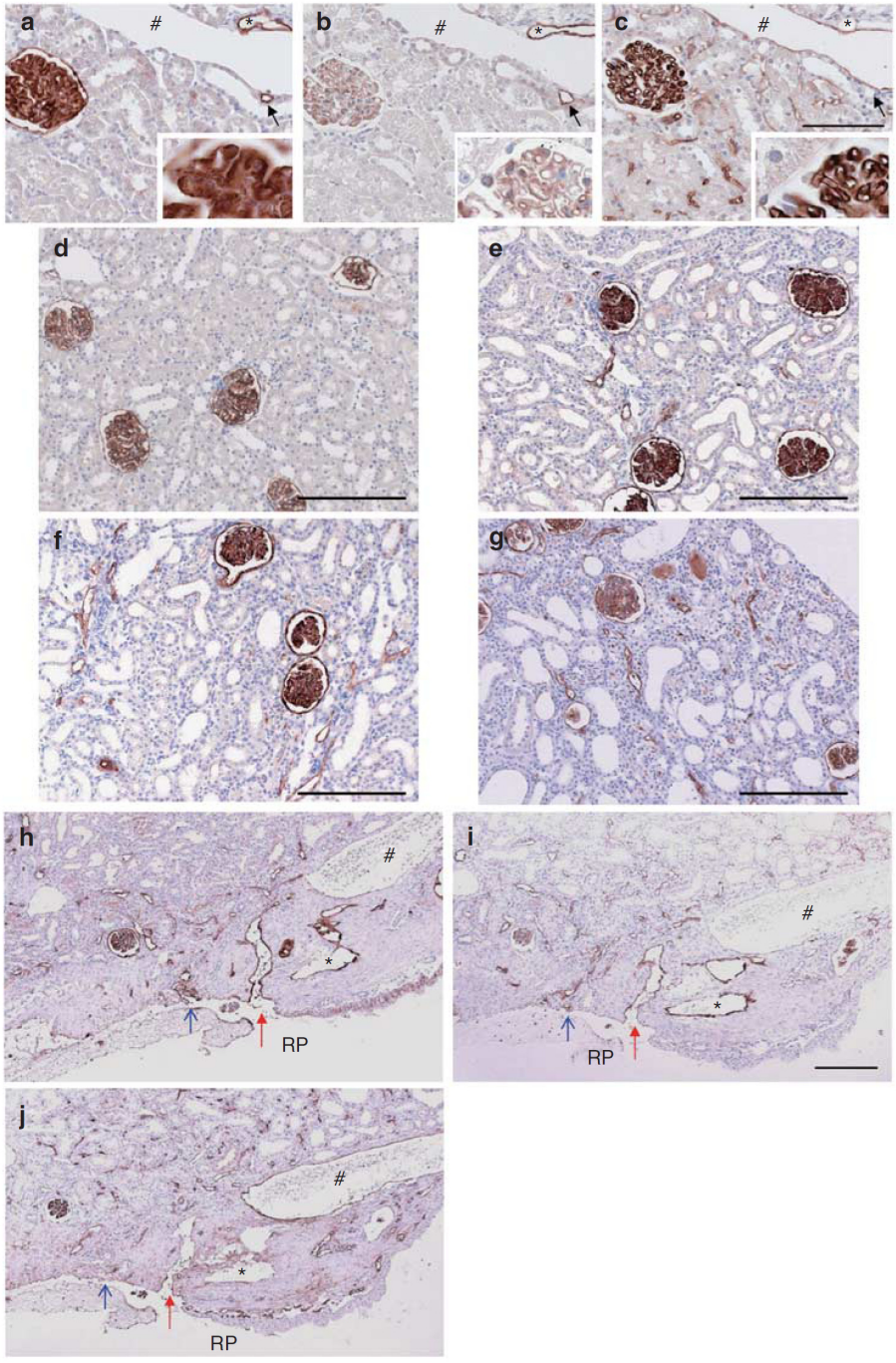

Figure 3 | Lymphatic vessels in normal and obstructed kidneys. (a–c) Immunohistochemical staining for podoplanin (a), lymphatic endothelial hyaluronan receptor-1 (LYVE-1) (b) and aminopeptidase P (c) on serial sections of normal rat kidney. Podoplanin and LYVE-1-positive lymphatic vessels were rarely detected in the normal architecture of the cortico-medullary tubulo-interstitial area. Lymphatics (* and arrows) were observed adjacent to the intermediate-sized vessels (#). In the glomeruli, podoplanin was detected in podocytes and parietal epithelial cells of Bowman's capsule (a). LYVE-1 was also expressed in the glomeruli (b). Expression of aminopeptidase P was observed in the peritubular capillaries and glomerular endothelial cells (c). Bar = 100μm. (d–g) Immunohistochemical staining for podoplanin in the cortex of the unilateral ureteral obstruction (UUO) model. No lymphatic vessels were detected on day 0 (d). There were only a few lymphatic vessels in the cortex of the UUO model on day 3 (e). On day 9 (f) and day 14 (g), the number of lymphatic vessels were increased in the tubulo-interstitial injured area. Bar = 200 μm. (h–j) Lymphatic vessels and blood vessels in the renal medulla in UUO on day 14. Immunohistochemical staining for podoplanin (h), LYVE-1 (i) and aminopeptidase P (j). Lymphatic vessels (*) expressed LYVE-1 and podoplanin, but did not express aminopeptidase P. The entry of the lymphatics (red and blue arrows) was confirmed in the renal pelvis (RP). Vein (#) was positive for aminopeptidase P, but negative for podoplanin and LYVE-1. Bar = 200 μm.

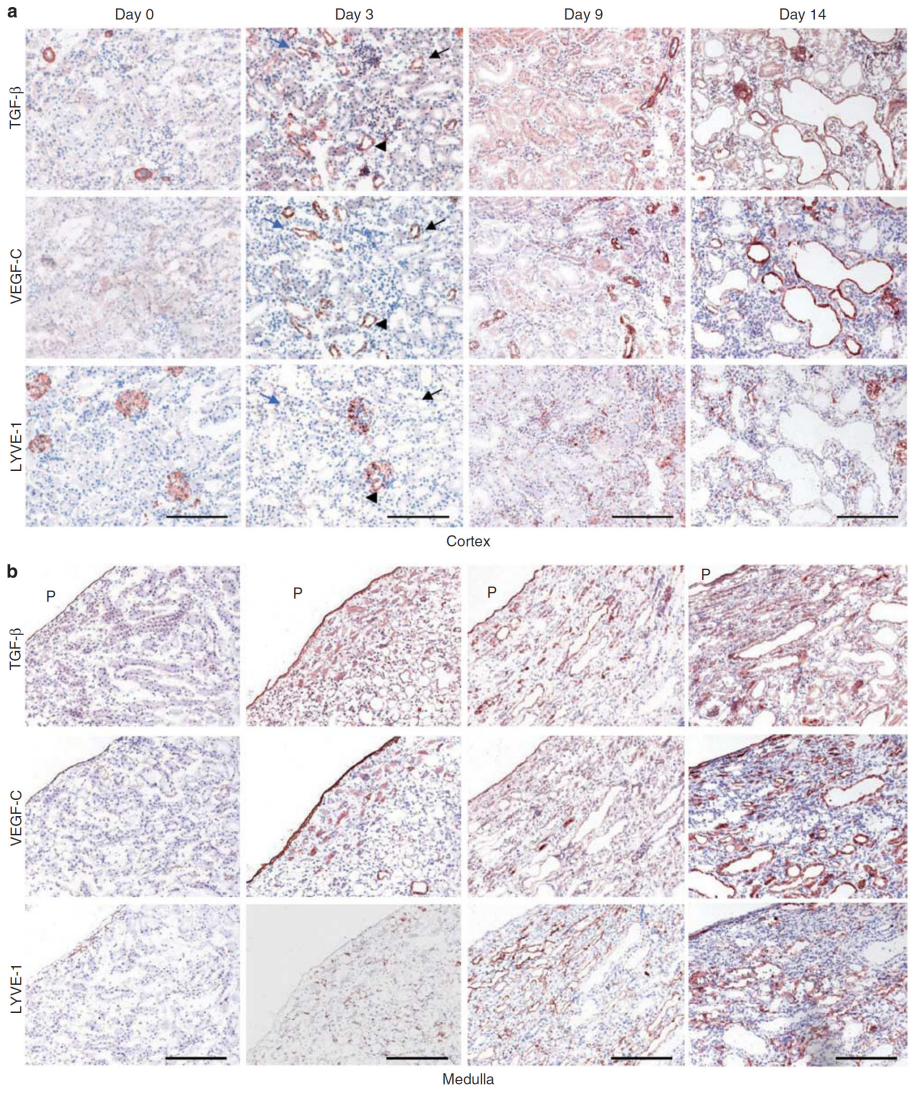

Figure 4 | Expression of growth factors and lymphatic vessels in unilateral ureteral obstruction. Immunohistochemical staining for transforming growth factor-β (TGF-β), vascular endothelial growth factor-C (VEGF-C), and lymphatic endothelial hyaluronan receptor-1 (LYVE-1) on serial frozen sections in the cortex (a) and in the medulla (b). TGF-β and VEGF-C were expressed in tubular epithelial cells (arrows and arrowheads), and were upregulated with time after ureteral obstruction in both the medulla and cortex. LYVE-1-positive lymphatic vessels were revealed and increased with time. Black and blue arrows and arrowheads indicate the same tubules. Bar = 200μm. P, renal pelvis.

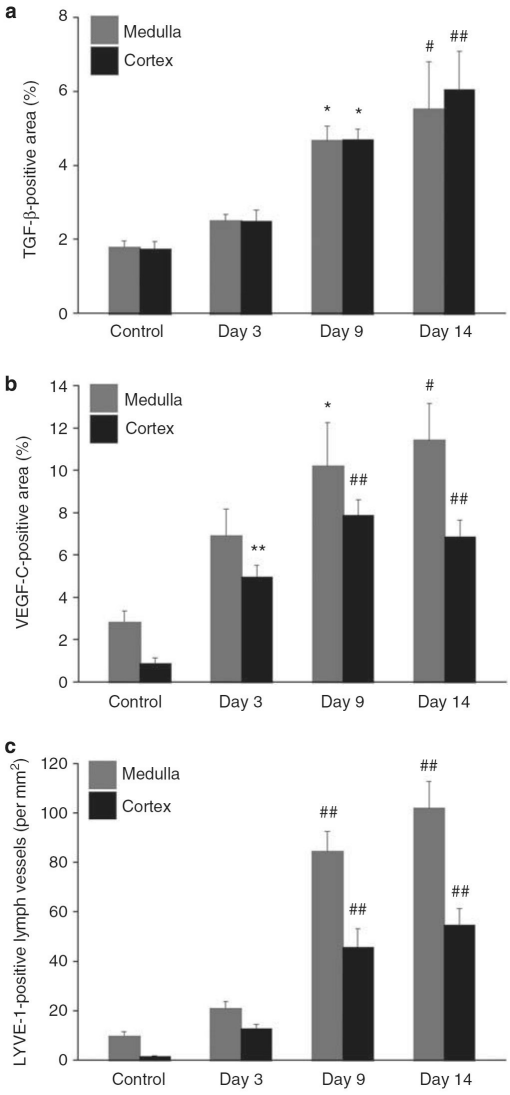

Figure 5 | Quantification of morphological analysis of transforming growth factor-β vascular endothelial growth factor-C (VEGF-C), and lymphatic endothelial hyaluronan receptor-1 (LYVE-1) expression in unilateral ureteral obstruction (UUO) model. TGF-β (a) and VEGF-C (b) expression increased with time. The number of LYVE-1-positive lymph vessels (c) was counted in ten random areas in the medulla and cortex of the UUO kidney. LYVE-1-positive lymphatics increased markedly in the medulla on day 9 and day 14. Values are means ± s.e. (N=5). *P<0.05; **P<0.005; #P<0.01; ##P<0.001 vs. control.

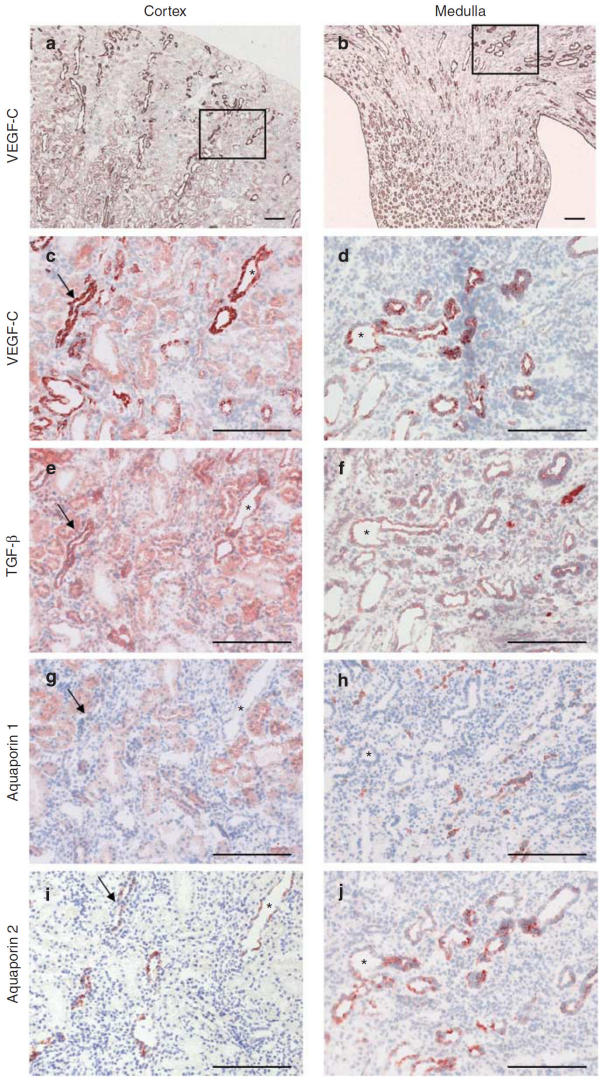

Figure 6 | Localization of vascular endothelial growth factor-C (VEGF-C) and transforming growth factor-β (TGF-β) protein in unilateral ureteral obstruction (UUO) (day 14). Immunohistochemical staining for VEGF-C, TGF-β, aquaporin-1, and aquaporin-2 in the same rat UUO kidney on day 14. VEGF-C is expressed in the aquaporin-1-positive proximal tubules and in the aquaporin-2-positive collecting ducts (arrows and *) in the injured tubulo-interstitial area. TGF-β is often co-localized with VEGF-C both in the cortex and the medulla. (a–d) VEGF-C staining; (e, f) TGF-β staining; (g, h) aquaporin-1 staining; (i, j) aquaporin-2 staining. Left panel (a, c, e, g, i): cortex; right panel (b, d, f, h, j): medulla. (c, d) Enlargement of the rectangular frame of a and b, respectively. Bar = 200μm.

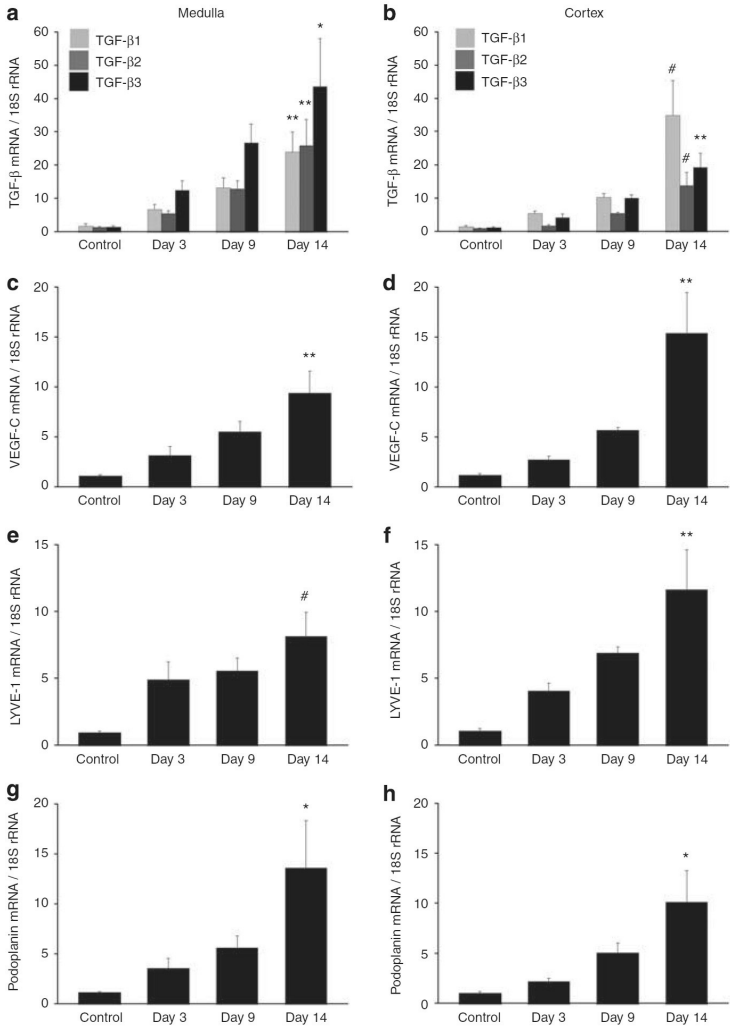

Figure 7 | Quantitative analysis of transforming growth factor-β (TGF-β), vascular endothelial growth factor-C (VEGF-C), lymphatic endothelial hyaluronan receptor-1 (LYVE-1) and podoplanin messenger RNA (mRNA) expression in unilateral ureteral obstruction (UUO) model. Expression of mRNA was analyzed by real-time reverse transcription-polymerase chain reaction. TGF-β, VEGF-C, LYVE-1, and podoplanin mRNA expression in both the medulla and cortex increased and peaked on day 14. (a, c, e, g) Medulla of UUO kidney; (b, d, f, h) cortex of UUO kidney. (a, b) TGF-β mRNA; (c, d) VEGF-C mRNA; (e, f) LYVE-1 mRNA; (g, h) podoplanin mRNA. Values are means ± s.e. (N=5). *P<0.05, **P<0.005, #P<0.01 vs. control.

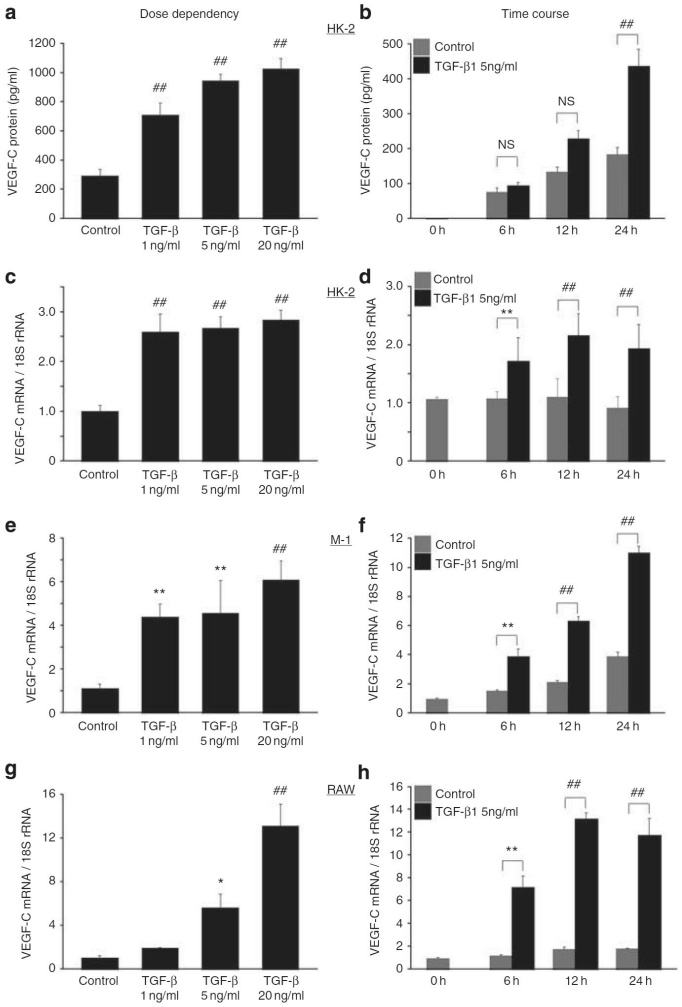

Figure 8 | Vascular endothelial growth factor-C (VEGF-C) expression in cultured proximal tubular epithelial cells (human kidney-2 (HK-2)), collecting duct cells (M-1) and macrophages (RAW 264.7) after treatment with transforming growth factor-β1 (TGF-β1). (a–d) HK-2 proximal tubular epithelial cell line; (e, f) M-1 collecting duct cell line; (g, h) RAW 264.7 macrophage cell line. (a–d) HK-2 cells, preincubated for 24 h in serum-free medium, were treated with TGF-β1. VEGF-C protein level in the supernatant was determined by enzyme-linked immunosorbent assay (a, b), and VEGF mRNA level was determined by real-time reverse transcription-polymerase chain reaction (c, d). 18s ribosomal RNA (rRNA) was used as an internal control. VEGF-C protein levels increased significantly in response to 1, 5, and 20 ng/ml TGF-β1 at 24h (a). VEGF-C mRNA expression was also elevated in response to 1, 5, and 20 ng/ml TGF-β1 at 24 h; it significantly increased at 6 h and peaked at 12 h with 5 ng/ml TGF-β1 (c, d). (e, f) M-1 cells were treated with TGF-β1. VEGF-C mRNA expression was significantly increased by stimulation with more than 1 ng/ml TGF-β1. (g, h) RAW264.7 cells were treated with TGF-β1. VEGF-C mRNA expression was elevated in response to TGF-β1 stimulation. Data are means ± s.e. (N=3). *P<0.05, **P<0.005, ##P<0.001 vs. control.

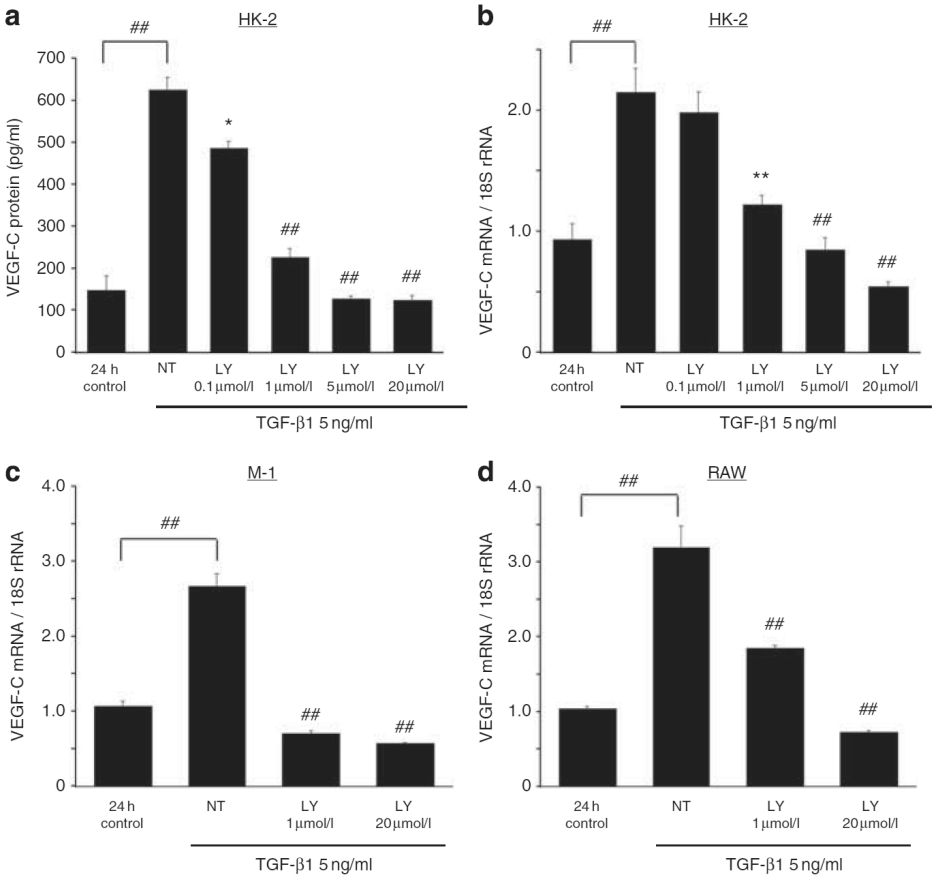

Figure 9 | Inhibition study of vascular endothelial growth factor-C (VEGF-C) expression in cultured proximal tubular epithelial cells (human kidney cells-2 (HK-2)), collecting duct cells (M-1), and macrophages (RAW 264.7) with TGF-β type I receptor inhibitor. (a, b) HK-2 cells were treated with 5 ng/ml TGF-β1 and TGF-β type I receptor inhibitor LY364947 (LY) for 24 h. VEGF-C protein levels in the supernatant were determined by ELISA. VEGF-C mRNA was analyzed by real-time PCR. VEGF-C protein (a) and mRNA (b) levels were suppressed by LY in a dose-dependent manner, as compared with non-treatment (NT; TGF-β1 stimulation only) at 24 h. (c, d) M-1 cells (c) and RAW264.7 cells (d) were incubated with TGF-β1 (5 ng/ml) and LY. Upregulation of VEGF-C mRNA by TGF-β1 was significantly inhibited by concentrations above 1µmol/l LY. Data are means ± s.e. (N=3). *P<0.05, **P<0.005, ##P<0.001 vs. NT.

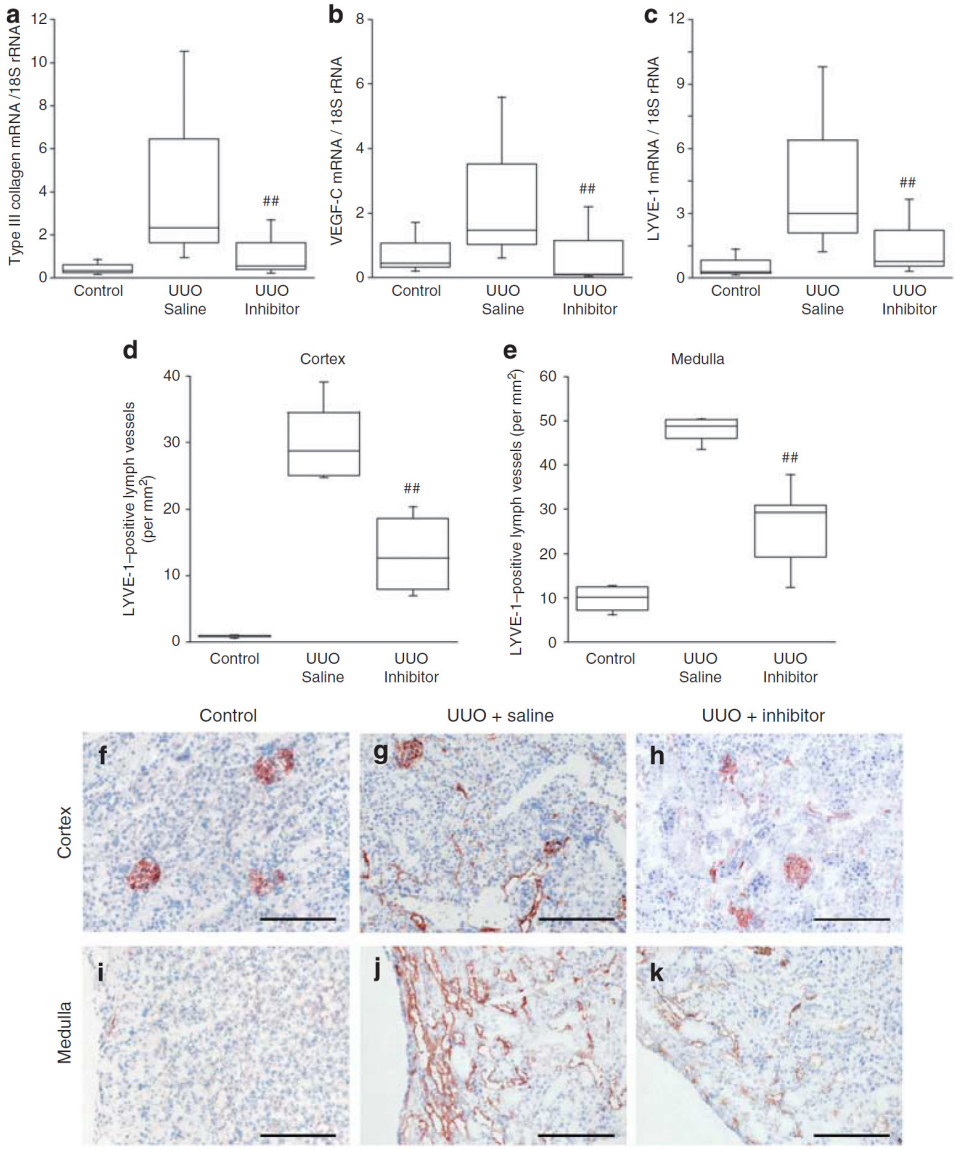

Figure 10 | Effects of transforming growth factor-β type I receptor inhibitor (LY364947) on lymphangiogenesis in unilateral ureteral obstruction (UUO). Type III collagen (a), vascular endothelial growth factor-C (VEGF-C) (b), and lymphatic endothelial hyaluronan receptor-1 (LYVE-1) (c) messenger RNA (mRNA) expression was suppressed by TGF-β type I receptor inhibitor (LY364947) administration via aorta. The number of lymphatics (LYVE-1) was significantly reduced by LY365947 in both the cortex (d) and medulla (e). Immunohistochemistry of LYVE-1 (f–k). (f–h) Cortex; (i–k) medulla; (f, i) control kidney; (g, j) UUO kidney injected with saline; (h, k) UUO kidney administered LY364947. Data are means = s.e. (N=6). ##P<0.001 vs. UUO injected with saline. Bar = 200μm. rRNA, ribosomal RNA.

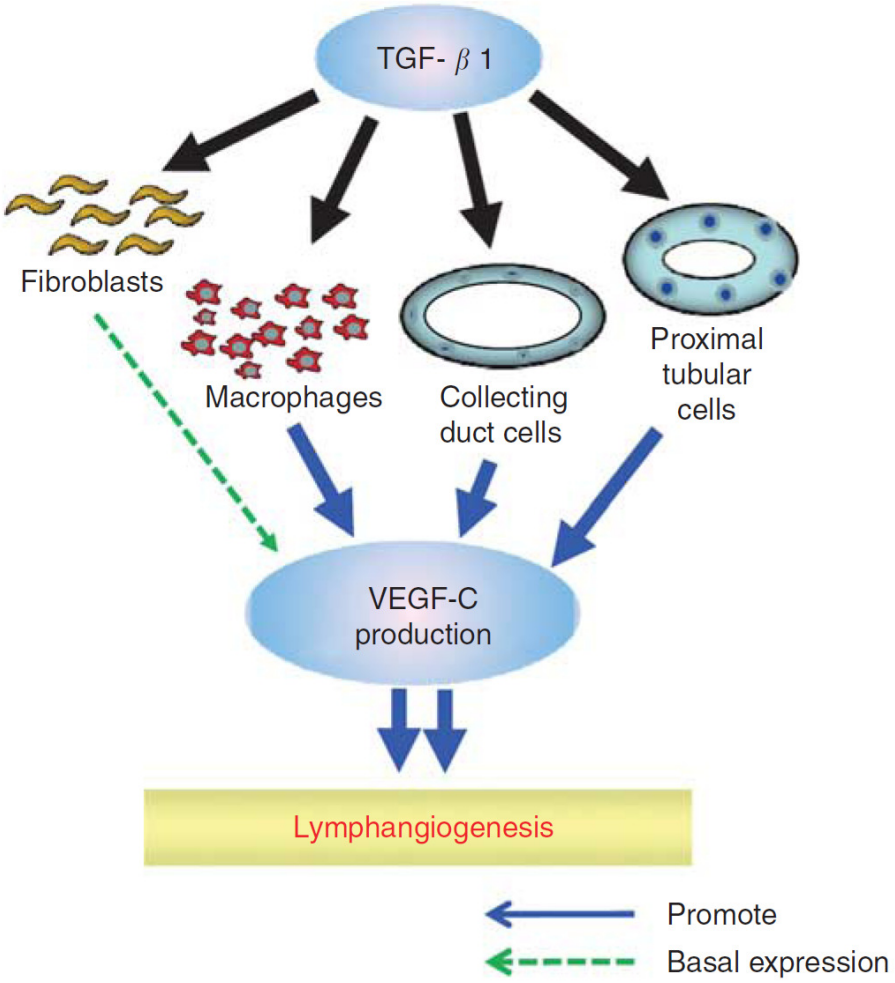

Figure 11 | Possible mechanisms of lymphangiogenesis via the transforming growth factor-β (TGF-β)–vascular endothelial growth factor-C (VEGF-C) pathway in unilateral ureteral obstruction (UUO). TGF-β expression is upregulated in the process of tubulo-interstitial fibrosis in UUO. TGF-β1 expressed by tubular epithelial cells and macrophages induces the upregulation of VEGF-C in proximal tubular epithelial cells (human kidney-2), collecting duct cells (M-1), and macrophages (RAW264.7), leading to lymphangiogenesis. In renal fibroblasts (NRK-49F), VEGF-C was not elevated by TGF-β1, despite basal secretion into the supernatant.

REFERENCES

1. Karpanen T, Alitalo K. Molecular biology and pathology of lymphangiogenesis. Annu Rev Pathol 2008; 3: 367–397.
2. Jones N, Iljin K, Dumont D et al. Tie receptors: new modulators of angiogenic and lymphangiogenic responses. Nat Rev Mol Cell Biol 2001; 2: 257–267.
3. Karkkainen M, Haiko P, Sainio K et al. Vascular endothelial growth factor C is required for sprouting of the first lymphatic vessels from embryonic veins. Nat Immunol 2004; 5: 74–80.
4. Schoppmann S, Birner P, Sto¨ ckl J et al. Tumor-associated macrophages express lymphatic endothelial growth factors and are related to peritumoral lymphangiogenesis. Am J Pathol 2002; 161: 947–956.
5. Kodama M, Kitadai Y, Tanaka M et al. Vascular endotherial growth factor c stimulates progression of human gastric cancer via both autocrine and paracrine mechanisms. Clin Cancer Res 2008; 14: 7205–7214.
6. Kitadai Y, Kodama M, Cho S et al. Quantitative analysis of lymphangiogenic markers for predicting metastasis of human gastric carcinoma to lymph nodes. Int J Cancer 2005; 115: 388–392.
7. Onogawa S, Kitadai Y, Tanaka S et al. Expression of VEGF-C and VEGF-D at the invasive edge correlates with lymph node metastasis and prognosis of patients with colorectal carcinoma. Cancer Sci 2004; 95: 32–39.
8. Baluk P, Tammela T, Ator E et al. Pathogenesis of persistent lymphatic vessel hyperplasia in chronic airway inflammation. J Clin Invest 2005; 115: 247–257.
9. Paavonen K, Puolakkainen P, Jussila L et al. Vascular endothelial growth factor receptor-3 in lymphangiogenesis in wound healing. Am J Pathol 2000; 156: 1499–1504.
10. Kerjaschki D, Huttary N, Raab I et al. Lymphatic endothelial progenitor cells contribute to de novo lymphangiogenesis in human renal transplants. Nat Med 2006; 12: 230–234.
11. Kerjaschki D, Regele H, Moosberger I et al. Lymphatic neoangiogenesis in human kidney transplants is associated with immunologically active lymphocytic infiltrates. J Am Soc Nephrol 2004; 15: 603–612.
12. Ishikawa Y, Akishima-Fukasawa Y, Ito K et al. Lymphangiogenesis in myocardial remodelling after infarction. Histopathology 2007; 51: 345–353.
13. Kajiya K, Detmar M. An important role of lymphatic vessels in the control of UVB-induced edema formation and inflammation. J Invest Dermatol 2005; 126: 920–922.
14. Maruyama K, Ii M, Cursiefen C et al. Inflammation-induced lymphangiogenesis in the cornea arises from CD11b-positive macrophages. J Clin Invest 2005; 115: 2363–2372.
15. Kataru R, Jung K, Jang C et al. Critical role of CD11b+ macrophages and VEGF in inflammatory lymphangiogenesis, antigen clearance, and inflammation resolution. Blood 2009; 113: 5650–5659.
16. Skobe M, Hawighorst T, Jackson DG et al. Induction of tumor lymphangiogenesis by VEGF-C promotes breast cancer metastasis. Nat Med 2001; 7: 192–198.
17. Ristima¨ki A, Narko K, Enholm B et al. Proinflammatory cytokines regulate expression of the lymphatic endothelial mitogen vascular endothelial growth factor-C. J Biol Chem 1998; 273: 8413–8418.
18. El-Chemaly S, Malide D, Zudaire E et al. Abnormal lymphangiogenesis in idiopathic pulmonary fibrosis with insights into cellular and molecular mechanisms. Proc Natl Acad Sci USA 2009; 106: 3958–3963.

19. Flister M, Wilber A, Hall K et al. Inflammation induces lymphangiogenesis through upregulation of VEGFR-3 mediated by NF-kappa B and Prox1. Blood 2010; 115: 418–429.
20. Sakamoto I, Ito Y, Mizuno M et al. Lymphatic vessels develop during tubulointerstitial fibrosis. Kidney Int 2009; 75: 828–838.
21. Matsui K, Nagy-Bojarsky K, Laakkonen P et al. Lymphatic microvessels in the rat remnant kidney model of renal fibrosis: aminopeptidase P and Podoplanin are discriminatory markers for endothelial cells of blood and lymphatic vessels. J Am Soc Nephrol 2003; 14: 1981–1989.
22. Liu Y. Renal fibrosis: new insights into the pathogenesis and therapeutics. Kidney Int 2006; 69: 213–217.
23. Boor P, Ostendorf T, Floege J. Renal fibrosis: novel insights into mechanisms and therapeutic targets. Nat Rev Nephrol 2010; 6: 643–656.
24. Ito Y, Goldschmeding R, Bende R et al. Kinetics of connective tissue growth factor expression during experimental proliferative glomerulonephritis. J Am Soc Nephrol 2001; 12: 472–484.
25. Klahr S, Morrissey J. Obstructive nephropathy and renal fibrosis: the role of bone morphogenic protein-7 and hepatocyte growth factor. Kidney Int 2003; 64: S105–S112.
26. Baluk P, Yao LC, Feng J et al. TNF-a drives remodeling of blood vessels and lymphatics in sustained airway inflammation in mice. J Clin Invest 2009; 119: 2954–2964.
27. Gordon EJ, Rao S, Pollard JW et al. Macrophages define dermal lymphatic vessel calibre during development by regulating lymphatic endothelial cell proliferation. Development 2010; 137: 3899–3910.
28. Teles-Grilo M, Leite-Almeida H, Martins dos Santos J et al. Differential expression of collagens type I and type IV in lymphangiogenesis during the angiogenic process associated with bleomycin-induced pulmonary fibrosis in rat. Lymphology 2005; 38: 130–135.
29. Oka M, Iwata C, Suzuki H et al. Inhibition of endogenous TGF-beta signaling enhances lymphangiogenesis. Blood 2008; 111: 4571–4579.
30. Clavin N, Avraham T, Fernandez J et al. TGF-β1 is a negative regulator of lymphatic regeneration during wound repair. Am J Physiol Heart Circ Physiol 2008; 295: H2113–H2127.
31. Avraham T, Clavin NW, Daluvoy SV et al. Fibrosis is a key inhibitor of lymphatic regeneration. Plast Reconstr Surg 2009; 124: 438–450.
32. Tammela T, Saaristo A, Holopainen T et al. Therapeutic differentiation and maturation of lymphatic vessels after lymph node dissection and transplantation. Nat Med 2007; 13: 1458–1466.
33. Kaneto H, Morrissey J, Klahr S. Increased expression of TGF-beta 1 mRNA in the obstructed kidney of rats with unilateral ureteral ligation. Kidney Int 1993; 44: 313–321.
34. Fukuda K, Yoshitomi K, Yanagida T et al. Quantification of TGF-b 1 mRNA along rat nephron in obstructive nephropathy. Am J Physiol Renal Physiol 2001; 281: F513–F521.
35. Ohashi R, Shimizu A, Masuda Y et al. Peritubular capillary regression during the progression of experimental obstructive nephropathy. J Am Soc Nephrol 2002; 13: 1795–1805.
36. Akishima Y, Ito K, Zhang L et al. Immunohistochemical detection of human small lymphatic vessels under normal and pathological conditions using the LYVE-1 antibody. Virchows Arch 2004; 444: 153–157.
37. Jackson D. The lymphatics revisited: new perspectives from the hyaluronan receptor LYVE-1. Trends Cardiovasc Med 2003; 13: 1–7.
38. Prevo R, Banerji S, Ferguson D et al. Mouse LYVE-1 is an endocytic receptor for hyaluronan in lymphatic endothelium. J Biol Chem 2001; 276: 19420–19430.

39. Mouta Carreira C, Nasser SM, di Tomaso E et al. LYVE-1 is not restricted to the lymph vessels: expression in normal liver blood sinusoids and down-regulation in human liver cancer and cirrhosis. Cancer Res 2001; 61: 8079–8084.
40. Goodwin W, Kaufman J. Renal lymphatics. II. Preliminary experiments. J Urol 1956; 76: 702–707.
41. Zhang T, Guan G, Liu G et al. Disturbance of lymph circulation develops renal fibrosis in rats with or without contralateral nephrectomy. Nephrology 2008; 13: 128–138.
42. Wilcox C, Sterzel R, Dunckel P et al. Renal interstitial pressure and sodium excretion during hilar lymphatic ligation. Am J Physiol Renal Physiol 1984; 247: 344–351.
43. Kuwana H, Terada Y, Kobayashi T et al. The phosphoinositide-3 kinase-gamma Akt pathway mediates renal tubular injury in cisplatin nephrotoxicity. Kidney Int 2008; 73: 430–445.
44. Lee H, Kim M, Song J et al. Sevoflurane-mediated TGF-beta1 signaling in renal proximal tubule cells. Am J Physiol Renal Physiol 2008; 294: F371–F378.
45. Nishimura H, Ito Y, Mizuno M et al. Mineralocorticoid receptor blockade ameliorates peritoneal fibrosis in new rat peritonitis model. Am J Physiol Renal Physiol 2008; 294: F1084–F1093.

SUPPLEMENTAL

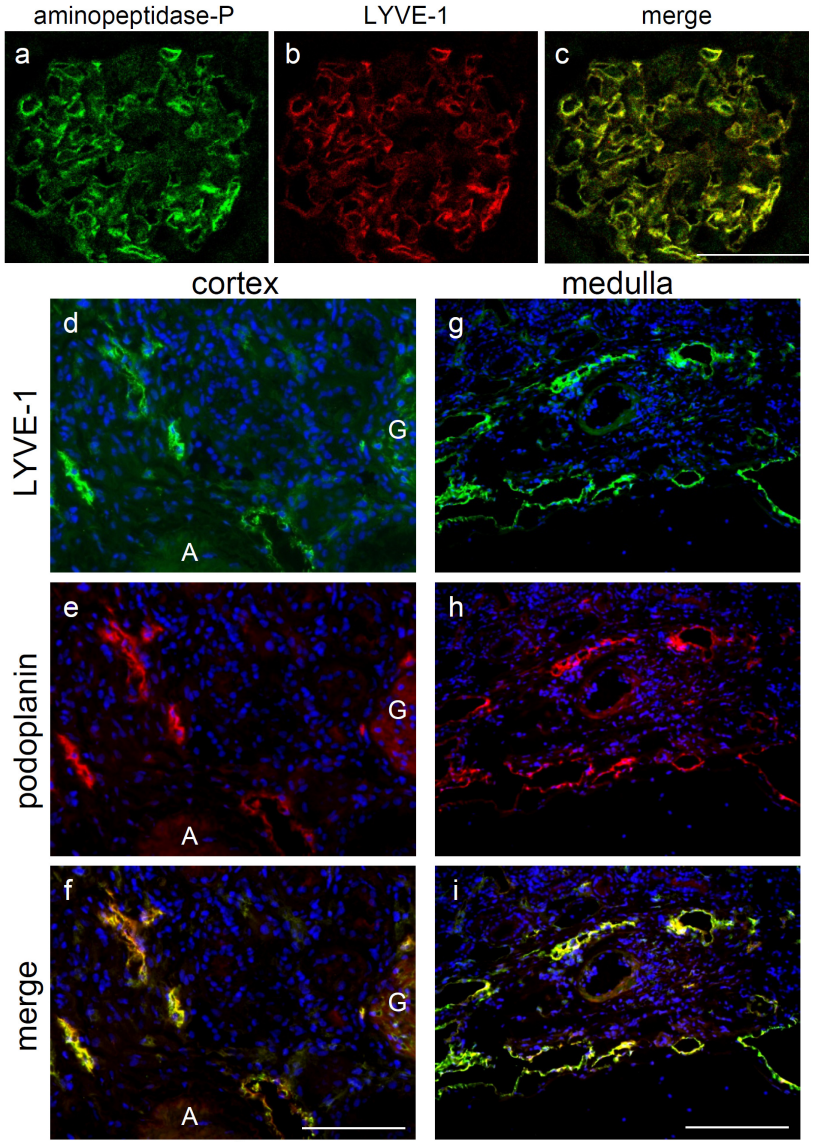

Supplementary Figure S1. Double-immunofluorescence staining for aminopeptidaseP and LYVE-1 in normal glomeruli.Aminopeptidase-P and LYVE-1 are co-localized in glomerular endothelial cells. Scale bar: 50 μm. a: aminopeptidase-P, b: LYVE-1, c: merge. Expression of LYVE-1 and podoplaninin UUO on Day14. d, e, f: cortex, g, h, i: medulla, d, g: LYVE-1, e, h: podoplanin, f, i: mergeG: glomerulus, A: artery, Scale bar: (d, e, f) 100μm, (g, h, i) 200 μm.

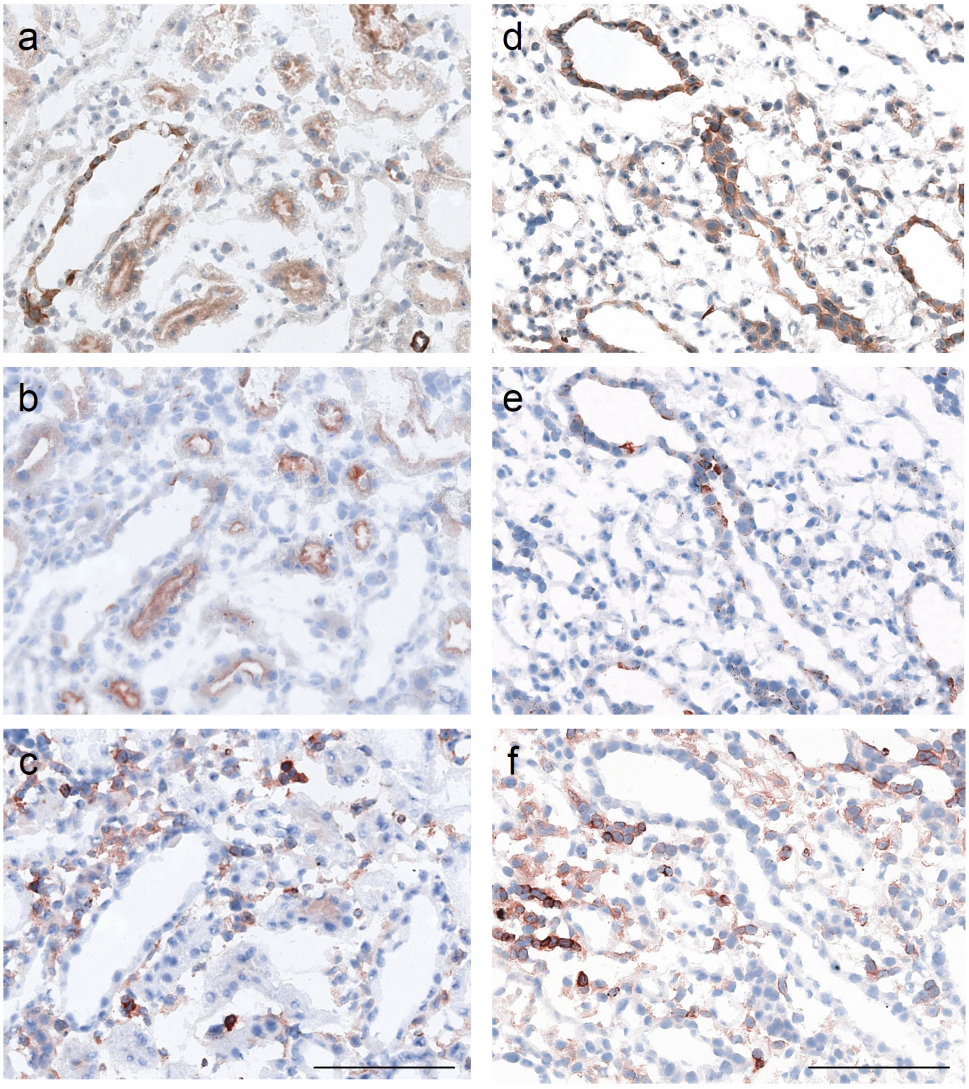

Supplementary Figure S2. Expression of TGF-β, VEGF-C and ED-1 positive macrophages in UUO on Day3.
Expression of TGF-β (a, d) and VEGF-C (b, e) was more remarkable in the tubules than in the macrophages (c, f).
a, b, c: cortex, d, e, f: medulla
a, d: TGF-β, b, e: VEGF-C, c, f: ED-1-positive macrophage
Scale bars 100 μm

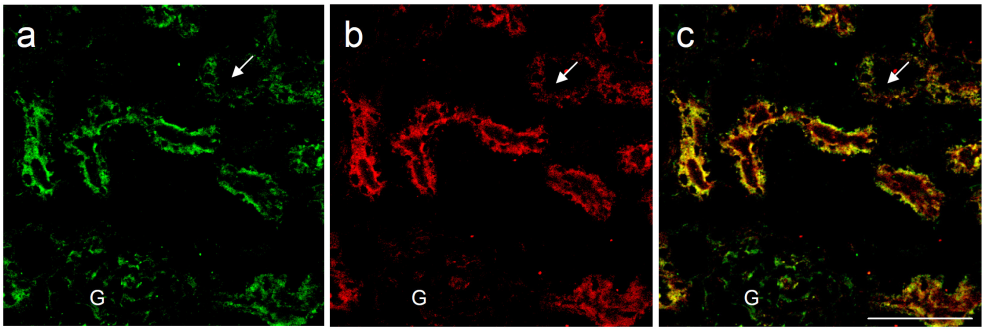

Supplementary Figure S3. Double staining for TGF-β and VEGF-C on the frozen section in UUO on Day14. Expression pattern of TGF-β in the tubules was similar to that of VEGF-C. In the glomerulus, there was a weak expression of TGF-β, but not VEGF-C. In the interstitium, TGF-β and VEGF-C was focally detected (arrows). Rabbit anti-TGF-β 1, 2, 3 antibody and mouse anti-VEGF-C antibody (Santa Cruz) were used as primary antibody. a: TGF-β, b: VEGF-C, c: merge. G: Glomerulus, Scale bar 100 μm.

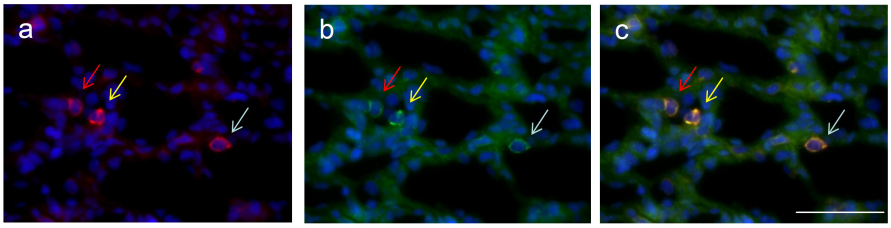

Supplementary Figure S4. VEGF-C was expressed by ED-1-positive macrophages in UUO on Day 9. VEGF-C was detected in the macrophages as well as tubular epithelial cells. Arrows of same colors indicate the same cells.
a: ED-1-positive macrophage, b: VEGF-C, c: merge. Scale bar: 50 μm.

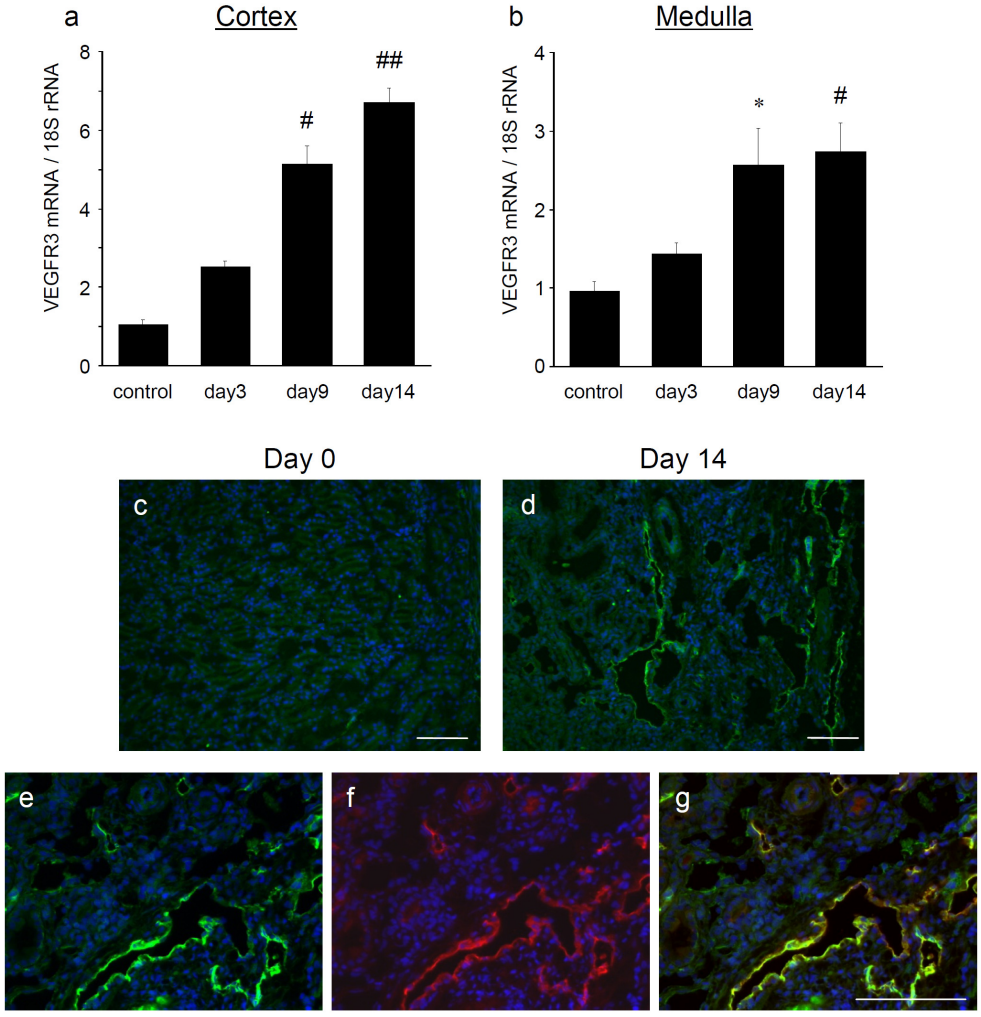

Supplementary Figure S5. Expression of VEGFR3 in UUO.
(a, b): Expression of VEGFR3 mRNA analyzed by real-time PCR was upregulatedwith time and peaked on Day 14 in both cortex (a) and medulla (b). ∗ $p<0.05$; # $p<0.01$; ## $p<0.001$ vs. control. On immunohistochemistry, VEGFR-3 was detected in the fibrotic tubulo-interstitial are on Day 14 (d), but not in the normal tubulo-interstitial area (c). In the cortex, staining pattern was similar. c: Day 0, d: Day 14, Scale bar: 100 μm.
(e-g):VEGFR3 expression (e) was co-localized with podoplanin-positive lymphatic vessels (f). e: VEGFR3, f: podoplanin, g: merge, Scale bar: 100 μm.

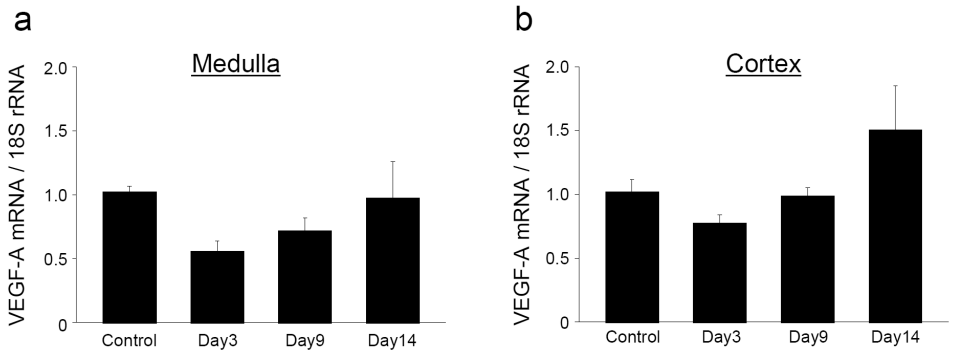

Supplementary Figure S6. Quantitative analysis of VEGF-A mRNA expression in UUO model. Expression of VEGF-A mRNA was analyzed by real-time reverse transcription-polymerase chain reaction. VEGF-A mRNA expression was not significantly changed at any time point in both the medulla (a) and the cortex (b). Values are means ± SE (N=5).

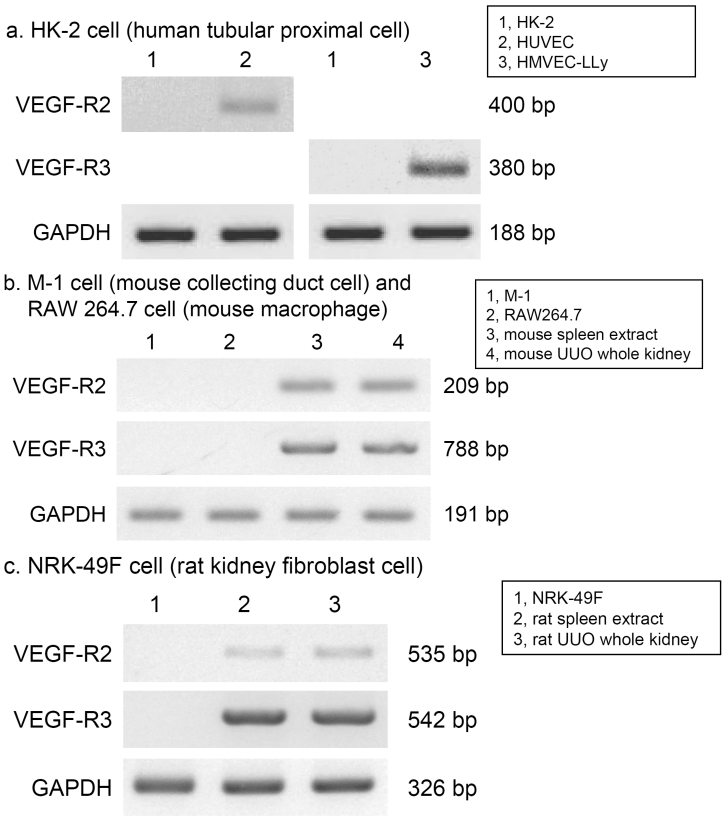

Supplementary Figure S7.
Expression of VEGF-receptor 2 and 3 mRNA in cultured proximal tubular epithelial cells (HK-2), collecting duct cells (M-1), macrophages (RAW 264.7) and fibroblasts (NRK-49F).
In order to clarify the expression of VEGFR2 and VEGFR3, which are involved in lymphangiogenesis, we performed RT-PCR.

Methods
Normal human lymphatic microvascular endothelial cells (HMVEC-LLy) and normal umbilical vein endothelial cells (HUVEC) were purchased from Lonza Bioscience (Basel Switzerland). Reverse Transcription Polymerase Chain Reaction (RT-PCR) was performed using the HOT-StarTaq PCR kit (Qiagen), as described previously. (1) Cycling conditions of the respective PCRs were as follows; initial denaturation (15 min at 94 °C), annealing (45 s at 62 °C for human VEGFR2 and VEGFR3, at 58 °C for Rat VEGFR2 and VEGFR3, and at 60 °C for Mouse VEGFR2 and VEGFR3) and elongation (1 min at 72 °C). After the last cycle, a final extension (7 min at 72 °C) was added and thereafter the samples were kept at 4 °C. PCR products were electrophoresed on 2% agarose gels in Trisacetate EDTA buffer, followed by staining with ethidium bromide. Primer sequences are shown in Table.

Results

(A) In HK-2 cells, VEGFR2 and -R3 mRNA was not detected. In contrast, HUVEC and HMVEC were positive for VEGFR2 and -R3, respectively. In both M-1 (B) and RAW 264.7 cells (C), VEGFR2 and -3 mRNA were not detected, on the other hand PCR products were positive in the rat and mouse UUO kidneys and spleen extracts.

HMVEC-LLy: normal human lymphatic microvascular endothelial cells; HUVEC: human umbilical vein endothelial cells.

Table

Table. RT-PCR primers

	sense	antisense	PCR product	Ref.
VEGFR2				
Human	5-CATCACATCCACTGGTATTGG	5-GCCAAGCTTGTACCATGTGAG	400 bp	(2)
Rat	5-CCAATGAAGGGGAACTG	5-TGACTGCTGGTGATGCT	535 bp	(3)
Mouse	5-TCCACCAAAGGGGCACGATTCCGTC	5-TTCTGTAACAGATGAGATGCTCCAAGG	209 bp	(4)
VEGFR3				
Human	5-CCCACGCAGACATCAAGACG	5-TGCAGAACTCCACGATCACC	380 bp	(2)
Rat	5-CTGAGGCAGAATATCAGTCTGGAG	5-AGATGCTCATACGTGTAGTTGTCC	542 bp	(5)
Mouse	5-TTGGCATCAATAAAGGCAG	5-CTGCGTGGTGTACACCTTA	788 bp	(6)
GAPDH				
Human	5-ATCATCCCTGCCTCTACTGG	5-CCCTCCGACGCCTGCTTCAC	188 bp	(1)
Rat	5-CGATCCCGCTAACATCAAAT	5-CCACAGTCTTCTGAGTGGCA	326 bp	(3)
Mouse	5-AACGACCCCTTCATTGAC	5-TCCACGACATACTCAGCAC	191 bp	(7)

References

1. Takei Y, Kadomatsu K, Yuzawa Y, et al. A small interfering RNA targeting vascular endothelial growth factor as cancer therapeutics. Cancer Res 2004; 64: 3365-3370.
2. Gockel I, Moehler M, Frerichs K, et al. Co-expression of receptor tyrosine kinases in esophageal adenocarcinoma and squamous cell cancer. Oncol Rep 2008; 20: 845-850.
3. Choi JS, Kim HY, Cha JH, et al. Upregulation of vascular endothelial growth factor receptors Flt-1 and Flk-1 following acute spinal cord contusion in rats. J Histochem Cytochem 2007; 55: 821-830.
4. Guan F, Villegas G, Teichman J, et al. Autocrine VEGF-A system in podocytes regulates podocin and its interaction with CD2AP. Am J Physiol Renal Physiol 2006; 291: F422-428.
5. Choi JS, Shin YJ, Lee JY, et al. Expression of vascular growth factor-3 mRNA in the rat developing forebrain and retina. J Comp Neurol 2010; 518: 1064-1081.
6. Ji RC, Eshita Y, Kato S. Investigation of intratumoural and peritumoural lymphatics expressed by podoplanin and LYVE-1 in the hybridoma-induced tumours. Int J Exp Pathol 2007; 88: 257-270.
7. Qiu H, Fan y, Joyee AG, etal. Type I IFNs Enhances susceptibility to Chlamydia muridarum lung infection by enhancing apoptosis of local macrophages. J Immunol 2008; 181: 2092-2102.

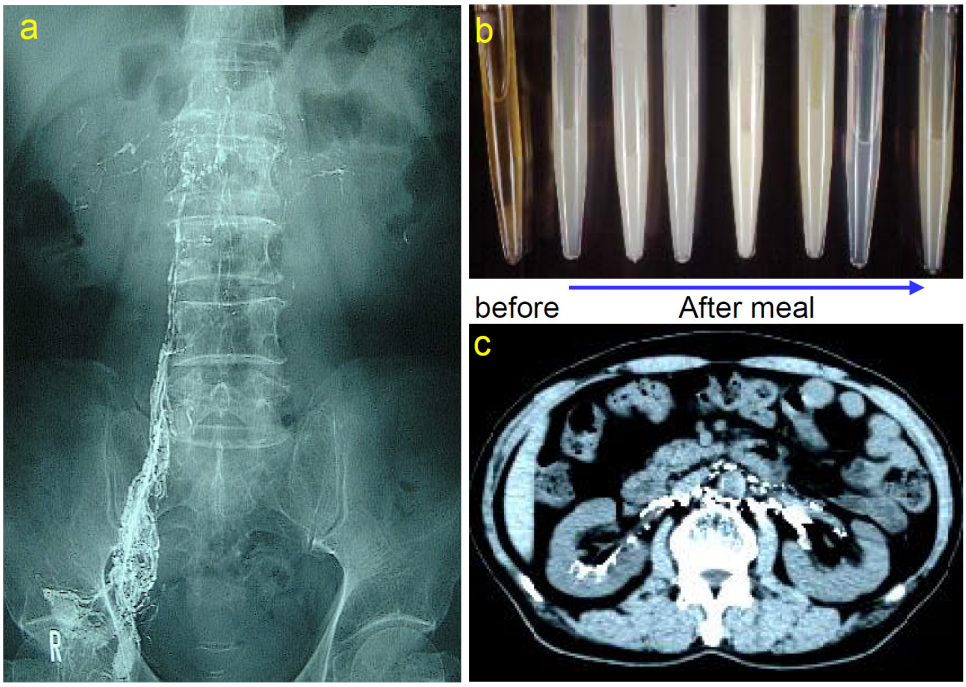

Supplementary Figure S8.
Lymphangiography in a case with chyluria due to filariasis.
a: Lymphangiography shows obliteration of the thoracic duct and lymphatic ducts were revealed at the hilus of bilateral kidneys.
b: Urine samples of a patient with chyluria. Urine was not cloudy after fasting; however, it became milky in appearance after the patient ate.
c: Computed tomography scan of lymphangiography demonstrated lymphatic vessels connected to the renal pelvis.

Supplementary Table S1

List of the antibodies

antibody	company
mouse anti α-SMA antibody (1A4)	Dako, Glostrup, Denmark
mouse anti-rat monocyte/macrophage antibody (ED1)	BMA Biomedicals AG, Augst, Switzerland
mouse anti-rat podoplanin antibody	Relia Tech GmbH, Braunschweig, Germany
mouse anti-rat aminopeptidase P antibody	Relia Tech GmbH, Braunschweig, Germany
rabbit anti-type III collagen antibody	LSL, Nagahama, Japan
rabbit anti-LYVE-1 antibody	Acris Antibodies GmbH, Herford, Germany
rabbit anti-VEGF-C antibody	Zymed Laboratories, South San Francisco, CA
rabbit anti-TGF-β1, 2, 3 antibody	Santa Cruz Biotechnology, Santa Cruz, CA
goat anti-VEGFR3 (Flt-4) antibody	R&D System, Minneapolis, MN
FITC-labeled rabbit anti-mouse IgG	Invitrogen, Camarillo, CA
Rhodamine labeled goat anti-rabbit IgG	Chemicon, Billerica, MA

Supplementary Table S2

Primers for real-time PCR (TaqMan Gene Expression Assays)

	Assay identification number
rat VEGF-A	Rn00582935_m1
rat VEGF-C	Rn00586458_m1
rat LYVE-1	Rn01510422_m1
rat podoplanin	Rn00571195_m1
rat TGF-β1	Rn00572010_m1
rat TGF-β2	Rn00579674_m1
rat TGF-β3	Rn00565937_m1
rat VEGFR3	Rn00586429_m1
rat type III collagen	Rn01437683_m1
mouse VEGF-C	Mm00437313_m1
human VEGF-C	Hs00153458_m1
18S ribosomal RNA	4319413E

7

CTGF/CCN2 is critically involved in the fibrosis-associated lymphangiogenesis of obstructive nephropathy

Provisionally accepted *(Kidney International)*

Hiroshi Kinashi*[1,2], Lucas L. Falke*[1], Tri Q. Nguyen[1], Niels Bovenschen[1], Jan Aten[3], Andrew Leask[4], Yasuhiko Ito[2], and Roel Goldschmeding[1]

[1]Department of Pathology, University Medical Center Utrecht, Utrecht, The Netherlands
[2]Department of Nephrology and Renal Replacement Therapy, Nagoya University Graduate School of Medicine, Nagoya, Japan
[3]Department of Pathology, Academic Medical Center, University of Amsterdam, Amsterdam, The Netherlands
[4]Department of Dentistry, Western University, London, Ontario, Canada
*Contributed equally

ABSTRACT
Lymphangiogenesis is correlated with the degree of renal interstitial fibrosis. TGF-β induces VEGF-C production, which is the main driver of lymphangiogenesis. Connective tissue growth factor (CTGF, CCN2) is an important determinant of fibrotic tissue remodeling, but its possible involvement in lymphangiogenesis has not been explored. We found that human obstructed kidney showed prominent lymphangiogenesis in tubulointerstitial fibrosis accompanied with increased expression of CTGF and VEGF-C. By making use of CTGF full-knockout mice, we investigated the involvement of CTGF in fibrotic development and associated lymphangiogenesis during obstructive nephropathy. The increase of lymphatic vessels and VEGF-C in obstructed wild-type kidneys was significantly reduced in CTGF knockout. In vitro, CTGF induced VEGF-C production in HK-2 cells, and CTGF siRNA suppressed TGF-β1-induced VEGF-C upregulation. Furthermore, CTGF and VEGF-C were shown to directly interact. Interestingly, VEGF-C-induced capillary-like tube formation was suppressed by full-length CTGF in human lymphatic endothelial cells. In conclusion, CTGF plays a significant role in renal lymphangiogenesis through the interaction with VEGF-C.

INTRODUCTION

Chronic kidney disease (CKD) is a major health problem with rising incidence and prevalence for which currently no effective therapy other than renal replacement therapy exists.[1] However, hemodialysis and renal transplantation are accompanied by a major economic and health burden, and the number of transplantable donor kidneys does not match the need.[2,3] As such, increasing effort is being put in the development of therapeutic interventional strategies to prevent CKD occurrence or limit progression to end stage renal disease. One potential strategy focuses on lymphangiogenesis.

The lymphatic vasculature is essential for the maintenance of tissue fluid balance, immune surveillance, and absorption fatty acids in the gut. Lymphatic vessels normally drain, filter, and return extravasated tissue fluid, cells, and proteins into the circulation through the thoracic and lymphatic ducts.[4] Lymphangiogenesis has been observed in various diseases, including tumor metastasis,[5] inflammatory disease,[6] heart disease,[7] and during transplant rejection.[8,9] Signaling via vascular endothelial growth factor (VEGF)-C/D and VEGF receptor (VEGFR)-3 is the central to lymphangiogenesis.[10,11] In addition, lymphangiogenesis is associated with fibrotic disease. We previously reported that lymphangiogenesis was observed in various types of human kidney diseases, and the number of renal lymphatics was related to the degree of renal interstitial fibrosis.[12] During obstructive nephropathy, transforming growth factor-β (TGF-β) increases VEGF-C expression, which leads to lymphangiogenesis.[13,14] We also demonstrated the similar mechanism of lymphangiogenesis in peritoneal fibrosis in association with peritoneal dialysis.[15]

The matricellular and multimodular protein connective tissue growth factor (CTGF, CTGF/Cyr61/Nov (CCN)2) is a major contributor to CKD development and progression.[16] TGF-β induces CTGF expression in multiple cell types including mesangial cells and renal tubular epithelial cells. CTGF plays a role in the development and progression of glomerulosclerosis and tubulointerstitial fibrosis as part of TGF-β-dependent and TGF-β-independent pathway.[17,18] Additionally CTGF modulates TGF-β signaling by direct physical interaction.[19] 50% reduction of CTGF reduces fibrotic development in relatively mild models of renal disease.[20,21] We have shown however, that 50% reduction of CTGF is insufficient to reduce fibrotic development in severe models of renal disease.[22] It should be noted however that 50% reduction under pathological circumstances still resulted in increased levels of CTGF compared to baseline physiological levels of expression.

Besides the major regulatory role during fibrosis, CTGF is an important regulator of angiogenesis.[23] Paradoxically, CTGF binding to VEGF-A, a strong angiogenic growth factor and VEGF family member, reduces tube formation of vascular endothelial cells and inhibits angiogenesis.[24,25] However, little is known about the role of CTGF in lymphangiogenesis and possible interaction with VEGF-C. With regards to CTGF, fibrotic development and lymphangiogenesis, we hypothesize that 1) CTGF reduction below baseline levels during a severe model of renal disease results in adequate reduction of fibrosis, and 2) there is a major role for CTGF in lymphangiogenesis in this setting. To test

our hypotheses, we assessed fibrotic development, lymphangiogenesis and associated VEGF-C expression in the human obstructive nephropathy and CTGF full-knockout ($CTGF^{-/-}$) mice in a severe model of unilateral ureteral obstruction (UUO). In addition, we analyzed CTGF effects on VEGF-C production in cultured human renal proximal tubular epithelial cells (HK-2). Finally, we clarified the interaction with VEGF-C by solid-phase binding assay, surface plasmon resonance analysis, and in cultured human lymphatic microvascular endothelial cells. We believe that this work is the first to show the effect of near total CTGF reduction on fibrotic development and lymphangiogenesis in the context of severe chronic kidney disease.

RESULTS

CTGF expression was increased around lymphangiogenesis of human obstructive nephropathy

A human obstructed kidney (OBK) and non-obstructed contralateral kidney (CLK) were derived from the same patient undergoing bilateral nephrectomy for bilateral renal pelvis tumors of which only one caused ureteral obstruction. We investigated both renal cortices by Masson's trichrome staining and immunohistochemistry (IHC) for CTGF, VEGF-C, and lymphatic marker D2-40. OBK showed prominent tubulointerstitial fibrosis and more lymphatics than CLK. Serial sections of OBK revealed that CTGF and VEGF-C expression were increased in atrophic tubules and interstitial infiltrating cells around lymphangiogenesis (Figure 1).

Near total reduction of CTGF reduced tubulointerstitial fibrosis 14 days after UUO

In order to investigate the effect of CTGF reduction of renal fibrosis 14 days after UUO, we made use of in conditional $CTGF^{-/-}$ mice. In wild-type (WT) mice, CTGF messenger RNA (mRNA) expression was increased 2.2-fold in OBK compared to CLK ($P < 0.05$). $CTGF^{-/-}$ CLK ($P < 0.05$) and OBK ($P < 0.001$) showed more than 90 % reduction of CTGF mRNA expression, and clear reduction of CTGF protein levels (Figure 2). Periodic acid Schiff (PAS) staining showed tubular dilatation, atrophy, and cast formation in renal cortex of both OBK (Figure 3a). Tubulointerstitial fibrosis in Masson's trichrome staining, alpha-smooth muscle actin (α-SMA)-positive myofibroblast expression, and collagen type I alpha 2 (Col1α2) mRNA expression were significantly increased in WT OBK compared to WT CLK ($P < 0.001$, Figure 3), and were significantly decreased in $CTGF^{-/-}$ OBK compared to WT OBK ($P < 0.01$, $P < 0.01$, $P < 0.001$, respectively, Figure 3). $CTGF^{-/-}$ mice (97.9±2.6 %) well maintained their body weight post UUO compared to WT mice (93.2±2.5 %, $P < 0.01$, Supplementary Figure S1).

Lymphangiogenesis and VEGF-C expression were reduced in $CTGF^{-/-}$ OBK

Next, we investigated whether near total reduction of CTGF was associated with a reduction in lymphangiogenesis. IHC of renal cortices showed that lymphatic endothelial hyaluronan receptor-1 (LYVE-1)-positive lymphatic vessels existed adjacent to renal blood

vessels in both CLK. In contrast, lymphatic vessels appeared in the injured tubulointerstitial area in both OBK (Figure 4a). VEGF-C expression was barely present in CLK, and mainly evident in renal tubules of OBK (Figure 4a). The density of LYVE-1-positive lymphatic vessels and VEGF-C-positive area were significantly increased in WT OBK compared to WT CLK ($P < 0.001$, Figure 4b and c), and were significantly decreased in $CTGF^{-/-}$ OBK compared to WT OBK ($P < 0.05$, $P < 0.001$, respectively, Figure 4b and c). Quantitative real-time PCR (qPCR) analysis showed that LYVE-1 and VEGF-C mRNA expression were increased 20.3- ($P < 0.001$) and 2.2-fold ($P < 0.05$), respectively in WT OBK compared to WT CLK. $CTGF^{-/-}$ OBK showed a significant decrease of both LYVE-1 and VEGF-C mRNA expression compared to WT OBK ($P < 0.05$, Figure 4d and e).

CTGF induces VEGF-C production in proximal tubular cells

We investigated CTGF-induced VEGF-C expression in HK-2 cells to assess the role of CTGF in renal lymphangiogenic signaling. Recombinant human full length (FL)-CTGF dose-dependently increased VEGF-C mRNA expression in HK-2 cells after 8h incubation ($P < 0.05$, Figure 5a). Next, we inhibited CTGF expression by CTGF short-interfering RNA (siRNA) with or without recombinant human TGF-β1 (10 ng/ml) treatment. CTGF mRNA expression was significantly increased by TGF-β1 after 8 h incubation ($P < 0.001$), and CTGF siRNA significantly reduced CTGF expression in both control ($P < 0.05$) and TGF-β1 treatment condition ($P < 0.001$) compared to Non-targeting control siRNA (Figure 5b). TGF-β1 significantly increased VEGF-C mRNA expression ($P < 0.001$, Figure 5c). Although CTGF siRNA did not affect VEGF-C mRNA expression in control condition, it significantly suppressed VEGF-C upregulation treated with TGF-β1 ($P < 0.01$, Figure 5c). VEGF-C protein levels in supernatants of HK-2 cells determined by enzyme-linked immunosorbent assay (ELISA) showed that increased VEGF-C protein levels treated with TGF-β1 after 24 h incubation ($P < 0.001$) was significantly decreased by CTGF siRNA compared to control siRNA ($P < 0.01$, Figure 5d). Plasminogen activator inhibitor-1 (PAI-1) is involved in extracellular matrix formation and regulated by TGF-β1. PAI-1 mRNA expression was significantly increased by TGF-β1 treatment after 8 h incubation ($P < 0.001$) that was significantly suppressed by CTGF siRNA ($P < 0.05$, Supplementary Figure S2).

CTGF directly binds to VEGF-C

To analyze the interaction between CTGF and VEGF-C, we performed solid-phase binding assay and surface plasmon resonance analysis. In solid-phase binding assay, recombinant human VEGF-C or bovine serum albumin (BSA) was coated on microtiter plates. Different dose of FL-CTGF was incubated on both proteins. FL-CTGF dose-dependently interacted with VEGF-C, but not with BSA ($P < 0.01$, Figure 6a). In surface plasmon resonance analysis, FL-CTGF and its proteolytic cleavage products, NH2- and COOH-terminal fragments (N-CTGF, C-CTGF), were incubated with immobilized VEGF-C. FL-CTGF and C-CTGF displayed specific association with immobilized VEGF-C followed by

dissociation (Figure 6b). In contrast, N-CTGF did not show any interaction with VEGF-C (Figure 6b). Dose-dependent response was observed with FL-CTGF and C-CTGF, and equilibrium dissociation constant (KD) were 243±24 (Mean ± SD) and 239±14 nM, respectively (Figure 6c). Similar binding behavior was observed with VEGF-A in that only FL-CTGF and C-CTGF, but not N-CTGF, bound to immobilized VEGF-A. KD values for FL-CTGF and C-CTGF binding to VEGF-A were 510±103 and 444±38 nM, respectively (data not shown).

CTGF suppressed VEGF-C-induced human dermal lymphatic microvascular endothelial cells (HMVEC-dLy) growth

We evaluated the effect of CTGF on VEGF-C-induced lymphatic endothelial cells growth. HMVEC-dLy were plated on Matrigel surface and incubated for 6 h. Cells growth was assessed by the number of capillary-like tube formation. HMVEC-dLy efficiently formed tube structures with VEGF-C treatment ($P < 0.001$, Figure 6a, b, and f). The addition of FL-CTGF significantly suppressed VEGF-C-induced tube formation ($P < 0.01$, Figure 6c and f). In contrast, equivalent amount of N-CTGF and C-CTGF showed no significant effect on VEGF-C-induced tube formation (Figure 6d-f).

DISCUSSION

In this study, we first demonstrated that CTGF expression was increased around lymphatic vessels growth within tubulointerstitial fibrosis of human OBK. The result suggested the possible involvement of CTGF in fibrosis and lymphangiogenesis of obstructive nephropathy. We next explored that inhibition of CTGF reduced tubulointerstitial fibrosis and suppressed lymphangiogenesis in $CTGF^{-/-}$ OBK. Several reports show that an approximate CTGF reduction of 50% is capable of reducing fibrotic development in moderate models of obstructive,[20] diabetic[21] and allograft nephropathy,[26] and the remnant kidney model.[27] However, previously demonstrated that 50% reduction in hemizygous CTGF knockout ($CTGF^{+/-}$) did not suffice to reduce fibrotic development in severe models of kidney injury, including 14 days UUO.[22] As mentioned, CTGF expression in these models never dropped below baseline levels despite hemizygous deletion, and as such expression remained relatively raised compared to control levels. We hypothesized that reduction of CTGF below baseline levels would have a beneficial effect in severe chronic kidney disease. As the CTGF gene full-knockout mouse exhibits perinatal lethality,[28] we generated time-conditional $CTGF^{-/-}$ mice by using a tamoxifen-inducible Cre-lox system. $CTGF^{-/-}$ mice showed dramatic reduction of CTGF proteins and mRNA expression in both CLK and OBK (Figure 2). Unlike $CTGF^{+/-}$ mice, pronounced CTGF reduction by $CTGF^{-/-}$ ameliorated tubulointerstitial fibrosis and α-SMA expression 14 days post UUO.

In parallel, we found that near total reduction of CTGF suppressed lymphangiogenesis accompanied with decreased expression of VEGF-C, which suggested the possible interaction between CTGF and VEGF-C. We also demonstrated that CTGF contributes to VEGF-C induction in HK-2 cells. In addition, CTGF gene inhibition by siRNA

significantly suppressed VEGF-C upregulation in HK-2 cells treated with TGF-β1, which is consistent with the finding in $CTGF^{-/-}$ OBK. Our results show that inhibition of CTGF could be a promising therapeutic approach targeting both fibrosis and lymphangiogenesis. TGF-β-induced VEGF-C expression also occurs during dialysis associated peritoneal fibrosis,[15] and might also be largely CTGF mediated. Especially since peritoneal fibrotic development is associated with high levels of CTGF.[29]

Induction of lymphangiogenesis via release of VEGF-C/D is correlated with a poor prognosis in a number of solid tumors.[30] Blocking VEGFR-3 signaling inhibits tumor lymphangiogenesis as well as lymph node metastasis in animal models.[31,32] Interestingly, WNT1-inducible-signaling pathway protein-1 (WISP-1), another member of the CCN family, was shown to promote lymphangiogenesis via upregulation of VEGF-C expression in oral squamous cell carcinoma.[33] A therapeutic monoclonal human antibody against CTGF, FG-3019 is under clinical investigation in a phase 1/2 trial of chemotherapy in pancreatic cancer patients (NCT02210559). FG-3019 enhanced chemotherapy response including reduction of liver metastasis in a mouse model of pancreatic cancer.[34] FG-3019 also inhibited the tumor progression and lung metastasis in a mouse model of metastatic melanoma.[35] It was similarly demonstrated that fibroblast-specific deletion of CTGF using the same CTGF-floxed mice reduced skin fibrosis and melanoma metastasis.[36-38] Possibly, this anti-metastatic effect of CTGF reduction might be due to reduction in tumor lymphangiogenesis.

Finally, we show that FL-CTGF directly binds to VEGF-C, and suppresses VEGF-C-induced lymphatic endothelial cells growth in vitro. CTGF binds to VEGF-A, and inhibits VEGF-A-induced angiogenesis in vitro and in vivo.[24] Some members of matrix metalloproteinases have been reported to process FL-CTGF of the complex with VEGF-A into N-CTGF and C-CTGF, and both of CTGF fragments were dissociated and released from the complex. The inhibited angiogenic activity of VEGF-A combined with FL-CTGF was reactivated to original levels after digestion of FL-CTGF.[25,39] In this study, we showed that FL-CTGF and C-CTGF directly bound to VEGF-C in surface plasmon resonance analysis. VEGF-C-induced capillary-like tube formation in cultured lymphatic endothelial cells was suppressed by FL-CTGF, but not by CTGF fragments. We hypothesize that FL-CTGF binds to VEGF-C through its C-CTGF portion, and the attached N-CTGF portion might sterically hinder VEGF-C binding to VEGFR-3 and inhibit lymphangiogenesis (Supplementary Figure S3). CTGF promotes VEGF-C production in renal tubules, binds to VEGF-C, and suppresses VEGF-C-induced lymphangiogenesis. It is estimated that the former effect is more important than the latter effect because $CTGF^{-/-}$ OBK showed less expression of VEGF-C and lymphatic vessels compared to WT OBK (Figure 8).

How blockage of lymphangiogenesis reduces disease progression remains somewhat illusive. It is speculated that lymphatic vessels not only drainage inflammatory infiltrate but also maintain the immune response by producing lymphatic chemokine which attracts inflammatory cells.[8] Results with regards to lymphangiogenesis blockage have been ambiguous. For instance, in renal transplantation model, sirolimus showed inhibition of

lymphangiogenesis associated with attenuated development of chronic kidney allograft injury.[40] In contrast, VEGF-C treatment attenuated lung allograft rejection by inducing lymphangiogenesis, which improved clearance of detrimental hyaluronan from the lung allografts.[9] During aspiration pneumonia increased lymphangiogenesis is observed, and treatment with VEGFR inhibitor or VEGFR-3 specific inhibitor improved inflammation and oxygen saturation.[41] Blocking of lymphangiogenesis by soluble VEGFR-3 improved ultrafiltration failure associated with peritoneal dialysis in a mouse peritoneal fibrosis model.[42] Interestingly, Yazdani S et al. reported that specific blocking of lymphangiogenesis by anti-VEGFR-3 antibody did not prevent inflammation, interstitial fibrosis, and proteinuria in a rat model of proteinuric nephropathy.[43] They also showed that macrophages depletion by clodronate liposome did not prevent lymphangiogenesis in this model. This is in stark contrast to another report that shows that treatment with clodronate liposomes markedly reduced the number of macrophages and lymphangiogenesis induced by UUO.[14,44] Thus the requirement for lymphangiogenesis and efficacy of therapeutic intervention varies depending on organ and etiology of disease, and further studies are needed to understand the role of renal lymphangiogenesis in a variety of kidney diseases.

In conclusion, near total reduction of CTGF suppressed fibrotic development, lymphangiogenesis and VEGF-C expression during obstructive nephropathy, and CTGF promoted VEGF-C production in renal tubular cells with or without TGF-β treatment. FL-CTGF directly bound to VEGF-C, and suppressed VEGF-C-induced lymphatic endothelial cells growth. Thus, CTGF plays a significant role in renal lymphangiogenesis through the interaction with VEGF-C. Further clarification of the mechanism of lymphangiogenesis in kidney fibrosis might lead to additional interventional strategies to combat chronic kidney disease.

MATERIALS AND METHODS

Human kidney specimens

A human OBK and CLK specimens were derived from the same 60 years old male patient undergoing bilateral nephrectomy for bilateral renal pelvis tumors at University Medical Center Utrecht.

Experimental animal model

The animal experiment was performed with the approval of the Experimental Animal Ethics Committee of the University of Utrecht. ROSA26-ERT2CRE/floxCTGF mice were injected with corn oil (n = 5) for WT mice or tamoxifen (n = 9) for $CTGF^{-/-}$ mice. Mice received 4 intraperitoneal injections of 100 µl (10mg/ml) tamoxifen. Two weeks after the last injection, the ureter of the left kidney was obstructed in all mice. 14 days after ligation, mice were sacrificed and organs were harvested for analysis. Non-obstructed CLK serve as control. Tissue was processed for western blot, IHC, and qPCR.

Immunohistochemistry

PAS and Masson's trichrome staining were performed using standard procedures. IHC for CTGF (sc-14939, Santa Cruz Biotechnology Inc., Dallas, TX), VEGF-C (Zymed Laboratories, South San Francisco, CA), D2-40 (Covance, Dedham, MA), α-SMA (Abcam, Cambridge, UK), and LYVE-1 (Acris Antibodies GmbH, Herford, Germany) were performed on formalin-fixed paraffin sections, as described previously.[12,22] To determine positive area percentage of Masson's trichrome, α-SMA, and VEGF-C stained slides, 10 random fields per section were chosen and photographed. Positive staining areas were quantitated using Image J software (NIH, USA). LYVE-1-positive lymphatic vessels were identified and counted in whole renal cortex of slides, and the density was calculated.[12]

Western blot

Frozen mouse renal cortex was homogenized in lysis buffer, and western blot was routinely performed as described previously.[22] Membranes were incubated with CTGF antibody (sc-14939, Santa Cruz Biotechnology Inc). Actin antibody (Sigma-Aldrich, St. Louis, MO) was used on the same blot for loading control.

HK-2 cell culture

HK-2 cells were cultured in Dulbecco's modified eagle's medium with 10% fetal calf serum. Cells were plated at a density of 1×10^5 cells in 6-well plates. The next day, culture medium was replaced with serum-free medium for 24 h to render cells quiescent. Subsequently, cells were incubated in serum-free medium supplemented with 0, 2.5, 5, or 10 nM FL-CTGF (FibroGen, South San Francisco, CA). In CTGF inhibition studies, 1 day after seeding cells in 6-well plates, cells were transfected with Lipofectamine RNAiMAX (Invitrogen, Carlsbad, CA) and 20 nM CTGF siRNA or Non-targeting siRNA (GE Healthcare, Little Chalfont, UK). After 6 h incubation, culture medium was replaced with serum-free medium and incubated for 24 h. Subsequently, cells were incubated in serum-free medium alone or medium with 10 ng/ml TGF-β1 (R&D System, Minneapolis, MN). Cells and cell supernatants were harvested after 8 or 24 h incubation.

Quantitative PCR

Total RNA was extracted from frozen mouse renal cortex and cultured cells using TRIzol (Life technologies, Carlsbad, CA). After cDNA synthesis, samples were mixed with TaqMan Gene Expression Assays (mouse CTGF, Mm01192932_g1; mouse Col1α2, Mm00483888_m1; mouse LYVE-1, Mm00475056_m1; mouse VEGF-C, Mm00437313_m1; human CTGF, Hs00170014_m1; human VEGF-C, Hs00153458_m1; human PAI-1, Hs00167155_m1, Applied Biosystems, Foster City, CA) and run on a Lightcycler 480 (Roche, Basel, Switzerland). TATA-box binding protein (TBP, mouse TBP, Mm00446971_m1; human TBP, Hs00427620_m1) was used as an internal reference.

VEGF-C ELISA

VEGF-C protein levels in cell culture supernatants were measured using the Human VEGF-C Assay Kit (IBL, Takasaki, Japan), according to the manufacturer's instruction.[13,15]

Solid-Phase Binding Assay
Microtiter plates were coated overnight at 4°C with 4 μg/ml recombinant human VEGF-C (R&D System) or 1% BSA. Wells were rinsed and blocked with 1% BSA for 2 h. After washing, a range of 0 to 2 μg/ml of FL-CTGF (BioVendor Laboratory Medicine, Brno, Czech Republic) was added and incubated overnight at 4°C, followed by alkaline phosphatase-conjugated antibody against CTGF (Leinco Technologies, Fenton, MO). After incubation for 15 min at 37°C, plates were washed and substrate solution containing p-nitrophenyl phosphate was added. Absorbance was read at 405 nm.

Surface plasmon resonance analysis
Protein interaction was analyzed by the Biacore T100 (GE Healthcare, Uppsala, Sweden). Carrier-free recombinant human VEGF-C or VEGF-A (R&D System) were immobilized on a CM5 sensor chip (GE Healthcare). One additional channel was routinely activated and blocked in the absence of protein, which served as a negative control. Recombinant human FL-CTGF, N-CTGF, or C-CTGF (25-1600 nM) (FibroGen) was diluted in HBS-EP buffer (GF Healthcare) and incubated with immobilized VEGF-C for 110s at a flow rate of 20 μl/min at 25 °C. Dissociation was allowed for 300s in the same buffer flow. Chips were regenerated by two pulses of 1M NaCl and 10mM Tris buffer (pH 7.4). Data were corrected for nonspecific binding to the control channel. Binding affinities (KD) were calculated from kinetic data, using steady-state affinity analysis from triplicate data.

Capillary-like tube formation assay
HMVEC-dLy Neo (Lonza, Walkersville, MD) were cultured in EGM-2MV BulletKit (Lonza). 2×10^5 cells in serum free medium were seeded in 6-well plates coated with Growth Factor Reduced Matrigel Matrix (Corning, Bedford, MA). Cells were treated with or without 500 ng/ml recombinant human VEGF-C (R&D System), and supplemented with 25nM FL-CTGF, N-CTGF, or C-CTGF (FibroGen) in the presence of VEGF-C. After 6 h incubation, 10 random fields in each well were photographed and the number of capillary-like tube formation was counted. Data was expressed as a percentage of the control.

Statistical analysis
Data are means±s.e. Differences were analyzed by t test or one-way ANOVA followed by Tukey's HSD multiple comparison test (SPSS, Chicago, IL). $P < 0.05$ was considered to be significant.

DISCLOSURES
R.G. has received research supports from FibroGen.

ACKNOWLEDGEMENTS

We are grateful for the technical assistance of Roel Broekhuizen (Department of Pathology, University Medical Center Utrecht, Utrecht, the Netherlands).

FIGURES

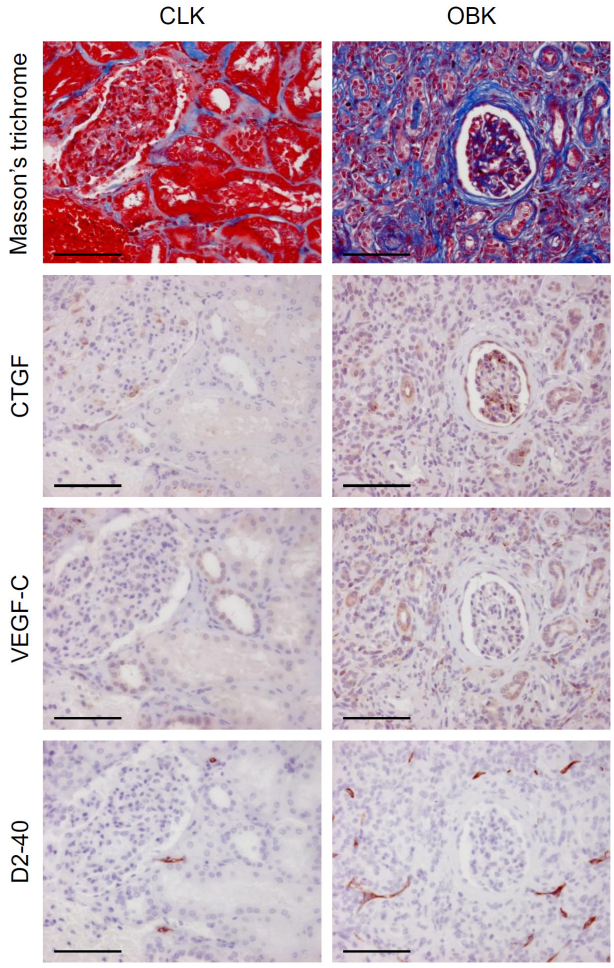

Figure 1 | Connective tissue growth factor (CTGF), vascular endothelial growth factor-C (VEGF-C), and D2-40 expression were increased in the human renal cortex undergoing fibrosis due to ureteral obstruction. A human obstructed kidney (OBK) and non-obstructed contralateral kidney (CLK) were derived from the same patient undergoing bilateral nephrectomy for bilateral renal pelvis tumors of which only one caused ureteral obstruction. Pictures show representative renal cortical areas in consecutive sections stained with Masson's trichrome, and for CTGF, VEGF-C, and D2-40. The increase of D2-40-positive lymphatic vessels in OBK undergoing tubulointerstitial fibrosis was associated with increased expression of CTGF and VEGF-C. Scale bars = 100 μm.

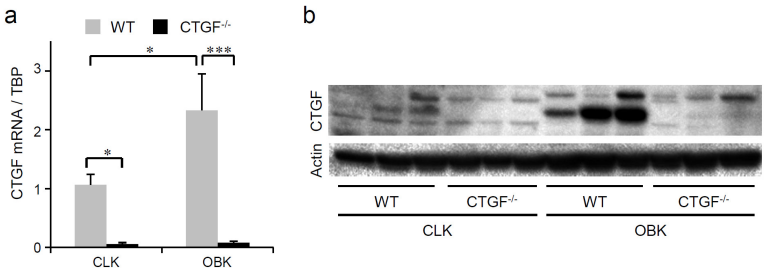

Figure 2 | Expression of connective tissue growth factor (CTGF) was dramatically decreased in CTGF knockout ($CTGF^{-/-}$) mouse kidneys. (a) Quantitative real-time PCR analysis showed that CTGF messenger RNA (mRNA) expression was significantly decreased in both of contralateral (CLK) and obstructed (OBK) kidneys of $CTGF^{-/-}$ mice compared to wild-type (WT) mice. Data are means ± s.e. (N = 5 for WT mice and N = 9 for CTGF-/- mice). TATA-box binding protein (TBP) was used as an internal control. *P < 0.05, ***P < 0.001. (b) Both of CLK and OBK lysates showed the decreased expression of CTGF protein levels in CTGF-/- mice compared to WT mice by western blot analysis. Actin was shown as a loading control.

Figure 3

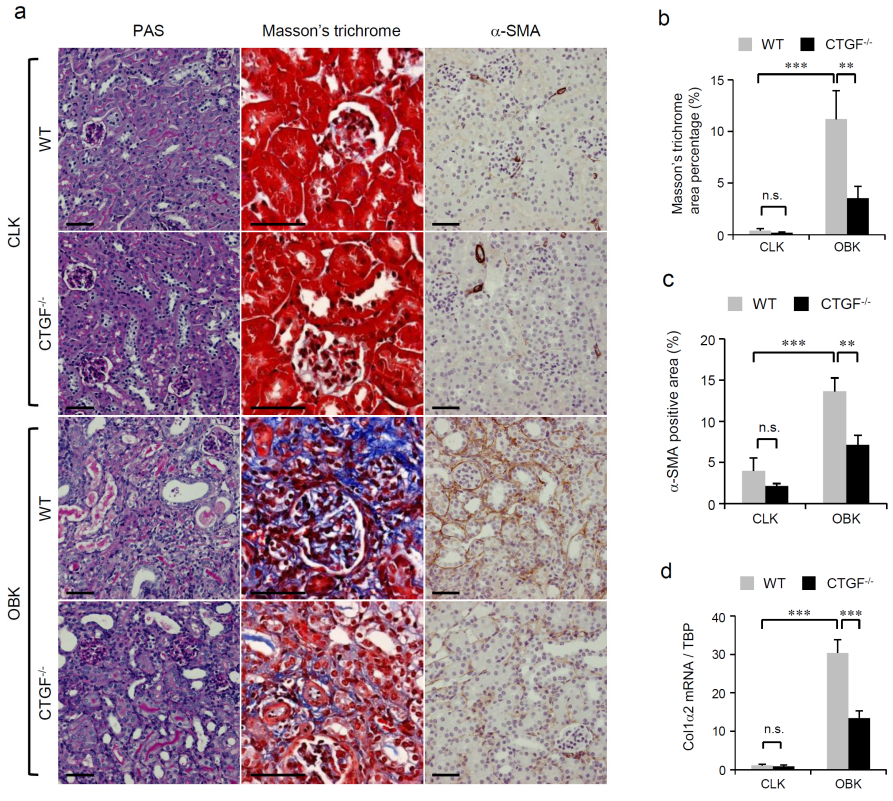

Figure 3 | Tubulointerstitial fibrosis was decreased in connective tissue growth factor knockout ($CTGF^{-/-}$) obstructed kidneys (OBK). (a) Representative micrographs of periodic acid-Schiff (PAS), Masson's trichrome, and α-smooth muscle actin (α-SMA) stained mouse renal cortex. Scale bars = 50 μm. (b and c) Quantification of Masson's trichrome staining and immunohistochemistry of α-SMA showed that an increased expression of tubulointerstitial fibrosis and α-SMA in OBK was significantly decreased in $CTGF^{-/-}$ mice compared to wild-type (WT) mice. (d) Quantitative real-time PCR analysis showed that an increased expression of collagen type I alpha 2 (Col1α2) messenger RNA (mRNA) in OBK was significantly decreased in $CTGF^{-/-}$ mice compared to WT mice. CLK: contralateral kidneys. TBP: TATA-box binding protein. Data are means ± s.e. (N = 5 for WT mice and N = 9 for $CTGF^{-/-}$ mice). $^{**}P < 0.01$, $^{***}P < 0.001$, n.s.: not significant.

Figure 4

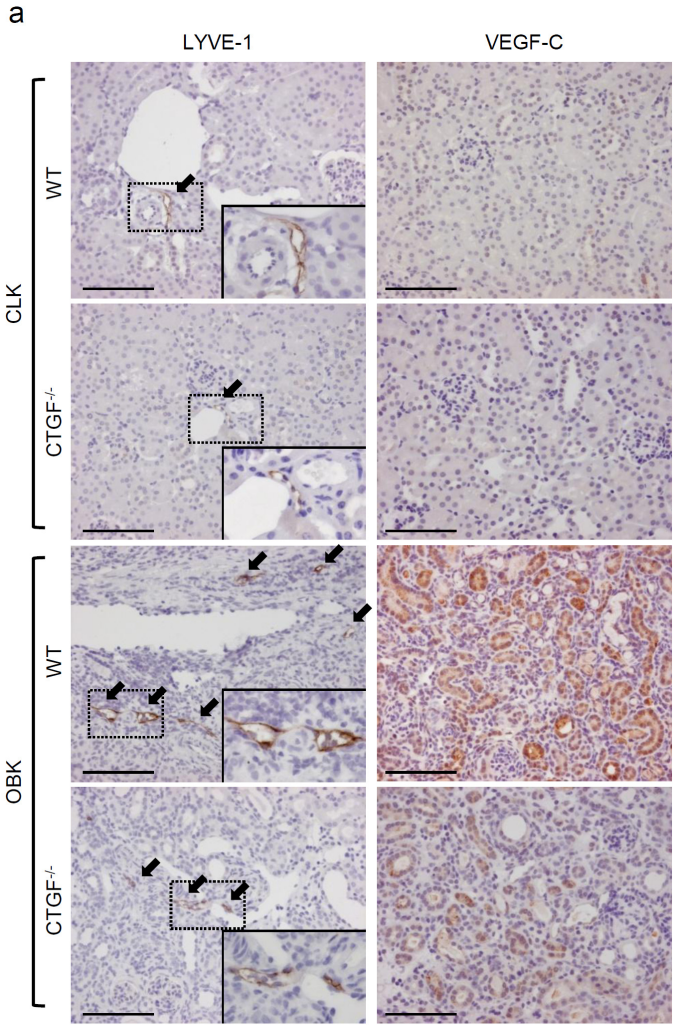

Figure 4 Continued

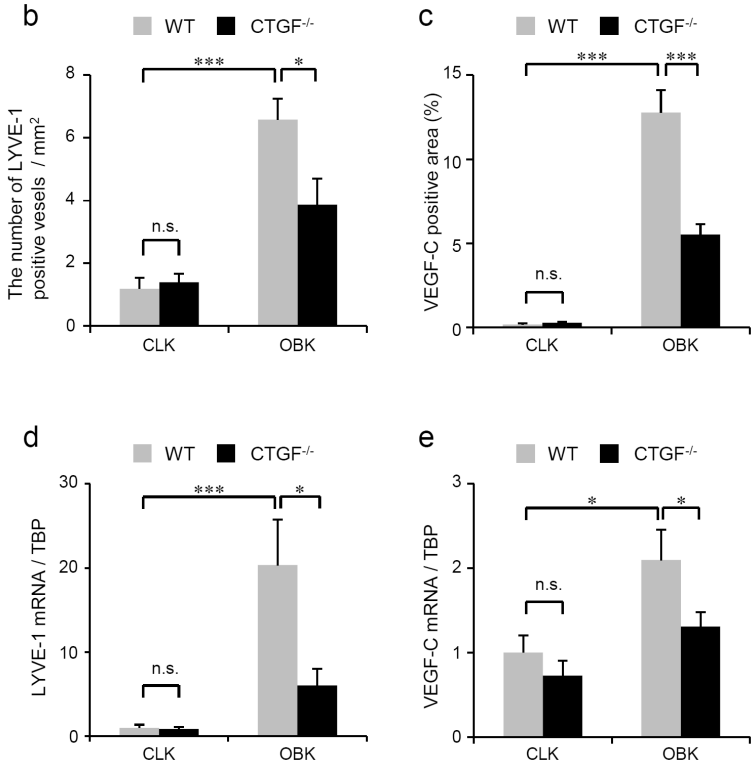

Figure 4 | Expression of lymphatic vessels and vascular endothelial growth factor-C (VEGF-C) was decreased in connective tissue growth factor knockout ($CTGF^{-/-}$) obstructed kidneys (OBK). (a) Representative micrographs of immunohistochemistry of lymphatic endothelial hyaluronan receptor-1 (LYVE-1) and VEGF-C in mouse renal cortex. Arrows indicate LYVE-1 positive lymphatic vessels. Insets indicate magnification of the black boxed area. Scale bars = 100 μm. (b and c) Quantification of immunohistochemistry showed that an increased number of LYVE-1 positive lymphatic vessels and an increased expression of VEGF-C in OBK were significantly decreased in $CTGF^{-/-}$ mice compared to wild-type (WT) mice. (d and e) Quantitative real-time PCR analysis showed that LYVE-1 and VEGF-C messenger RNA (mRNA) expression were significantly decreased in $CTGF^{-/-}$ OBK compared to WT OBK. CLK: contralateral kidneys. TBP: TATA-box binding protein. Data are means ± s.e. (N = 5 for WT mice and N = 9 for $CTGF^{-/-}$ mice). *P < 0.05, ***P < 0.001, n.s.: not significant.

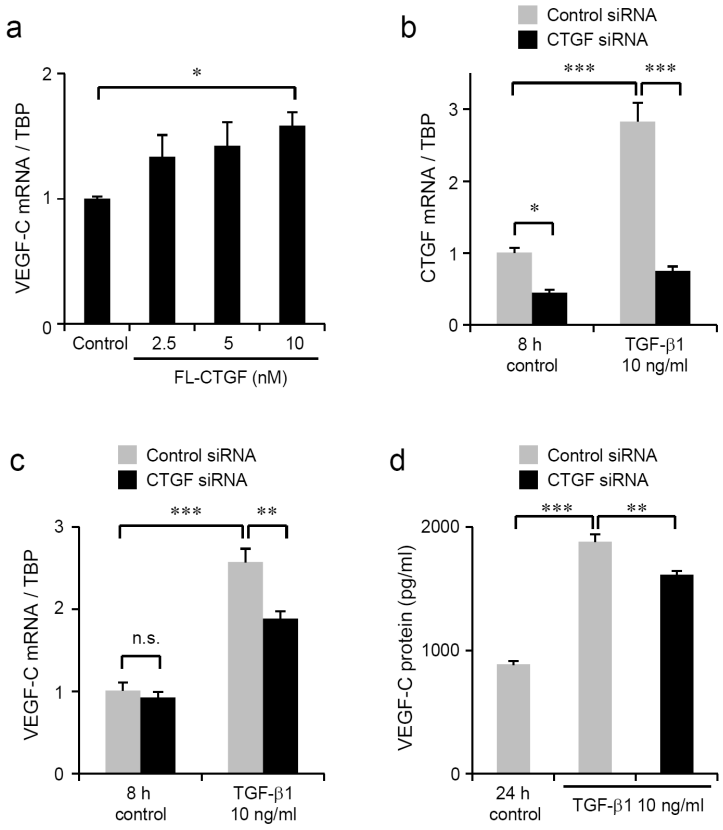

Figure 5 | Connective tissue growth factor (CTGF) induced vascular endothelial growth factor-C (VEGF-C) production in cultured human renal proximal tubular epithelial cells (HK-2). (a) HK-2 cells were treated with recombinant human full-length CTGF (FL-CTGF). (b-d) HK-2 cells were transfected with CTGF small interfering RNA (siRNA) and treated with transforming growth factor-β1 (TGF-β1). Non-targeting siRNA was used as a control siRNA. CTGF (b) and VEGF-C (a and c) messenger RNA (mRNA) were determined by quantitative real-time PCR. (a-c) TATA-box binding protein (TBP) was used as an internal control. (d) VEGF-C protein level in the supernatant was determined by enzyme-linked immunosorbent assay. (a) VEGF-C mRNA expression was increased dose-dependently by FL-CTGF treatment after 8 h incubation. (b) CTGF mRNA expression was significantly increased by TGF-β1 treatment after 8 h incubation. CTGF siRNA significantly reduced CTGF mRNA expression both in control and TGF-β1 treatment condition. (c) VEGF-C mRNA expression was significantly increased by TGF-β1 treatment after 8 h incubation. TGF-β1-incuced VEGF-C mRNA upregulation was significantly suppressed by CTGF siRNA. (d) VEGF-C protein level upregulated by TGF-β1 treatment was significantly reduced by CTGF siRNA after 24 h incubation. Data are means ± s.e. (N = 4). *P < 0.05, **P < 0.01, ***P < 0.001, n.s.: not significant.

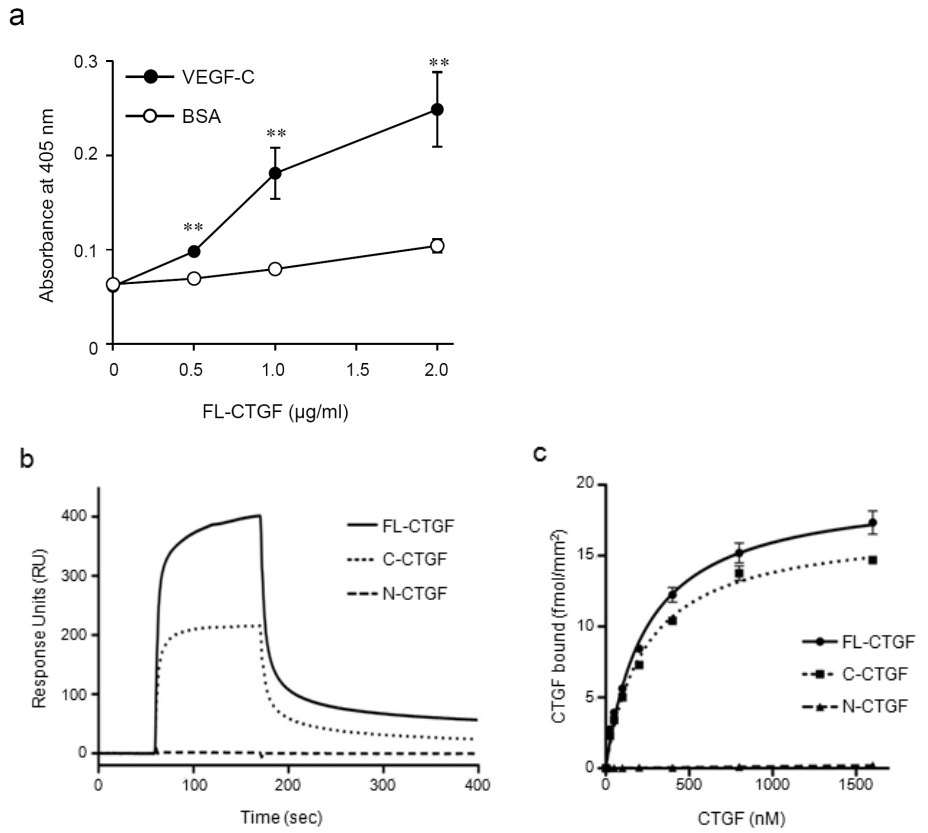

Figure 6 | Connective tissue growth factor (CTGF) directly bound to vascular endothelial growth factor-C (VEGF-C). Physical interaction between CTGF and VEGF-C was demonstrated by solid-phase binding assay and surface plasmon resonance analysis. (a) Increasing concentrations of recombinant human full-length CTGF (FL-CTGF) were added to microtiter plates coated with 4 μg/ml recombinant human VEGF-C or 1 % bovine serum albumin (BSA). Bound proteins were detected with an alkaline phosphatase-conjugated antibody against CTGF. Data are from three independent experiments. $^{**}P < 0.01$ compared to the value for BSA. (b) Recombinant human VEGF-C was immobilized and FL-CTGF, NH2- (N-CTGF) and COOH-terminal (C-CTGF) fragmants were incubated. Representative curves at 400 nM CTGF are shown (corrected for background binding). (c) FL-CTGF and C-CTGF, but not N-CTGF, dose-dependently interacted with VEGF-C. The response at maximal binding are shown. Data are from triplicates.

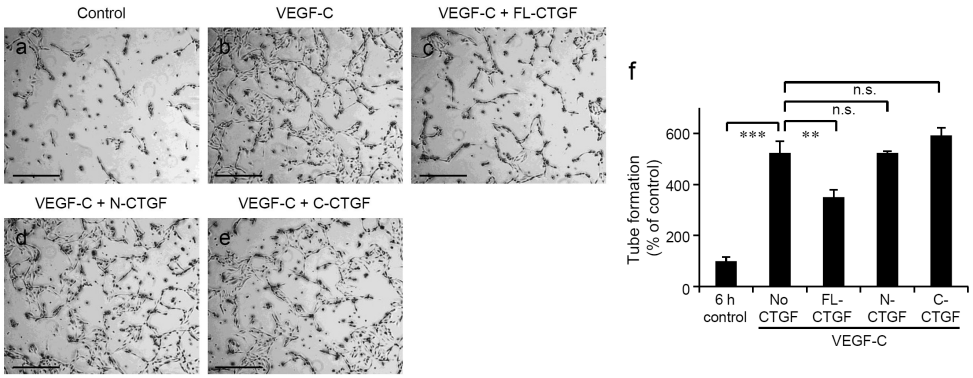

Figure 7 | Connective tissue growth factor (CTGF) suppressed vascular endothelial growth factor-C (VEGF-C)-induced capillary-like tube formation in human dermal lymphatic microvascular endothelial cells (HMVEC-dLy). (a and b) VEGF-C efficiently induced capillary-like tube formation in HMVEC-dLy seeded on Matrigel in serum free medium for 6 h (a and b). HMVEC-dLy were treated with recombinant human full-length CTGF (FL-CTGF) (c) or NH2-terminal fragmant of CTGF (N-CTGF) (d) or COOH-terminal fragmant of CTGF (C-CTGF) (e) in the presence of VEGF-C. Scale bars = 400 μm. (f) Tube formation was quantified by counting the number of tubes. FL-CTGF suppressed VEGF-C-induced tube formation. N-CTGF and C-CTGF had no significant effect on tube formation induced by VEGF-C. Data are means ± s.e. (N = 3). **P < 0.01, ***P < 0.001, n.s.: not significant.

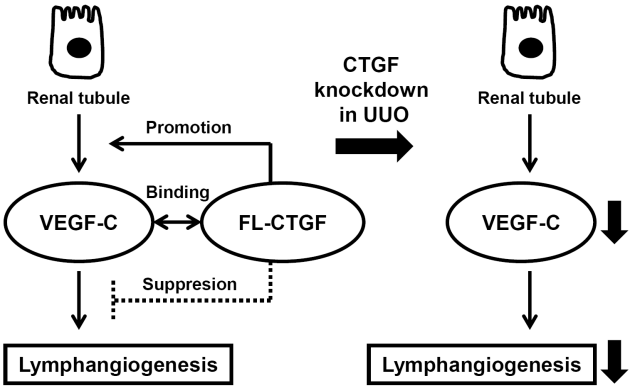

Figure 8 | Connective tissue growth factor (CTGF) plays a significant role in renal lymphangiogenesis. Full-length CTGF (FL-CTGF) promotes vascular endothelial growth factor-C (VEGF-C) production in renal tubular epithelial cells. FL-CTGF binds to VEGF-C, and suppresses VEGF-C-induced lymphangiogenesis. NH2-terminal fragmant and COOH-terminal fragmant of CTGF have no influence on VEGF-C function. CTGF knockdown suppresses VEGF-C expression and lymphangiogenesis in an unilateral ureteral obstruction (UUO) model.

Supplementary Material

Figure S1

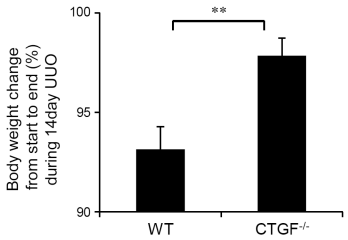

Figure S2

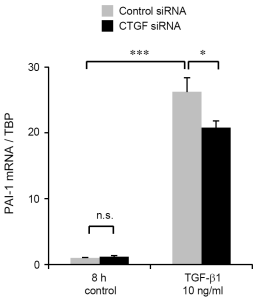

Figure S1. Connective tissue growth factor knockout ($CTGF^{-/-}$) mice showed a beneficial effect for maintaining body weight during 14-days unilateral ureteral obstruction (UUO) model. Percentage of mouse body weight 14 days after UUO is shown. $CTGF^{-/-}$ mice (97.9±2.6 %) showed a beneficial effect for maintaining body weight during an experimental period compared with wild-type (WT) mice (93.2±2.5 %). Data are means ± s.e. ($N = 5$ for WT mice and $N = 9$ for $CTGF^{-/-}$ mice). $^{**}P < 0.01$.

Figure S2. Connective tissue growth factor short-interfering RNA (CTGF siRNA) suppressed plasminogen activator inhibitor-1 (PAI-1) messenger RNA (mRNA) expression in cultured human renal proximal tubular epithelial cells (HK-2) treated with transforming growth factor-β1 (TGF-β1). HK-2 cells were transfected with CTGF siRNA and treated with TGF-β1. Non-targeting siRNA was used as a control siRNA. PAI-1 mRNA expression was determined by quantitative real-time PCR. TATA-box binding protein (TBP) was used as an internal control. PAI-1 mRNA expression was significantly increased by TGF-β1 treatment after 8 h incubation. TGF-β1-induced PAI-1 mRNA upregulation was significantly suppressed by CTGF siRNA. Data are means ± s.e. ($N = 4$). $^{*}P < 0.05$, $^{***}P < 0.001$, n.s.: not significant.

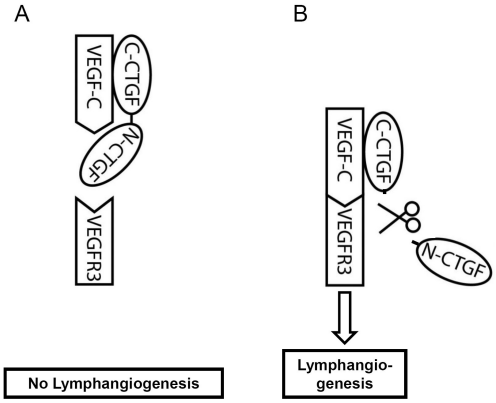

Figure S3. Hypothetical model for connective tissue growth factor (CTGF) – vascular endothelial growth factor-C (VEGF-C) – VEGF receptor (VEGFR)2/3 interaction. (A) Full-length CTGF (FL-CTGF) binds to VEGF-C through its C-CTGF portion. The attached N-CTGF portion might sterically hinder VEGF-C binding to VEGFR2/3 and inhibit lymphangiogenesis. (B) VEGF-C-induced lymphangiogenesis might be restored by proteolytic cleavage of FL-CTGF separating the N-CTGF fragment from the bound C-CTGF portion, thereby eliminating the steric hindrance and restoring VEGF-C signaling through VEGFR2/3.

REFERENCES

1. Fung E, Kurella Tamura M. Epidemiology and Public Health Concerns of CKD in Older Adults. Adv Chronic Kidney Dis. 2016;23:8-11.
2. Thomas B, Wulf S, Bikbov B, et al. Maintenance Dialysis throughout the World in Years 1990 and 2010. J Am Soc Nephrol. 2015;26:2621-2633.
3. Ghanta M, Jim B. Renal Transplantation in Advanced Chronic Kidney Disease Patients. Med Clin North Am. 2016;100:465-476.
4. Norrmén C, Tammela T, Petrova TV, et al. Biological basis of therapeutic lymphangiogenesis. Circulation. 2011;123:1335-1351.
5. Alitalo A, Detmar M. Interaction of tumor cells and lymphatic vessels in cancer progression. Oncogene. 2012;31:4499-4508.
6. Kim H, Kataru RP, Koh GY. Inflammation-associated lymphangiogenesis: a double-edged sword? J Clin Invest. 2014;124:936-942.
7. Dashkevich A, Hagl C, Beyersdorf F, et al. VEGF Pathways in the Lymphatics of Healthy and Diseased Heart. Microcirculation. 2016;23:5-14.
8. Kerjaschki D, Regele HM, Moosberger I, et al. Lymphatic neoangiogenesis in human kidney transplants is associated with immunologically active lymphocytic infiltrates. J Am Soc Nephrol. 2004;15:603-612.
9. Cui Y, Liu K, Monzon-Medina ME, et al. Therapeutic lymphangiogenesis ameliorates established acute lung allograft rejection. J Clin Invest. 2015;125:4255-4268.
10. Zheng W, Aspelund A, Alitalo K. Lymphangiogenic factors, mechanisms, and applications. J Clin Invest. 2014;124:878-887.
11. Coso S, Bovay E, Petrova TV. Pressing the right buttons: signaling in lymphangiogenesis. Blood. 2014;123:2614-2624.
12. Sakamoto I, Ito Y, Mizuno M, et al. Lymphatic vessels develop during tubulointerstitial fibrosis. Kidney Int. 2009;75:828-838.
13. Suzuki Y, Ito Y, Mizuno M, et al. Transforming growth factor-β induces vascular endothelial growth factor-C expression leading to lymphangiogenesis in rat unilateral ureteral obstruction. Kidney Int. 2012;81:865-879.
14. Lee AS, Lee JE, Jung YJ, et al. Vascular endothelial growth factor-C and -D are involved in lymphangiogenesis in mouse unilateral ureteral obstruction. Kidney Int. 2013;83:50-62.
15. Kinashi H, Ito Y, Mizuno M, et al. TGF-β1 promotes lymphangiogenesis during peritoneal fibrosis. J Am Soc Nephrol. 2013;24:1627-1642.
16. Falke LL, Goldschmeding R, Nguyen TQ. A perspective on anti-CCN2 therapy for chronic kidney disease. Nephrol Dial Transplant. 2014;29(suppl 1):i30-i37.
17. Gupta S, Clarkson MR, Duggan J, et al. Connective tissue growth factor: potential role in glomerulosclerosis and tubulointerstitial fibrosis. Kidney Int. 2000;58:1389-1399.
18. Phanish MK, Winn SK, Dockrell ME. Connective tissue growth factor-(CTGF, CCN2)--a marker, mediator and therapeutic target for renal fibrosis. Nephron Exp Nephrol. 2010;114:e83-e92.

19. Abreu JG, Ketpura NI, Reversade B, et al. Connective-tissue growth factor (CTGF) modulates cell signalling by BMP and TGF-beta. Nat Cell Biol. 2002;4:599-604.
20. Yokoi H, Mukoyama M, Nagae T, et al. Reduction in connective tissue growth factor by antisense treatment ameliorates renal tubulointerstitial fibrosis. J Am Soc Nephrol. 2004;15:1430-1440.
21. Guha M, Xu ZG, Tung D, et al. Specific down-regulation of connective tissue growth factor attenuates progression of nephropathy in mouse models of type 1 and type 2 diabetes. FASEB J. 2007;21:3355-3368.
22. Falke LL, Dendooven A, Leeuwis JW, et al. Hemizygous deletion of CTGF/CCN2 does not suffice to prevent fibrosis of the severely injured kidney. Matrix Biol. 2012;31:421-431.
23. Pi L, Shenoy AK, Liu J, et al. CCN2/CTGF regulates neovessel formation via targeting structurally conserved cystine knot motifs in multiple angiogenic regulators. FASEB J. 2012;26:3365-3379.
24. Inoki I, Shiomi T, Hashimoto G, et al. Connective tissue growth factor binds vascular endothelial growth factor (VEGF) and inhibits VEGF-induced angiogenesis. FASEB J. 2002;16:219-221.
25. Hashimoto G, Inoki I, Fujii Y, et al. Matrix metalloproteinases cleave connective tissue growth factor and reactivate angiogenic activity of vascular endothelial growth factor 165. J Biol Chem. 2002;277:36288-36295.
26. Luo GH, Lu YP, Song J, et al. Inhibition of connective tissue growth factor by small interfering RNA prevents renal fibrosis in rats undergoing chronic allograft nephropathy. Transplant Proc. 2008;40:2365-2369.
27. Okada H, Kikuta T, Kobayashi T, et al. Connective tissue growth factor expressed in tubular epithelium plays a pivotal role in renal fibrogenesis. J Am Soc Nephrol. 2005;16:133-143.
28. Ivkovic S, Yoon BS, Popoff SN, et al. Connective tissue growth factor coordinates chondrogenesis and angiogenesis during skeletal development. Development. 2003;130:2779-2791.
29. Mizutani M, Ito Y, Mizuno M, et al. Connective tissue growth factor (CTGF/CCN2) is increased in peritoneal dialysis patients with high peritoneal solute transport rate. Am J Physiol Renal Physiol. 2010;298:F721-F733.
30. Sleeman JP, Thiele W. Tumor metastasis and the lymphatic vasculature. Int J Cancer. 2009;125:2747-2756.
31. He Y, Rajantie I, Pajusola K, et al. Vascular endothelial cell growth factor receptor 3-mediated activation of lymphatic endothelium is crucial for tumor cell entry and spread via lymphatic vessels. Cancer Res. 2005;65:4739-4746.
32. Quagliata L, Klusmeier S, Cremers N, et al. Inhibition of VEGFR-3 activation in tumor-draining lymph nodes suppresses the outgrowth of lymph node metastases in the MT-450 syngeneic rat breast cancer model. Clin Exp Metastasis. 2014;31:351-365.

33. Lin CC, Chen PC, Lein MY, ey al. WISP-1 promotes VEGF-C-dependent lymphangiogenesis by inhibiting miR-300 in human oral squamous cell carcinoma cells. Oncotarget. 2016;7:9993-10005.
34. Neesse A, Frese KK, Bapiro TE, et al. CTGF antagonism with mAb FG-3019 enhances chemotherapy response without increasing drug delivery in murine ductal pancreas cancer. Proc Natl Acad Sci U S A. 2013;110:12325-12330.
35. Finger EC, Cheng CF, Williams TR, et al. CTGF is a therapeutic target for metastatic melanoma. Oncogene. 2014;33:1093-1100.
36. Liu S, Shi-wen X, Abraham DJ, et al. CCN2 is required for bleomycin-induced skin fibrosis in mice. Arthritis Rheum. 2011;63:239-246.
37. Liu S, Parapuram SK, Leask A. Fibrosis caused by loss of PTEN expression in mouse fibroblasts is crucially dependent on CCN2. Arthritis Rheum. 2013;65:2940-2944.
38. Hutchenreuther J, Vincent KM, Carter DE, et al. CCN2 Expression by Tumor Stroma Is Required for Melanoma Metastasis. J Invest Dermatol. 2015;135:2805-2813.
39. Dean RA, Butler GS, Hamma-Kourbali Y, et al. Identification of candidate angiogenic inhibitors processed by matrix metalloproteinase 2 (MMP-2) in cell-based proteomic screens: disruption of vascular endothelial growth factor (VEGF)/heparin affin regulatory peptide (pleiotrophin) and VEGF/Connective tissue growth factor angiogenic inhibitory complexes by MMP-2 proteolysis. Mol Cell Biol. 2007;27:8454-8465.
40. Palin NK, Savikko J, Koskinen PK. Sirolimus inhibits lymphangiogenesis in rat renal allografts, a novel mechanism to prevent chronic kidney allograft injury. Transpl Int. 2013;26:195-205.
41. Nihei M, Okazaki T, Ebihara S, et al. Chronic inflammation, lymphangiogenesis, and effect of an anti-VEGFR therapy in a mouse model and in human patients with aspiration pneumonia. J Pathol. 2015;235:632-645.
42. Terabayashi T, Ito Y, Mizuno M, et al. Vascular endothelial growth factor receptor-3 is a novel target to improve net ultrafiltration in methylglyoxal-induced peritoneal injury. Lab Invest. 2015;95:1029-1043.
43. Yazdani S, Hijmans RS, Poosti F, et al. Targeting tubulointerstitial remodeling in proteinuric nephropathy in rats. Dis Model Mech. 2015;8:919-930.
44. Jung YJ, Lee AS, Nguyen-Thanh T, et al. Hyaluronan-induced VEGF-C promotes fibrosis-induced lymphangiogenesis via Toll-like receptor 4-dependent signal pathway. Biochem Biophys Res Commun. 2015;466:339-345.

8

Age-dependent shifts in renal response to injury relate to altered BMP6/CTGF expression and signaling

Am J Physiol Renal Physiol. 2016;311(5):F926-F934

Lucas L. Falke[1], Hiroshi Kinashi[1,2], Amelie Dendooven[3], Roel Broekhuizen[1], Reinout Stoop[4], Jaap A. Joles[5], Tri Q. Nguyen[1], and Roel Goldschmeding[1]

[1]Department of Pathology, University Medical Center Utrecht, Utrecht, The Netherlands
[2]Department of Nephrology and Renal Replacement Therapy, Nagoya University, Nagoya, Japan
[3]Department of Pathology, University Medical Center, Antwerp, Belgium
[4]Department of Metabolic Health Research, TNO, Leiden, The Netherlands
[5]Department of Nephrology and Hypertension, University Medical Center Utrecht, Utrecht, The Netherlands

ABSTRACT
Age is associated with an increased prevalence of chronic kidney disease (CKD), which, through progressive tissue damage and fibrosis, ultimately leads to loss of kidney function. Although much effort is put into studying CKD development experimentally, age has rarely been taken into account. Therefore, we investigated the effect of age on the development of renal tissue damage and fibrosis in a mouse model of obstructive nephropathy (i.e., unilateral ureter obstruction; UUO). We observed that after 14 days, obstructed kidneys of old mice had more tubulointerstitial atrophic damage but less fibrosis than those of young mice. This was associated with reduced connective tissue growth factor (CTGF), and higher bone morphogenetic protein 6 (BMP6) expression and pSMAD1/5/8 signaling, while transforming growth factor-β expression and transcriptional activity were no different in obstructed kidneys of old and young mice. In vitro, CTGF bound to and inhibited BMP6 activity. In summary, our data suggest that in obstructive nephropathy atrophy increases and fibrosis decreases with age and that this relates to increased BMP signaling, most likely due to higher BMP6 and lower CTGF expression.

INTRODUCTION

Chronic kidney disease (CKD) primarily affects the aging population (11, 37, 42). Decline of kidney function with age might result from multifactorial changes in kidney physiology, primarily due to "senescence" itself, and a more adverse response to injury (1, 5, 22, 43, 45, 47). As such, it has been proposed that the aging kidney increasingly accumulates extracellular matrix, leading to glomerulosclerosis and interstitial fibrosis (1, 25) and ultimately to loss of renal mass and reduced glomerular and tubular function (17, 51). Parameters such as diabetes, vitamin D deficiency, alterations in renin-angiotensin-aldosterone system (RAAS) signaling, oxidative stress by reactive oxygen species (ROS) production, and advanced glycation end (AGE) products are thought to underlie these morphological and functional changes in the kidney parenchyma (8). Furthermore, the age-associated gradual decline in Klotho, a transmembrane FGF23 coreceptor expressed in the convoluted distal tubule under physiological conditions, renders kidneys more susceptible to injury, dysregulation of mineral homeostasis, and fibrosis (28).

In young mice, the kidney response to injury is profoundly influenced by the transforming growth factor-β (TGF-β) superfamily, including TGF-β1, bone morphogenetic protein 7 (BMP7), and BMP6 (14, 35). Canonical signaling of the TGF-β superfamily is accomplished via activin-like kinase (ALK) activation and subsequent downstream SMAD phosphorylation. Activation of ALK4, 5, or 7 by TGF-β leads to fibrosis-associated SMAD2/3 phosphorylation. ALK1-3 or 6 activation by BMPs leads to renoprotection-associated SMAD1/5/8 phosphorylation (10). Under specific conditions, TGF-β has been shown to activate ALK1 (36). Upon injury, TGF-β levels rise and BMP levels drop rapidly (34). The shift in these factors is regarded as a major early event in the ensuing tissue damage with subsequent fibrosis following injury.

Connective tissue growth factor (CTGF) is another immediate early factor shown to greatly influence the response to kidney injury. CTGF is a matricellular protein involved in various fibrosis-associated phenomena, such as extracellular matrix production, proliferation, and myofibroblast differentiation (19). Although no exclusive CTGF receptor has been identified, CTGF has been known to interact with TGF-β and BMP7, thereby modulating signaling in favor of profibrotic TGF-β while inhibiting BMP7 signaling (2, 35). As such, TGF-β, BMP6 and 7, and CTGF are regarded as major factors influencing the renal response to injury. The age-associated production of reaction oxygen species (ROS) is related to increased levels of profibrotic growth factors (41), but little is known about the impact of aging on the regulation of these factors in the kidney. It has been reported that profibrotic TGF-β signaling generally increases with age, which might at least in part be due to the gradual decline of Klotho (15).

The effect of aging on renal CTGF expression is largely unknown, but CTGF/CCN2 was found to be reduced in aged skin in association with loss of collagen (39). Interestingly, conditional overexpression of CTGF prevented age-related degenerative changes in epiphyseal cartilage in rats (27). In contrast, aging is associated with increased cardiac

CTGF expression in mice (40, 48), suggesting that age-related differential expression of CTGF is context dependent.

Reports on age-associated changes in expression and signaling of the (antifibrotic) BMPs are scarce, but it has been noted that BMP7 expression declines in aging cartilage (3), while increased expression of BMP6 was found in Alzheimer brains (12), and early aging in Klotho-deficient mice was associated with increased BMP signaling and vascular calcification (23). To the best of our knowledge, there are no previous data on age-related changes in renal BMP expression and signaling. Based on our findings in the current study, we hypothesize that old and young kidneys respond differently to injury in association with differential TGF-β/BMP/CTGF signaling.

Unilateral ureter obstruction (UUO) is a commonly used model of renal injury characterized by inflammation, extensive morphological damage, and fibrosis (7, 29). Upon obstruction, the quick rise in TGF-β levels and subsequent phosphorylation of SMAD2/3 and PAI-1 upregulation are regarded as key events ultimately leading to fibrosis (26, 44). We studied morphological damage and fibrosis following 14 days of UUO and observed a shift from a largely fibrotic phenotype in young kidneys to a more atrophic phenotype of tubulointerstitial damage in old kidneys, although BMP7 and TGF-β were not different. This phenotypic shift might derive from a synergistic effect of the observed decrease in CTGF and increase in BMP6, even more so since we noted in vitro that CTGF directly binds to BMP6 and inhibits its signaling activity. Together, these findings provide further understanding of the age-associated response to injury and might help to identify better diagnostic methods and therapeutic interventions in the aging population.

MATERIALS AND METHODS

Animals

Two groups of C57BL6/J mice [16 wk old (n = 6; Young) and 50 wk old (n = 6; Old)] were housed under standard conditions and subjected to UUO. Under general isoflurane anesthesia, the left ureter was ligated with silk suture through the left flank, after which the wound was closed and stitched. One young and one old mouse deteriorated in condition rapidly after surgery and both were euthanized within a week. These mice were excluded from further analysis. After 13 days, the remaining mice were housed in metabolic cages for 16 h for urine collection. At day 14, they were euthanized and organs and plasma were collected for analysis. Animal experiments were carried out with the approval of the Experimental Animal Ethics Committee of the University of Utrecht conforming with Dutch law.

Immunohistochemistry

Fresh kidney tissue was fixed in buffered 4% paraformaldehyde solution and embedded in paraffin. Sections (3 ┘ m) were cut, embedded on object slides, and incubated in a stove at 60°C for 16 h. Sections were deparaffinized and rehydrated in xylene, 100 and 70% ethanol, respectively, after which the sections were rinsed in demineralized water. Periodic acid-

Schiff (PAS) and Masson trichrome staining were performed using standard procedures. For quantification of morphological damage, 10 arbitrary cortical fields/kidney were scored in PAS-stained sections with regard to atrophy and dilatation (0 = <1%, 1 = 1–25%, 2 = 25–50%, 3 = 50–75%, and 4 = 75–100%). For immunohistochemistry, antigen retrieval consisted of 20-min boiling in either citrate buffer (pH = 6), EDTA buffer (pH = 9), or 10-min pepsin digestion depending upon the primary antibody. Slides were incubated with the following antibodies: α-smooth muscle actin (α-SMA; EDTA, 1:200, Abcam, Cambridge, UK), CTGF (citrate, 1:200, Santa Cruz Biotechnology, Santa Cruz, CA), pSMAD2/3 (pepsin, 1:400, Santa Cruz Biotechnology), or pSMAD1/5/8 (citrate, 1:50, Cell Signaling Technology, Danvers, MA). To determine positive area percentages of Masson trichrome- and CTGF-stained slides, 10 random fields/section were chosen and photographed. using Photoshop (version 12.0). Positive-staining areas were selected and quantitated using ImageJ software (NIH, Baltimore, MD).

Hydroxyproline, Urea, Protein, and Senescence-Associated β-Galactosidase Assay
Hydroxyproline. Paraffin sections were analyzed for hydroxyproline levels as a measurement of collagen content using HPLC (18); proline ratio was taken as a measure of relative abundance of collagen. Plasma urea. Plasma urea levels were measured by colorimetric assay using standard procedures (DiaSys, Holzheim, Germany). Urinary protein. Urinary protein was measured by BCA assay (Bio-Rad, Hercules, CA). Senescence-associated β-galactosidase. Senescence-associated (SA)- β-galactosidase (Gal) activity was detected as described (13).

Western Blotting
Snap-frozen renal cortex was homogenized and lysed using NP-40 lysis buffer containing Na-orthovanadate, Na-fluoride, and complete protease inhibitor cocktail. Lysates were spun down, and pellets were discarded. Total protein concentration in the supernatant was measured using BCA (Pierce Thermo, Rockford, IL). Twenty micrograms of protein was boiled with Laemmli/DTT and run for 90 min on 10% SDS-PAGE gels (Bio-Rad). Gels were subsequently blotted for 90 min on polyvinylidene difluoride membrane using a wet blotting transfer system (Bio-Rad). For pSmad1/5/8 analysis, membranes were incubated with primary antibody (pSMAD1/5/8, 1:2,000, Cell Signaling Technology; SMAD1/5/8, 1:1,000, Santa Cruz Biotechnology) in TBS-Tween containing 3% BSA overnight. After a thorough rinsing, membranes were incubated with secondary horseradish peroxidaseconjugated antibody and imaged using chemiluminescence substrate (GE Healthcare Life Sciences, Buckinghamshire, UK).

RT-Quantitative PCR
RNA was isolated from both tissue homogenate and cell cultures using TRIzol (Life Technologies, Carlsbad, CA). RNA was reversely transcribed to cDNA using standard procedures. Expression of target genes was determined using commercially available

predesigned TaqMan probes (Bmp6, Mm00432095_m1; Bmp7, Mm00432102_m1; Col1− 2, Mm00483888_m1; Ctgf, Mm00515790_g1; Hsp47, Mm00438058_g1; Klotho, Mm00502002_m1; Pai1, Mm00435860_m1; Tgfβ1, Mm01178820_m1; Id1: Mm00775963_g1; and Tbp: Mm01277042_m1; Thermo Fisher, Waltham, MA). Samples were run on a Lightcycler 480 (Roche, Basel, Switzerland), and relative expression was determined by the ΔΔCT method. Application of GeNorm identified TATA box binding protein (Tbp) as the most stable reference gene (out of Gapdh, Yhwaz, Actb, and Tbp).

Solid-Phase BMP6/CTGF Binding Assay

Microtiter plates were coated with fixed concentration of 200 ng/ml full-length rhCTGF (BioVendor, Modrice, Czech Republic) at 4°C overnight. Plates were rinsed and blocked with 1% BSA for 2 h. After rinsing, a range of 0–1,000 ng/ml rhBMP6 (R&D Systems, Minneapolis, MN) was added. Bound BMP6 was detected by using a BMP6 antibody (Santa Cruz Biotechnology).

Cell Culture

HK-2 cells were maintained in DMEM (GIBCO/Thermo, Waltham, MA) with 10% FCS, penicillin, and streptomycin in humidified air with 5% CO2 at 37°C. HK-2 cells were plated at a density of 1×10^5 cells in six-well plates. Cells were serum starved for 24 h and subsequently incubated with serum-free medium alone, 50 ng/ml rhBMP6 (R&D Systems) with or without 400 ng/ml rhCTGF. Cells were harvested after 1 h for Western blot analysis and after 2 h for quantitative PCR.

Statistics

Data were analyzed using GraphPad Prism version 6.02 (GraphPad software, La Jolla, CA). All data were statistically tested with Student's t-test for two groups, or two-way ANOVA followed by post hoc Tukey correction for multiple testing when more groups were compared, unless stated otherwise. $P < 0.05$ was considered statistically significant. Error bars represent SE.

RESULTS

General Characteristics

To investigate potential age-related differential responses to injury, we performed UUO in both groups for 14 days. Post-UUO, kidney weight loss, diuresis, plasma urea, and proteinuria were similar at both ages (data not shown). However, old mice lost more body weight compared with young mice (Fig. 1A). Old contralateral kidneys (CLKs; 50 wk) showed sporadic SA-β-Gal activity whereas this was not detected in any of sections from kidneys of young mice (16 wk) (data not shown). Glomerulosclerosis, a phenomenon associated with aging, was not seen in old CLKs (Fig. 1B).

Ureteral Ligation Induces a More Severe Morphological Phenotype in Aged Kidneys

To assess the extent of injury, dilatation and atrophy (2 hallmarks of UUO-induced renal damage) were scored. Morphological interstitial damage after obstruction was more severe in old obstructed kidneys (OBKs), as exemplified by higher kidney tubular morphological damage scores for dilatation and atrophy in old OBKs compared with young OBKs (Fig. 1, B and C).

Development of Fibrosis Is Reduced in Aged Kidneys

Since fibrosis is a second major phenomenon occurring during UUO-mediated renal injury, we studied the level of ECM deposition and associated myofibroblast accumulation in OBKs of both age groups. Quantification of Masson trichrome staining, a staining for fibrillary collagen, showed a reduced area positivity (%) in old OBKs compared with young OBKs (Fig. 2A). An increase in Masson trichrome-positive surface area in young OBKs was observed, whereas no significant increase was seen in old OBKs compared with CLKs (Fig. 2B). Furthermore, myofibroblast numbers as assessed by α-SMA were also lower in old OBKs compared with young OBKs (Fig. 2A, bottom, B and C). No difference was observed in CLKs (data not shown). Old OBKs show a reduced Col1α2 upregulation compared with young OBKs (Fig. 2D). Correspondingly, a significant increase in the message for collagen chaperone Hsp47 was seen in young kidneys upon obstruction whereas this was not observed in old OBKs (Fig. 2E). Hydroxyproline levels were higher in old CLKs compared with young CLKs, but were similar in OBKs of both age groups (Fig. 2F). The fold-increase (OBK/CLK) in hydroxyproline was reduced in old compared with young kidneys (Fig. 2F, right). Taken together, this suggests a decreased de novo synthesis of collagen in old compared with young kidneys upon ureteral obstruction.

Age Is Associated with an Altered Profibrotic/Regenerative Balance

To gain insight into potential underlying differences in profibrotic signaling resulting in the altered phenotype, we studied several important known mediators of aging or fibrosis. For assessment of proregenerative gene expression, we investigated Klotho, Bmp6, and Bmp7 mRNA expression levels (Fig. 3, A–C). The renoprotective factor Klotho is strongly associated with aging and interacts with the TGF-β pathway during fibrogenesis in the kidney (4, 31, 50). Despite the 38-wk age difference, Klotho expression was not differentially regulated in unobstructed CLKs of 50- and 12-wk-old mice (Fig. 3A). Also, Klotho was similarly downregulated in OBKs of both age groups, and no significant change in Klotho expression was observed between old and young OBKs (Fig. 3A). In young mice, OBKs had significantly reduced gene expression levels of Bmp6 and Bmp7 (Fig. 3, B and C). In old and young OBKs, Bmp7 expression was similarly suppressed (Fig. 3B). However, unlike young OBKs, old OBKS showed no reduction of Bmp6 expression (Fig. 3C).

The increase in Tgf-β1 as a key profibrotic regulator, and Pai-1 as important downstream mediator of TGF-β1 in kidney fibrosis (24), were not different in old and young OBKs ($P = 0.96$, $P = 0.36$, respectively; Fig. 3, D and E). To further evaluate downstream signaling of

TGF-β1 we performed pSMAD2/3 immunohistochemistry on the kidney cortex. However, the number of cortical cells showing TGF-β-associated nuclear SMAD2/3 phosphorylation was not significantly different between old and young OBKs ($P = 0.95$; data not shown). CTGF greatly influences the fibrotic/regenerative balance by positively modulating TGF-β and negatively modulating BMP signaling and is commonly regarded as profibrotic (2, 35). In CLKs, Ctgf mRNA expression levels were identical in old and young mice (Fig. 3F). In OBKs, mean Ctgf gene expression tended to be higher in young OBKs compared with old OBKs, and compared with young CLKs ($P = 0.07$); the mean increase vs. age-matched CLK was 7-fold in young OBKs compared with 3.5-fold in old OBKs (Fig. 3F). This increase was significant in young OBKs but not in old OBKs ($P = 0.013$ vs. 0.54, respectively). Furthermore, CTGF immunohistochemistry showed a decrease in CTGF-positive area both in CLK and OBK old kidneys compared with CLK and OBK young kidneys, respectively (Fig. 3, G and H: $P < 0.05$), while the increase in OBK compared with CLK was significant only in young mice. Signal loss occurred mainly in cortical tubules. The Bmp6/Ctgf ratio in individual OBKs was significantly higher in old than in young OBKs (12.1 ± 2.6 vs. 4.1 ± 0.4; $P < 0.05$).

Canonical BMP Signaling is Better Preserved in Cortical Tubular Epithelium of Old Mice

Given the increased BMP6/CTGF ratio, we next studied whether this resulted in an increase in canonical BMP signaling. In old OBKs, the pSMAD1/5/8 signal was better preserved compared with young OBKs (Fig. 4, A and B). Immunostaining for pSMAD1/5/8 shows that glomerular and interstitial pSMAD1/5/8 is similar in young and old OBKs (Fig. 4, C and D). However, preservation of pSMAD1/5/8 signal occurred in the tubuli.

CTGF Binds BMP6 and Inhibits Canonical Downstream Signaling

CTGF inhibits canonical BMP7 signaling in proximal tubular (HK-2) cells via direct interaction (35). Whether CTGF holds similar potential with regard to BMP6 is unknown. By solid-phase assay, we observed concentration-dependent binding of rhBMP6 in rhCTGF-coated microtiter plates (Fig. 5A). Stimulating HK-2 cells with rhBMP6 increased downstream transcriptional Id1 expression significantly ($P < 0.05$) (Fig. 5B). When costimulating HK-2 cells with rhBMP6 and rhCTGF, however, this increase was significantly less profound (Fig. 5B). Consistently, Western blot analysis showed increased SMAD1/5/8 phosphorylation upon rhBMP6 stimulation, which was less profound when rhBMP6 was preincubated with rhCTGF before stimulation (Fig. 5C). Thus in vivo the increased BMP6 expression and associated SMAD1/5/8 phosphorylation might be further complemented by reduced physical inhibition by CTGF.

DISCUSSION

In this study, we revealed an age-related differential response to persistent renal injury. We show that age-associated changes in the fibrotic response to kidney injury occur already

before the appearance of typical senescence markers like SA-β-Gal activity, Klotho loss, and spontaneous glomerulosclerosis. In particular, increased morphological damage and a reduced fibrotic response were observed in 1-yr-old mice without alteration of canonical TGF-β transcriptional activity. Instead, a decrease in CTGF and increase of BMP6 expression was found, associated with increased downstream pSMAD1/5/8 activity in cortical tubules, which might at least in part explain the observed reduced fibrogenesis to kidney injury in aging.

In human diagnostics and experimental animal research, interstitial fibrosis and tubular atrophy (IFTA) are often assessed together and thought to "go hand in hand" (21). We show that following injury in the aged kidney, the proportion of fibrosis and atrophy can be shifted in favor of atrophy, suggesting ramifications for clinical assessment of IFTA in the aging kidney. Previously, it has been shown that renal damage in response to ischemia-reperfusion injury, in terms of GFR loss, morphological injury, and fibrosis, is increased in aging (9, 46). Inverse correlations have been reported previously (38). Age-related acceleration of progressive kidney senescence and CKD development, after the initial acute injury has subsided, is becoming a widely recognized phenomenon, and considered to be due to a decrease in reparative capacity (20). It remains to be established whether, in addition to decreased regenerative capacity, the observed "weaker" but possibly more persistent fibrotic renal response to injury might also be involved in more progressive loss of function upon transient injury in old kidneys.

The kidney is a major contributor to Klotho production, and Klotho loss is strongly associated with aging and the renal response to damage (6, 16, 30, 31, 33). Klotho is an important inhibitor of TGF-β, one of the most important mediators of fibrotic renal response to damage and aging (34, 43). However, we found that at the age of 50 wk Klotho and Tgfβ expression were not yet affected by aging but diminished and increased, respectively, to a similar extent in young OBKs. Thus the observed differential renal damage response occurred before the well-established changes in baseline Klotho and TGF-β expression at a more advanced age.

Interestingly, expression of the well-established antifibrotic and proregenerative BMP7 gene was also not different in old compared with young OBKs, but the older OBKs had an increased BMP6/CTGF ratio, resulting from retained BMP6 expression and suppressed CTGF expression. The finding that preserved Bmp6 expression in old OBKs was associated with less fibrosis is congruent with our previous observation that loss of BMP6, together with the ensuing overexpression of CTGF, aggravated renal fibrosis and myofibroblast (α-SMA) accumulation (14). The study by Dendooven et al. (14) also showed that the level of tubular dilatation was unaltered, suggesting BMP6 to be unrelated to dilatation. We propose that direct BMP6 effects might mainly attenuate fibrosis, while the other morphological differences observed might be secondary to this.

In our experiment, the increased BMP6 expression might at least partially account for the 50% reduction of CTGF in old OBKs. Figure 5 shows that CTGF directly interacts with BMP6 and as such inhibits canonical signaling. Since old OBKs show less CTGF but more

BMP6 expression, this increased BMP6/CTGF ratio might underlie the found pSMAD158 increase in cortical tubules, especially since we have an indication that the inhibitory effects of CTGF on pSMAD158 might be due to direct physical interaction with BMP6.

In the cortex, mainly distal tubules and collecting ducts display canonical BMP signaling, and it has been noted previously that upon UUO, signaling decreases (32). The phenomenon of epithelial-to-mesenchymal transition (EMT) is a large contributor to the development of renal fibrosis (49). Possibly, the increase in tubular pSMAD1/5/8 seen in Fig. 4 reflects a reduced EMT rate underlying the reduction in fibrosis.

Previously, we reported that a 50% reduction of CTGF as such is not sufficient to hamper the phenotype observed in 14-day UUO and other severe models of CKD (18). In conjunction with the present observations, this might suggest that, at least in the UUO model, BMP6/CTGF balance is more important for fibrosis control than the absolute CTGF level.

One might speculate that, in conjunction with less pronounced fibrosis, an increase in morphological damage in terms of atrophy and dilatation in old OBKs might result from less fibrogenic growth factor activity, with the resulting reduction of matrix deposition hampering generation of sufficient structural support to withstand increased pressure developing upon obstruction. As previously mentioned, there are many factors playing a role in the process of renal aging. However, the production of profibrotic cytokines is a common end point (e.g., TGF-β). Since there is no differential regulation of TGF-β or downstream PAI-1 expression, the observed effects might have different drivers than the usual suspects of aging.

In conclusion, our studies have revealed an age-dependent shift in renal response to injury, developing a more atrophic and less fibrotic phenotype. This change is associated with altered BMP6/CTGF balance and already occurs before mice have lived through half of their life span and before the appearance of classic signs of senescence, namely, spontaneous loss of Klotho and an increase in TGF-β expression and SA-β-Gal. Figure 6 depicts a proposed mechanism distilled from the observations presented in this manuscript. While most experimental studies addressing CKD have been performed in young rodents, these might not appropriately reflect renal response to injury in aging patients. This should be taken into account in interpreting existing and designing future studies addressing CKD progression in the aging population.

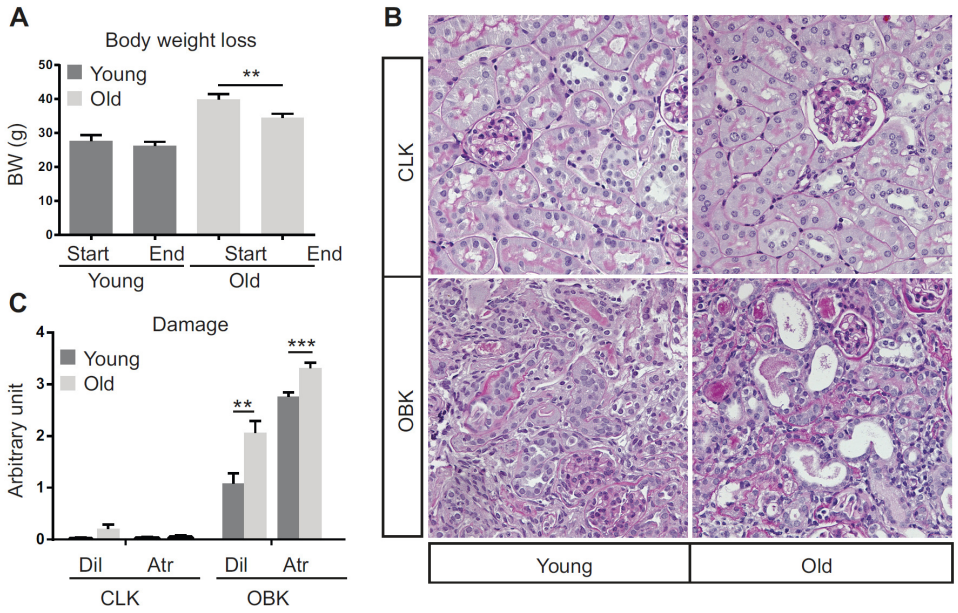

Fig. 1. Unilateral ureter obstruction (UUO) causes more morphological damage in old kidneys. A: total body weight (BW) before UUO (Start) and after death (End). B: representative micrographs of periodic acid-Schiff (PAS)-stained slides of contralateral kidney (CLK) and obstructed kidney (OBK) in both age groups (×200). C: quantification of microscopically observed atrophy (Atr) and dilatation (Dil) observed. Error bars represent SE. Statistics used: 2-way ANOVA with Sidak correction for multiple comparison (A); nonpaired 2-way ANOVA with Tukey correction (C and E). **P < 0.01. ***P < 0.005.

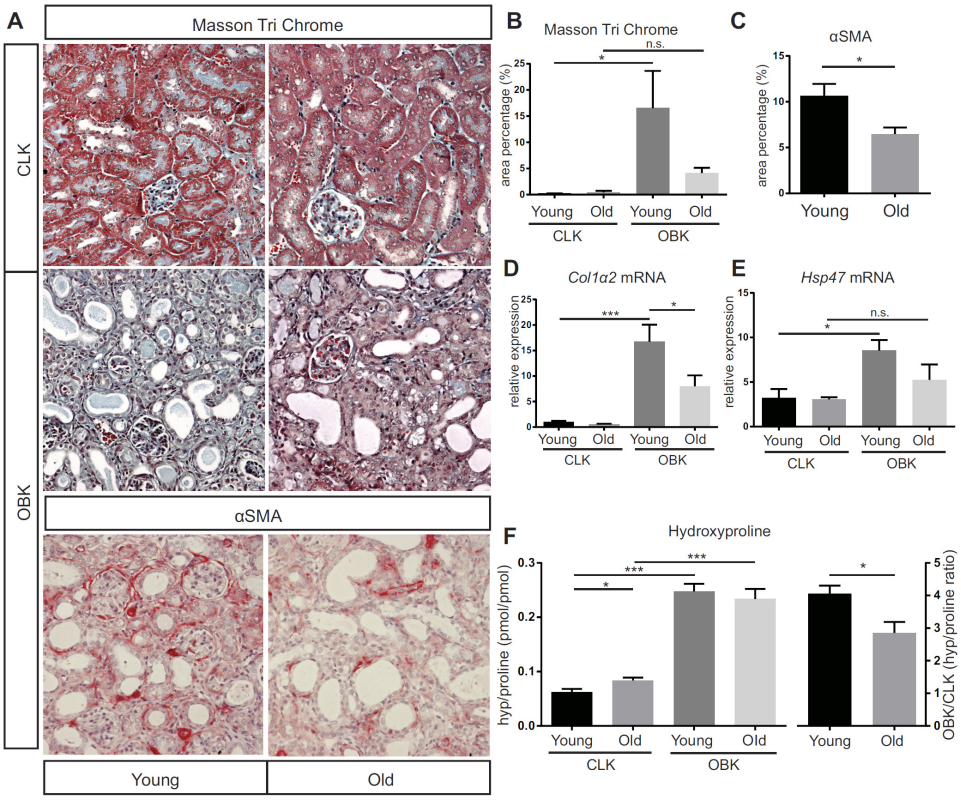

Fig. 2. Old kidneys show less ECM deposition upon UUO. A: representative micrographs of Masson trichrome (MTC)- and α-smooth muscle actin (SMA)-stained kidneys of both age groups (×200). B: morphometric quantification of fibrosis as seen with MTC staining; C: morphometric quantification of myofibroblasts as seen with α-SMA staining. D: Col1α2 expression levels in CLK and OBK. E: Hsp47 expression levels in CLK and in OBKs. F: hydroxyproline/proline ratio. Error bars represent SE. Statistics used: nonpaired two-way ANOVA with Tukey correction (B–D).*$P < 0.05$. ***$P < 0.005$.

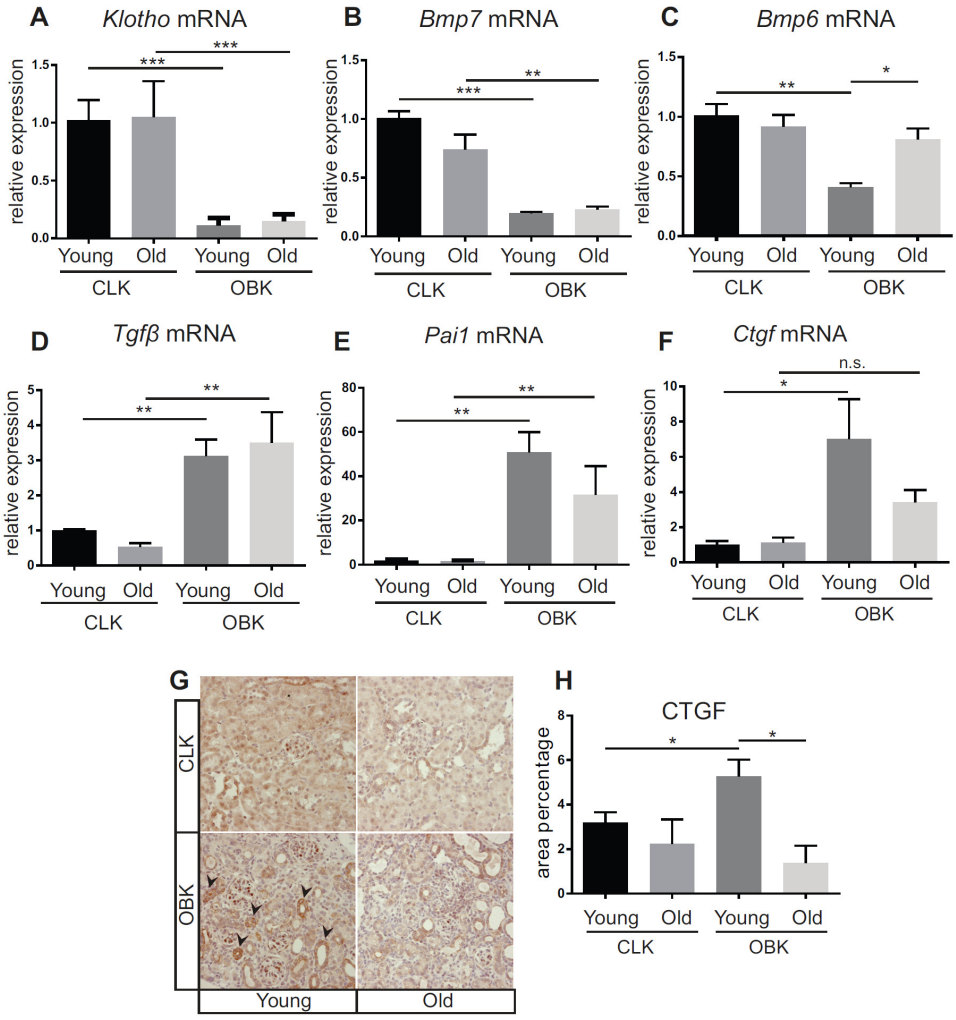

Fig. 3. CTGF/bone morphometric protein (BMP) 6 ratio is altered before differential Klotho or transforming growth factor (TGF)-β regulation in old OBKs. A: Klotho expression levels in CLK and OBK of both age groups. B: Bmp7 expression levels in CLKs and OBKs. C: Bmp6 expression levels in CLKs and OBKs. D: TGF-β expression levels in CLKs and OBKs. E: Pai1 expression levels in CLKs and OBKs. F: Ctgf expression levels in CLKs and OBKs. G: representative micrographs of CTGF-stained slides of CLKs and OBKs (×200). H: morphometric quantification of CTGF-positive staining area. Arrowheads indicate positive tubular staining. Error bars represent SE. Statistics used: nonpaired 2-way ANOVA with Tukey correction (A–F and H). *P < 0.05. **P < 0.01. ***P < 0.005.

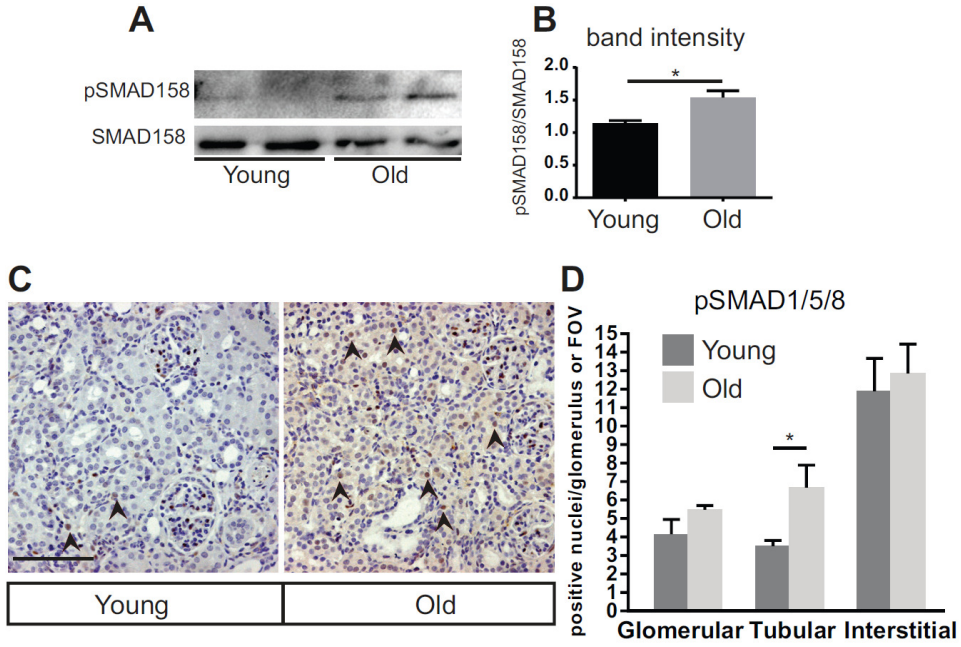

Fig. 4. Tubular pSMAD1/5/8 signaling is preserved in old OBKs. A: Western blot of OBK cortical lysates showing pSMAD1/5/8 and SMAD1/5/8 level band intensity. B: pSMAD1/5/8 band intensity quantification corrected for total SMAD1/5/8 levels. C: representative micrographs of pSMAD1/5/8 OBKs (×200). Arrowheads indicate pSMAD1/5/8-positive tubular cells. D: quantification of the number of cortical pSMAD1/5/8-positive nuclei in glomerular, tubular, and interstitial cells. Error bars represent SE. *$P < 0.05$.

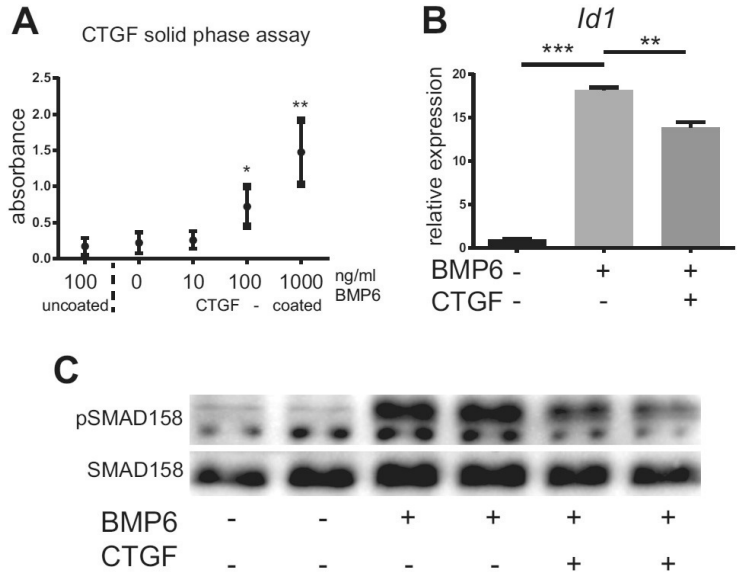

Fig. 5. CTGF binds BMP6 and inhibits canonical BMP signaling. A: absorbance levels of CTGF/BMP6 solid-phase assay. B: Western blot of HK-2 cell lysate 1 h after stimulation with rhBMP6 and/or rhCTGF. Top: pSMAD1/5/8. Bottom: SMAD1/5/8. C: Id1 expression levels of HK-2 cells stimulated with rhBMP6 and/or rhCTGF. Error bars represent SE. Statistics used: nonpaired 2-way ANOVA with Tukey correction. *P < 0.05, **P < 0.01, ***P < 0.005.

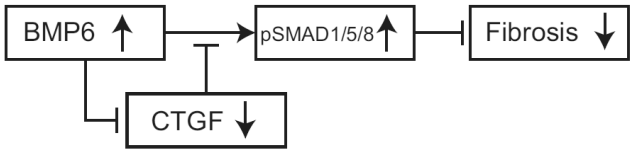

Fig. 6. Proposed model for age-associated change in the response to renal injury. In the aged kidneys, there is an increased expression of BMP6 that in itself is capable of reducing CTGF expression. Both the increase in BMP6 and the reduction of CTGF lead to increased levels of pSMAD1/5/8 (partially due to loss of physical binding to and inhibition of BMP6 by CTGF). The increase in pSMAD1/5/8 leads to reduced fibrosis, possibly via inhibition of epithelialto-mesenchymal transition.

REFERENCES

1. Abrass CK, Adcox MJ, Raugi GJ. Aging-associated changes in renal extracellular matrix. Am J Pathol 146: 742–752, 1995.
2. Abreu JG, Ketpura NI, Reversade B, De Robertis EM. Connectivetissue growth factor (CTGF) modulates cell signalling by BMP and TGF-beta. Nat Cell Biol 4: 599–604, 2002.
3. Abula K, Muneta T, Miyatake K, Yamada J, Matsukura Y, Inoue M, Sekiya I, Graf D, Economides AN, Rosen V, Tsuji K. Elimination of BMP7 from the developing limb mesenchyme leads to articular cartilage degeneration and synovial inflammation with increased age. FEBS Lett 589: 1240–1248, 2015.
4. Arking DE, Krebsova A, Macek M Sr., Macek M Jr, Arking A, Mian IS, Fried L, Hamosh A, Dey S, McIntosh I, Dietz HC. Association of human aging with a functional variant of klotho. Proc Natl Acad Sci USA 99: 856–861, 2002.
5. Bolignano D, Mattace-Raso F, Sijbrands EJ, Zoccali C. The aging kidney revisited: a systematic review. Ageing Res Rev 14C: 65–80, 2014.
6. Buendia P, Carracedo J, Soriano S, Madueno JA, Ortiz A, Martin-Malo A, Aljama P, Ramirez R. Klotho prevents nfkappab translocation and protects endothelial cell from senescence induced by uremia. J Gerontol A Biol Sci Med Sci 70: 1198–1209, 2015.
7. Chevalier RL, Forbes MS, Thornhill BA. Ureteral obstruction as a model of renal interstitial fibrosis and obstructive nephropathy. Kidney Int 75: 1145–1152, 2009.
8. Choudhury D, Levi M. Kidney aging—inevitable or preventable? Nat Rev Nephrol 7: 706–717, 2011.
9. Clements ME, Chaber CJ, Ledbetter SR, Zuk A. Increased cellular senescence and vascular rarefaction exacerbate the progression of kidney fibrosis in aged mice following transient ischemic injury. PLoS One 8:e70464, 2013.
10. Conidi A, Cazzola S, Beets K, Coddens K, Collart C, Cornelis F, Cox L, Joke D, Dobreva MP, Dries R, Esguerra C, Francis A, Ibrahimi A, Kroes R, Lesage F, Maas E, Moya I, Pereira PN, Stappers E, Stryjewska A, van den Berghe V, Vermeire L, Verstappen G, Seuntjens E, Umans L, Zwijsen A, Huylebroeck D. Few Smad proteins and many Smad-interacting proteins yield multiple functions and action modes in TGFbeta/BMP signaling in vivo. Cytokine Growth Factor Rev 22: 287–300, 2011.
11. Coresh J, Astor BC, Greene T, Eknoyan G, Levey AS. Prevalence of chronic kidney disease and decreased kidney function in the adult US population: Third National Health and Nutrition Examination Survey. Am J Kidney Dis 41: 1–12, 2003.
12. Crews L, Adame A, Patrick C, Delaney A, Pham E, Rockenstein E, Hansen L, Masliah E. Increased BMP6 levels in the brains of Alzheimer's disease patients and APP transgenic mice are accompanied by impaired neurogenesis. J Neurosci 30: 12252–12262, 2010.
13. Debacq-Chainiaux F, Erusalimsky JD, Campisi J, Toussaint O. Protocols to detect senescence-associated beta-galactosidase (SA-betagal) activity, a biomarker of senescent cells in culture and in vivo. Nat Protoc 4: 1798–1806, 2009.

14. Dendooven A, van Oostrom O, van der Giezen DM, Leeuwis JW, Snijckers C, Joles JA, Robertson EJ, Verhaar MC, Nguyen TQ, Goldschmeding R. Loss of endogenous bone morphogenetic protein-6 aggravates renal fibrosis. Am J Pathol 178: 1069–1079, 2011.
15. Doi S, Zou Y, Togao O, Pastor JV, John GB, Wang L, Shiizaki K, Gotschall R, Schiavi S, Yorioka N, Takahashi M, Boothman DA, Kuro-o M. Klotho inhibits transforming growth factor-beta1 (TGF-beta1) signaling and suppresses renal fibrosis and cancer metastasis in mice. J Biol Chem 286: 8655–8665, 2011.
16. Duce JA, Podvin S, Hollander W, Kipling D, Rosene DL, Abraham CR. Gene profile analysis implicates Klotho as an important contributor to aging changes in brain white matter of the rhesus monkey. Glia 56:106–117, 2008.
17. Epstein M. Aging and the kidney. J Am Soc Nephrol 7: 1106–1122, 1996.
18. Falke LL, Dendooven A, Leeuwis JW, Nguyen TQ, van Geest RJ, van der Giezen DM, Broekhuizen R, Lyons K, Stoop R, Kemperman H, Schlingemann R, Joles JA, Goldschmeding R. Hemizygous deletion of CTGF/CCN2 does not suffice to prevent fibrosis of the severely injured kidney. Matrix Biol 31: 421–431, 2012.
19. Falke LL, Goldschmeding R, Nguyen TQ. A perspective on anti-CCN2 therapy for chronic kidney disease. Nephrol Dial Transplant 29, Suppl 1:i30 –i37, 2014.
20. Ferenbach DA, Bonventre JV. Mechanisms of maladaptive repair after AKI leading to accelerated kidney ageing and CKD. Nat Rev Nephrol 11: 264–276, 2015.
21. Forbes MS, Thornhill BA, Minor JJ, Gordon KA, Galarreta CI, Chevalier RL. Fight-or-flight: murine unilateral ureteral obstruction causes extensive proximal tubular degeneration, collecting duct dilatation, and minimal fibrosis. Am J Physiol Renal Physiol 303: F120–F129, 2012.
22. Frenkel-Denkberg G, Gershon D, Levy AP. The function of hypoxiainducible factor 1 (HIF-1) is impaired in senescent mice. FEBS Lett 462: 341–344, 1999.
23. Gomez D, Kessler K, Michel JB, Vranckx R. Modifications of chromatin dynamics control Smad2 pathway activation in aneurysmal smooth muscle cells. Circ Res 113: 881–890, 2013.
24. He W, Tan R, Dai C, Li Y, Wang D, Hao S, Kahn M, Liu Y. Plasminogen activator inhibitor-1 is a transcriptional target of the canonical pathway of Wnt/beta-catenin signaling. J Biol Chem 285: 24665–24675, 2010.
25. Hewitson TD. Renal tubulointerstitial fibrosis: common but never simple. Am J Physiol Renal Physiol 296: F1239–F1244, 2009.
26. Inazaki K, Kanamaru Y, Kojima Y, Sueyoshi N, Okumura K, Kaneko K, Yamashiro Y, Ogawa H, Nakao A. Smad3 deficiency attenuates renal fibrosis, inflammation, and apoptosis after unilateral ureteral obstruction. Kidney Int 66: 597–604, 2004.
27. Itoh S, Hattori T, Tomita N, Aoyama E, Yutani Y, Yamashiro T, Takigawa M. CCN family member 2/connective tissue growth factor (CCN2/CTGF) has anti-aging effects that protect articular cartilage from age-related degenerative changes. PLoS One 8: e71156, 2013.

28. Kim JH, Hwang KH, Park KS, Kong ID, Cha SK. Biological role of anti-aging protein Klotho. J Lifestyle Med 5: 1–6, 2015.
29. Klahr S. Urinary tract obstruction. Semin Nephrol 21: 133–145, 2001.
30. Koh N, Fujimori T, Nishiguchi S, Tamori A, Shiomi S, Nakatani T, Sugimura K, Kishimoto T, Kinoshita S, Kuroki T, Nabeshima Y. Severely reduced production of klotho in human chronic renal failure kidney. Biochem Biophys Res Commun 280: 1015–1020, 2001.
31. Kuro-o M, Matsumura Y, Aizawa H, Kawaguchi H, Suga T, Utsugi T, Ohyama Y, Kurabayashi M, Kaname T, Kume E, Iwasaki H, Iida A, Shiraki-Iida T, Nishikawa S, Nagai R, Nabeshima YI. Mutation of the mouse klotho gene leads to a syndrome resembling ageing. Nature 390: 45–51, 1997.
32. Leeuwis JW, Nguyen TQ, Chuva de Sousa Lopes SM, van der Giezen DM, van der Ven K, Rouw PJ, Offerhaus GJ, Mummery CL, Goldschmeding R. Direct visualization of Smad1/5/8-mediated transcriptional activity identifies podocytes and collecting ducts as major targets of BMP signalling in healthy and diseased kidneys. J Pathol 224: 121–132, 2011.
33. Lindberg K, Amin R, Moe OW, Hu MC, Erben RG, Ostman Wernerson A, Lanske B, Olauson H, Larsson TE. The kidney is the principal organ mediating klotho effects. J Am Soc Nephrol 25: 2169–2175, 2014.
34. Meng XM, Chung AC, Lan HY. Role of the TGF-beta/BMP-7/Smad pathways in renal diseases. Clin Sci (Lond) 124: 243–254, 2013.
35. Nguyen TQ, Roestenberg P, van Nieuwenhoven FA, Bovenschen N, Li Z, Xu L, Oliver N, Aten J, Joles JA, Vial C, Brandan E, Lyons KM, Goldschmeding R. CTGF inhibits BMP-7 signaling in diabetic nephropathy. J Am Soc Nephrol 19: 2098–2107, 2008.
36. Oh SP, Seki T, Goss KA, Imamura T, Yi Y, Donahoe PK, Li L, Miyazono K, ten Dijke P, Kim S, Li E. Activin receptor-like kinase 1 modulates transforming growth factor-beta 1 signaling in the regulation of angiogenesis. Proc Natl Acad Sci USA 97: 2626–2631, 2000.
37. Prakash S, O'Hare AM. Interaction of aging and chronic kidney disease. Semin Nephrol 29: 497–503, 2009.
38. Pulskens WP, Rampanelli E, Teske GJ, Butter LM, Claessen N, Luirink IK, van der Poll T, Florquin S, Leemans JC. TLR4 promotes fibrosis but attenuates tubular damage in progressive renal injury. J Am Soc Nephrol 21: 1299–1308, 2010.
39. Quan T, Shao Y, He T, Voorhees JJ, Fisher GJ. Reduced expression of connective tissue growth factor (CTGF/CCN2) mediates collagen loss in chronologically aged human skin. J Invest Dermatol 130: 415–424, 2010.
40. Reed AL, Tanaka A, Sorescu D, Liu H, Jeong EM, Sturdy M, Walp ER, Dudley SC Jr, Sutliff RL. Diastolic dysfunction is associated with cardiac fibrosis in the senescence-accelerated mouse. Am J Physiol Heart Circ Physiol 301: H824–H831, 2011.

41. Richter K, Kietzmann T. Reactive oxygen species and fibrosis: further evidence of a significant liaison. Cell Tissue Res 365: 591–605, 2016.
42. Rosner M, Abdel-Rahman E, Williams ME. Geriatric nephrology: responding to a growing challenge. Clin J Am Soc Nephrol 5: 936–942, 2010.
43. Ruiz-Torres MP, Bosch RJ, O'Valle F, Del Moral RG, Ramirez C, Masseroli M, Perez-Caballero C, Iglesias MC, Rodriguez-Puyol M, Rodriguez-Puyol D. Age-related increase in expression of TGF-beta1 in the rat kidney: relationship to morphologic changes. J Am Soc Nephrol 9: 782–791, 1998.
44. Samarakoon R, Overstreet JM, Higgins SP, Higgins PJ. TGF-beta1 → SMAD/p53/USF2 → PAI-1 transcriptional axis in ureteral obstructioninduced renal fibrosis. Cell Tissue Res 347: 117–128, 2012.
45. Schmitt R, Cantley LG. The impact of aging on kidney repair. Am J Physiol Renal Physiol 294: F1265–F1272, 2008.
46. Shimizu MH, Araujo M, Borges SM, de Tolosa EM, Seguro AC. Influence of age and vitamin E on post-ischemic acute renal failure. Exp Gerontol 39: 825–830, 2004.
47. Tanaka T, Kato H, Kojima I, Ohse T, Son D, Tawakami T, Yatagawa T, Inagi R, Fujita T, Nangaku M. Hypoxia and expression of hypoxiainducible factor in the aging kidney. J Gerontol A Biol Sci Med Sci 61: 795–805, 2006.
48. van Almen GC, Verhesen W, van Leeuwen RE, van de Vrie M, Eurlings C, Schellings MW, Swinnen M, Cleutjens JP, van Zandvoort MA, Heymans S, Schroen B. MicroRNA-18 and microRNA-19 regulate CTGF and TSP-1 expression in age-related heart failure. Aging Cell 10: 769–779, 2011.
49. Zeisberg M, Kalluri R. The role of epithelial-to-mesenchymal transition in renal fibrosis. J Mol Med (Berl) 82: 175–181, 2004.
50. Zhou L, Li Y, Zhou D, Tan RJ, Liu Y. Loss of Klotho contributes to kidney injury by derepression of Wnt/beta-catenin signaling. J Am Soc Nephrol 24: 771–785, 2013.
51. Zhou XJ, Rakheja D, Yu X, Saxena R, Vaziri ND, Silva FG. The aging kidney. Kidney Int 74: 710–720, 2008.

9

Tubulointerstitial expression and urinary secretion of connective tissue growth factor 3 months after renal transplantation predict interstitial fibrosis and tubular atrophy at 5 years

Submitted

Thomas Vanhove[1], Hiroshi Kinashi[2,3], Tri Q. Nguyen[2], Christoph Metalidis[1], Koen Poesen[4], Evelyne Lerut[5], Roel Goldschmeding[2], and Dirk R.J. Kuypers[1]

[1]Department of Microbiology and Immunology, KU Leuven - University of Leuven, and Department of Nephrology, University Hospitals Leuven, Leuven, Belgium
[2]Department of Pathology, University Medical Center Utrecht, Utrecht, the Netherlands
[3]Department of Nephrology, Nagoya University Hospital, Nagoya, Japan
[4]Clinical Department of Laboratory Medicine, University Hospitals Leuven, Belgium
[5]Department of Imaging and Pathology, KU Leuven - University of Leuven, and Department of Pathology, University Hospitals Leuven, Leuven, Belgium

ABSTRACT

Background. Connective tissue growth factor (CTGF) is an important mediator of renal allograft fibrosis and urinary CTGF (CTGFu) levels correlate with the development of human allograft interstitial fibrosis.

Methods. We evaluated the added predictive value of CTGF protein expression in 160 kidney transplant recipients with paired protocol biopsies at 3 months, 1 year and 5 years after transplantation. At month 3 and year 1, CTGFu was measured using a sandwich ELISA and biopsies were immunohistochemically stained for CTGF, with semiquantitative scoring of tubulointerstitial CTGF positive surface area (CTGFti).

Results. Independent predictors of the sum of interstitial fibrosis and tubular atrophy scores (IF/TA) at 5 years were donor age (OR 1.04 [1.02-1.07], p=0.001) and CTGFti > 10% at month 3 (OR 3.03 [1.47-6.23], p=0.003). In various subgroups of patients with little histologic damage at 3 months [either ci score 0 (n=119), IF/TA score ≤ 1 (n=123), or absence of interstitial fibrosis, tubular atrophy, interstitial inflammation and tubulitis (n=45)], consistent predictors of progression of chronic histologic damage by 5 years were donor age, CTGFti > 10% and CTGFu.

Conclusions. These results suggest that, even in patients with favorable histology at 3 months, fibrogenic processes might often be active early after transplantation, which result in accelerated accumulation of histologic damage.

Abbreviations

A1M	α1-microglobulin
AUC	area under the curve
BPAR	biopsy-proven acute rejection
CI	confidence interval
CTGF	connective tissue growth factor
CTGFti	tubulointerstitial CTGF positive surface area
CTGFu	urine CTGF concentration
DCD	deceased of cardiac death
DGF	delayed graft function
ECD	extended criteria donor
eGFR	estimated glomerular filtration rate
IF/TA	interstitial fibrosis and tubular atrophy
NPV	negative predictive value
PPV	positive predictive value
PRA	panel reactive antibody
PTDM	posttransplant diabetes mellitus
PVAN	polyomavirus-associated nephropathy
ROC	receiver operating characteristic
SCD	standard criteria donor

INTRODUCTION

Connective tissue growth factor (CTGF; CCN2) is a growth factor that plays a critical role in fibrogenesis in a variety of tissues. In kidney disease, CTGF expression by renal tubular epithelial cells is a key mediator of TGF-β1-dependent interstitial fibrogenesis in vitro[1] and in renal allografted mice.[2] CTGF mRNA is overexpressed by interstitial fibroblasts, epithelial and mesangial cells in proliferative glomerulopathies and tubulointerstitial fibrotic areas in chronic transplant rejection.[3] We have previously demonstrated that CTGFu is higher in the presence of interstitial fibrosis on human renal allograft biopsies.[4] In that study, high levels of CTGFu in renal recipients without fibrosis (ci score = 0) at 3 months after transplantation were also independently predictive of development of moderate to severe fibrosis (ci score ≥ 2) by 2 years.

CTGF has also come under interest as a potential therapeutic target. A CTGF antisense oligodeoxynucleotide attenuated the upregulation of CTGF, fibronectin and α1-collagen genes and decreased the number of renal myofibroblasts in rats with unilateral ureter obstruction.[5] In Lewis-Fischer transplanted rats, injection of small inhibitory RNA against CTGF was associated with a lower incidence of chronic allograft nephropathy and lower serum creatinine after 8 weeks.[6] Finally, in a phase I study in 24 diabetic patients with micro-albuminuria, administration of the monoclonal anti-CTGF antibody FG-3019 resulted in a reduction of the urinary albumin-creatinine ratio from 48 to 20 mg/g.[7]

There is relatively little data regarding the expression of CTGF in human renal allografts. In a microarray analysis of consecutive renal protocol biopsies, development of early interstitial fibrosis and tubular atrophy (IF/TA) was predicted by upregulation of 30 unique genes, one of which was CTGF.[8] Another study, however, reported that CTGF mRNA expression in 3-month protocol biopsies in 101 renal recipients did not predict chronic allograft damage index (CADI) at 12 months,[9] but longer histologic follow-up was not available. The goals of the current study were to evaluate whether early tubulointerstitial CTGF expression predicts progression of interstitial fibrosis and tubular atrophy (IF/TA) as well as functional deterioration over the first 5 years after transplantation.

MATERIALS AND METHODS

Study design

This was a single center, observational retrospective cohort study. Adult tacrolimus-treated patients who had received a single kidney allograft between March 2004 and May 2009 were included if repeat protocol biopsies at 3 months and 5 years were available. Blood samples for routine biochemistry and morning midstream urine sample were collected on the day of the biopsy. This study was performed in accordance with the Declaration of Helsinki and was approved by the ethics committee of the University Hospitals Leuven (S53364; ML7499). All patients provided written informed consent.

Histology and renal function

Biopsies were obtained under real-time ultrasound guidance using a Biopty-Cut® gun with a 16-gauge needle. The tissue cylinder was fixed in buffered formalin and embedded in paraffin. Slides containing 4 to 10 paraffin sections (2-3 µm) were routinely stained with hematoxylin-eosin, periodic acid-Schiff and silver methenamine (Jones) for light microscopic examination. The severity of histologic lesions was semiquantitatively scored according to the revised Banff 1997 criteria.[21] For the purpose of this analysis, the sum of ci and ct scores is referred to as IF/TA score; fibrosis with inflammation is defined as ci score > 0 and i score > 0. All episodes of biopsy-proven acute rejection (BPAR) and subclinical BPAR were treated with high-dose steroids and/or anti-thymocyte globulin. Borderline rejection was not treated. Estimated glomerular filtration rate (eGFR) was calculated using the Modification of Diet in Renal Disease (MDRD) formula.[22] Delayed graft function (DGF) was defined as the need for dialysis in the first 7 days after transplantation. Posttransplant diabetes mellitus (PTDM) was defined as need for treatment with oral antidiabetic drugs and/or insulin after transplantation.

Quantification of CTGF and α1-microglobulin

Plasma and urines samples were stored at -80°C within 4 hours after collection. CTGFu and plasma CTGF (CTGFp) concentrations were determined with a proprietary sandwich enzyme-linked immunosorbent assay (FibroGen, San Francisco, CA, USA) using two monoclonal antibodies against distinct epitopes on the N-terminal part of human CTGF, detecting full-length CTGF as well as the N-fragment, as previously described.[23] Urinary CTGF was normalized to urinary creatinine and is expressed as pmol/g creatinine. Fractional excretion of CTGF (FeCTGF) was calculated as [(CTGFu x plasma creatinine)/(urinary creatinine x CTGFp]. Urinary α1-microglobulin (A1M) concentration was determined using nephelometry. A1M was selected as a marker for tubular proteinuria because urine had not been alkalinized, precluding reliable measurement of β2-microglobulin (B2M).

CTGF immunohistochemistry and analysis

Renal biopsies processed for light microscopy were stained for CTGF in a single batch, as previously described.[24] Tubulointerstitial CTGF positive surface area (CTGFti) in the entire cortical area was assessed by a single researcher (HK) blinded to clinical information and semiquantitavely categorized as absent (<1%), minimal (1-10%), moderate (11-25%) or extensive (>25%).

Statistical analysis

Data are reported as mean ± SD, unless stated otherwise. Normality was tested using the Shapiro-Wilk test. Urinary and plasma CTGF and A1M were not normally distributed and 10-log transformed for analyses. Proteinuria was categorized as < 0.3 g/g, 0.3-1 g/g and > 1 g/g creatinine for analysis. Undetectable concentrations of A1M were set at half the lowest observed concentration prior to log transformation. Difference in continuous variables

between both time points were assessed using paired-samples t-test, differences in categorical variables using Mcnemar's test, differences in histologic score distribution using the Friedman test and correlations using chi square test (Pearson's r). Differences in a continuous variable between categories of a categorical variable were assessed using ANOVA. Ordinal multivariable regression models were constructed using the SPSS GENLIN procedure to assess which variables predicted ci and ct score at 5 years. All clinical and histologic variables presented in tables 1 and 2 were considered as potential predictors of histologic and renal functional outcome. Of these, only variables that were significant at $p < 0.2$ in univariate analysis were considered for the final model. Ci and ct score at 3 months were always included as predictors in the respective models, regardless of significance. Similarly, the outcomes of IF/TA score ≥ 2 and chronicity score ≥ 3 at 5 years were assessed using binary logistic regression with backward conditional inclusion of predictors. When, in case of (quasi-)complete separation of data for a particular predictor variable, estimates could not be calculated, Firth's penalized maximum likelihood estimation was used, utilizing the Firth binary logistic regression extension via the SPSS R-plugin (R logistf package).[25] Resulting odds ratio confidence intervals for these variables were still typically very wide; the exact value of the odds ratios should not be overinterpreted. Intercepts were included in all models but are not reported. A two-sided p-value < 0.05 was considered statistically significant. All analyses were performed using IBM SPSS Statistics version 22 (IBM, NY, USA). Figures were generated using Graphpad Prism version 6 (San Diego, CA, USA).

RESULTS

Demographics and evolution of histology

Repeat protocol biopsies were available for 171 patients. Eleven patients were excluded because insufficient renal tissue was available for CTGF staining. Demographics of the final 160 patients are presented in Table 1. Evolution of renal function, proteinuria and selected histologic parameters are presented in Table 2. Evolution of all individual Banff scores is presented in Supplementary Table S1, available online.

CTGF staining and CTGFu

In the tubulointerstitial compartment, CTGF staining was mainly positive in the cytoplasm of proximal (and, to a lesser degree, distal) tubular epithelial cells (Figure 1). Staining was less pronounced at the tubular brush border and in interstitial cells. Table 2 shows CTGFti, urinary and plasma CTGF and FeCTGF at 3 and 12 months as well as A1M values at 3 months. As CTGF is known to be upregulated in the context of inflammatory renal pathology[3], we first examined the cross-sectional relationship between CTGF staining and morphological evidence of inflammation at 3 months. CTGFti > 10% was present in 21 out of the 24 patients with i score > 0 ($p=0.182$) and in 18 out of 21 patients with borderline or subclinical acute rejection at month 3 ($p=0.049$). Additionally, CTGFti > 10% was present in 88% of extended criteria donor (ECD) kidneys, versus 64% of kidneys from living

donors, 62% of standard criteria donors (SCD) and 59% of deceased of cardiac death (DCD) kidneys (p=0.011 for ECD vs. other groups). In multivariable logistic regression, independent predictors of moderate to extensive CTGF staining were ECD kidney and i score > 0 ($p<0.05$ for both).

In cross-sectional analysis at 3 months, CTGFu correlated with proteinuria (r=0.375, $p<0.001$) and CTGFp (r=0.196, p=0.013), but not with A1M, eGFR, FeCTGF or CTGFti. In multivariable analysis, independent predictors of CTGFu were proteinuria and CTGFp (B = 3.320 [1.825-4.816], R^2 0.136, $p<0.0001$ and B = 0.484 [0.131-0.837], R^2 0.034, p=0.007, respectively), together explaining 17% of variability in CTGFu. There was a significant interaction between proteinuria and CTGFp the predictive model for CTGFu (B = 1.631 [0.901-2.361], R^2 for full model including interaction term 0.228, $p<0.0001$), indicating that the increase in CTGFu observed with increasing proteinuria became more strongly pronounced when CTGFp was high.

CTGF staining did not correlate with plasma CTGF (CTGFp) (p=0.776) or FeCTGF (p=0.290). CTGFp is not further discussed, as it was not predictive of any outcome parameter (data not shown). At the 12 month time point, CTGFu correlated weakly with CTGFp (r=0.178, p=0.032) and eGFR (r=-0.211, p=0.011), but not with proteinuria, CTGFti or FeCTGF.

Prediction of fibrosis at 5 years

First, predictive models were constructed using only predictor variables available at 3 months. Uni- and multivariable predictors of IF/TA at 5 years are presented in Table 3. Independent predictors of IF/TA were donor age and CTGFti > 10%; CTGFu was not (p=0.066). Donor age and CTGFti > 10% were also independent predictors of the individual ci and ct scores (Supplementary Tables S2-3). The relative value of CTGFti and CTGFu when added to donor age to predict development of fibrosis and/or tubular atrophy was evaluated in several subgroups of patients with favorable histologic features at 3 months, namely either no fibrosis (ci score 0), very low IF/TA score (≤ 1) or absence of any fibrosis, tubular atrophy, tubulitis or interstitial inflammation, as shown in Table 4 and Supplementary Tables S4-6. Donor age, CTGFti > 10% and CTGFu were independently predictive of progression of fibrosis or IF/TA score in all 3 of these subgroups. Figure 2 illustrates the fact that in patients with IF/TA score ≤ 1 at 3 months, progression of IF/TA by 5 years was more pronounced in those who had 3-month CTGF > 10%. The final model for development of de novo fibrosis had a positive predictive value (PPV) of 89.3% and negative predictive value (NPV) of 53.5%, with receiver operating characteristic (ROC) curve area under the curve (AUC) of 0.76. When only donor age was included in this model, PPV was 84.0%, NPV 46.5% and ROC AUC 0.70. Model performance of other combinations of predictor variables for these 3 subgroups are reported in Supplementary Tables S7-9. ROC curves for development of de novo fibrosis and IF/TA progression are shown in Figure 3.

All of the above analyses were repeated using 1-year histologic lesions, clinical variables and CTGFti and CTGFu values (available for 146 patients) as predictors of histology at 5 years. Independent predictors of ci, ct and IF/TA ≥ 2 are presented in Supplementary Tables S10-15. At his time point, CTGFti and CTGFu were not predictive of 5-year histology. This remained true if the cut-off for 'positive' CTGF staining was raised from 11% to 25% (data not shown).

Renal function and graft loss

Average renal function remained stable over the 5-year follow-up period, as shown in Table 2. Renal function declined > 10 ml/min/1.73m² in 16.2% of patients. In cross-sectional analysis at month 3, independent predictors of eGFR were ECD kidney, DGF, IF/TA score and fractional excretion of CTGF (Supplementary Table S16). Independent (month 3) predictors of eGFR at 5 years were eGFR at 3 months and donor age (Supplementary Table S17).

Reduction in eGFR (%) between month 3 and year 5 was independently predicted by 3-month eGFR (B = 0.895 [0.566-1.224], p<0.001), donor age (B = 0.703 [0.376-1.030], p<0.001) and 3-month IF/TA score (B = 4.861 [0.229-9.492], p=0.040). Increase in IF/TA score over time was correlated with decrease in eGFR, but only to a limited degree (r= 0.167, p=0.039). In the subgroup of patients with IF/TA score ≤ 1 at month 3 (n=123), average change in eGFR did not differ between patients who progressed to IF/TA score ≥ 2 and patients who demonstrated no IF/TA score progression (p=0.412). CTGFti or CTGFu at month 3 or 12 and the degree of change (delta) in CTGFti or CTGFu between month 3 and 12 did not correlate with eGFR at any time point and did not predict change in eGFR over time.

After the 5-year protocol biopsy, there were 7 cases of death with a functioning graft and 0 cases of graft loss censored for death over an average follow up period of 7.6 years (range 5.6 – 10.8). As a result, whether CTGFti and CTGFu predict death-censored graft loss could not be assessed.

DISCUSSION

In this study, tubulointerstitial CTGF expression was an independent predictor of interstitial fibrosis and tubular atrophy at 5 years after transplantation in a cohort of low-risk, stable renal recipients. These findings are in agreement with some,[8] but not all,[9] earlier studies assessing the prognostic value of early (mRNA level) CTGF gene expression. Particularly in patients with only minimal chronic histologic damage (either ci score 0 or IF/TA score ≤ 1) at 3 months, development of fibrosis and progression of IF/TA were determined by donor age, CTGFti and CTGFu. Even though CTGF expression was higher in the presence of subclinical inflammation and in ECD kidneys, only CTGFti independently predicted allograft fibrosis in multivariable analysis. This could be due to the fact that CTGF expression might reflect early fibrogenic processes across the full spectrum of renal allografts, including non-ECD kidneys without any histologic evidence of subclinical

inflammation. This is illustrated by the fact that in the subgroup of patients with ci, ct, i and t scores of 0 at 3 months, 71% (n=32) had CTGFti > 10%, which was associated with a 8-fold higher risk of progressing to IF/TA score ≥ 2 by 5 years, after correction for donor age and CTGFu. These findings are compatible with microarray data, which have demonstrated frequent and significant upregulation of genes related to immunity, inflammation, remodeling and fibrosis in histologically normal protocol biopsies.[8,10]

Our results confirm that donor age is not only of the dominant predictors of baseline histologic damage,[11,12] but is also associated with an accelerated progression of IF/TA regardless of baseline histology.[13–15] The predictive model for de novo development of fibrosis was only modestly improved by adding CTGFti and CTGFu to donor age, which is not surprising given that 5-year fibrosis reflects the cumulative burden of injury sustained over the entire follow-up period. Many factors that may have contributed after the 3 month point.

CTGF undergoes glomerular filtration, tubular reabsorption (which is quasi complete under normal circumstances) and can be produced by tubular epithelial cells, immune cells and mesangial cells (including fibroblasts).[3,16,17] The presence of CTGF in urine can theoretically indicate (1) intrarenal production, (2) tubular dysfunction and (3) saturation of tubular reabsorption, either resulting from increased filtration due to glomerular damage or because of high plasma concentrations. In this analysis, however, CTGFu did not correlate with A1M, an established marker of tubular proteinuria. Proteinuria and CTGFp did correlate with CTGFu, and the presence of an interaction between proteinuria and CTGFp indicates that they magnified each other's effect: CTGF was particularly prone to be present in urine if high systemic CTGF concentrations were combined with (presumed) glomerular damage. However, the fact that CTGFp and proteinuria only explained 17% of interindividual variability in CTGFu seems to indicate that filtration and glomerular damage are not dominant factors. It is likely that intrarenal fibrogenesis is another key factor. Ideally, quantification of CTGF mRNA expression on biopsies would clarify the relative contributions of these mechanisms but, unfortunately, this was not possible on the current cohort (discussed under limitations). Previous research suggests that the relative importance of intrarenal fibrogenesis, filtration and tubular dysfunction depend on study context and underlying pathology. Gerritsen et al. performed a study in which recombinant CTGF was infused in diabetic mice, which led them to estimate that 60% of CTGFu was produced intrarenally and 40% originated from plasma.[18] The same authors reported a strong correlation (r=0.85) between CTGFu and B2M in a variety of human glomerular diseases, suggesting that, in this population, it mainly reflected tubular dysfunction,[16] contrasting with our population of renal recipients. Regardless of the origins and biology of CTGF in renal recipients, these results indicate that it is an attractive candidate biomarker to include in future studies examining early prediction of long-term allograft outcome. It would almost certainly perform best when combined with other markers, as no single predictor can be expected to capture the complexities and temporal dynamics of renal inflammation and fibrogenesis.

This study has several limitations. First, study design was based on availability of paired protocol biopsies, which allowed for an analysis of factors that predict evolution of histology in individual recipients. However, the resulting cohort was selected for graft survival and compliance (as patients often refuse their 5-year protocol biopsy) and therefore biased with regard to clinical endpoints. This precludes a reliable analysis of the predictive performance of CTGFti and CTGFu concerning renal function and graft loss, particularly since no death-censored graft loss occurred during the extended follow-up period. Renal function was stable in most patients and correlated cross-sectionally with the degree of IF/TA, but progression of IF/TA and decrease in eGFR were only weakly correlated. CTGF expression was not predictive of renal function at 5 years. As it is known that chronic histologic damage is a risk factor for graft loss,[19] it is likely that the accelerated progression of IF/TA related to high early CTGF expression will eventually translate into renal functional decline. However, this will need to be addressed separately in future studies correlating CTGFti at 3 months with hard outcome parameters in an unselected population. Second, protocol biopsies have limitations, such as interobserver variability and sampling error. The former does not apply to this study because a single pathologist (EL) scored all biopsies. Sampling error was partly offset by the use of paired biopsies, where every patient was his own historic control. Third, CTGF expression could not be assessed on the mRNA level because, at the time, biopsies were not yet stored in an RNA stabilization solution and in situ hybridization of mRNA on paraffin slides was not successful, possibly because of mRNA degradation over time. We cannot exclude that part of the tubulointerstitial CTGF protein originated from tubular reabsorption of circulating CTGF. However, CTGF protein and mRNA expression have been shown to correlate well in the tubulointerstitium of renal allografts in mice[2] and the glomeruli of adult humans.[20]

In conclusion, early tubulointerstitial expression and urinary secretion of CTGF are independent predictors of IF/TA at 5 years after transplantation in stable renal recipients. These results suggest that, even in patients with very favorable histology at 3 months (little chronic histologic damage and/or absence of inflammation), fibrogenic processes might often be active early after transplantation, which result in accelerated accumulation of histologic damage over the following years.

ACKNOWLEDGEMENTS

The authors thank R. Broekhuizen, T. Coopmans, J. de Loor and M. Dekens for their technical assistance.

REFERENCES

1. Okada H, Kikuta T, Kobayashi T, et al. Connective tissue growth factor expressed in tubular epithelium plays a pivotal role in renal fibrogenesis. J Am Soc Nephrol. 2005;16(1):133-143.
2. Cheng O, Thuillier R, Sampson E, et al. Connective tissue growth factor is a biomarker and mediator of kidney allograft fibrosis. Am J Transplant. 2006;6(10):2292-2306.
3. Ito Y, Aten J, Bende RJ, et al. Expression of connective tissue growth factor in human renal fibrosis. Kidney Int. 1998;53(4):853-861.
4. Metalidis C, van Vuuren SH, Broekhuizen R, et al. Urinary connective tissue growth factor is associated with human renal allograft fibrogenesis. Transplantation. 2013;96(5):494-500.
5. Yokoi H, Mukoyama M, Nagae T, et al. Reduction in connective tissue growth factor by antisense treatment ameliorates renal tubulointerstitial fibrosis. J Am Soc Nephrol. 2004;15(6):1430-1440.
6. Luo GH, Lu YP, Song J, Yang L, Shi YJ, Li YP. Inhibition of connective tissue growth factor by small interfering RNA prevents renal fibrosis in rats undergoing chronic allograft nephropathy. Transplant Proc. 2008;40(7):2365-2369.
7. Adler SG, Schwartz S, Williams ME, et al. Phase 1 study of anti-CTGF monoclonal antibody in patients with diabetes and microalbuminuria. Clin J Am Soc Nephrol. 2010;5(8):1420-1428.
8. Vitalone MJ, O'Connell PJ, Wavamunno M, Fung CL-S, Chapman JR, Nankivell BJ. Transcriptome changes of chronic tubulointerstitial damage in early kidney transplantation. Transplantation. 2010;89(5):537-547.
9. Menon MC, Chuang PY, Li Z, et al. Intronic locus determines SHROOM3 expression and potentiates renal allograft fibrosis. J Clin Invest. 2015;125(1):208-221.
10. Park W, Griffin M, Grande JP, Cosio F, Stegall MD. Molecular evidence of injury and inflammation in normal and fibrotic renal allografts one year posttransplant. Transplantation. 2007;83(11):1466-1476.
11. De Vusser K, Lerut E, Kuypers D, et al. The predictive value of kidney allograft baseline biopsies for long-term graft survival. J Am Soc Nephrol. 2013;24(11):1913-1923.
12. Cosio FG, Grande JP, Wadei H, Larson TS, Griffin MD, Stegall MD. Predicting Subsequent Decline in Kidney Allograft Function from Early Surveillance Biopsies. Am J Transplant. 2005;5(10):2464-2472.
13. Nankivell BJ, Borrows RJ, Fung CL-S, O'Connell PJ, Allen RDM, Chapman JR. The natural history of chronic allograft nephropathy. N Engl J Med. 2003;349(24):2326-2333.
14. Naesens M, Lerut E, de Jonge H, et al. Donor age and renal P-glycoprotein expression associate with chronic histological damage in renal allografts. J Am Soc Nephrol. 2009;20(11):2468-2480.

15. Vanhove T, Vermeulen T, Annaert P, Lerut E, Kuypers DRJ. High intrapatient variability of tacrolimus concentrations predicts accelerated progression of chronic histologic lesions in renal recipients. Am J Transplant. 2016;(10):1-10.
16. Gerritsen KG, Peters HP, Nguyen TQ, et al. Renal proximal tubular dysfunction is a major determinant of urinary connective tissue growth factor excretion. Am J Physiol Renal Physiol. 2010;298(6):F1457-F1464.
17. Gerritsen KG, Abrahams AC, Peters HP, et al. Effect of GFR on plasma N-terminal Connective Tissue Growth Factor (CTGF) concentrations. Am J Kidney Dis. 2012;59:619-627.
18. Gerritsen KGF, Leeuwis JW, Koeners MP, et al. Elevated Urinary Connective Tissue Growth Factor in Diabetic Nephropathy Is Caused by Local Production and Tubular Dysfunction. J Diabetes Res. 2015;2015:539787.
19. Naesens M, Kuypers DRJ, De Vusser K, et al. Chronic histological damage in early indication biopsies is an independent risk factor for late renal allograft failure. Am J Transplant. 2013;13(1):86-99.
20. Ito Y, Goldschmeding R, Kasuga H, et al. Expression patterns of connective tissue growth factor and of TGF-beta isoforms during glomerular injury recapitulate glomerulogenesis. Am J Physiol Renal Physiol. 2010;299(3):F545-F558.
21. Racusen LC, Colvin RB, Solez K, et al. Antibody-mediated rejection criteria - an addition to the Banff 97 classification of renal allograft rejection. Am J Transplant. 2003;3(6):708-714.
22. Levey AS, Greene T, Schluchter MD, et al. Glomerular filtration rate measurements in clinical trials. Modification of Diet in Renal Disease Study Group and the Diabetes Control and Complications Trial Research Group. J Am Soc Nephrol. 1993;4(5):1159-1171.
23. Nguyen TQ, Tarnow L, Andersen S, et al. Urinary connective tissue growth factor excretion correlates with clinical markers of renal disease in a large population of type 1 diabetic patients with diabetic nephropathy. Diabetes Care. 2006;29(1):83-88.
24. Falke LL, Dendooven A, Leeuwis JW, et al. Hemizygous deletion of CTGF/CCN2 does not suffice to prevent fibrosis of the severely injured kidney. Matrix Biol. 2012;31(7-8):421-431.
25. Heinze G, Schemper M. A solution to the problem of separation in logistic regression. Stat Med. 2002;21(16):2409-2419.

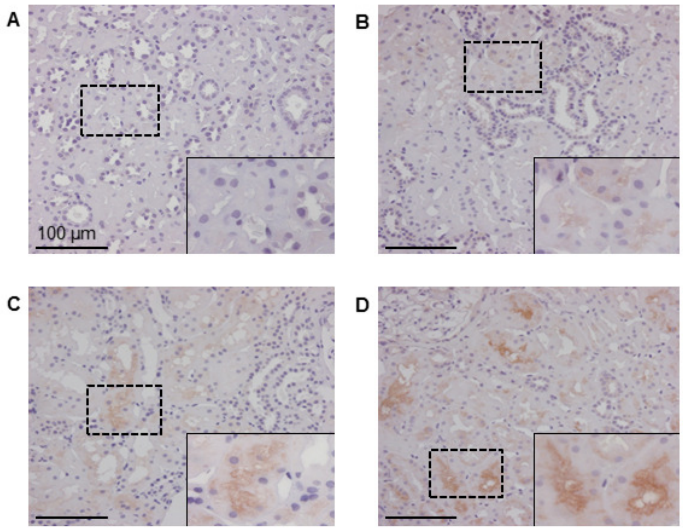

Figure 1. Representative tubulointerstitial CTGF staining pattern. The 4 categories of staining intensity are (A) absent (<1%), (B) minimal (1-10%), (C) moderate (11-25%) and (D) extensive (>25%).

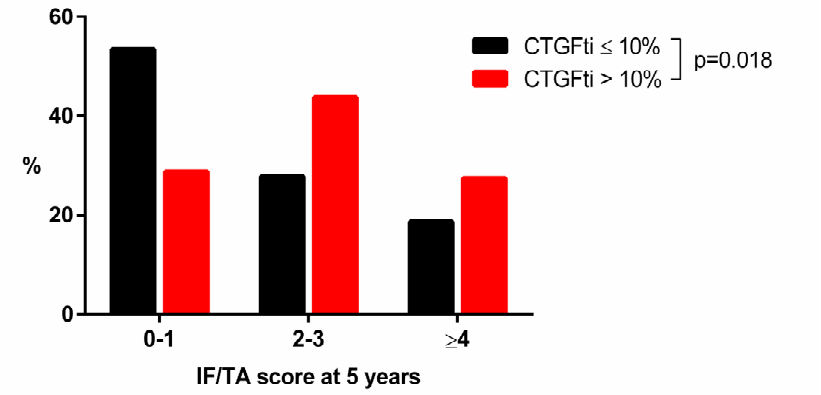

Figure 2. Differences in 5-year IF/TA score (sum of Banff ci and ct scores) by 3-month CTGF staining intensity in the subgroup of patients with IF/TA score ≤ 1 at 3 months.

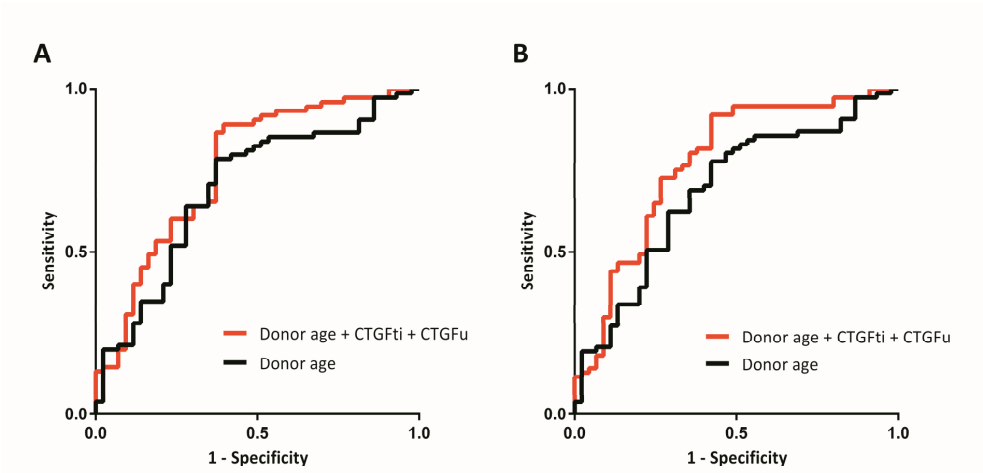

Figure 3. ROC analysis. The combination of donor age, CTGFti and CTGFu outperformed donor age alone in (A) predicting de novo fibrosis (ci > 0) by year 5 in the subgroup without fibrosis at 3 months (AUC=0.76 vs. 0.70) and in (B) predicting progression to IF/TA score ≥ 2 in the subgroup with IF/TA score ≤ 1 at 3 months (AUC=0.78 vs. 0.68).

Table 1. Donor, recipient and transplant characteristics.

Characteristic	Value
Donor characteristics	
Age (years)	42.8 ± 14.8
Gender (male)	96 (60%)
Donor type: living	14 (8.8%)
DCD	27 (16.9%)
SCD	91 (56.9%)
ECD	26 (16.3%)
Cold ischemia time (hours)	13.9 ± 6.2
Recipient characteristics	
Age (years)	51.4 ± 12.2
Gender (male)	96 (60%)
PRA > 20%*	3 (2.7%)
Diabetes mellitus pretransplant	24 (15%)
Transplant characteristics	
Repeat transplant	16 (10%)
Number of HLA mismatches	2.5 ± 1.3
Induction therapy	56 (35%)
Delayed graft function	15 (9.4%)

* PRA information only available for 110 patients
DCD, deceased of cardiac death; SCD, standard criteria donor; ECD, extended criteria donor; PRA, panel reactive antibody. HLA mismatch is the sum of broad antigen mismatches.

Table 2. Patient characteristics over time.

Characteristic	Month 3	Year 1	Year 5	P value
Clinical characteristics				
eGFR (ml/min/1.73 m²)	50.3 ± 15.0	55.5 ± 16.2	52.5 ± 18.1	0.063
Proteinuria (g/g creatinine):				0.051
< 0.3	155 (96.9%)	153 (95.6%)	140 (90.9%)	
0.3 – 1	5 (3.1%)	5 (3.1%)	13 (8.4%)	
> 1	0	2 (1.3%)	1 (0.6%)	
PTDM (cumulative incidence)	15 (9.4%)	27 (16.9%)	35 (21.9%)	<0.001
Selected histology				
Number of available protocol biopsies	160	146	160	
CTGFti area				0.001
< 1%	18 (11.3%)	4 (2.8%)	-	
1 - 10%	36 (22.5%)	28 (19.6%)	-	
11 - 25%	58 (36.3%)	38 (26.6%)	-	
> 25%	30 (30.0%)	73 (51%)	-	
BPAR (cumulative incidence)	28 (17.5%)	31 (19.4%)	34 (21.3%)	0.332
PVAN (cumulative incidence)	2 (1.3%)	5 (3.1%)	8 (5%)	0.031
IF/TA score	1.0 ± 1.0	1.6 ± 1.1	2.5 ± 1.8	<0.001
Subclinical acute rejection	1 (0.6%)	3 (2.1%)	3 (1.9%)	0.625
Borderline acute rejection	20 (12.5%)	9 (6.2%)	10 (6.3%)	0.078
Fibrosis with inflammation	3 (1.9%)	7 (2.7%)	14 (8.8%)	0.013
Urinary markers				
Urinary CTGF (pmol/g creatinine)	270 (178-470)	238 (141-389)	-	0.039
Plasma CTGF (pmol)	18.7 (14.2-25.7)	18.0 (13.9-25.5)	-	0.981
Fractional excretion of CTGF (%)	4.4 ± 3.2	4.6 ± 4.2	-	0.601
Urinary A1M (mg/g creatinine)	2.4 (0-4.6)	-	-	NA

IF/TA score is the sum of ci and ct scores. Fibrosis with inflammation is defined as ci > 0 and i > 0. CTGF and A1M values are median (interquartile range).

A1M, α1-microglobulin; BPAR, biopsy-proven acute rejection; CTGF, connective tissue growth factor; CTGFti, tubulointerstitial CTGF positive surface area; eGFR, estimated glomerular filtration rate; NA, not available; PTDM, posttransplant diabetes mellitus; PVAN, polyomavirus-associated nephropathy.

Table 3. Uni- and multivariate predictors of IF/TA score ≥ 2 at 5 years.

Predictors	Univariate analysis			Multivariate analysis		
	OR	CI	P value	OR	CI	P value
Donor characteristics						
Age (years)	1.04	1.02-1.07	<0.001	1.043	1.017-1.071	0.001
Gender (female)	0.62	0.32-1.22	0.167			
Donor type (ECD vs other)	3.49	1.14-10.70	0.029			
Cold ischemia time (hours)	0.99	0.94-1.05	0.773			
Recipient characteristics						
Age (years)	0.99	0.97-1.02	0.515			
Gender (female)	2.14	1.07-4.30	0.032			
PRA > 20%[a]	3.88	0.34-526.37	0.301			
Diabetes mellitus pretransplant	0.88	0.36-2.16	0.781			
Transplant characteristics						
Repeat transplant	0.66	0.23-1.89	0.442			
Number of HLA mismatches	1.27	0.97-1.65	0.082			
Induction therapy	1.78	0.87-3.62	0.112			
Delayed graft function	1.09	0.35-3.35	0.887			
Variables at 3 months						
eGFR (ml/min/1.73 m²)	0.99	0.97-1.02	0.687			
Proteinuria > 300mg/g [b]	0.80	0.13-4.95	0.812			
Urinary A1M	0.61	0.33-1.12	0.113			
BPAR	1.34	0.55-3.30	0.522			
Subclinical/borderline acute rejection	1.86	0.64-5.36	0.254			
Fibrosis with inflammation[c]	3.90	0.37-527.42	0.297			
CTGFti > 10%	3.00	1.51-5.96	0.002	3.03	1.47-6.23	0.003
CTGFu	1.50	1.03-2.18	0.034	1.42	0.98-2.22	0.066
IF/TA score ≥ 2	2.52	0.69-9.26	0.163	1.05	0.43-2.55	0.914

[a] Complete separation of data: all 3 patients with PRA > 20% had IF/TA score ≥ 2 at 5 years

[b] At 3 months, no patients had proteinuria > 1 g/g creatinine

[c] Complete separation of data: all 3 patients with fibrosis with inflammation at 3 months had IF/TA score ≥ 2 at 3 months and 5 years

Fibrosis with inflammation is defined as ci > 0 and i > 0.

A1M, α1-microglobulin; BPAR, biopsy-proven acute rejection; CI, 95% confidence interval; CTGF, connective tissue growth factor; CTGFti, tubulointerstitial CTGF positive surface area; CTGFu, urinary CTGF concentration; ECD, extended criteria donor; eGFR, estimated glomerular filtration rate; OR, odds ratio; PRA, panel reactive antibody titer

Table 4. Analyses for progression of fibrosis and tubular atrophy.

Outcome parameter	Predictors at month 3	Odds ratio (CI)		P value
Subgroup with IF/TA score ≤ 1 at month 3 (n=123)				
IF/TA ≥ 2 at 5 years (n=77)	Donor age	1.04	(1.01 – 1.07)	0.005
	CTGFti > 10%	3.71	(1.56 – 8.84)	0.003
	CTGFu	6.03	(1.66 – 21.99)	0.006
Subgroup with ci score 0 at month 3 (n=119)				
ci score ≥ 1 at 5 years (n=75)	Donor age	1.04	(1.02 – 1.07)	0.003
	CTGFti > 10%	2.68	(1.12 – 6.42)	0.027
	CTGFu	5.51	(1.52 – 19.99)	0.009
Subgroup with IF/TA, t and i scores of 0 at month 3 (n=45)				
IF/TA ≥ 2 at 5 years (n=32)	Donor age	1.07	(1.00 – 1.13)	0.037
	CTGFti > 10%	8.65	(1.48 – 50.66)	0.017
	CTGFu	9.01	(1.09 – 74.23)	0.041

CTGFu is 10-log transformed

CI, 95% confidence interval; IF/TA, interstitial fibrosis and tubular atrophy (sum of ci and ct scores)

Supplementary Table S1. Evolution of histologic lesions over time.

Histologic lesion	Category	3 months	1 year	5 years	P value
t	0	74.4% (n=119)	78.8% (n=115)	61.9% (n=99)	0.012
	1	18.1% (n=29)	13.7% (n=20)	28.8% (n=46)	
	2	6.3% (n=10)	4.1% (n=6)	6.9% (n=11)	
	3	1.3% (n=2)	3.4% (n=5)	2.5% (n=4)	
i	0	85.0% (n=136)	90.4% (n=132)	88.1% (n=141)	0.480
	1	13.1% (n=21)	5.5% (n=8)	5.6% (n=9)	
	2	0.6% (n=1)	3.4% (n=5)	3.1% (n=5)	
	3	1.3% (n=2)	0.7% (n=1)	3.1% (n=5)	
g	0	93.1% (n=149)	89.0% (n=130)	89.4% (n=143)	0.297
	1	3.8% (n=6)	7.5% (n=11)	8.8% (n=14)	
	2	2.5% (n=4)	2.7% (n=4)	1.3% (n=2)	
	3	0.6% (n=1)	0.7% (n=1)	0.6% (n=1)	
v	0	95.6% (n=153)	98.6% (n=144)	100.0% (n=160)	0.008
	1	2.5% (n=4)	1.4% (n=2)	0% (n=0)	
	2	1.3% (n=2)	0% (n=0)	0% (n=0)	
	3	0.6% (n=1)	0% (n=0)	0% (n=0)	
mm	0	94.4% (n=151)	93.8% (n=137)	88.8% (n=142)	0.041
	1	4.4% (n=7)	4.8% (n=7)	8.1% (n=13)	
	2	0.6% (n=1)	1.4% (n=2)	2.5% (n=4)	
	3	0.6% (n=1)	0% (n=0)	0.6% (n=1)	
ci	0	74.4% (n=119)	55.0% (n=88)	35.0% (n=56)	<0.001
	1	15.6% (n=25)	33.8% (n=54)	33.8% (n=54)	
	2	7.5% (n=12)	8.8% (n=14)	15.0% (n=24)	
	3	2.5% (n=4)	2.5% (n=4)	16.3% (n=26)	
ct	0	40.6% (n=65)	13.0% (n=19)	8.1% (n=13)	<0.001
	1	57.5% (n=92)	80.1% (n=117)	62.5% (n=100)	
	2	1.9% (n=3)	6.2% (n=9)	16.3% (n=26)	
	3	0% (n=0)	0.7% (n=1)	13.1% (n=21)	
ah	0	70.6% (n=113)	77.4% (n=113)	38.1% (n=61)	<0.001
	1	21.3% (n=34)	18.5% (n=27)	31.3% (n=50)	
	2	6.9% (n=11)	4.1% (n=6)	27.5% (n=44)	
	3	1.3% (n=2)	0% (n=0)	3.1% (n=5)	
cv	0	55.0% (n=88)	50.0% (n=73)	42.5% (n=68)	0.051
	1	26.3% (n=42)	30.8% (n=45)	34.4% (n=55)	
	2	18.1% (n=29)	17.8% (n=26)	22.5% (n=36)	
	3	0.6% (n=1)	1.4% (n=2)	0.6% (n=1)	
cg	0	98.1% (n=157)	96.6% (n=141)	98.1% (n=157)	1.000
	1	0.6% (n=1)	1.4% (n=2)	0.6% (n=1)	
	2	0.6% (n=1)	0.7% (n=1)	0% (n=0)	
	3	0.6% (n=1)	1.4% (n=2)	1.3% (n=2)	

P values refer to Friedman test for difference in distribution between month 3 and year 5.

Table S2. Uni- and multivariable predictors of ci score at 5 years.

Predictors	Univariable analysis			Multivariable analysis		
	OR	CI	P value	OR	CI	P value
Donor characteristics						
Age (years)	1.04	1.02-1.06	<0.001	1.03	1.01-1.05	0.002
Gender (female)	0.48	0.27-0.87	0.016	0.46	0.25-0.86	0.015
Donor type (ECD vs other)	1.84	0.84-3.78	0.095			
Cold ischemia time (hours)	0.98	0.94-1.03	0.409			
Recipient characteristics						
Age (years)	0.99	0.97-1.01	0.353			
Gender (female)	1.96	1.10-3.51	0.023	2.00	1.09-3.63	0.025
PRA > 20%	2.41	0.34-17.33	0.382			
Diabetes mellitus pretransplant	1.25	0.57-2.74	0.560			
Transplant characteristics						
Repeat transplant	1.08	0.33-2.59	0.885			
Number of HLA mismatches	1.22	0.97-1.54	0.083			
Induction therapy	1.20	0.67-2.15	0.546			
Delayed graft function	0.75	0.28-2.00	0.563			
Variables at 3 months						
eGFR (ml/min/1.73 m²)	1.00	0.82-1.02	0.952			
Proteinuria > 300mg/g [a]	1.43	0.23-8.94	0.700			
Urinary A1M	0.58	0.34-0.99	0.045			
BPAR	1.36	0.65-2.84	0.419			
Subclinical/borderline acute rejection	1.44	0.65-3.20	0.368			
CTGFti > 10%	2.23	1.20-4.16	0.012	1.89	1.01-3.56	0.048
CTGFu	1.31	0.96-1.79	0.094			
ci score	1.58	1.06-2.35	0.025	1.43	0.95-2.14	0.083

[a] At 3 months, no patients had proteinuria > 1 g/g creatinine

Fibrosis with inflammation is defined as ci > 0 and i > 0.

A1M, α1-microglobulin; BPAR, biopsy-proven acute rejection; CI, 95% confidence interval; CTGF, connective tissue growth factor; CTGFti, tubulointerstitial CTGF positive surface area; CTGFu, urinary CTGF concentration; ECD, extended criteria donor; eGFR, estimated glomerular filtration rate; OR, odds ratio; PRA, panel reactive antibody titer

Table S3. Uni- and multivariable predictors of ct score at 5 years.

Predictors	Univariable analysis			Multivariable analysis		
	OR	CI	P value	OR	CI	P value
Donor characteristics						
Age (years)	1.02	0.99-1.04	0.083			
Gender (female)	0.51	0.23-1.13	0.097			
Donor type (ECD vs other)	1.07	0.46-2.48	0.876			
Cold ischemia time (hours)	1.12	0.62-1.07	0.722			
Recipient characteristics						
Age (years)	1.36	0.69-2.66	0.374			
Gender (female)	1.73	0.92-3.27	0.092			
PRA > 20%	0.46	0.05-3.93	0.477			
Diabetes mellitus pretransplant	1.05	0.43-2.56	0.907			
Transplant characteristics						
Repeat transplant	0.46	0.10-2.19	0.328			
Number of HLA mismatches	1.25	0.96-1.62	0.098			
Induction therapy	1.09	0.51-2.31	0.831			
Delayed graft function	0.95	0.26-3.48	0.942			
Variables at 3 months						
eGFR (ml/min/1.73 m^2)	1.01	0.98-1.03	0.823			
Proteinuria > 300mg/g [a]	0.59	0.03-9.97	0.711			
Urinary A1M	0.58	0.32-1.04	0.066			
BPAR	1.48	0.57-3.88	0.420			
Subclinical/borderline acute rejection	1.35	0.46-4.00	0.585			
Fibrosis with inflammation	2.02	0.20-20.01	0.549			
CTGFti > 10%	2.02	1.02-4.02	0.045	2.11	1.05-4.20	0.035
CTGFu	1.07	0.75-1.54	0.711			
ct score	1.32	0.70-2.48	0.393	1.42	0.78-2.59	0.257

[a] At 3 months, no patients had proteinuria > 1 g/g creatinine

Fibrosis with inflammation is defined as ci > 0 and i > 0.

A1M, α1-microglobulin; BPAR, biopsy-proven acute rejection; CI, 95% confidence interval; CTGF, connective tissue growth factor; CTGFti, tubulointerstitial CTGF positive surface area; CTGFu, urinary CTGF concentration; ECD, extended criteria donor; eGFR, estimated glomerular filtration rate; OR, odds ratio; PRA, panel reactive antibody titer

Subgroups with little/no fibrosis at 3 months

Table S4. Subgroup with ci score 0 at month 3 (n=119): predictors of progression to ci score ≥ 1 at 5 years (n=75).

Predictors	Univariable analysis			Multivariable analysis		
	OR	CI	P value	OR	CI	P value
Donor characteristics						
Age (years)	1.05	1.02-1.08	0.001	1.04	1.02-1.07	0.003
Gender (female)	0.80	0.37-1.72	0.565			
Donor type (ECD vs other)	2.71	0.84-8.71	0.094			
Cold ischemia time (hours)	0.98	0.92-1.05	0.552			
Recipient characteristics						
Age (years)	0.99	0.96-1.02	0.533			
Gender (female)	1.78	0.81-3.88	0.149			
PRA > 20%[a]	4.26	0.39-579.98	0.031			
Diabetes mellitus pretransplant	2.30	0.71-7.47	0.168			
Transplant characteristics						
Repeat transplant	0.38	0.11-1.27	0.116			
Number of HLA mismatches	1.34	0.98-1.83	0.067			
Induction therapy	1.51	0.69-3.31	0.303			
Delayed graft function	0.44	0.11-1.73	0.240			
Variables at 3 months						
eGFR (ml/min/1.73 m²)	1.01	0.98-1.03	0.882			
Proteinuria > 300mg/g[b]	1.79	0.09-263.75	0.711			
BPAR	1.79	0.60-5.36	0.298			
Subclinical/borderline acute rejection	2.30	0.71-7.47	0.168			
Fibrosis with inflammation[c]	-	-	-			
CTGFti > 10%	2.14	0.98-4.67	0.055	2.68	1.12-6.42	0.027
CTGFu	5.39	1.60-18.12	0.007	5.51	1.52-19.99	0.009

[a] Complete separation of data: all 3 patients with PRA > 20% progressed to ci score ≥ 1 at 5 years

[b] Complete separation of data: the 1 patient with proteinuria > 300mg/g progressed to ci score ≥ 1 at 5 years

[c] No cases of fibrosis with inflammation in this subgroup

Table S5. Subgroup with IF/TA score ≤ 1 at month 3 (n=123): predictors of progression to IF/TA ≥ 2 at 5 years (n=77)

Predictors	Univariable analysis			Multivariable analysis		
	OR	CI	P value	OR	CI	P value
Donor characteristics						
Age (years)	1.05	1.02-1.07	0.001	1.04	1.01-1.07	0.005
Gender (female)	0.80	0.38-1.70	0.558			
Donor type (ECD vs other)	2.75	0.86-8.82	0.088			
Cold ischemia time (hours)	1.00	0.94-1.06	0.969			
Recipient characteristics						
Age (years)	1.00	0.97-1.02	0.751			
Gender (female)	2.23	1.02-4.87	0.045			
PRA > 20%[a]	4.01	0.37-546.21	0.290			
Diabetes mellitus pretransplant	1.67	0.55-5.02	0.365			
Transplant characteristics						
Repeat transplant	0.39	0.12-1.30	0.125			
Number of HLA mismatches	1.30	0.97-1.76	0.084			
Induction therapy	1.90	0.87-4.17	0.108			
Delayed graft function	0.89	0.24-3.33	0.859			
Variables at 3 months						
eGFR (ml/min/1.73 m²)	1.00	0.98-1.03	0.990			
Proteinuria > 300mg/g[b]	1.82	0.10-268.27	0.703			
BPAR	1.98	0.67-5.88	0.216			
Subclinical/borderline acute rejection	1.67	0.55-5.02	0.365			
Fibrosis with inflammation[c]	-	-	-			
CTGFti > 10%	2.85	1.32-6.16	0.008	3.71	1.56-8.84	0.003
CTGFu	5.42	1.62-18.15	0.006	6.03	1.66-21.99	0.006

[a] Complete separation of data: all 3 patients with PRA > 20% progressed to IF/TA score ≥ 2 at 5 years

[b] Complete separation of data: the 1 patient with proteinuria > 300mg/g progressed to IF/TA score ≥ 2 at 5 years

[c] No cases of fibrosis with inflammation in this subgroup

Table S6. Subgroup with IF/TA, t and i scores of 0 at month 3 (n=45): predictors of progression to IF/TA score ≥ 2 at 5 years (n=32).

Predictors	Univariable analysis			Multivariable analysis		
	OR	CI	P value	OR	CI	P value
Donor characteristics						
Age (years)	1.06	1.01-1.12	0.014	1.07	1.00-1.13	0.037
Gender (female)	0.92	0.27-3.08	0.888			
Donor type (ECD vs other)	4.75	0.51-44.48	0.172			
Cold ischemia time (hours)	0.96	0.86-1.06	0.407			
Recipient characteristics						
Age (years)	1.00	0.95-1.05	0.926			
Gender (female)	2.15	0.63-7.42	0.224			
PRA > 20%[a]						
Diabetes mellitus pretransplant	2.25	0.39-13.07	0.366			
Transplant characteristics						
Repeat transplant	1.23	0.19-8.16	0.832			
Number of HLA mismatches	1.52	0.92-2.51	0.102			
Induction therapy	2.53	0.73-8.71	0.142			
Delayed graft function[b]	4.36	0.33-615.23	0.288			
Variables at 3 months						
eGFR (ml/min/1.73 m²)	0.99	0.95-1.03	0.548			
Proteinuria > 300mg/g[c]	-	-	-			
BPAR	1.79	0.39-8.29	0.457			
Subclinical/borderline acute rejection[c]	-	-	-			
Fibrosis with inflammation[c]	-	-	-			
CTGFti > 10%	4.30	1.08-17.17	0.039	8.65	1.48-50.66	0.017
CTGFu	6.45	0.94-44.77	0.057	9.01	1.09-74.23	0.041

[a] Complete separation of data: the 1 patient with PRA > 20% progressed to IF/TA score ≥ 2 at 5 years

[b] Complete separation of data: all 2 patients with DGF progressed to IF/TA score ≥ 2 at 5 years.

[c] No cases in this subgroup

Table S7. Performance of different models in predicting de novo ci score ≥ 1 at 5 years in patients with ci score 0 at month 3 (n=119)

Combination of predictors	PPV	NPV	ROC AUC
Donor age + CTGFti > 10% + CTGFu	89.3%	53.5%	0.76
Donor age + CTGFti > 10%	84.0%	39.5%	0.68
Donor age + CTGFu	84.0%	44.2%	0.70
Donor age	84.0%	46.5%	0.70

PPV, positive predictive value; NPV, negative predictive value; ROC AUC, area under the curve of multivariable logistic regression receiver operating characteristic analysis

Table S8. Performance of different models in predicting de novo IF/TA score ≥ 2 at 5 years in patients with IF/TA score ≤ 1 at month 3 (n=123)

Combination of predictors	PPV	NPV	ROC AUC
Donor age + CTGFti > 10% + CTGFu	89.6%	57.8%	0.78
Donor age + CTGFti > 10%	85.9%	39.0%	0.69
Donor age + CTGFu	83.1%	42.2%	0.68
Donor age	84.4%	44.4%	0.70

Table S9. Performance of different models in predicting de novo IF/TA score ≥ 1 at 5 years in patients with IF/TA, t and i scores of 0 at month 3 (n=45)

Combination of predictors	PPV	NPV	ROC AUC
Donor age + CTGFti > 10% + CTGFu	80.0%	78.9%	0.80
Donor age + CTGFti > 10%	72.0%	57.9%	0.66
Donor age + CTGFu	76.0%	63.2%	0.71
Donor age	72.0%	73.7%	0.73

12-month predictors of 5-year histology

Table S10. Twelve month predictors of ci score at 5 years.

Predictors	Univariable analysis			Multivariable analysis		
	OR	CI	P value	OR	CI	P value
Donor characteristics						
Age (years)	1.04	1.02-1.06	<0.001	1.04	1.01-1.05	0.001
Gender (female)	0.48	0.27-0.87	0.016	0.43	0.23-0.80	0.007
Donor type (ECD vs other)	1.84	0.84-3.78	0.095			
Cold ischemia time (hours)	0.98	0.94-1.03	0.409			
Recipient characteristics						
Age (years)	0.99	0.97-1.01	0.353			
Gender (female)	1.96	1.10-3.51	0.023	1.97	1.08-3.58	0.027
PRA > 20%	2.41	0.34-17.33	0.382			
Diabetes mellitus pretransplant	1.25	0.57-2.74	0.576			
Transplant characteristics						
Repeat transplant	1.08	0.33-2.59	0.885			
Number of HLA mismatches	1.22	0.97-1.54	0.083			
Induction therapy	1.20	0.67-2.15	0.546			
Delayed graft function	0.75	0.28-2.00	0.563			
Variables at 12 months						
eGFR (ml/min/1.73 m²)	0.99	0.97-1.01	0.247			
Proteinuria > 300mg/g	0.57	0.12-2.76	0.482			
BPAR	1.32	0.67-2.62	0.424			
Subclinical/borderline acute rejection	2.32	0.86-6.22	0.096			
Fibrosis with inflammation	2.71	0.74-9.94	0.133			
CTGFti > 10%	0.82	0.39-1.73	0.599			
CTGFu	1.10	0.79-1.51	0.578			
ci score at month 12	1.82	1.24-2.68	0.002	1.69	1.14-2.51	0.009

Table S11. Twelve month predictors of ct score at 5 years.

Predictors	Univariable analysis			Multivariable analysis		
	OR	CI	P value	OR	CI	P value
Donor characteristics						
Age (years)	1.02	0.99-1.04	0.083			
Gender (female)	0.51	0.23-1.13	0.097	0.36	0.17-0.78	0.009
Donor type (ECD vs other)	1.07	0.46-2.48	0.876			
Cold ischemia time (hours)	1.12	0.62-1.07	0.722			
Recipient characteristics						
Age (years)	1.36	0.69-2.66	0.374			
Gender (female)	1.73	0.92-3.27	0.092			
PRA > 20%	0.46	0.05-3.93	0.477			
Diabetes mellitus pretransplant	1.05	0.43-2.56	0.907			
Transplant characteristics						
Repeat transplant	0.46	0.10-2.19	0.328			
Number of HLA mismatches	1.25	0.96-1.62	0.098			
Induction therapy	1.09	0.51-2.31	0.831			
Delayed graft function	0.95	0.26-3.48	0.942			
Variables at 12 months						
eGFR (ml/min/1.73 m^2)	0.99	0.97-1.01	0.268			
Proteinuria > 300mg/g	2.57	0.43-15.55	0.303			
BPAR	1.38	0.62-3.06	0.432			
Subclinical/borderline acute rejection	2.17	0.71-6.61	0.174			
Fibrosis with inflammation	2.98	0.63-14.00	0.167			
CTGFti > 10%	1.20	0.52-2.78	0.672			
CTGFu	0.88	0.61-1.25	0.468			
ct score at month 12	1.82	0.90-3.70	0.097	1.61	0.76-3.43	0.215

Table S12. Twelve month predictors of IF/TA ≥ 2 at 5 years.

Predictors	Univariable analysis			Multivariable analysis		
	OR	CI	P value	OR	CI	P value
Donor characteristics						
Age (years)	1.04	1.02-1.07	<0.001	1.04	1.01-1.07	0.005
Gender (female)	0.62	0.32-1.22	0.167			
Donor type (ECD vs other)	3.49	1.14-10.70	0.029			
Cold ischemia time (hours)	0.99	0.94-1.05	0.773			
Recipient characteristics						
Age (years)	0.99	0.97-1.02	0.515			
Gender (female)	2.14	1.07-4.30	0.032			
PRA > 20%[a]	3.88	0.34-526.37	0.301			
Diabetes mellitus pretransplant	0.88	0.36-2.16	0.781			
Transplant characteristics						
Repeat transplant	0.66	0.23-1.89	0.442			
Number of HLA mismatches	1.27	0.97-1.65	0.082			
Induction therapy	1.78	0.87-3.62	0.112			
Delayed graft function	1.09	0.35-3.35	0.887			
Variables at 12 months						
eGFR (ml/min/1.73 m²)	0.98	0.96-1.00	0.125			
Proteinuria > 300mg/g	0.39	0.08-1.79	0.224			
BPAR	1.90	0.79-4.55	0.150			
Subclinical/borderline acute rejection[b]	15.27	1.94-1970.42	0.004	19.91	2.23-2646.52	0.003
Fibrosis with inflammation[c]	7.77	0.90-1007.27	0.065			
CTGFti > 10%	1.30	0.57-2.96	0.527			
CTGFu	1.23	0.84-1.80	0.298			
IF/TA score ≥ 2 at month 12	4.83	2.20-10.59	<0.001	4.04	1.83-9.37	<0.001

[a] Complete separation of data: all 3 patients with PRA > 20% had IF/TA score ≥ 2 at 12 months and at 5 years

[b] Complete separation of data: all 12 patients with subclinical/borderline acute rejection on month 12 protocol biopsy had IF/TA score ≥ 2 at 5 years (6 of these already had IF/TA score ≥ 2 at 12 months)

[c] Complete separation of data: all 7 patients with fibrosis with inflammation on month 12 protocol biopsy had IF/TA score ≥ 2 at 12 months and at 5 years

Subgroups with little/no fibrosis at 12 months

Table S13. Subgroup with ci score 0 at month 12 (n=88): predictors of progression to ci score ≥ 1 at 5 years.

Predictors	Univariable analysis			Multivariable analysis		
	OR	CI	P value	OR	CI	P value
Donor characteristics						
Age (years)	1.05	1.01-1.08	0.004	1.05	1.01-1.08	0.008
Gender (female)	0.79	0.33-1.89	0.595			
Donor type (ECD vs other)	7.88	1.65-37.70	0.010			
Cold ischemia time (hours)	1.01	0.94-1.08	0.857			
Recipient characteristics						
Age (years)	0.99	0.96-1.03	0.741			
Gender (female)	2.92	1.20-7.10	0.018			
PRA > 20%[a]	1.04	0.94-1.15	0.448			
Diabetes mellitus pretransplant	1.23	0.35-4.38	0.748			
Transplant characteristics						
Repeat transplant	1.00	0.23-4.28	1.000			
Number of HLA mismatches	1.18	0.83-1.67	0.354			
Induction therapy	1.55	0.61-3.91	0.351			
Delayed graft function	1.00	0.23-4.28	1.000			
Variables at 12 months						
eGFR (ml/min/1.73 m²)	1.00	0.98-1.03	0.999			
Proteinuria > 300mg/g[b]	0.13	0.01-1.43	0.104			
BPAR	1.41	0.45-4.46	0.561			
Subclinical/borderline acute rejection[c]	15.03	1.69-1984.26	0.011	23.17	2.28-3171.63	0.005
Fibrosis with inflammation[d]	-	-	-			
CTGFti > 10%	1.78	0.62-5.10	0.286			
CTGFu	1.04	0.64-1.68	0.889			

Out of 88 patients with ci score 0 at month 12, 44 (50%) progressed to ci score ≥ 1 at 5 years

[a] Complete separation of data: all 2 patients with PRA > 20 progressed to IF/TA score ≥ 2 at 5 years

[b] Complete separation of data: none of the 3 patients with proteinuria > 300mg/g at month 12 progressed to ci score ≥ 1 by 5 years

[c] Complete separation of data: all 6 patients with subclinical/borderline acute rejection on the month 12 protocol biopsy progressed to ci score ≥ 1 by 5 years

d No cases of fibrosis with inflammation in this subgroup

Table S14. Subgroup with IF/TA score ≤ 1 at month 12 (n=76): predictors of progression to IF/TA score ≥ 2 at 5 years.

Predictors	Univariable analysis			Multivariable analysis		
	OR	CI	P value	OR	CI	P value
Donor characteristics						
Age (years)	1.04	1.01-1.07	0.015	1.039	1.01-1.07	0.022
Gender (female)	0.93	0.37-2.34	0.873			
Donor type (ECD vs other)	3.67	0.92-14.60	0.065			
Cold ischemia time (hours)	1.04	0.96-1.13	0.313			
Recipient characteristics						
Age (years)	0.98	0.95-1.02	0.399			
Gender (female)	3.87	1.42-10.53	0.008	3.78	1.33-10.70	0.012
PRA > 20%[a]	4.27	0.33-600.64	0.294			
Diabetes mellitus pretransplant	1.13	0.26-4.87	0.875			
Transplant characteristics						
Repeat transplant	1.22	0.25-5.87	0.802			
Number of HLA mismatches	1.18	0.77-1.61	0.553			
Induction therapy	1.62	0.60-4.37	0.345			
Delayed graft function	1.57	0.35-7.10	0.557			
Variables at 12 months						
eGFR (ml/min/1.73 m²)	1.00	0.97-1.03	0.794			
Proteinuria > 300mg/g[b]	0.29	0.01-5.66	0.421			
BPAR	3.19	0.79-12.90	0.103			
Subclinical/borderline acute rejection[c]	2.62	0.42-5.95	0.812			
Fibrosis with inflammation[d]	-	-	-			
CTGFti > 10%	1.76	0.62-5.03	0.291			
CTGFu	0.98	0.60-1.58	0.917			

Out of 76 patients with IF/TA score ≤ 1 at month 12, 40 (52.6%) progressed to IF/TA score ≥ 2 at 5 years

[a] Complete separation of data: all 2 patients with PRA > 20 progressed to IF/TA score ≥ 2 at 5 years

[b] Complete separation of data: the 1 patient with proteinuria > 300mg/g at month 12 did not progress to IF/TA score ≥ 2 at 5 years

[c] Complete separation of data: all 6 patients with subclinical/borderline acute rejection on the month 12 protocol biopsy progressed to IF/TA score ≥ 2 at 5 years

[d] No cases of fibrosis with inflammation in this subgroup

Table S15. Subgroup with IF/TA score, t and I scores of 0 at month 12 (n=16): predictors of progression to IF/TA score ≥ 2 at 5 years.

As this subgroup was limited to 16 patients, no analysis was performed.

Predictors of renal function

Table S16. Month 3 predictors of renal function at month 3.

Predictors	Univariable analysis			Multivariable analysis		
	B value	CI	P value	B value	CI	P value
Donor age (years)	-0.23	-0.39-(-0.08)	0.004			
ECD kidney	-5.67	-11.99-0.65	0.078	-6.49	-12.34-(-0.74)	0.027
DGF	-7.68	-15.66-(0.31)	0.059	-9.34	-16.62-(-2.06)	0.012
Proteinuria	-17.4	-30.6-(-4.1)	0.010			
IF/TA score	-5.27	-7.35-(-3.20)	<0.001	-5.09	-7.10-(-3.08)	<0.001
Fractional excretion of CTGF (%)	-0.96	-1.69-(-0.23)	0.011	-1.12	-1.79-(-0.45)	0.001

Table S17. Month 3 predictors of renal function at 5 years.

Predictors	Univariable analysis			Multivariable analysis		
	B value	CI	P value	B value	CI	P value
Donor age (years)	-0.54	-0.72-(-0.37)	<0.001	-0.40	-0.55-(-0.24)	<0.001
ECD kidney	-8.87	-16.45-(-1.30)	0.022			
Proteinuria	-18.09	-34.12-(-2.06)	0.027			
eGFR	0.67	0.51-0.84	<0.001	0.62	0.47-0.78	<0.001
IF/TA score	-6.39	-8.90-(-3.88)	<0.001			

10

Summary and Perspectives

SUMMARY

Chapter 1 describes the pathophysiology of the peritoneal membrane in association with peritoneal dialysis (PD). Long-term PD treatment induces production of proinflammatory cytokines and growth factors, and epithelial-mesenchymal transition (EMT) in peritoneal mesothelial cells. Uremia, exposure to dialysate, and peritonitis episodes cause submesothelial fibrosis, which is mainly mediated by transforming growth factor-β (TGF-β). Neoangiogenesis and high vascular permeability are induced by vascular endothelial growth factor (VEGF)-A and proinflammatory cytokines, which contribute to high peritoneal solute transport and ultrafiltration failure (UFF). Peritoneal lymphangiogenesis with increased lymphatic absorption is very likely to contribute to UFF in peritoneal fibrosis.

Lymphangiogenesis is also associated with tubulointerstitial fibrosis in a variety of primary kidney diseases. Particularly prominent lymphangiogenesis was observed in acute kidney transplant rejection. Unlike the contribution of lymphatic vessels in the physiology of PD, the role of lymphangiogenesis and the therapeutic potential of targeting this phenomenon in the kidney might depend on the specific etiologies of different kidney diseases.

Connective tissue growth factor (CTGF/CCN2) is an important determinant of fibrotic tissue remodeling. Inhibition of CTGF reduced fibrotic development in several experimental kidney diseases. CTGF expression is also associated with PD-related peritoneal fibrosis. Thus, CTGF plays an important role in both renal and peritoneal fibrosis. However, its possible role also in lymphangiogenesis remains unknown.

Chapter 2 is a review article focusing on rodent models of peritoneal injury in association with peritonitis. Bacteria-induced animal models basically show the transient inflammation and peritoneal dysfunction, which do not lead to morphological changes such as peritoneal fibrosis and neoangiogenesis. We newly generated two non-bacterial rat models, i.e. a mechanical scraping model, and model based on intraperitoneal zymosan injection. The scraping model, which is produced by scratching the rat parietal peritoneal surface, initially shows strong inflammation that is a typical sign of peritonitis, which lead to fibrosis and neoangiogenesis two weeks after scraping. The addition of a yeast cell wall component, zymosan, to the scraped peritoneum produces sustained peritoneal thickening with severe inflammatory cell infiltration five weeks after scraping, which is dependent on complement activation. We conclude that these non-bacterial peritonitis models are useful for investigating the pathophysiology of fibrosis, neoangiogenesis, and lymphangiogenesis triggered by peritonitis-induced inflammation.

Chapter 3 is the first report showing the relation between lymphangiogenesis and PD-associated peritoneal fibrosis. VEGF-C protein levels in human PD effluents were correlated with peritoneal solute transport rate and TGF-β1 levels. Expression of VEGF-C

and lymphatic markers in human peritoneal biopsies was the highest in UFF patients, and was correlated with peritoneal thickness. VEGF-C expression was upregulated in mesothelial cells and macrophages in human peritoneal samples with peritonitis. In vitro, TGF-β1 increased VEGF-C production in human peritoneal mesothelial cells. The magnitude of the response to TGF-β1 stimulation correlated with peritoneal function of the corresponding PD patient. The rat peritoneal fibrosis model induced by chlorhexidine gluconate (CG) showed an increase of lymphatic vessels both in a parietal peritoneum and particularly in the diaphragm. The treatment with TGF-β type I receptor inhibitor reduced VEGF-C expression and lymphangiogenesis in parallel with reduction of inflammation and fibrosis in the CG rat peritoneum. Newly generated lymphatic vessels in the CG rat diaphragm effectively absorbed large molecules, as indicated by the redistribution of fluorescein isothiocyanate (FITC)-dextran (MW 2,000,000) from the peritoneal cavity. As an underlying pathway, we identified induction of VEGF-C production in peritoneal cells by TGF-β, leading to lymphangiogenesis during peritoneal fibrosis.

In **Chapter 4**, we investigated the effect of specific inhibition of lymphangiogenesis using soluble VEGF receptor-3 (VEGFR-3), a decoy receptor, to trap VEGF-C/D, in a mouse peritoneal fibrosis model induced by intraperitoneal injection with methylglyoxal (MGO), which is a toxic glucose degradation product (GDP) that sometimes can also be found in PD effluents. MGO-induced morphological changes were prominent especially in the diaphragm. The observed lymphangiogenesis appeared to be driven by increased VEGF-D rather than by VEGF-C, since the expression of the latter was not found to be altered in the model. Remarkably, both VEGF-C and VEGF-D expression was increased in the peritoneum of UFF patients. Treatment with soluble VEGFR-3 specifically suppressed lymphangiogenesis, and did not change inflammation, fibrosis, and blood vessel formation in the diaphragm of MGO model. The treatment also improved impaired ultrafiltration without changes of peritoneal solute transport in this model, which indicates that peritoneal lymphatic vessels directly absorb PD solution without modification of solute composition, which is in agreement with the open structure of the lymphatic capillary wall. We conclude that the inhibition of VEGFR-3 signaling might be a useful strategy to improve lymphangiogenesis-dependent UFF.

Chapter 5 showed the relationship between CTGF and peritoneal lymphangiogenesis. There was a positive correlation between CTGF and VEGF-C protein levels in human PD effluents. CTGF mRNA expression positively correlated with VEGF-C, lymphatic vessel endothelial hyaluronan receptor 1 (LYVE-1), and podoplanin mRNA expression in human peritoneal biopsies. There was a positive correlation between CTGF and VEGF-C mRNA enhancement in human peritoneal mesothelial cells treated with TGF-β1. Expression of CTGF, VEGF-C, and lymphatic vessels was significantly increased in a diaphragm of rat CG model. CTGF expression was positively correlated with expression of VEGF-C and lymphatic vessels in a diaphragm of rat CG model. Peritoneal mesothelial cells produce

CTGF and VEGF-C in parallel, and there is a close relationship between CTGF and PD-associated peritoneal lymphangiogenesis. In our kidney damage models, we have obtained evidence suggesting that CTGF itself is actively involved in the regulation of lymphangiogenesis (Chapter 7). It remains to be established whether this is also the case in peritoneal lymphangiogenesis.

In **Chapter 6**, we investigated the mechanism of renal lymphangiogenesis in a rat unilateral ureteral obstruction (UUO) model. Expression of TGF-β, VEGF-C, and lymphatic vessels was time-dependently increased and peaked around two weeks post UUO. VEGF-C production was induced by TGF-β treatment in cultured renal tubular cells and macrophages. The direct administration of TGF-β type I receptor inhibitor via renal artery reduced expression of VEGF-C and lymphatic vessel formation in the UUO model. In parallel with Chapter 3, we showed TGF-β–VEGF-C pathway in renal and peritoneal lymphangiogenesis.

In **Chapter 7** we clarified the involvement of CTGF in renal lymphangiogenesis. We observed prominent lymphangiogenesis accompanied with increased expression of CTGF and VEGF-C in human obstructive nephropathy. CTGF knockdown in mice resulted in less VEGF-C expression and decreased lymphangiogenesis in parallel with significant reduction of fibrosis in the UUO model. In vitro, CTGF induced VEGF-C production in renal tubular cells, but CTGF also directly bound to VEGF-C, and thereby suppressed VEGF-C-induced lymphatic endothelial cells growth. In vivo, not only intact CTGF, but also CTGF fragments can be detected. Unlike full length CTGF, these CTGF fragments did not affect VEGF-C function, which suggests that the direct inhibitory effect of CTGF on VEGF-C can be prevented and maybe also terminated by the cleavage of CTGF. Thus, CTGF appears to be directly involved in renal lymphangiogenesis through the regulation of VEGF-C production and activity.

Chapter 8 focuses on the effect of aging on tissue response to injury in the mouse UUO model. We observed that old mice developed more severe tubular morphological damage, while less interstitial fibrosis appeared, compared to young mice after UUO. There was no significant difference in the expression of established profibrotic cytokines and renoprotective factors including TGF-β, plasminogen activator inhibitor-1 (PAI-1), Klotho, and bone morphogenetic protein 7 (BMP7) between young and old UUO kidneys. However, old UUO kidneys showed increased BMP6 expression and decreased CTGF expression, which might be associated with less fibrotic development. In vitro, we found that CTGF directly bound to BMP6 and suppressed BMP6 downstream signaling, which suggested that the renoprotective effects of BMP6 could be further upregulated by less CTGF expression in old UUO kidneys. The contrast with the more extensive tubular damage in old UUO kidneys suggests the involvement of different mechanisms driving this phenotype. Our findings are important because, although chronic kidney disease (CKD) mainly affects

older individuals, experimental studies of kidney fibrosis have generally been performed in young animals, without taking into account, that age may have important effects on renal response to injury.

In **Chapter 9**, investigated the relation of CTGF expression in transplanted kidneys with histological and functional outcome. We identified tubulointerstitial CTGF expression (CTGFti) at 3 months was an independent predictor of interstitial fibrosis (IF) and tubular atrophy (TA) at 5 years after transplantation in stable renal transplant recipients. Donor age is known as a dominant predictor of histological damage. In predictive models, the data of CTGFti and urinary CTGF levels (CTGFu) at 3 months when added to donor age improved prediction of IF/TA at 5 years. CTGF expression was not predictive of renal function at 5 years, which might be caused by the relatively stable renal function within this cohort. Further studies with a longer observation period will be necessary to determine whether the observed progression of IF/TA related to high early CTGF expression will finally result in renal functional decline and graft loss.

PERSPECTIVES

I propose that the observations throughout this thesis support the notion that pharmacological targeting of CTGF might have beneficial effects on the regulation of lymphangiogenesis associated with renal and peritoneal fibrosis.

Loss of ultrafiltration is a critical problem leading to discontinuation of PD treatment and poor survival rate of PD patients. I suggest a possible involvement of lymphangiogenesis with increased lymphatic absorption in the context of UFF in association with peritoneal fibrosis. As based on the findings in Chapter 3 I argue that lymphangiogenesis is associated with UFF in human PD patients. Newly generated lymphatic vessels effectively transported fluid and solutes in a rat peritoneal fibrosis model, which supported the concept that lymphangiogenesis leads to the increase of peritoneal lymphatic absorption. In addition, Chapter 4 confirmed the potential of targeting peritoneal lymphangiogenesis to improve impaired ultrafiltration in association with peritoneal fibrosis. Chapter 5 showed the close relationship between CTGF expression and peritoneal lymphangiogenesis. In our previous report, we did not find a significant correlation between CTGF and blood vessel density in human peritoneal biopsies. Thus, CTGF might be more closely related to lymphangiogenesis than angiogenesis in peritoneal fibrosis. I therefore would expect that inhibition of CTGF could reduce peritoneal fibrosis and improve impaired ultrafiltration at least partly through suppression of lymphangiogenesis. This might become even more important in the near future, considering the development and introduction of new biocompatible osmotic agents with higher molecular weight, like icodextrin, in peritoneal dialysates, which will not be easily diffuse over the wall of blood capillaries, but can be readily absorbed from the peritoneal cavity by lymphatic vessels.

Chapter 6 and 7 showed the involvement of both TGF-β and CTGF in lymphangiogenesis of obstructive nephropathy. Furthermore, Chapter 7 suggested that inhibition of CTGF might be a useful therapeutic strategy to reduce fibrosis even in severe CKD. Interestingly, Chapter 8 demonstrated that CTGF increment in response to renal injury was less in old mice compared to young mice, which suggests that CTGF inhibition strategy might be more effective in young population than in old population. Inhibition of CTGF also resulted in less VEGF-C expression and decreased lymphangiogenesis. Little is known about how lymphangiogenesis affects inflammation and fibrosis in renal response to injury. It is not even clear whether it contributes to damage or rather supports the resolution of the injury. One might speculate that, under certain conditions it might therefore even be harmful to inhibit lymphangiogenesis in renal response to injury. However, if newly generated lymphatic vessels would mainly act to support persistence of detrimental renal inflammation by producing chemokines and attracting inflammatory cells, suppression of lymphangiogenesis could also be part of the beneficial effect of anti-CTGF therapy in reducing renal damage. Chapter 9 revealed the potential of CTGF as a biomarker predicting human renal allograft fibrosis. Such a biomarker might be useful in patient stratification and management, especially in the context of clinical trials, although the strength of its predictive value is not sufficient to rely on as a guide for clinical decision making in daily practice.

As for options for anti-CTGF therapy, FG-3019, a human monoclonal antibody against CTGF, has already been found to be safe and well-tolerated in several clinical conditions. It was studied in a small phase-1 clinical trial on patients with diabetic nephropathy, and found to significantly reduce albuminuria. Unfortunately, a phase-2 study of FG-3019 in subjects with type 2 diabetic nephropathy has been terminated early due to the sub-optimal study design. However, phase-2 studies of FG-3019 in patients with idiopathic pulmonary fibrosis and other conditions are underway (https://clinicaltrials.gov/ct2/results?term=FG-3019&Search=Search).

In conclusion, I propose that the role of CTGF and lymphangiogenesis in peritoneal and renal fibrosis as demonstrated in this thesis will contribute to the development of novel strategies to the benefit of patients with kidney diseases and those being treated with peritoneal dialysis.

Summary in Japanese / 日本語の要約

第 1 章では腹膜透析 (peritoneal dialysis, PD) に関連した腹膜の病態生理変化の概要が述べられている。長期腹膜透析の継続により炎症性サイトカインや各種成長因子が産生され、腹膜中皮細胞において上皮間葉移行が誘導される。尿毒症、透析液の暴露、腹膜炎の合併により transforming growth factor-β (TGF-β) を介した中皮下の線維化が進行する。血管内皮成長因子 (vascular endothelial growth factor, VEGF)-A や炎症性サイトカインは血管新生と血管透過性亢進を引き起こし、腹膜透過性亢進、除水機能不全の一因となる。腹膜におけるリンパ管新生は腹腔のリンパ管吸収を増加させ、腹膜線維症における除水機能不全の一因と考えられる。

リンパ管新生はさまざまな腎臓病における尿細管間質線維化とも関連がみられる。特に腎移植の急性拒絶反応では顕著なリンパ管新生が観察される。腹膜透析における明確なリンパ管の役割とは異なり、腎臓におけるリンパ管新生の役割とその治療戦略はさまざまな腎臓病の病因によって異なると考えられる。

Connective tissue growth factor (CTGF/CCN2) は組織線維化における重要な進展因子である。CTGF の抑制はさまざまな腎臓病モデルにおいて線維化の減少につながる。また CTGF は PD 腹膜線維症とも関連がみられる。このように CTGF は腎臓と腹膜の線維化において重要な働きをもつ。しかしながら CTGF のリンパ管新生における役割については解明されていない。

第 2 章は腹膜炎に関連した腹膜傷害動物モデルについての総説である。細菌を使用した動物モデルの腹膜の炎症と機能不全は基本的に一過性であり、腹膜線維症や血管新生などの形態学的変化には至らない。我々は新たに「腹膜擦過モデル」とその擦過モデルの腹腔内にザイモザンを投与した「ザイモザンモデル」の二つの非感染性の動物モデルを確立した。腹膜擦過モデルはラットの壁側腹膜表面を擦過することにより惹起され、初期には腹膜炎の典型的な特徴である強い炎症を示し、2 週間後には腹膜線維化と血管新生が観察される。擦過した腹膜に真菌の壁成分であるザイモザンを投与することにより、補体活性に依存した強い炎症細胞浸潤が持続し、5 週間後においても腹膜肥厚が観察される。これらのモデルは腹膜炎による炎症を誘因とした腹膜の線維化、血管新生、リンパ管新生の病態生理の解明に有用であると考えられる。

第 3 章はリンパ管新生と PD 腹膜線維症との関連についての最初の報告である。ヒト腹膜透析排液において、リンパ管新生を誘導する成長因子である VEGF-C 濃度と腹膜透過性、TGF-β1 濃度との間に相関を認めた。ヒト腹膜生検組織において VEGF-C とリンパ管マーカーの発現は除水機能不全患者群において最も上昇しており、また腹膜の肥厚との間に相関を認めた。ヒト腹膜炎生検組織において VEGF-

C の発現上昇は腹膜中皮細胞とマクロファージにて観察された。PD 排液由来腹膜中皮細胞において TGF-β1 刺激により VEGF-C の発現が増強し、その増加の程度は PD 患者の腹膜機能と相関を認めた。グルコン酸クロルヘキシジン (chlorhexidine gluconate, CG) を用いたラット腹膜線維症モデルにおいて、リンパ管の発現増加が壁側腹膜、横隔膜に観察され、特に横隔膜で顕著であった。TGF-β 受容体阻害剤投与により CG ラット腹膜の炎症と線維化が減少するとともに、VEGF-C 発現とリンパ管新生が抑制された。CG ラット腹腔内に投与した蛍光標識デキストラン (分子量 2,000,000) の追跡により、横隔膜の新生リンパ管が効果的に腹腔内分子を吸収することが明らかとなった。我々は腹膜線維症において TGF-β が VEGF-C 産生を誘導しリンパ管新生を促進する根本的なメカニズムを明らかにした。

第 4 章では腹膜透析液中に生じる有毒なグルコース分解産物であるメチルグリオキサール (methylglyoxal, MGO) を用いたマウス腹膜線維症モデルを、VEGF-C/D を捉えるおとり受容体である可溶性 VEGF receptor-3 (VEGFR-3)を用いて治療することにより、腹膜線維症におけるリンパ管新生の抑制効果を検討した。MGO による腹膜の形態学的変化は横隔膜にて顕著に観察され、MGO モデルにおいて VEGF-D の増加がみられたのに対して VEGF-C の変化は乏しく、観察されたリンパ管新生は主に VEGF-D に誘導されたものと考えられた。また VEGF-C、VEGF-D の発現は共に除水機能不全の患者群で顕著な上昇を示した。MGO モデルの横隔膜において、可溶性 VEGFR-3 治療により特異的にリンパ管新生が抑制され、炎症、線維化、血管新生には変化が見られなかった。また可溶性 VEGFR-3 治療により腹膜の溶質移動を変化させることなく除水量の低下が改善したことにより、間隙の多い壁構造を伴う腹膜の毛細リンパ管は成分を変化させることなくそのまま腹膜透析液を吸収することが示唆された。腹膜線維症における VEGFR-3 シグナルの抑制はリンパ管新生に依存した除水機能不全の改善に有用であると考えられた。

第 5 章では CTGF と腹膜のリンパ管新生との関連を示した。ヒト腹膜透析排液において CTGF 蛋白濃度と VEGF-C 蛋白濃度との間に相関を認めた。またヒト腹膜生検組織において CTGF messenger RNA (mRNA) 発現は VEGF-C、リンパ管マーカーである lymphatic endothelial hyaluronan receptor-1 (LYVE-1)、ポドプラニンと正の相関を示した。TGF-β1 刺激により腹膜中皮細胞における CTGF、VEGF-C mRNA 発現は増加し、そのそれぞれの増加の程度は正の相関を示した。ラット CG モデルの横隔膜において CTGF、VEGF-C、リンパ管の発現は有意に上昇し、CTGF 発現は VEGF-C、リンパ管の発現と正の相関を示した。腹膜中皮細胞は CTGF と VEGF-C を同程度に並行して産生すると考えられ、CTGF と PD 関連の腹膜リンパ管新生との間に有意な相関がみられる。我々は腎障害モデルにおいて CTGF がリ

ンパ管新生を誘導することを示したが、腹膜においても同様のメカニズムが存在するか検討の余地がある。

第 6 章ではラット片側尿管結紮 (UUO) モデルにおける腎臓リンパ管新生のメカニズムを検討した。TGF-β、VEGF-C、リンパ管の発現は 2 週間の UUO モデルにおいて経時的な上昇を示した。培養腎尿細管上皮細胞とマクロファージにおいて、TGF-β1 刺激により VEGF-C 発現の増加がみられた。腎動脈経由の TGF-β 受容体阻害剤投与により UUO モデルにおける VEGF-C とリンパ管の発現が抑制された。第 3 章と共に我々は腎臓と腹膜のリンパ管新生における TGF-β–VEGF-C 経路を示した。

第 7 章では腎臓リンパ管新生における CTGF の関与を明らかにした。ヒト閉塞性腎症例において CTGF と VEGF-C の発現増加を伴った顕著なリンパ管新生が観察された。CTGF 欠損マウスの UUO モデルにおいて、正常マウス UUO と比較して線維化が減少するとともに VEGF-C 発現とリンパ管新生が抑制された。インビトロの検討において、CTGF は培養腎尿細管上皮細胞における VEGF-C 発現を増加させた一方で、CTGF は VEGF-C と結合し VEGF-C によるリンパ管内皮細胞の成長を抑制した。生体内には全長の CTGF だけではなくその断片も存在し、これらの CTGF 断片は全長 CTGF とは異なり VEGF-C の機能に影響を及ばさなかった。このことにより CTGF が分解されることで VEGF-C に対する直接的な影響は抑制されると考えられた。このように CTGF は VEGF-C の産生と活性を調節することで腎臓リンパ管新生に関与すると考えられる。

第 8 章ではマウス UUO モデルの組織応答に対して加齢が及ぼす影響に着目している。UUO 術後、老齢マウスは若いマウスに比べて形態学的により強い尿細管傷害を示したのに対し、間質線維化の程度は軽度であった。UUO モデルにおいて若いマウスと老齢マウスとの間に TGF-β1、plasminogen activator inhibitor-1 (PAI-1)、Klotho、bone morphogenetic protein (BMP) 7 などの線維化に関わるサイトカインや腎保護因子の発現の差はみられなかった。しかしながら老齢マウス UUO 腎は BMP6 発現増加と CTGF 発現低下を示し、それらが線維化の減少に関係していると考えられた。またインビトロにおいて CTGF は BMP6 と結合しその結果 BMP6 の下流シグナルを抑制したため、老齢マウス UUO 腎において CTGF 発現低下により BMP6 の腎保護効果がさらに増強されることが示唆された。老齢マウス UUO 腎にみられた尿細管傷害の増強は異なるメカニズムの関与が考えられた。加齢が腎線維化の病態に影響を及ぼした我々の所見は重要である。なぜならば慢性腎臓病 (chronic kidney disease, CKD) は高齢者を中心に発症するが、一般的な腎線維化の研究は若い動物を用いて行われており、加齢の影響は考慮されていないからである。

第 9 章では移植腎の組織学的、機能的変化における CTGF 発現の関与について検討した。移植 3 ヶ月後の尿細管間質の CTGF 発現 (tubulointerstitial CTGF expression, CTGFti) は移植 5 年後の間質線維化 (interstitial fibrosis, IF) と尿細管萎縮 (tubular atrophy, TA) の独立した予測因子であった。移植腎提供者の年齢は組織学的障害の主要な予測因子として知られている。我々の予測モデルにおいて移植 3 ヶ月後の CTGFti と尿中 CTGF は移植腎提供者の年齢による 5 年後の IF/TA の予測をさらに改善させた。CTGF 発現は 5 年後の腎機能に関しては有意な予測因子ではなかった。このことは今回の研究コホートでは比較的腎機能が保たれていたことが原因として考えられた。CTGF の初期発現上昇を伴った IF/TA の進行が最終的に腎機能低下と移植腎廃絶に至るのかどうかを検討するために、より長期の観察期間を設けたさらなる研究が必要と考えられる。

展望

この論文を通して、薬理学的に CTGF を標的とすることが腎臓線維化と腹膜線維症におけるリンパ管新生の調節に有用であることが推測された。

腹膜透析における除水機能低下は腹膜透析中止や生命予後悪化につながる深刻な問題である。リンパ管吸収増加を伴ったリンパ管新生は腹膜線維症に関連した除水機能不全の一因と考えられる。第 3 章で示したようにリンパ管新生は腹膜透析患者の除水機能不全と関連している。ラット腹膜線維症モデルにおいて新生リンパ管が効果的に腹腔内溶液を吸収したことにより、リンパ管新生がリンパ管吸収増加に至る概念が補足された。さらに第 4 章では腹膜リンパ管新生を標的とすることで腹膜線維症に関連した除水機能低下が改善することが示された。第 5 章では CTGF 発現が腹膜リンパ管新生と密接に関連することが示された。我々は過去にヒト腹膜生検組織において CTGF 発現と血管密度の間に有意な関連がなかったことを報告しており、CTGF は腹膜線維症において血管新生よりもリンパ管新生に深く関連することが示唆された。これらのことから CTGF の抑制は腹膜線維症とリンパ管新生を減少させ、そのリンパ管新生の抑制は除水機能低下の改善に少なくともある程度寄与していることが推測された。イコデキストリンのような大分子量の浸透圧物質は腹膜の毛細血管壁を通過せずリンパ管から体内に吸収されるため、このことは近い将来生体適合性の高い大分子量の浸透圧物質を使用した新しい腹膜透析液が開発された場合においても重要に関わってくる。

第 6、7 章では TGF-β と CTGF が共に閉塞性腎症のリンパ管新生に関わることが示された。さらに第 7 章では重度な慢性腎臓病においても CTGF の抑制は線維化を減少させる有用な治療方針であることが示された。興味深いことに第 8 章において、腎傷害に反応した CTGF 発現の増加は若いマウスに比べて老齢マウスでは

軽微であったため、CTGF の抑制は高齢患者よりも若年患者により効果的である可能性が考えられた。また CTGF の抑制は VEGF-C 発現を減少させリンパ管新生を抑制させた。リンパ管新生が腎傷害における炎症と線維化にどのように影響を及ぼすのか、また傷害をさらに悪化させるのかまたは治癒に貢献するのかについてはほとんど明らかになっていない。それゆえにある状況下の腎傷害においてはリンパ管新生を抑制することが有害であると考えられるかもしれない。しかしながら新生リンパ管が主にケモカインを産生し、炎症細胞を呼び寄せることによって有害な腎の炎症を堅持しているならば、リンパ管新生の抑制は腎傷害減少を目的とした抗 CTGF 療法における有益な作用となり得る。第 9 章ではヒト移植腎線維化を予測するバイオマーカーとしての CTGF の意義を明らかにした。その予測値は日常診療での臨床決定指針としては不十分であるが、そのようなバイオマーカーは患者の選別と管理に有用である。

抗 CTGF 療法の可能性として、ヒト抗 CTGF モノクローナル抗体である FG-3019 の安全性と耐用性がすでにいくつかの臨床病態において示されている。FG-3019 は糖尿病性腎症患者を対象とした小規模第 1 相臨床試験において有意に尿蛋白を減少させた。残念ながら 2 型糖尿病性腎症患者を対象とした第 2 相臨床試験は最適ではない研究デザインのために中止となった。しかしながら特発性肺線維症患者や他疾患患者を対象とした第 2 相臨床試験が進行中である。
(https://clinicaltrials.gov/ct2/results?term=FG-3019&Search=Search)

結論として、この論文で証明された腹膜線維症と腎臓線維化における CTGF とリンパ管新生の役割は腎臓病患者と腹膜透析患者のための新規治療法開発に貢献することが期待される。

Summary in Dutch / Samenvatting in het Nederlands

Hoofdstuk 1 beschrijft de pathofysiologische veranderingen van de peritoneaal membraan bij peritoneaal dialyse (PD). Langdurige PD therapie leidt tot productie van proinflammatoire cytokines en groeifactoren en epitheliale-naar-mesenchymale transitie (EMT) in peritoneale mesotheelcellen. Uremie, blootstelling aan het dialysaat en episoden van peritonitis veroorzaken submesotheliale fibrose, waarbij transforming growth factor (TGF)-β de belangrijkste mediator is. Neoangiogenese en toegenomen vasculaire permeabiliteit worden geïnduceerd door vascular endothelial growth factor (VEGF)-A en proinflammatoire cytokines en dragen bij aan het toegenomen peritoneale transport van opgeloste stoffen en ultrafiltratiefalen (UFF). Ook peritoneale lymfangiogenese en toegenomen lymfatische absorptie dragen hoogstwaarschijnlijk bij aan UFF in peritoneale fibrose.

Lymfangiogenese is ook geassocieerd met tubulointerstitiële fibrose in meerdere primaire nierziekten. Ook wordt prominente lymfangiogenese gezien in acute rejectie van getransplanteerde nieren. In tegenstelling tot de eenduidige rol van lymfvaten in de fysiologie van PD, is de bijdrage van lymfangiogenese in de nier en het therapeutische potentieel om dit fenomeen in de nier te remmen waarschijnlijk afhankelijk van de desbetreffende onderliggende oorzaak van de verschillende nierziekten.

Connective tissue growth factor (CTGF/CCN2) is een belangrijke determinant van fibrotische weefselremodelering. Remming van CTGF vermindert de ontwikkeling van fibrose in verschillende experimentele nierziekten. CTGF expressie is ook geassocieerd met PD-gerelateerde peritoneale fibrose. CTGF speelt dus een belangrijke rol in het ontstaan van zowel nier- als peritoneaal fibrose, maar een mogelijke rol van CTGF in lymfangiogenese was nog niet bekend.

Hoofdstuk 2 betreft een review artikel dat gericht is op proefdiermodellen van peritoneale schade geassocieerd met peritonitis. Bacterie-geïnduceerde proefdiermodellen laten meestal slechts voorbijgaande inflammatie en peritoneale disfunctie zien, die niet leiden tot morfologische veranderingen zoals peritoneale fibrose en neoangiogenese. We hebben twee nieuwe non-bacteriële rattenmodellen ontwikkeld, namelijk het mechanische schraapmodel en het intraperitoneale zymosan-injectie model. Het mechanische schraapmodel, dat berust op het aanbrengen van krassen op het pariëtale peritoneumoppervlak, leidt in de acute fase tot ernstige inflammatie van het peritoneum en resulteert na twee weken in fibrose en neoangiogenese. De toevoeging van zymosan, een component van de gistcelwand, aan het gekraste peritoneum veroorzaakt een blijvende verdikking van het peritoneum met sterke infiltratie van inflammatoire cellen. Deze veranderingen worden 5 weken na het schrapen gezien en zijn afhankelijk van complement activatie. We concluderen dat deze non-bacteriële peritonitismodellen van nut kunnen zijn om de pathofysiologie van fibrose, neoangiogenese en lymfangiogenese in het kader van peritonitis-geïnduceerde inflammatie te onderzoeken.

Hoofdstuk 3 is de eerste publicatie waarin de relatie wordt getoond van lymfangiogenese met PD-geassocieerde peritoneaal fibrose. De hoeveelheid VEGF-C eiwit in PD effluent van patiënten correleert met de peritoneale solute transport rate en met TGF-β1 spiegels. De expressie van VEGF-C en die van lymfatische markers zijn het hoogst in patiënten met UFF en correleren met de dikte van het peritoneum. De expressie van VEGF-C is verhoogd in mesotheelcellen en in macrofagen in peritoneumbiopten van patiënten met peritonitis. TGF-β1 stimuleert de VEGF-C productie in peritoneale mesotheelcellen van patiënten. De sterkte van deze respons correleert met de peritoneumfunctie van de desbetreffende PD patiënt. In een rattenmodel van peritoneaal fibrose geïnduceerd door chloorhexidine gluconaat (CG) is het aantal lymfvaten toegenomen in het pariëtale peritoneum en vooral in het diafragma. Behandeling met een remmer van de TGF-β type I receptor verlaagt de VEGF-C expressie en de lymfangiogenese, in parallel met een afgenomen inflammatie en fibrose in het CG rattenperitoneum. Nieuwgevormde lymfvaten in het CG rattendiafragma zijn in staat grote moleculen op een effectieve wijze te absorberen, zoals blijkt uit de redistributie van FITC-dextraan (MW 2.000.000) in de peritoneumholte. Als onderliggend mechanisme hebben we aangetoond dat de TGF-β geïnduceerde VEGF-C productie in peritoneale cellen leidt tot lymfangiogenese gedurende het proces van peritoneale fibrose.

In **Hoofdstuk 4** hebben we het effect onderzocht van specifieke remming van lymfangiogenese in een muizenmodel van peritoneale fibrose geïnduceerd door intraperitoneale injecties met methylglyoxal (MGO), een toxisch glucose degradatie product (GDP) dat soms ook gevonden wordt in PD effluent. Voor remming van lymfangiogenese wordt gebruik gemaakt van soluble VEGFR-3, een decoy receptor, met als doel om VEGF-C/D weg te vangen. De MGO-geïnduceerde morfologische veranderingen in het peritoneum, inclusief lymfangiogenese, zijn prominent aanwezig, met name in het diafragma. De lymfangiogenese in het MGO model lijkt gedreven te worden door VEGF-D en niet door VEGF-C, omdat alleen de expressie van VEGF-D toegenomen is in dit model. Opmerkelijk hierbij is dat in het peritoneum van patiënten met UFF de expressie van zowel VEGF-C als VEGF-D is verhoogd. Behandeling met soluble VEGFR-3 onderdrukt de lymfangiogenese, maar heeft geen effect op de inflammatie, fibrose en bloedvatvorming in het diafragma in het MGO model. Deze behandeling leidt ook tot verbetering van de gestoorde ultrafiltratie, terwijl de peritoneale solute transport rate niet veranderd is. Deze bevindingen suggereren dat peritoneale lymfvaten in staat zijn om PD vloeistof direct te absorberen, waarbij geen modificatie plaatsvindt van de compositie van opgeloste stoffen. Dit is overeenkomstig met de open structuur van de wand van lymfvaten. We concluderen dat het remmen van VEGFR-3 signalering een nuttige strategie zou kunnen zijn om lymfangiogenese-geïnduceerde UFF te verbeteren.

Hoofdstuk 5 toont de relatie tussen CTGF en peritoneale lymfangiogenese. Er is een positieve correlatie tussen de eiwitspiegels van CTGF en VEGF-C in PD effluent. CTGF

mRNA expressie is positief gecorreleerd met VEGF-C, LYVE-1 en podoplanine mRNA expressie in peritoneumbiopten van patiënten. Er is een positieve correlatie tussen CTGF en VEGF-C mRNA toename in humane peritoneale mesotheelcellen na stimulatie met TGF-β1. Expressie van CTGF, VEGF-C en markers van lymfvaten is significant verhoogd in het diafragma in het ratten CG-model. In ditzelfde model is de CTGF expressie positief gecorreleerd met de expressie van VEGF-C en markers van lymfvaten. CTGF en VEGF-C worden door peritoneale mesotheelcellen in parallel geproduceerd en er is een nauwe relatie tussen CTGF en PD-geassocieerde lymfangiogenese in het peritoneum. In experimentele modellen voor nierschade hebben we aanwijzingen dat CTGF zelf direct betrokken is bij de regulatie van lymfangiogenese (Hoofdstuk 7), maar het is nog niet bekend of dit ook het geval is bij lymfangiogenese in het peritoneum.

In **Hoofdstuk 6** hebben we het mechanisme onderzocht van lymfangiogenese in de nier in het rattenmodel van unilaterale ureter obstructie (UUO). De expressie van TGF-β, VEGF-C en markers van lymfvaten is toegenomen, waarbij de relatie tijdsafhankelijk is met een hoogste piek rond twee weken na UUO. TGF-β stimuleert de VEGF-C productie in gekweekte niertubulusepitheelcellen en macrofagen. Directe toediening van de remmer van de TGF-β type I receptor via de arteria renalis resulteert in verminderde expressie van VEGF-C en lymfangiogenese in het UUO model. Overeenkomstig met Hoofdstuk 3, laten we zien dat de TGF-β-VEGF-C pathway een belangrijke rol speelt in nier- en peritoneaal fibrose.

In **Hoofdstuk 7** hebben we de rol van CTGF met betrekking tot lymfangiogenese in de nier opgehelderd. In een nefrectomiepreparaat afkomstig van een patiënt met obstructieve nefropathie is prominente lymfangiogenese aanwezig, die gepaard gaat met toegenomen expressie van CTGF en VEGF-C. CTGF knockdown in muizen resulteert in een lagere VEGF-C expressie en afgenomen lymfangiogenese, met in parallel een significante afname van fibrose in het UUO model. CTGF stimuleert in vitro de productie van VEGF-C in niertubulusepitheelcellen, maar CTGF bindt ook direct aan VEGF-C, met als gevolg dat de VEGF-C geïnduceerde groei van lymfendotheelcellen geremd wordt. In vivo kan niet alleen het intacte CTGF molecuul, maar ook CTGF fragmenten gedetecteerd worden. In tegenstelling tot het intacte CTGF molecuul, hebben deze CTGF fragmenten geen invloed op de functie van VEGF-C. Dit suggereert dat het direct remmende effect van CTGF op VEGF-C kan worden voorkomen of mogelijk worden opgeheven door het klieven van CTGF. CTGF lijkt dus direct betrokken te zijn bij de lymfangiogenese in nierfibrose door het reguleren van zowel de productie als de activiteit van VEGF-C.

Hoofdstuk 8 is gericht op de effecten van veroudering op de reactie van de nier op schade in het UUO muizenmodel. Qua morfologie ontwikkelen oude muizen vergeleken met jonge muizen meer tubulusschade, maar minder interstitiële fibrose. Tussen oude en jonge muizen is geen significant verschil aanwezig in de expressie van bewezen profibrotische en

nierbeschermende factoren, zoals TGF-β, plasminogen activator inhibitor-1 (PAI-1), Klotho en bone morphogenetic protein 7 (BMP7). Wel wordt in geobstrueerde nieren van oude muizen een hogere expressie van BMP6 en een lagere expressie van CTGF gezien, dat mogelijk geassocieerd is met de waargenomen mindere fibrose. CTGF bindt in vitro direct aan BMP6 en remt hiermee de signalering van BMP6. Dit suggereert dat de beschermende effecten van BMP6 op de nier nog sterker zijn in de oude UUO nieren waarin CTGF expressie lager is. De combinatie van meer tubulusschade en minder fibrose in de oude UUO nieren suggereert dat nog andere mechanismen betrokken zijn bij dit fenotype. Onze bevinden zijn relevant, omdat chronische nierziekten vooral optreden in oudere mensen, terwijl proefdierstudies naar nierfibrose in het algemeen uitgevoerd worden in jonge muizen, zonder rekening te houden dat de leeftijd belangrijke effecten zou kunnen hebben op de reactie van de nier op schade.

In **Hoofdstuk 9** hebben we de relatie onderzocht van CTGF expressie in getransplanteerde nieren met histologische en functionele uitkomsten. We hebben ontdekt dat tubulointerstitiële CTGF expressie (CTGFti) in patiënten met een stabiele nierfunctie op 3 maanden na transplantatie een onafhankelijke voorspeller is voor het ontstaan van interstitiële fibrose (IF) en tubulusatrofie (TA) op 5 jaar na transplantatie. Het is bekend dat de leeftijd van de donor een belangrijke voorpeller is voor het ontstaan van histologische schade. Met behulp van voorspellingsmodellen laten wij zien dat de combinatie van CTGFti en CTGF spiegels in de urine (CTGFu) op 3 maanden na transplantatie samen met de leeftijd van de donor de voorspellende waard voor het ontstaan van IF/TA op 5 jaar na transplantatie sterk doen toenemen. De bevinding dat CTGF expressie geen voorspeller is voor de nierfunctie op 5 jaar na transplantatie kan mogelijk verklaard worden door het gegeven dat binnen dit cohort de nierfunctie relatief stabiel is gebleven. Derhalve zijn meer studies met een langere observatieperiode nodig om een uitspraak te kunnen doen of de waargenomen progressie van IF/TA gerelateerd aan de vroege verhoging van CTGF expressie in het nierbiopt uiteindelijk zal leiden tot verlies van de nierfunctie en het transplantaat.

Perspectieven

Ik leg voor dat de observaties die beschreven staan in dit proefschrift het idee ondersteunen dat het farmacologisch targeten van CTGF gunstige effecten heeft op de regulatie van lymfangiogenese-geassocieerde nier- en peritoneaal fibrose.

Verlies van ultrafiltratie is een belangrijke oorzaak voor het staken van de PD behandeling en voor de slechte overleving van PD patiënten. Ik veronderstel een mogelijke betrokkenheid van lymfangiogenese met toegenomen lymfatische absorptie in de context van UFF geassocieerd met peritoneale fibrose. Gebaseerd op de bevindingen in Hoofdstuk 3, argumenteer ik dat lymfangiogenese geassocieerd is met UFF in PD patienten. Nieuwgevormde lymfvaten transporteren op een effectieve wijze vloeistof en opgeloste

stoffen in een rattenmodel van peritoneale fibrose. Deze bevinding ondersteunt het concept dat lymfangiogenese leidt tot toegenomen peritoneale lymfatische absorptie. Tevens heb ik in Hoofdstuk 4 bevestigd dat het targeten van peritoneale lymfangiogenese succesvol is om de gestoorde ultrafiltratie die geassocieerd is met peritoneale fibrose te verbeteren. In Hoofdstuk 5 laat ik de nauwe relatie zien tussen CTGF expressie en peritoneale lymfangiogenese. In een eerdere studie hebben we geen significante relatie gevonden tussen CTGF en de dichtheid van bloedvaten in peritoneumbiopten van patiënten. Derhalve is CTGF waarschijnlijk meer betrokken bij angiogenese van lymfvaten dan bij angiogenese van bloedvaten in peritoneale fibrose. Ik zou derhalve verwachten dat het reduceren van peritoneale fibrose en het verbeteren van gestoorde ultrafiltratie door remming van CTGF deels gemedieerd wordt door onderdrukking van lymfangiogenese. Deze observatie zou in de nabije toekomst nog meer van belang kunnen zijn bij het voorkomen van UFF, gezien de ontwikkeling en introductie van nieuwe biocompatibele osmotische agentia met een hogere molecuulgewicht, zoals icodextrine, in peritoneale dialysevloeistoffen. Deze dialysevloeistoffen zullen namelijk niet makkelijk kunnen diffunderen via de wand van bloedcapillairen, maar wel makkelijk geabsorbeerd kunnen worden via de lymfvaten.

In Hoofdstuk 6 en 7 wordt de betrokkenheid getoond van zowel TGF-β als CTGF bij lymfangiogenese in het kader van obstructieve nefropathie. Verder wordt in Hoofdstuk 7 gesuggereerd dat remming van CTGF een nuttige therapeutische strategie zou kunnen zijn om fibrose te remmen in zelfs ernstige chronische nierziekten. Het is daarbij interessant dat, zoals in Hoofdstuk 8 wordt getoond, de verhoging van CTGF als reactie op nierschade minder verhoogd is in oude muizen dan in jonge muizen. Dit is een aanwijzing dat de strategie om CTGF te remmen meer succesvol zou kunnen zijn in een jonge patiëntenpopulatie dan in een oudere patiëntenpopulatie. Remming van CTGF resulteert ook in een lagere VEGF-C expressie en in minder lymfangiogenese. Het is niet goed bekend welke effecten lymfangiogenese heeft op inflammatie en fibrose in nierziekten. Het is tevens nog onduidelijk of lymfangiogenese in de nier bijdraagt aan de schade of juist nuttig is om de schadelijke effecten te doen verminderen. Men kan zelfs speculeren dat het in bepaalde omstandigheden juist schadelijk is om lymfangiogenese in de nier te remmen. Echter, indien nieuwgevormde lymfvaten een rol spelen bij het in stand houden van de inflammatie in de nier door het produceren van chemokines en het aantrekken van ontstekingscellen, zou het onderdrukken van lymfangiogenese ook een belangrijk element kunnen zijn van de gunstige anti-CTGF therapie bij nierpatiënten. In Hoofdstuk 9 beschrijven we het potentieel van CTGF als biomarker voor het voorspellen van nierfibrose in patiënten die een niertransplantatie hebben gehad. Zo'n biomarker zou nuttig kunnen zijn voor patiëntstratificatie en –behandeling, vooral in de context van klinische trials, hoewel de sterkte van de voorspellende waarde niet voldoende is om als leidraad te dienen voor het klinische beleid in de dagelijkse praktijk.

Wat de behandeling voor anti-CTGF therapie in patiënten betreft, komt FG-3019, een humaan monoclonaal antilichaam dat gericht is tegen CTGF, hiervoor in aanmerking. FG-3019 is al voldoende veilig en goed verdraagbaar bevonden in meerdere klinische studies.

In een kleine fase 1 studie bestaande uit patiënten met diabetische nefropathie bleek FG-3019 albuminurie significant te verlagen. Een fase 2 studie met FG-3019 in patiënten met diabetes type 2 en nefropathie werd helaas voortijdig beëindigd vanwege een suboptimaal design van de studie, maar momenteel lopen fase 2 studies met FG-3019 in patiënten met idiopathische longfibrose en andere studies (https://clinicaltrials.gov/ct2/results?term=FG-3019&Search=Search).

Ter conclusie wil ik voorleggen dat met de identificatie van CTGF als belangrijke factor in peritoneaal- en nierfibrose, alsmede in lymfangiogenese, nieuwe therapieën kunnen worden ontwikkeld worden voor patiënten met nierziekten en patiënten die peritoneaal dialyse ondergaan.

Acknowledgements

This thesis was supported by the department of Pathology at University Medical Center Utrecht and the department of Nephrology and Renal Replacement Therapy at Nagoya University Graduate School of Medicine.

I am really grateful to prof. **R. Goldschmeding** and **Tri** for supporting my life in Utrecht and all studies. I am also grateful to prof. **Y. Ito** for giving me a chance to study abroad.

I would like to thank the kidney research group, **Roel Broekhuizen**, **Irma**, **Lucas**, **Ellen**, and **Aernoud** for assistance with all experiments. Roel and Ellen will also support this thesis defense as paranimfen.

I thank the Granzyme research group, **Niels**, **Jan**, and **Liling** for technical assistance and useful discussions. I also thank prof. **P. J. van Diest**, prof. **G. J. A. Offerhaus**, and **Stefan** for nice discussions.

I thank **Andrew Leask**, **Jan Aten**, **Ken Lipson**, and **Alferso Abrahams** for technical assistance and beneficial advice. I also thank **Thomas** and prof. **Dirk Kuypers** for collaboration with the human kidney transplantation study.

I thank **Petra**, **Domenico**, and **Eline** for working at the histological laboratory. I also thank **Marja**, **Joyce**, and **Remco** for working at the molecular laboratory.

I would like to thank PRL members, **Folkert**, **Cathy**, **Wendy**, **Manon**, **Shoko**, **Robert**, **Marise**, **Pauline**, **Koos**, **Huijing**, **Rob**, **Justin**, **Willemijne**, **Natalie**, **Laurien**, **Quirine**, **Emma**, **Lilian**, and **Joost** for technical assistance, discussion, talking, lunch, and entertaining events.

I would also like to take this opportunity to thank **Toki Saito**, **Tim Voss**, **Selina**, **Emina**, and **Ayana** for supporting the life and education for my family. I thank **Wilco Tielemans**, **Feemke**, **Hannah**, and **Fleurtje** for being good neighbors and having fun together. I thank **Jochem** and **George** for the house in Utrecht.

I finally thank my family, **Kana** and **Tatsuya** for coming along with me and enjoying the Dutch life. I am grateful to **Noriko Okazaki**, **Toshiyuki Okazaki**, **Yusuke Okazaki**, **Tomoko Okazaki**, **Mitsutaka Kaneko**, **Setsuko Kaneko**, **Shigeno Okazaki**, **Misako Ito**, **Makoto Kinashi**, **Kyoko Kinashi**, **Fukue Kinashi**, **Noriko Matsumoto**, **Hiroshi Togawa**, and **Tomoko Togawa** for assistance from Japan.

Curriculum vitae: Hiroshi Kinashi

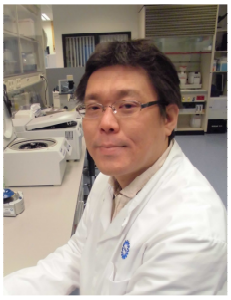

Date of Birth: 11th Feb 1978
Nationality: Japanese
Marial Status: Married with one child

Education
M.D., School of Medicine, Nagoya University, Japan, 2002
Ph.D. in Medicine, Nagoya University Graduate School, 2013

Medical Training
Internship
Handa City Hospital, Japan, 2002-2003
Residency
Handa City Hospital, Department of Nephrology, 2004-2006

Professional Experience
Staff Physician, Department of Nephrology
Handa City Hospital, 2007
Komaki City Hospital, Japan, 2008
Nagoya University Hospital, 2012
Yokkaichi Municipal Hospital, Japan, 2013

Postdoctoral Studies
Graduate School of Medicine, Nagoya University, 2008-2011
Research fellow at Nagoya University, 2012-2013
Visiting scientist at the department of Pathology in University Medical Center Utrecht, The Netherlands, April 2014-March 2017

List of Publications

Falke LL, **Kinashi H**, Dendooven A, Broekhuizen R, Stoop R, Joles JA, Nguyen TQ, Goldschmeding R. Age-dependent shifts in renal response to injury relate to altered BMP6/CTGF expression and signaling. *Am J Physiol Renal Physiol*. 2016;311(5):F926-F934.

Terabayashi T, Ito Y, Mizuno M, Suzuki Y, **Kinashi H**, Sakata F, Tomita T, Iguchi D, Tawada M, Nishio R, Maruyama S, Imai E, Matsuo S, Takei Y. Vascular endothelial growth factor receptor-3 is a novel target to improve net ultrafiltration in methylglyoxal-induced peritoneal injury. *Lab Invest*. 2015;95(9):1029-43.

Kinashi H, Ito Y, Mizuno M, Suzuki Y, Terabayashi T, Nagura F, Hattori R, Matsukawa Y, Mizuno T, Noda Y, Nishimura H, Nishio R, Maruyama S, Imai E, Matsuo S, Takei Y. TGF-β1 promotes lymphangiogenesis during peritoneal fibrosis. *J Am Soc Nephrol*. 2013;24(10):1627-42.

Suzuki Y, Ito Y, Mizuno M, **Kinashi H**, Sawai A, Noda Y, Mizuno T, Shimizu H, Fujita Y, Matsui K, Maruyama S, Imai E, Matsuo S, Takei Y. Transforming growth factor-β induces vascular endothelial growth factor-C expression leading to lymphangiogenesis in rat unilateral ureteral obstruction. *Kidney Int*. 2012;81(9):865-79.

Kato H, Mizuno T, Mizuno M, Sawai A, Suzuki Y, **Kinashi H**, Nagura F, Maruyama S, Noda Y, Yamada K, Matsuo S, Ito Y. Atrial natriuretic peptide ameliorates peritoneal fibrosis in rat peritonitis model. *Nephrol Dial Transplant*. 2012;27(2):526-36.